



HAL
open science

Towards a better valorization of *Arthrospira platensis* (Spirulina) biomass: Contribution to the optimization of its culture and its refinery

Alejandra Gutiérrez Márquez

► To cite this version:

Alejandra Gutiérrez Márquez. Towards a better valorization of *Arthrospira platensis* (Spirulina) biomass: Contribution to the optimization of its culture and its refinery. Chemical and Process Engineering. Aix-Marseille Université, 2024. English. NNT: . tel-04632679

HAL Id: tel-04632679

<https://theses.hal.science/tel-04632679v1>

Submitted on 2 Jul 2024

HAL is a multi-disciplinary open access archive for the deposit and dissemination of scientific research documents, whether they are published or not. The documents may come from teaching and research institutions in France or abroad, or from public or private research centers.

L'archive ouverte pluridisciplinaire **HAL**, est destinée au dépôt et à la diffusion de documents scientifiques de niveau recherche, publiés ou non, émanant des établissements d'enseignement et de recherche français ou étrangers, des laboratoires publics ou privés.

THÈSE DE DOCTORAT

Soutenue à Aix-Marseille Université
le 10 avril 2024 par

Alejandra GUTIERREZ MARQUEZ

Towards a better valorization of Arthrospira platensis (Spirulina) biomass: Contribution to the optimization of its culture and its refinery

Discipline

Sciences pour l'ingénieur

Spécialité

Génie des procédés

École doctorale

ED 353 - Sciences pour l'ingénieur:
mécanique, physique, micro et
nanoélectronique

Laboratoire/Partenaires de recherche

Laboratoire de Mécanique, Modélisation
& Procédés Propres, M2P2 (UMR CNRS
7340)

Plateforme « Microalgues et procédés »,
MAP, CEA, Cadarache

Composition du jury

• Céline LAROCHE	Rapporteuse
• PR, Université Clermont Auvergne	
• Miguel HERRERO	Rapporteur
• Senior Researcher, CIAL	
• Abril LANSOY	Examinatrice
• IR, CRES-TOTAL ENERGIES	
• Luc MARCHAL	Président du jury
• PR, Université de Nantes	
• Elisabeth BADENS	Directrice de thèse
• PR, Aix-Marseille Université	
• Christelle CRAMPON	Co-directrice de thèse
• PR, Aix-Marseille Université	
• Gatien FLEURY	Co-encadrant
• IR, CEA	

Affidavit

I, undersigned, Alejandra GUTIERREZ MARQUEZ, hereby declare that the work presented in this manuscript is my own work, carried out under the scientific supervision of Elisabeth BADENS, Christelle CRAMPON and Gatien FLEURY in accordance with the principles of honesty, integrity and responsibility inherent to the research mission. The research work and the writing of this manuscript have been carried out in compliance with both the French national charter for Research Integrity and the Aix-Marseille University charter on the fight against plagiarism.

This work has not been submitted previously either in this country or in another country in the same or in a similar version to any other examination body.

Aix-En-Provence, 3 February, 2024

Alejandra GUTIERREZ MARQUEZ



Cette œuvre est mise à disposition selon les termes de la [Licence Creative Commons Attribution - Pas d'Utilisation Commerciale - Pas de Modification 4.0 International](https://creativecommons.org/licenses/by-nc-nd/4.0/).

Liste de publications et participation aux conférences

1) Liste de publications et/ou brevet dans le cadre du projet de thèse :

1. Márquez, A.G., Fleury, G., Dimitriades-Lemaire, A., Alvarez, P., Santander, G., Crampon, C., Badens, E., Sassi, J.-F., 2023. Potential of the worldwide-cultivated cyanobacterium *Arthrospira platensis* for CO₂ mitigation: Impacts of photoperiod lengths and abiotic parameters on yield and efficiency. *Bioresource Technology Reports* 22, 101439. <https://doi.org/10.1016/j.biteb.2023.101439>

2) Participation aux conférences et écoles d'été au cours de la période de thèse :

1. Márquez, A.G., Fleury G., Alvarez Diaz P., Delrue F., Dimitriades-Lemaire A., Crampon C., Badens E., Sassi J.-F., Challenges and opportunities of CO₂ remediation through *A. platensis* culture, *Algaeurope*, December 2021 (Poster presentation).
2. Márquez A.G, Fleury G., Alvarez Diaz P., Dimitriades-Lemaire A., Crampon C., Badens E., Sassi J.-F., High-value molecule production by CO₂ remediation: Culture optimization of *Arthrospira platensis* (Spirulina) in phototrophic conditions, VII Congreso Latinoamericano de Biotecnología Algal (CLABA) y el V Congreso de la Sociedad Latinoamericana de Biotecnología Ambiental y Algal (SOLABIAA), November, 2022 (Poster presentation).
3. Márquez A.G, Fleury G., Alvarez Diaz P., Santander G., Dimitriades-Lemaire A., Crampon C., Badens E., Sassi J.-F., CO₂ bio-sequestration for antioxidant production: optimization of the cultivation and biorefining of *Arthrospira platensis* (Spirulina), 30th congress of the Environmental Sciences doctoral school, May 2023. (Oral presentation).

Résumé

Utilisée en agroalimentaire, nutraceutique et cosmétique sous forme brute ou de produit raffiné, *A. platensis* suscite un intérêt croissant mais sa culture et son bioraffinage représentent un réel défi. Ce doctorat s'est attaché à proposer et tester des procédés durables pour améliorer ces deux aspects.

Ce travail contribue à évaluer le potentiel de réutilisation du CO₂ par *A. platensis* lors de sa culture et l'impact des photopériodes sur sa productivité en biomasse et pigments. L'assimilation du CO₂ est caractérisée via un modèle adossé à des mesures expérimentales. Dans les conditions de laboratoire testées, une photopériode de 24 heures augmente à la fois la productivité en biomasse de 74 % et la teneur en phycocyanine de 35 %.

Les extractions sous pression sont réalisées par des mélanges éthanol/eau (PLE) et CO₂ supercritique (scCO₂). Les conditions optimales trouvées en PLE sont 60°C/100 % d'éthanol et 65 °C/90 % d'éthanol (v/v) à 103 bar, respectivement pour une biomasse avec et sans extraction préalable des phycobiliprotéines par macération. L'extraction par scCO₂, dont la cinétique a été modélisée par les équations de Sovová, induit une perte de masse de 7,7 % à 60 °C et 300 bar.

Ce travail permet de proposer un schéma de bioraffinerie en trois étapes, commençant par une première extraction de la biomasse par macération aqueuse afin d'extraire les phycobiliprotéines. Une deuxième étape d'extraction à l'éthanol sous pression permet ensuite la séparation d'un mélange de pigments lipophiles et composés phénoliques antioxydants. Puis, après séchage, l'extraction de la fraction apolaire par scCO₂ permet d'isoler une fraction huileuse riche en caroténoïdes et d'obtenir une biomasse résiduelle riche en protéines.

Mots-clés : *A. platensis*, CO₂-mitigation, pigments, valorisation, solvants verts

Abstract

The rising popularity of vegan diets is driving demand for *A. platensis* biomass, known for its nutritional density. Widely utilized in food, nutraceuticals, and cosmetics, *A. platensis* encounters challenges in cultivation and extraction. This doctoral program focuses on developing sustainable processes to improve both cultivation and extraction methods.

The study assesses *A. platensis*' CO₂ reutilization potential and the impact of photoperiods on biomass and pigment productivity (phycobiliproteins, Chlorophyll a, and carotenoids) in both laboratory and greenhouse settings. CO₂ assimilation is characterized using a cross-model with experimental measurements. A 24-hour photoperiod increases biomass productivity by 74%, and laboratory phycocyanin content by 35%.

The second part of the study focuses on pigment extraction using a water/ethanol mixture (PLE) and supercritical CO₂ (scCO₂). Optimal PLE conditions are 60°C/100% ethanol and 65°C/90% ethanol (v/v) at 103 bar, for biomass undergoing maceration of phycobiliproteins and without prior extraction, respectively. ScCO₂ extraction results in a mass loss of 7.7% at 60°C and 300 bar. Kinetics are modeled using Sovová's equations to identify phenomena limiting material transfer based on pretreatment.

A valorization process is proposed, starting with the extraction of fresh biomass through aqueous maceration to extract phycobiliproteins. A second step involves ethanol pressurized extraction, yielding a mixture of lipophilic pigments and antioxidant phenolic compounds. After drying, supercritical CO₂ extraction of the apolar fraction isolates an oily portion rich in carotenoids and a residual biomass with nutritional value.

Key-words: *A. platensis*, CO₂-mitigation, pigments, valorization, green-solvents

Remerciements

Cette thèse de doctorat a été réalisée à la Plateforme de microalgues (MAP) du CEA-Cadarache et au Laboratoire de Mécanique, Modélisation & Procédés Propres (M2P2) de l'Université Aix-Marseille, en co-financement avec le Conseil National de la Science et de la Technologie du Mexique (CONACyT) sous le financement numéro 786324. Je tiens à exprimer ma sincère gratitude aux organismes impliqués dans le développement de ce projet.

Ce manuscrit de thèse est le résultat d'un rêve qui a commencé il y a un peu plus de trois ans. Je peux affirmer sans aucun doute que cette expérience a été l'une des plus enrichissantes et stimulantes de ma vie, compte tenu des exigences intellectuelles et personnelles qu'elle implique. Cependant, je peux dire que Dieu m'a béni en mettant sur mon chemin des personnes merveilleuses qui ont été de grands guides, enseignants et soutiens tout au long de ces années.

Je tiens à commencer en exprimant ma gratitude envers mes directeurs de thèse, Gatien FLEURY, Elisabeth BADENS et Christelle CRAMPON, pour leur grande qualité humaine et professionnelle. Leur encadrement tout au long de ce projet a été fondamental pour moi. Merci de partager vos connaissances précieuses, votre expérience, et votre temps avec moi. Travailler avec vous a été un grand honneur. Votre passion pour votre métier est contagieuse et une grande source d'inspiration pour moi.

Je tiens à exprimer ma sincère gratitude envers les membres du jury, Céline LAROCHE, Miguel HERRERO, Luc MARCHAL et Abril LANSOY, d'avoir accepté de participer à l'évaluation de mon projet de thèse doctorale.

Un grand merci à l'équipe de la MAP de m'avoir ouvert ses portes dès mon stage ; cela a été un plaisir de travailler avec vous tout ce temps. Sincèrement, vous avez fait en sorte que le fait de me lever à 6 heures du matin en vaille la peine. Un immense merci à Alexandra DIMITRIADES-LEMAIRE pour le formidable travail qu'elle accomplit en chimie analytique, son soutien tout au long des analyses de cette thèse, et sa grande qualité humaine a vraiment fait la différence pour moi. Merci également à Sophie FON SING, Pablo ALVAREZ, Florian DELRUE et Jean-François SASSI pour leur disponibilité, leurs conseils techniques et leur bonne humeur tout au long de ce projet. Merci également à Patricia MURRISCH, Eliane LAURINO et Juliette IMBACH pour leur soutien avec les procédures internes du CEA.

Toute ma gratitude au laboratoire M2P2 pour avoir ouvert ses portes à mon projet, en particulier à Adil MOUAHID pour avoir partagé avec moi ses connaissances précieuses et son expérience dans les extractions au CO₂ supercritique. Son soutien a été d'une aide immense pour ce projet.

Je tiens à exprimer du fond du cœur ma gratitude envers mes collègues, pour leurs conseils, leur soutien moral, les rires, les cafés et les moments partagés au laboratoire et en dehors. Sans vous, tout aurait été beaucoup plus difficile. Un grand merci particulièrement à Adriana, Alex, Maria, Thao, Ana, Jeanne, Anne, Chloé, Aymeric, Olivia, Javier, Marie, Raphael, Charlotte, Olivier, Sandrine, Fred, Vénicia, Carolina, Alex P., Shuxin, Giovanni, Fatimatou, Zoya, Antonello, Paul, Fiona, Laura et Giulia. Je suis très chanceuse d'avoir partagé cette étape avec vous.

Je considère avoir été chanceuse d'avoir bénéficié d'un réseau de soutien aussi solide tout au long de ce parcours. Un merci particulier à Luca, qui a été le compagnon idéal, ma main droite en permanence et « casa » en France. J'exprime toute ma gratitude envers Enrique pour être cet ami qui conseille, comprend et écoute, son amitié est très précieuse pour moi. Merci Diana pour ton amitié précieuse, depuis que je suis arrivé en France, tu es cette amie qui écoute et accompagne chacun de mes pas. Un remerciement infini à mes amies d'enfance Kim et Liz qui ne m'ont jamais lâchée et m'ont soutenue depuis l'autre côté du monde. Un immense merci au groupe Shalom-Aix pour apporter de la joie et me soutenir durant l'étape aixoise de ma thèse.

Je tiens à dédier cette thèse à mes parents, Laura et Alejandro. Vous avez été la source de ma motivation et de ma force tout au long de ce parcours que j'ai choisi d'entreprendre dans la vie. Merci de m'avoir fourni les moyens d'atteindre mes rêves et de toujours avoir eu confiance en moi. Si j'ai réussi à aller aussi loin, c'est en grande partie grâce à vous. Merci de m'entourer de votre amour depuis le Mexique.

Merci bon Dieu pour tant de bénédictions.

*Mais, ceux qui comptent sur l'Eternel
renouvellent leur force.
Ils prennent leur envol comme les aigles.
Ils courent sans s'épuiser,
ils marchent sans se fatiguer.
Ésaïe 40:31*

Content

Affidavit	2
Liste de publications et participation aux conférences	3
Résumé	4
Abstract	5
Remerciements	6
List of abbreviations	12
Introduction	14
Chapter 1 State of the art	17
1.1 <i>Arthrospira platensis</i> general aspects	17
1.1.1 <i>Arthrospira platensis</i> in human history.....	17
1.1.2 Microorganism morphology, reproduction, and habitat.....	18
1.2 <i>Arthrospira platensis</i> as a source of bioactive compounds	19
1.2.1 Total sugars	19
1.2.2 Lipids	20
1.2.3 Proteins.....	21
1.2.4 Phycocyanin (PC)	22
1.2.5 Allophycocyanin.....	22
1.2.6 Phycoerythrin	23
1.2.7 Chlorophylls	23
1.2.8 Carotenoids.....	24
1.2.9 Phenolic compounds	24
1.3 <i>Arthrospira platensis</i> culture	25
1.3.1 Autotrophic culture	25
1.3.2 Culture media and nutrient supplementation.....	26
1.3.3 Bioreactors for <i>Arthrospira platensis</i> culture.....	31
1.3.4 Environmental Parameters Influencing <i>Arthrospira platensis</i> Growth.....	32
1.3.5 <i>Arthrospira platensis</i> strains.....	35
1.4 <i>Arthrospira platensis</i> culture monitoring parameters	37
1.5 Downstream processing of <i>Arthrospira platensis</i> for pigment industrial applications ...37	
1.5.1 Harvest methods	37
1.5.2 Biomass drying methods	42
1.5.3 Cell-disruption techniques.....	46
1.6 Extraction techniques applied to <i>Arthrospira platensis</i> valorization	48
1.6.1 Organic solvent extractions	49
1.6.1 Maceration.....	50
1.6.2 Green solvent extractions	50
1.6.3 Pressurized Liquid Extraction (PLE)	50
1.6.4 Supercritical CO ₂ (scCO ₂) extraction.....	53

1.6.5	Pressurized Fluid Extraction (PFE) Scale-up	57
1.7	High-value molecule quantification techniques for biomass extracts	58
1.7.1	Protein quantification.....	58
1.7.2	Total sugars	59
1.7.3	Lipids	60
1.7.4	Chlorophylls and carotenoids	61
1.7.5	Antioxidant properties of the extracts	61
1.8	Integral valorization of <i>Arthrospira platensis</i> biomass in a biorefinery approach	64
1.8.1	Vegan proteins.....	64
1.8.2	Aquaculture feed.....	64
1.8.3	Bioplastics	65
1.8.4	Bioethanol	65
1.8.5	Biogas	66
1.9	Aims and objectives	66
Chapter 2 Materials and methods		70
2.1	Phase I: Biomass culture optimization	72
2.1.1	<i>Arthrospira platensis</i> culture as a CO ₂ mitigation technique	72
2.1.2	Project strain choice.....	73
2.1.3	Culture conditions for project strain choice	73
2.1.4	Dry weight determination for project strain choice	74
2.1.5	Generic dry weight determination	74
2.1.6	Growth and productivity calculations	74
2.1.7	Lipophilic pigments (Chl and carotenoids)	75
2.1.8	Chl a and carotenoids spectrophotometer quantification	76
2.1.9	HPLC Chlorophyll a and carotenoids quantification	76
2.1.10	Phycobiliproteins extraction.....	77
2.1.11	Dry biomass phycobiliproteins extraction.....	77
2.1.12	Phycobiliproteins spectrophotometer quantification.....	78
2.1.13	Laboratory scale <i>Arthrospira platensis</i> CO ₂ mitigation characterization.....	78
2.1.14	Cultivation conditions for the laboratory scale CO ₂ mitigation characterization	78
2.1.15	Sampling for Analytical determinations in the laboratory scale CO ₂ mitigation characterization	79
2.1.16	Supernatant analysis.....	80
2.1.17	Biomass analysis.....	80
2.1.18	Kinetic parameters and CO ₂ fixation rate.....	81
2.1.19	Statistical Analysis of the determinations in the Laboratory Scale CO ₂ mitigation characterization	81
2.1.20	Numerical modeling of <i>Arthrospira platensis</i> culture CO ₂ mitigation at laboratory scale 81	
2.1.21	<i>Arthrospira platensis</i> CO ₂ mitigation in a 3 L system	83

2.1.22	<i>Arthrospira platensis</i> CO ₂ mitigation in a 3 m ³ system	86
2.1.23	3 m ³ culture conditions	87
2.1.24	3 m ³ culture sampling	88
2.1.25	Carbon mass balance for culture CO ₂ assimilation.....	88
2.2	Phase I: Enhancement of pigment productivity in <i>Arthrospira platensis</i> cultures by photoperiod modification.....	92
2.2.1	Artificial light conditions seed culture for the photoperiod modification experiment...92	92
2.2.2	Artificial light culture conditions.....92	92
2.2.3	Artificial light conditions sampling	92
2.2.4	Natural light conditions experimental set-up.....93	93
2.2.5	Natural light conditions seed culture	95
2.2.6	Sampling and analysis.....96	96
2.3	Phase II: <i>Arthrospira platensis</i> production for green solvent extractions.....	97
2.3.1	<i>Arthrospira platensis</i> culture for application of biomass valorization techniques	97
2.3.2	<i>Arthrospira platensis</i> biomass harvesting for biomass extraction	98
2.3.3	<i>Arthrospira platensis</i> biomass drying for biomass extraction	98
2.3.4	Drying efficiency test.....98	98
2.3.5	Lyophilization.....99	99
2.3.6	Spray-dryer.....99	99
2.3.7	Air-flow drying.....100	100
2.4	Phase II: Biomass characterization.....	100
2.4.1	Biomass moisture.....100	100
2.4.2	Total lipids.....101	101
2.4.3	Sugars.....102	102
2.4.4	Ashes.....103	103
2.5	Phase II: Green solvent <i>Arthrospira platensis</i> valorization.....	104
2.5.1	Valorization of hydrophilic pigments in <i>Arthrospira platensis</i> biomass	104
2.5.2	Configuration of ASE extraction cells	105
2.5.3	Phycobiliprotein extraction before ASE	106
2.5.4	Selective lipophilic pigment extraction of the initial biomass.....106	106
2.5.5	Accelerated Solvent Extraction (ASE) device.....106	106
2.5.6	Central composite design (CCD).....107	107
2.5.7	ASE extract characterization	109
2.6	Phase II: Valorization of lipophilic fraction in <i>Arthrospira platensis</i> biomass.....	115
2.6.1	Studied biomass for scCO ₂ extraction.....115	115
2.6.2	20 mL semi-continuous extractor	115
2.6.3	Supercritical CO ₂ extraction conditions for extraction kinetics.....116	116
2.6.4	Extraction kinetics operating mode	117
2.6.5	ScCO ₂ extract characterization	118

2.6.6	Supercritical CO ₂ extraction modeling.....	120
Chapter 3 Results and Discussions		126
3.1	Phase I: Biomass culture optimization	126
3.1.1	<i>Arthrospira platensis</i> culture as a CO ₂ mitigation technique	126
3.1.2	Strain screening	127
3.1.3	Laboratory scale <i>Arthrospira platensis</i> CO ₂ mitigation characterization.....	130
3.1.4	Conclusions of laboratory scale <i>Arthrospira platensis</i> CO ₂ mitigation characterization 136	
3.1.5	<i>Arthrospira platensis</i> CO ₂ mitigation in a 3 L system	137
3.1.6	<i>Arthrospira platensis</i> CO ₂ mitigation in a 3 m ³ system	139
3.1.7	Conclusions of greenhouse conditions <i>Arthrospira platensis</i> CO ₂ mitigation characterization	143
3.1.8	Enhancement of pigment productivity in <i>Arthrospira platensis</i> cultures.....	144
3.1.9	Conclusions of the enhancement of pigment productivity in <i>Arthrospira platensis</i> cultures 156	
3.2	Phase II: <i>Arthrospira platensis</i> production for the application of biomass valorization techniques.....	157
3.2.1	Drying techniques comparison	157
3.2.2	Biomass characterization.....	160
3.3	Phase II: Green solvent <i>Arthrospira platensis</i> valorization.....	161
3.3.1	Valorization of hydrophilic pigments in <i>Arthrospira platensis</i> biomass	161
3.3.2	Pigment Extraction by Accelerated Solvent Extraction Preliminary study.....	161
3.3.3	Conclusions	183
3.4	Phase II: Valorization of lipophilic pigments in <i>Arthrospira platensis</i> biomass	184
3.4.1	Supercritical CO ₂ valorization of <i>Arthrospira platensis</i> biomass.....	184
3.4.2	Repeatability test	184
3.4.3	Evaluation of the modeled parameters	187
3.4.4	Extract characterization.....	188
3.4.5	Conclusions	190
3.5	Proposition of a new <i>Arthrospira platensis</i> valorization scheme.....	191
General Conclusions and perspectives		193
List of tables.....		197
List of figures		199
Bibliography.....		203
Annex		225

List of abbreviations

ABTS	2,2'-Azinobis-(3-Ethylbenzthiazolin-6-Sulfonic Acid)
ATEX	ATmosphère EXplosible (Explosive Atmospheres)
AP	<i>Arthrospira platensis</i>
APIs	Active Pharmaceutical Ingredients
APC	Allophycocyanin
ASE	Accelerated Solvent Extraction
ATP	Adenosine-5'-triphosphate
BHT	Butylated hydroxytoluene
CA	Carbonic Anhydrase
CCM	Carbon Concentrating Mechanisms
Chl	Chlorophyll
C-PC	C-Phycocyanin
CSTR	Completely Stirred Tank Reactors
DHA	Docosahexaenoic Acid
DIC	Dissolved Inorganic Carbon
DOC	Dissolved Organic Carbon
DPPH	2,2,1-Diphenyl-1-Picrylhydrazyl
DW	Dry Weight
EPS	Exopolysaccharides
EPA	Eicosapentaenoic Acid
FAO	Food and Agriculture Organization of the United Nations
FAMEs	Fatty Acid Methyl Esters
FC	Folin Ciocalteu
FID	Flame Ionic Detector
FPD	Flame Photometric Detector
GA	Gallic Acid
GAE	Gallic Acid Equivalent
GLA	Gamma Linoleic Acid

HPH	High-Pressure Homogenization
HPLC	High-Performance Liquid Chromatography
LCA	Life Cycle Analysis
MAP	MicroAlgae Process platform
NADH	Nicotinamide Adenine Dinucleotide
NADP ⁺	Nicotinamide Adenine Dinucleotide Phosphate
OD	Optical Density
PAR	Photosynthetic Active Radiation
PAHs	Polycyclic Aromatic Hydrocarbons
PBP	Phycobiliproteins
PBR	Photobioreactors
PC	Phycocyanin
PE	Phycoerythrin
PEF	Pulsed Electric Field
PFTR	Plug Flow Tubular Reactor
PFE	Pressurized Liquid Extraction
PHA	Polyhydroxyalkanoates
PHB	Polyhydroxybutyrates
PhC	Phenolic Compounds
PLE	Pressurized Liquid Extraction
PSII	Photosystem II
PUFA	Polyunsaturated Fatty Acids
ROS	Reactive Oxygen Species
R-PC	R-Phycocyanin
RUBISCO	Ribulose-1,5-bisphosphate carboxylase/oxygenase
scCO ₂	Supercritical CO ₂
SFA	Saturated Fatty Acids
TAG	Triacylglycerol
TPC	Total Phenolic Compounds
UAE	Ultrasound-Assisted Extraction
wt	Weight

Introduction

The present manuscript is the result of a 3 year Ph.D. research that aims to contribute to the sustainable development challenges that our society faces nowadays. We find ourselves in a transitional era where there is a growing awareness of the importance of consuming food and products that promote health and environmental responsibility. The establishment and maturation of technologies allowing to manufacture safe bio-sourced molecules for human use, is a critical stage in the way of building a sustainable society. The diversification of the feedstocks is a step forward to reaching sustainability. *Arthrospira platensis* (AP) biomass has been consumed worldwide by different civilizations thanks to its composition rich in nutrients and bioactive molecules. Nowadays, more than 10,000 tons of dry biomass of AP are produced annually for food-grade purposes [1]. However, the produced biomass is primarily utilized as a dietary supplement for human consumption, overlooking the untapped potential of the antioxidant pigments and proteins inherent in AP biomass for alternative applications. These include but are not limited to uses in cosmetics and agri-food industry applications.

This doctoral research titled: “*Towards a better valorization of Arthrospira platensis (Spirulina) biomass: Contribution to the optimization of its culture and its refinery*” represents the collaborative efforts of two research groups. “The Microalgae Process platform” (MAP) at CEA-Cadarache, for the cultivation phase and the “Mechanics, Modeling, and Clean Processes Laboratory” (M2P2) for the fractioning of the biomass. The project is integrated to the doctoral school ED 353 of Aix-Marseille University Engineering Sciences: Mechanics, Physics, Micro and Nanoelectronics, under the specialty of Process engineering. This research was funded by the Mexican National Council of Sciences and Technologies (CONACyT) via the scholarship no. 786324 , the MAP and M2P2 laboratories, and by Ecosynia company SIRET: 889 424 503 00023.

This study aims to explore alternative approaches for optimizing both the upstream and downstream processes involved in the valorization of AP biomass. The investigation comprised four main stages: 1) optimizing the cultivation of AP biomass by substituting the conventional mineral carbon source with gaseous CO₂ as the sole carbon source, 2) inducing the accumulation of bioactive molecules, such as *phycocyanin* (PC), *Chl a*, and carotenoids in the biomass induced by photoperiod modifications and 3) extracting high-value molecules using environmentally friendly solvent technologies such as supercritical CO₂ (scCO₂) and pressured liquid extraction (PLE) to valorize various biomass fractions, and 4) evaluating the antioxidant activities of the extracts (Figure 1). Two well defined complementary parts can be highlighted,

Part I: Upstream optimization, that includes stage 1 and 2, and Part II: Downstream optimization that includes stages 3 and 4.

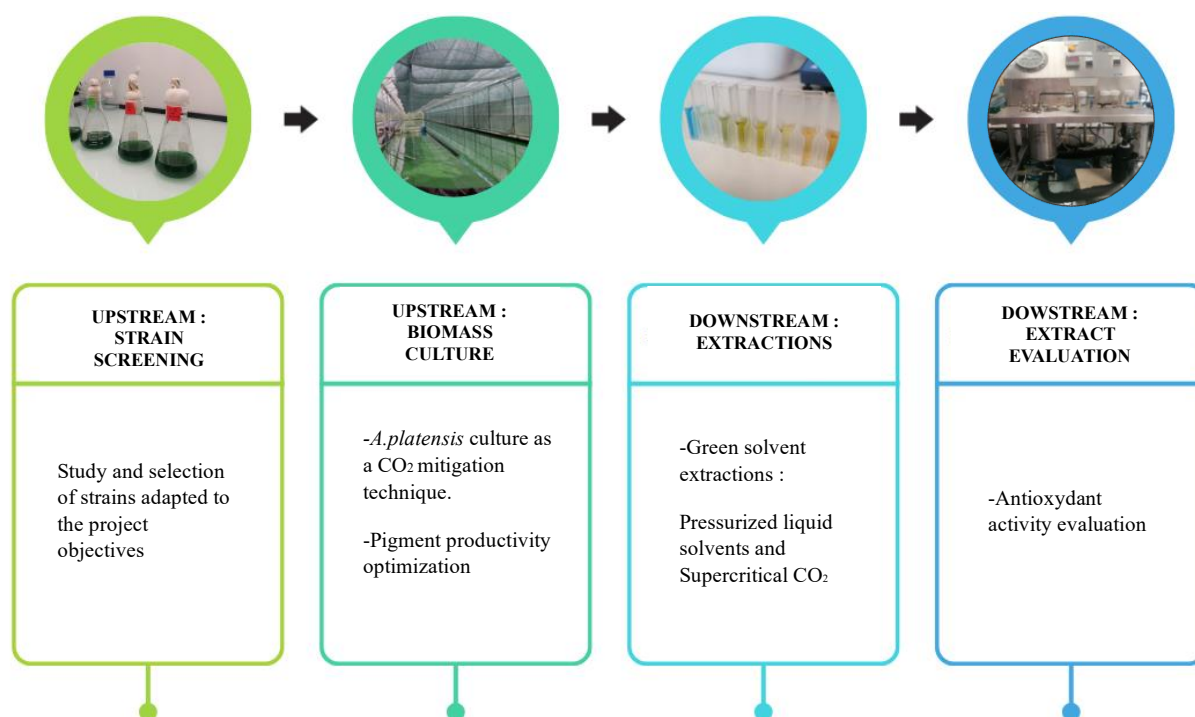


Figure 1 Project view of *Arthrospira platensis* valorization chain

The organization of this work is designed to provide crucial information for outlining the issues and responses that it aims to address. The goal is to facilitate the cultivation and fractioning of *Arthrospira platensis* (AP) biomass for its application in the food, nutraceutical, and cosmetic industries. This is encouraged by its content in bioactive compounds like antioxidants and proteins.

Chapter 1, “State of the art”, initiates this exploration by introducing the fundamental aspects of the operations involved in this study. From the microorganism characterization as a source of bioactive compounds (1.2.2) to the application of green solvents for its biomass valorization (1.6.1). The chapter navigates through key aspects such as biomass culture (1.3), pre-treatments for biomass extraction (1.5), evaluations of the extracts (1.7), and alternative applications of biomass (1.8). In conclusion, this chapter outlines the primary aims and objectives of the work.

Chapter 2, "Materials and Methods", furnishes details about the methodologies employed to attain the set objectives outlined in the aims and objectives. Sections 2.1 and 2.2 explore the optimization methodologies for the upstream processes, focusing on the assessment of AP cultivation as a CO₂ mitigation technique and the enhancement of pigment productivity through

photoperiod modification. In the context of downstream processes, Sections 2.3 and 2.4 outline the techniques utilized for the cultivation, harvest, pre-treatment, and characterization of the biomass intended for the green solvent extraction tests. Finally, Section 2.5 describes the methodology employed for evaluating PLE and scCO₂ extraction in AP biomass for its fractionation and valorization.

Chapter 3, entitled "Results and Discussions", explores the outcomes acquired for the components addressed in this study: the cultivation and fractionation optimization of AP. In Section 3.1, the potential of AP as a CO₂ mitigation technique is discussed, both through the application of a model and experimental investigation under laboratory conditions. The evaluation of CO₂ mitigation yields by the microorganism culture was also carried out for different Photobioreactor (PBR) configurations. Section 3.2 evaluates the efficiency of different drying methods as pre-treatments for extraction. This assessment involves a comparison of spray drying, freeze-drying, and air-flow drying techniques, considering the concentration of PBP biomass after treatment. This section also explores the composition of the biomass cultivated for the green solvent extractions. Section 3.3 covers the discussion of optimal extraction conditions for Pressurized Liquid Extraction (PLE) concerning temperature and solvent mixture composition at the laboratory scale. It also addresses the results of supercritical CO₂ (scCO₂) extraction under optimal conditions at the laboratory scale. Towards the end of this chapter, an analysis is conducted on the applicability of the proposed techniques.

In the concluding section of this document, the research work conclusions and future perspectives are presented. This part highlights the outcomes of the conducted experiments and outlines the proposed approaches to address areas that may have uncertainties or gaps.

Chapter 1 State of the art

1.1 *Arthrospira platensis* general aspects

1.1.1 *Arthrospira platensis* in human history

This cyanobacterium is known to have a long-term relationship with human nutrition. The first evidence of its consumption in modern history dates between 1519 and 1521, by the Spanish explorer Bernal Diaz del Castillo during his expeditions to Central America. He witnessed the Aztec people harvesting “Tecuitlatl”, the name given by the Aztecs to AP biomass cultivated straight from Texcoco Lake (Figure 2), in present-day Mexico City [2, 3]. More than 400 years later, in 1940 the French phycologist Pierre Dangeard described in a communication to the Linnean Society of Bordeaux a sort of cookie named “Dihé” consumed by the Kanembou people in the market of Massakory, 100 km from Chad Lake, in Central Africa. In 1960, Belgian botanist Jean Léonard rediscovered "Dihé" during an expedition to Chad, confirming its composition as *Arthrospira platensis* (AP) collected from the alkaline waters of Northeast Lake Chad. [4]. These events awoke interest in the research about the properties of this blue-green algae. In 1996, the first doctoral project for the understanding of AP culture was performed by Claude Zarrouk at the University of Paris [5], and the research about the culture and valorization of this microorganism is still on track.

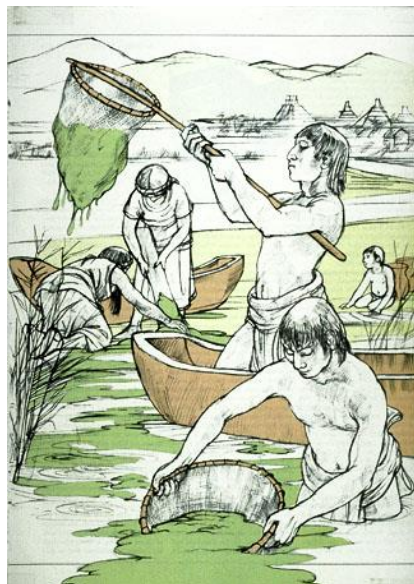


Figure 2 Illustration of the Aztecs collecting *Arthrospira platensis* biomass from Texcoco Lake, reproduced from [2]

During the last decades, AP received increased attention from researchers, mainly for its interesting protein content, in addition to the pigments of interest in the food, cosmetic, and pharmaceutical industries [6]. In 2002, the FDA, classified AP as Generally Recognized as Safe (GRAS), its biomass stands out for its rich composition in bioactive molecules, such as essential

amino acids, unsaturated fatty acids, and colored pigments like Chl a, carotenoids, and phycobiliproteins. These compounds can serve as both colorants and natural antioxidants, thereby enhancing human nutrition and development [7].

Nowadays, eating habits and healthy lifestyle awareness have been rising to reduce the incidence of chronic diseases [8]. The main biological activities of AP as a neuroprotector, anticancer, and anti-inflammatory effect make its biomass a potential candidate for functional foods [9].

The present work explores the potential of AP as a source of bioactive molecules for different applications and proposes sustainable strategies to optimize its culture and biorefinery.

1.1.2 Microorganism morphology, reproduction, and habitat

AP is a prokaryotic microorganism exclusively phototrophic. This filamentous blue-green cyanobacterium reproduces by binary fission. Its cells are composed of multicellular cylindrical trichomes that group to form a sole long trichome, with an length range of 50–500 μm and a width range of 3–4 μm (Figure 3) [10].



Figure 3 Microscope picture (40x) of *Arthrospira platensis* SAG-21.99 from DRT MAP, Cadarache

The natural blooms of AP are mainly found in tropical areas of the world, like central and East Africa and South America. The microorganisms develop rapidly, in soil, marshes, brackish water, salty water, freshwater, and thermal springs. Alkaline (pH 8.5-11), salty water ($\text{Na} < 30 \text{ g/L}$), and high solar radiation promote its development [11]. AP development is favored by temperatures between 35-39°C [12].

Chapter I : State of the art

1.2 *Arthrospira platensis* as a source of bioactive compounds

Microalgae and cyanobacteria are known to be a rich source of bioactive molecules. Generally, the chemical composition of these microorganisms is 70-230 g lipids/kg of biomass, 50-230 g carbohydrates/kg of biomass, and 60-700 g proteins/kg biomass on a dry weight basis, which varies as a function of the genus and species and on the growing conditions of the microorganisms [13]. AP specie is an interesting source of nutritional compounds, such as macro and micronutrients, including proteins, carbohydrates, lipids, vitamins, and minerals which are fundamental for human nutrition. Moreover, some of the compounds, such as the phycobiliproteins (PBP) and the long-chain polyunsaturated fatty acids (PUFA) present different biological activities, like neuroprotective, anti-inflammatory, and antioxidant activities [14]. Figure 4 provides a visual representation of the organelles within a cyanobacterial cell, such as AP. Each organelle has a specific function in the cell and can be a source of bioactive molecules.

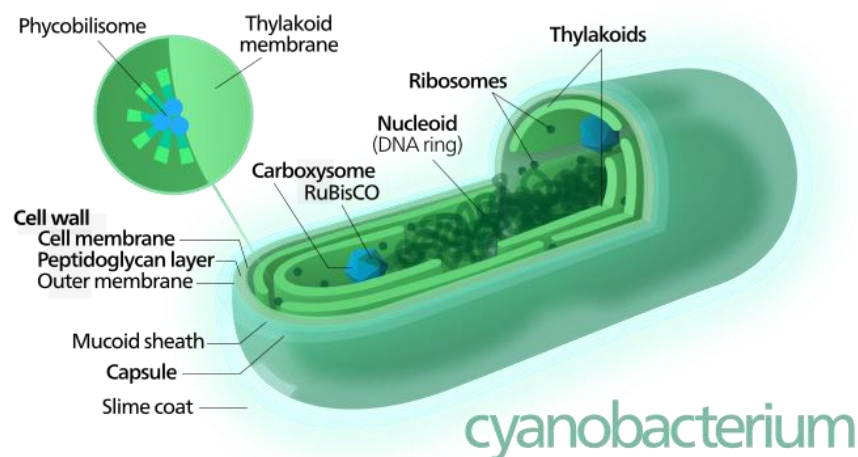


Figure 4 Typical cyanobacterium structure reproduced from [15]

1.2.1 Total sugars

AP exhibits a preference for accumulating carbohydrates as its primary storage compounds, prioritizing them over lipids [16]. Between 10-20% of AP dry weight is usually constituted by sugars. However, AP biomass can reach up to 64.3% dry wt of sugars by nutrient starvation techniques [18],[19]. Cyanobacteria utilize sugars for two purposes: as components of the cell and as reserve molecules. Notably to constitute its cell wall, providing structural support in the composition of intracellular components. Regarding its role as a reserve molecule, cyanobacteria store glycogen, a multibranched polysaccharide of glucose, that serves as an energy reserve. Glycogen can be considered as a high-value molecule, that can be applied in the pharmaceutical industry as a drug carrier [18] [19], in the cosmetic industry as a moisturizer and antiaging agent, and in the food industry as an additive agent to enhance the food

texture[20][21]. AP demonstrated to be a promising feedstock of sugars for bioethanol production in a biorefinery approach [16]. Its biomass lacks lignin, hemicellulose, and cellulose, this eases the access to the cell's metabolites and decreases the energetic cost of AP biomass pretreatment [22].

1.2.2 Lipids

AP biomass is an interesting source of lipids having important bioactive effects [23]. AP biomass contains between 5 and 15%_{wt} of total lipids [24]. According to Ramadan [23], AP biomass contains about 45% neutral lipids, 39% glycolipids, and 16% phospholipids with all values given as percentages of total lipids. In AP biomass, PUFA can constitute up to 21% of the total lipids [25]. The lipids found in AP biomass are classified as neutral lipids, like triacylglycerols (TAG), which play an important role in cell energy storage [26] and phosphoglycolipids. Phospholipids and glycolipids are polar lipids, that form part of the cell-membranes, maintaining the communication of the membrane with the external environment, acting as transporters [27]. Lipids with a polar nature incorporate oxygen and functional groups, facilitating interactions with water. In contrast, nonpolar or neutral lipids are hydrocarbon-based compounds with minimal oxygen and no charges, resulting in limited interaction with water.

The lipids in cyanobacterial biomass are rich in polyunsaturated fatty acids (PUFA), like γ -linoleic acid and α -linolenic 18:3n3 acids and their C₂₀ derivatives, eicosatetraenoic acids 20:4n3 and arachidonic acids 20:4n6 [23] [28]. As the human metabolism is incapable of synthesizing PUFA, obtaining these molecules from sustainable sources such as microalgae and cyanobacteria has the potential to enhance future food and feed production [29] [30].

Numerous studies, including those conducted by Zhou, 2016 [31] and Jun Li, 2020 [25], have established the proven effects of linoleic, γ -linoleic, and α -linolenic acids on human health. Notably, these studies, such as the one by Zhou, demonstrate the positive impact of linoleic acid in reducing the risk of breast cancer. In the same line, the investigation of Farvid *et al.*, 2014 [32] claimed that the dietary intake of linoleic acid reduces by 15% the risk of coronary heart disease. Globally, the intake of polyunsaturated fatty acids may offer favorable effects in resolving inflammatory processes like cellular inflammation linked to various diseases such as obesity, diabetes, and cancer.

Chapter I : State of the art

1.2.3 Proteins

AP biomass is abundant in proteins and essential amino acids, serving as an alternative protein source with protein content comparable to that of meat and soybeans [33]. Its protein content can reach up to 70% dry weight when cultivated in optimal conditions. The study published by Volkmann *et al.* in 2008 [34] shows that the amino acid concentrations, except lysine and tryptophan found on AP biomass cultivated under controlled conditions were superior to the amino acid concentrations recommended by the Food and Agriculture Organization of the United Nations (FAO). For example, FAO recommends consuming 600 mg/day of lysine, while AP dry biomass contains 22.62 mg of lysine per gram. A quantity of 26 520 mg of AP dry biomass satisfies then the daily recommended dose of lysine for one healthy adult.

The most relevant proteins for food applications found on AP biomass are the PBP, which are fluorescent pigmented proteins namely, phycoerythrin (PE), which is cyan color, allophycoerythrin (APE), which is purple-blue color and phycoerythrin (PE), which is fuchsia [35]. These proteins are located in the phycobilisome (Figure 5), which is a light-harvesting antenna developed by all the cyanobacteria [36]. The phycobilisome absorbs energy and transfers it to the Chls in photosystem 2 (PSII) reaction centers. The PBP comprise around 20% of cellular proteins quantitatively and are the majoritarian pigments in AP biomass [37].

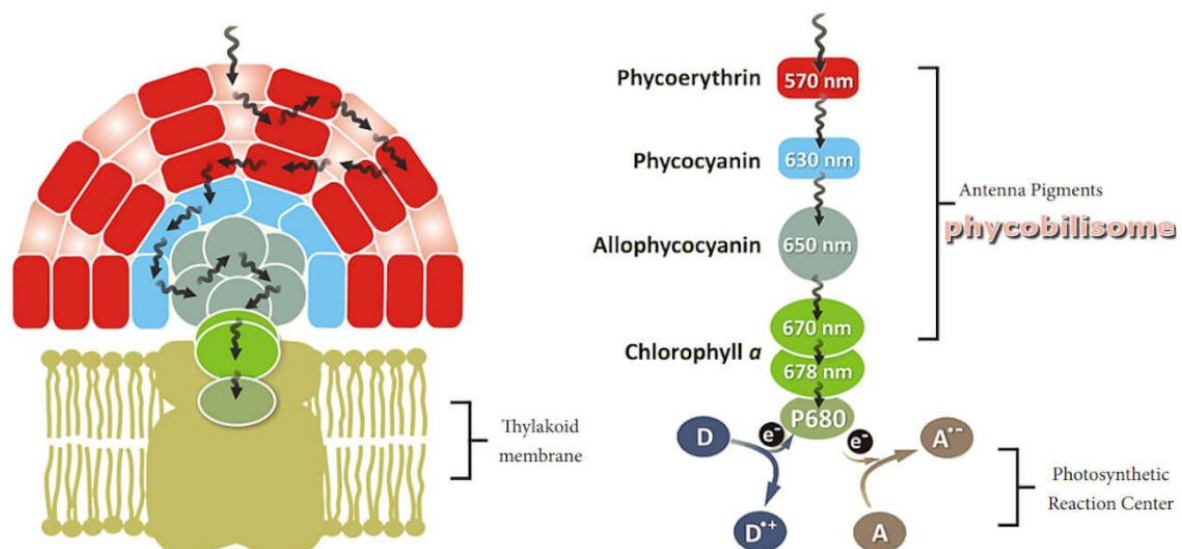


Figure 5 Phycobilisome over thylakoid schematic representation for general cyanobacteria [38]

The role of the PBP is to enhance the photosynthesis light caption, by capturing energy between 450-650 nm [39]. The main physiological function of the PBP is to absorb energy in the light wavelengths where the Chl has poor absorption, between 500 and 650 nm, a gap zone

commonly named “the green gap”[39] (Figure 6). The PBP are located on the surface of the thylakoid membranes and may comprise between 40-60% of the total soluble proteins [40].

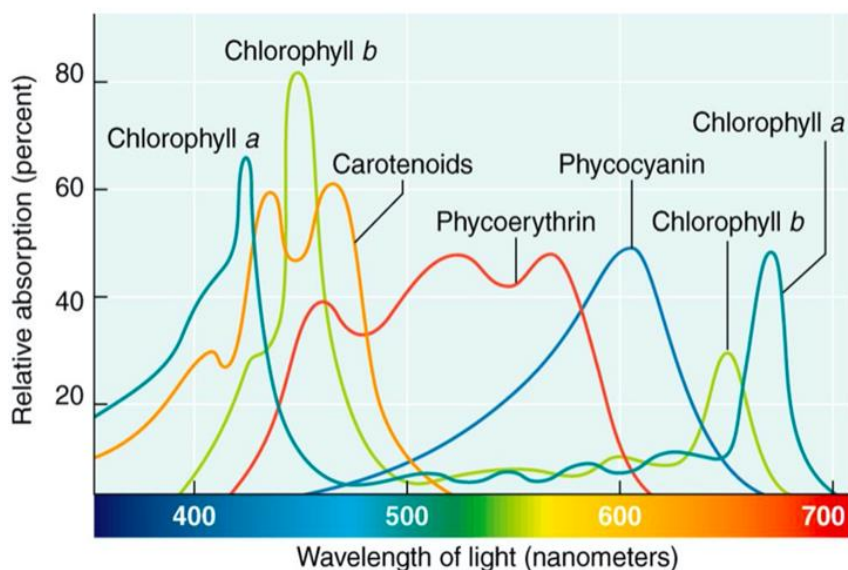


Figure 6 Phycobiliprotein and Chlorophyll Absorption spectra [41]

1.2.4 Phycocyanin (PC)

This PBP is present in cyanobacteria and red algae. PC is known to be the main bioactive compound present in AP biomass, it is a water-soluble blue-red fluorescent pigment, absorbing around 630-650 nm (orange-red absorbing). PC can be classified as a function of its spectrophotometric absorbance; C-PC (C-Phycocyanin) and R-PC (R-Phycocyanin). C-PC is present in most of the cyanobacteria, its absorption spectrum shows a single maximal absorption at 620 nm (Figure 6). Meanwhile, R-PC is present only in red algae, this type of PC shows two absorption maxima, one at 555 nm and the other at 619 nm [39]. PC pigment has proved to have important biological activities, like antioxidant, anti-inflammatory, antimetabolic, anticancer, and anti-neurodegenerative activities [42]. This pigment shows food, cosmetic, nutraceutical, and medical applications.

1.2.5 Allophycocyanin

This molecule is found in cyanobacteria and red algae, it absorbs light between 650-662 nm and has a maximum absorption at 650 nm in red spectrum [43] (Figure 7). Due to its fluorescence, it is applied in cytometry assays [44]. This pigment finds especially application in immunoassays and flow cytometry [45].

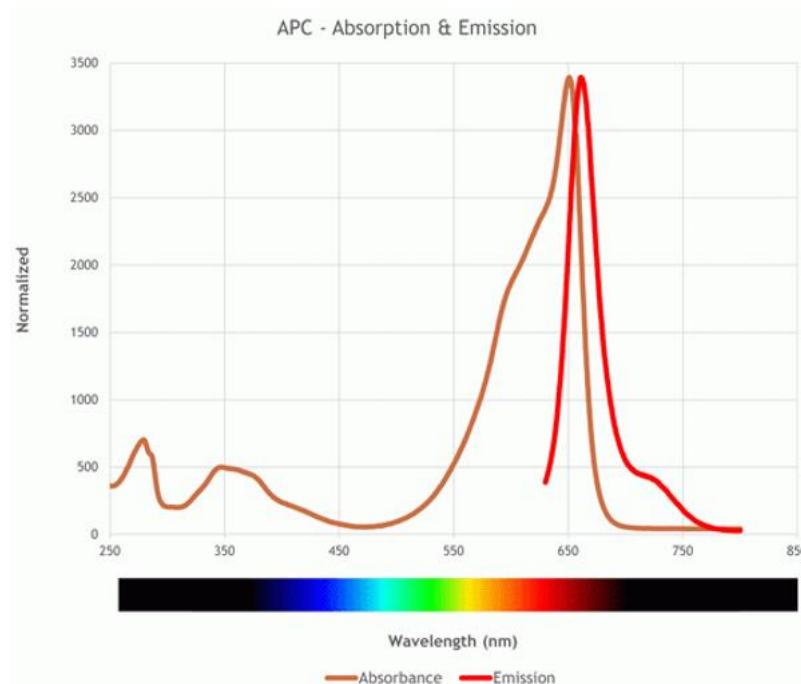


Figure 7 Allophycocyanin maximum absorption and emission wavelengths, reproduced from [46]

1.2.6 Phycoerythrin

The PE is a red-colored pigment that presents a maximum absorption at 576 nm (green absorbing). This PBP phycobiliprotein has proven to have an anticancer and anti-neurodegenerative effect [47]. It also finds applications as a fluorescent marker, labeling antibodies, most often for flow cytometry. It emits light at a maximum wavelength of 573 nm.

1.2.7 Chlorophylls

Chlorophyll (Chl) is the main photosynthetic pigment, it is associated with multiprotein complexes known as reaction centers of photosystems [39]. More specifically in the thylakoid membrane, in the Chloroplasts. Its primary role is to absorb light and converts it into energy to accomplish photosynthesis. Chl absorbs energy close to violet-blue and orange-red light wavelengths, and it is a poor absorber of green and near-green portions of the spectrum. There are six different types of Chl, but the main ones are Chl a and b. All photosynthetic organisms contain Chl a, since they all derived from a common ancestor, however, not all of the photosynthetic organisms contain Chl b. Chl is a molecular structure consisting of a Chlorin ring, where four nitrogen atoms surround a central magnesium atom, and has several other attached side chains and a hydrocarbon tail formed by a phytol ester [48]. AP only contains Chlorophyll a (Chl a) in its biomass. All different Chl types can efficiently absorb light energy between 400 and 500 nm and between 650 and 720 nm. This molecule is employed in the food industry as a colorant, and is also known to have antioxidant and antimutagenic properties [49].

1.2.8 Carotenoids

Carotenoids are a class of natural lipid-soluble pigments that are responsible for the red, yellow, and orange colors found in various plants and microorganisms. These pigments can be found in plants, algae, cyanobacteria, mushrooms, and animals. Notably, lutein and zeaxanthin have been found in human eye tissues [50]. However, they are only synthesized by photosynthetic microorganisms. More than 750 structures of carotenoids have been isolated from natural sources. This family of molecules belongs to the isoprenoids, with forty carbon atoms C_{40} . Two types of carotenoids can be discerned: carotenes and xanthophylls [51]. Both are structural elements of the photosynthetic apparatus. The main difference between both is the presence of oxygen in xanthophylls and its lack in carotene. The greater absorptions are exhibited at 450 and 435 nm for carotene and xanthophylls, respectively [52].

They are primarily used as photosynthesis aids and used in the photoprotection process. Different carotenoids possess different physical, chemical, and functional properties as a function of their structure. Carotenoids possess a range of important and well-documented biological activities. They exhibit several functions in cells, preventing cell damage, reducing oxidative stress, and increasing vitamin A activity. Based on their benefits they have been largely documented and used in the pharmaceutical, nutraceutical, and food industries [53]. The carotenoids found in AP biomass are the β -carotene, zeaxanthin, diatoxanthin, and myxoxanthophyll [54]. Carotenoids are potent antioxidants and free radical scavengers [55] and can modulate the pathogenesis of cancers.

1.2.9 Phenolic compounds

These compounds (PhC) represent the largest group of secondary metabolites in photosynthetic microorganisms, from simple aromatic rings to more complex molecules, comprising, flavonoids, phenolic acids, tannins, lignans, and coumarins (Figure 8). Generally, their primary function is to protect from ultraviolet radiation and harsh conditions. Phenolic acids are the most simple and most important non-flavonoid compounds, they are classified by the length of their chain that contains the carboxylic group [46]. These molecules are known to present bioactive activities, such as the prevention of oxidative damage. The phenolic acids found in AP biomass are gallic acid, hydroxybenzoic acid, Chlorogenic acid, caffeic acid, ferulic acid, and cinnamic acid, representing 0.18-1.98% in dry weight content [6]. They have numerous beneficial health effects due to their antioxidant and chelating capacities. Their antioxidant, anti-inflammatory, and antimicrobial activities have been demonstrated [56] [54]. The flavonoids found in AP biomass are quercetin, genistein, eugenol and galangine 0.05-0.73% in dry weight content [6].

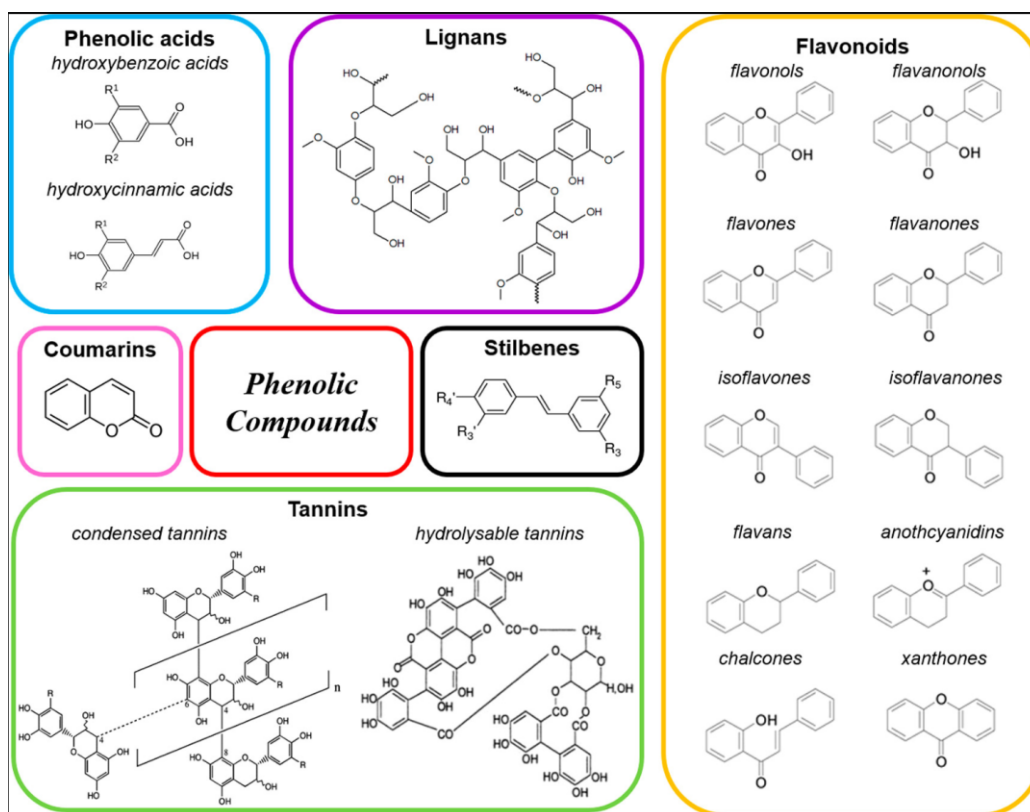


Figure 8 Different classes of phenolic compounds with their backbone structures, reproduced from [57].

1.3 *Arthrospira platensis* culture

1.3.1 Autotrophic culture

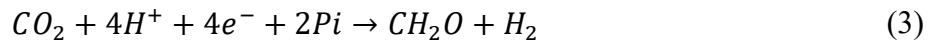
Photosynthesis is the biochemical process that enables photoautotrophic organisms to convert light energy and CO₂ into chemical energy in the form of carbohydrates [58], in the case of microalgae and cyanobacteria, CO₂ must be in the form of dissolved inorganic carbon (DIC), defined as :

$$DIC = [H_2CO_3] + [HCO_3^-] + [CO_3^{2-}] \quad (1)$$

The CO₂ must be completely diluted in the aqueous phase to be available for the cell, and fixed by the carboxylase enzyme RUBISCO [11]. The sunlight energy is used to transport water electrons to NADP⁺, which is a coenzyme that has a reduction effect on the CO₂, converting it into organic carbon. The ATP (energy storage molecule in living cells) and the NADH (coenzyme for electron exchange in photosynthesis) generated during this light-driven process are used for the enzymatic conversion of atmospheric CO₂ into nutrients in the biomass, the reaction is described as:



Dark reactions are also part of the photoautotrophic processes, these reactions include the inorganic carbon assimilation and the photorespiration. Firstly, the CO₂ is assimilated by the ATP and the NADPH₂, as shown in equation (3)



Where,

Molecule	Meaning	Role
<i>NADPH₂</i>	Nicotinamide Adenine Dinucleotide Phosphate	Coenzyme
<i>NADPH</i>	Nicotinamide adenine dinucleotide phosphate	Coenzyme
<i>ADP</i>	Adenosine diphosphate	Energetic molecule
<i>ATP</i>	Adenosine triphosphate	Energetic molecule
<i>Pi</i>	Pyruvate	Enzyme
<i>CH₂O</i>	Carbohydrate general formula	

The Nutrients in the media along with carbon substrate play a vital role in developing biomass and secondary metabolites such as lipids and pigments [59]. For phototrophic cultivation, the light intensity not only strongly influences the cell growth of the microorganism, but also changes the levels of light-related molecules in the photosynthetic system [60].

1.3.2 Culture media and nutrient supplementation

In microorganisms that develop mainly in an aqueous phase as AP, the culture medium is responsible for supplying the essential nutrients to the cells, to promote their growth [11]. The elementary composition of microalgae and cyanobacteria cells can provide a hint about the optimal nutrient ratio in the liquid medium. Stumm's formula for microalgae and cyanobacteria is C₁₀₆H₂₆₃O₁₁₀N₁₆P (molar N/P ratio = 7.2:1). The former empirical formula is consistent with the Redfield ratio, which sets an empirical ratio for oceanic biomass as 106:16:1 for C:N:P respectively. However, the average composition of microalgal cells depends on the strain and growth conditions [61]. Globally, the nutrient mass ratio of the AP biomass grown in usual conditions (without any significant abiotic stress) is given below [62] (Table 1).

Chapter I : State of the art

Table 1 Element mass composition (%) of AP [62]

	C	H	O	N	P	S	Total
<i>A. platensis</i>	48.6%	6.35%	29.72%	9.80%	0.75%	0.78%	96%

1.3.2.1 Carbon source

Carbon is the main component of biomass, thus its availability in the culture media is critical to culture growth and product formation. In large-scale cultures, the carbon source is often provided as a salt form such as NaHCO_3 , NaCO_3 , or even CaCO_3 due to its economical viability, compared to compressed CO_2 directly injected into the cultures [63]. However, CO_2 is often used as a pH regulator in small and pilot-scale cultures. It is important to take into account that the addition of carbonated salts leads to an increase in the culture pH and an accumulation of salts in the culture media. According to Pruvost *et al.* [62], the minimum carbon concentration in a culture medium for cyanobacteria is between 360–480 mgC/L.

1.3.2.2 Carbon capture

Cyanobacteria and microalgae are known for effectively sequestering CO_2 through photosynthesis. Previous research indicates that a microalgae culture with a productivity of 12.7 g/m²/day can capture 102.13 t CO_2 /ha/year, surpassing the CO_2 removal capacity of terrestrial plants like forests (4.5 to 40.7 t CO_2 /ha/year) [64]. These findings emphasize the potential significance of using microalgae and cyanobacteria cultivation for CO_2 mitigation. Establishing a microalgae cultivation system aimed at capturing CO_2 from concentrated gas emissions for biomass and high-value molecule (HVM) production could simultaneously lead to carbon credit generation. Notably, the European Emission Trading System (EU ETS) imposes a tax of 78.91 euros per metric ton of CO_2 [65].

However, to permit the microalgae and cyanobacteria to use the CO_2 , it must be dissolved in the aqueous phase to be available for cyanobacteria. The CO_2 solubility in aqueous solutions is a function of the pH, temperature, and ionic strength. It can be theoretically described by Henry's law principle, which states that the concentration of a dissolved gas in a liquid is proportional to its partial pressure [66], see equation (4):

$$[\text{H}_2\text{CO}_3]_{\text{Henry}} = K_H \cdot p_{\text{CO}_2} \quad (4)$$

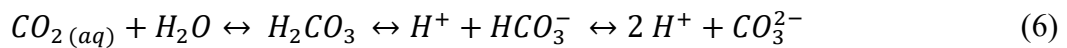
Where:

K_H = Henry's equilibrium constant (mol /atm.L)

$[H_2CO_3]_{Henry}$ = Concentration of CO_2 in aqueous phase (mol/L)

p_{CO_2} = Partial pressure (atm)

The DIC switches from one equilibrium form to another influenced by the pH, ionic strengths, and temperature, as shown in the following equations:



The formed carbon forms depend on the pH and temperature, mainly. Ionic strength can have a slight influence on the promoted equilibria (Figure 9) [67]. In pure water, at a low pH <5 and high temperature, the predominant carbon forms in solution is carbonic acid (H_2CO_3). While at pH [5-8], the promoted form is bicarbonate (HCO_3^-) and at pH >8.5 and low temperatures the predominant speciation of the DIC is carbonate (CO_3^{2-}).

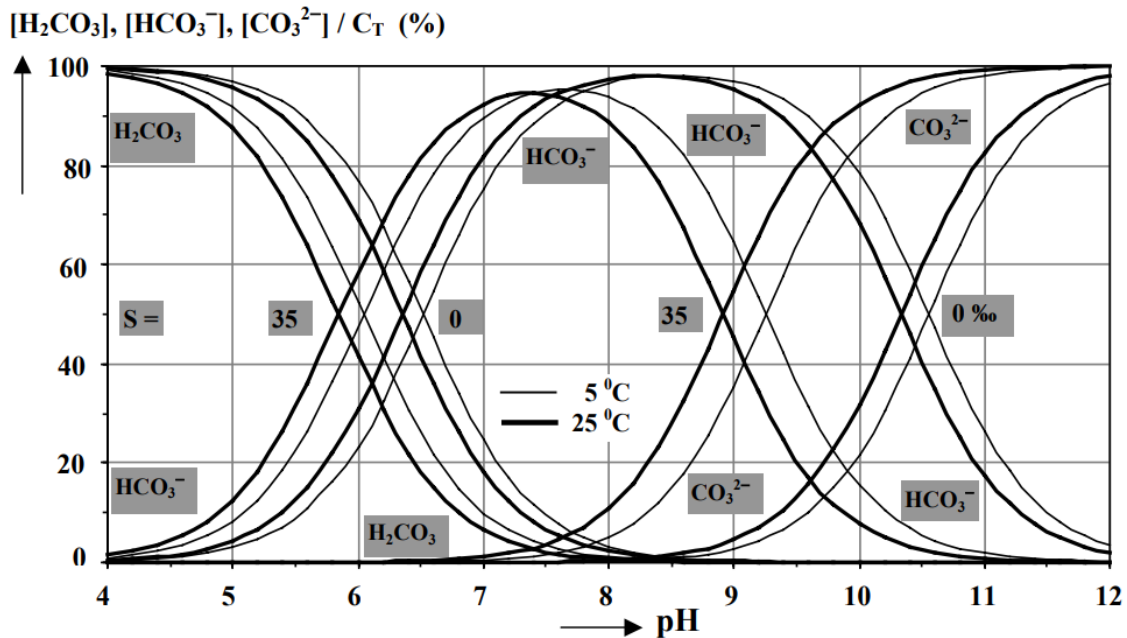


Figure 9 Distribution of the dissolved inorganic carbon species as percentages of the total carbon content, C_T . The values are calculated using Henry's law for temperatures of 5 and 25°C and for salinities of 0 and 35 ‰ as a function of the pH. To illustrate the dependence of the carbon distribution on salinity, reproduced from [68].

Chapter I : State of the art

Inorganic carbon delivery methods depend on the strains and culture conditions of the microorganisms [69]. The cyanobacteria, such as AP, prefer the C_3 -metabolism, followed by the higher plants. This metabolism consists of CO_2 fixation into a compound containing three carbon atoms before entering the Calvin cycle of photosynthesis [11]. Cyanobacteria are unable to incorporate into their metabolism gaseous CO_2 , it must be dissolved into the liquid phase (culture medium). The dissolving phenomenon from gas to liquid phase is often slow in environmental conditions and inorganic concentration in the aqueous phase is kept low. Therefore, the cyanobacteria developed carbon-concentrating mechanisms (CCM) (Figure 10). CCM enables them to grow and accumulate carbon under variable concentrations of inorganic carbon. They use bicarbonate transporters (HCO_3^-) and CO_2 receptors to generate high intercellular concentrations of dissolved inorganic carbon (DIC) and improve intracellular CO_2 concentration to promote carbon utilization efficiency. It is proven that the photosynthetic microorganisms can change their relative affinities for DIC (HCO_3^- and CO_2), depending on the concentration in the external medium, and there are some active accumulation mechanisms that allow CO_2 to be concentrated inside the cell [70] [71].

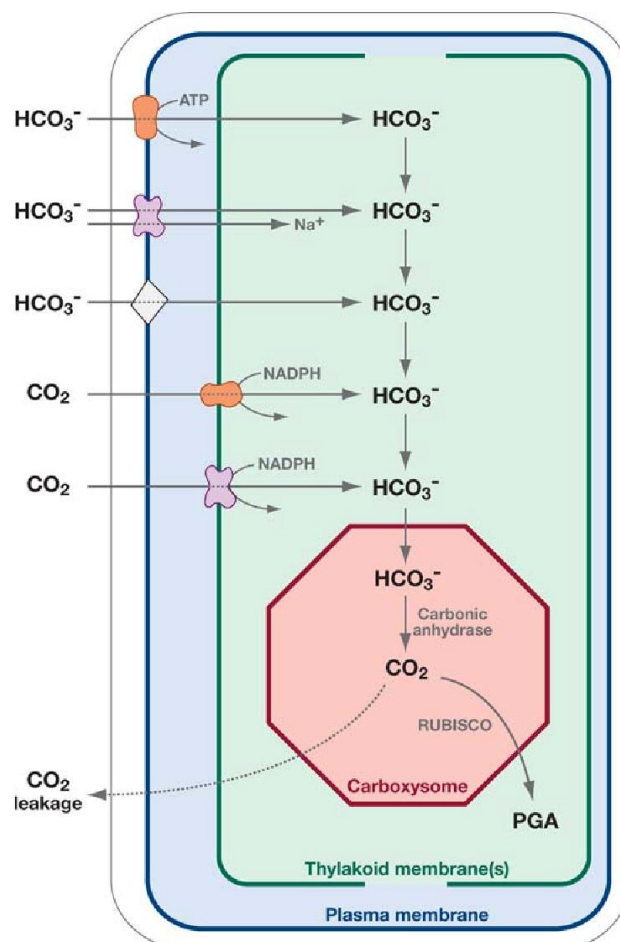


Figure 10 Schematic model for inorganic carbon transport and CO_2 accumulation in the cyanobacterial cell, reproduced from [72].

The carbon form the most available for the CCM cell metabolism is the bicarbonate ion HCO_3^- , which will be metabolized as CO_2 by RUBISCO, after a transformation catalyzed by the carbonic anhydrase (CA) enzyme. CA is the central enzyme in CO_2 fixation. This enzyme enhances the carbon fixation activity of the enzyme RUBISCO. Its primary role is to facilitate the presence of CO_2 molecules for RUBISCO through the reversible conversion of CO_2 into HCO_3^- , as CO_2 escapes easily through the cell membrane, as opposed to bicarbonates. The described mechanism ensures the carbon availability for biomass development.

1.3.2.3 Nitrogen source

Inorganic nitrogen is essential for biomass development, it contributes to the formation of amino acids, proteins, and nucleotides that are at the basis of cells' development [73]. Cyanobacteria can metabolize nitrogen in different forms, notably, as dinitrogen nitrate, ammonium, and urea, these forms are translocated across the cell membrane in the following order: $\text{NH}_4^+ > \text{NO}_3^- > \text{NO}_2^-$ [74]. These oxidized nitrogen forms are subsequently reduced to N and assimilated into amino acids for the formation of proteins. NH_4^+ uptake is the preferred form due to the reduced energy requirement necessary for its reduction and assimilation. Cyanobacteria need energy to reduce NO_3^- and NO_2^- . Although AP can assimilate all these nitrogen sources, the choice of the source has to be taken into consideration, because it might influence the gene expression associated with the metabolism of the nitrogen source. For example, when nitrate is depleted from the medium, an increase of glycogen can be induced in the biomass [75].

1.3.2.4 Phosphorus source

It is an essential element for biomass development. Its role is to store and exchange energy within the cell, forming important molecules, such as Ribulose 1,5-bisphosphate carboxylase/oxygenase (RUBISCO), phospholipids, and adenosine triphosphate (ATP). This element is soluble as its phosphate forms PO_4^{3-} and is typically included in culture media as K_2HPO_4 . The available form of phosphate in an aqueous medium is the orthophosphate (PO_4^{3-} , HPO_4^{2-} , H_2PO_4^-) [76].

Previous studies have reported that to accomplish carbohydrate-rich biomass, it is important to decrease phosphate concentration to the minimum intracellularly, within a range of 1.78-8.9 mg phosphorus/L of medium [77]. The results reported by Zarrouk (1966), regarding the $[\text{P}]_i$ concentrations show that to maintain the *Spirulina* growth for 3 days, an initial concentration of $[\text{P}]_i \sim 10 \text{ mg L}^{-1}$ is enough. After these 3 days, the growth inhibition is observed [5]. An elevated pH can cause phosphates to precipitate by complexation with metal ions such as calcium, magnesium, and iron present in the water.

Chapter I : State of the art

1.3.2.5 Microelement's role

The need for ionic forms of Na, Ca, Fe, Mo, and Mg is weak compared to the ones of C, N, and P [5]. However the activities of these ions in cellular metabolism have been reported, notably, the iron and molybdenum have displayed activity for the nitrogen metabolism [78]. The bioavailability of these metals in the culture medium is crucial for biomass development, and pH, alkalinity, and chelating compound concentrations must be monitored to ensure the solubilization of these ions [79]. Moreover, a regulated presence of these trace metals in the biomass has a positive effect on the consumption of AP for food and nutraceutical industries.

1.3.2.6 Formulated media

AP is a microorganism that has been studied for a long time, hence various media have been employed for its culture, notably, BG-11, Jourdan, Hiri, CFTRI, etc. [80]. The medium has to provide the nutrients listed previously. All culture media formulated for AP contain a carbonate source as NaCO_3 , NaHCO_3 , and CaCO_3 , the sodium bicarbonate provides a medium with high alkalinity and allows maintenance of the pH of the culture [81] [82]. Previous studies have shown that the Zarrouk medium [5] enhances the culture of the microorganism, compared to other media. The composition of the Zarrouk medium is displayed in Table 57 from Annex in p. 225.

1.3.3 Bioreactors for *Arthrospira platensis* culture

This microorganism can be cultivated in open or closed photobioreactors (PBRs). The type of PBR needs to be chosen as a function of different factors: the application of the cultivated biomass, the downstream process, and the scalability of the whole process [83]. Open PBRs allow good scalability of productivity, however, there is a lack of control over the environmental parameters, and the risk of contamination increases, the most common type of open PBR for AP culture is the raceway. On the other hand, the close PBRs enable better control of the process variables and allow an easy optimization of the process. Different types of enclosed PBRs have been established, such as tubular ones, flat panels, columns, and system optimized to grow biofilms. It is known that the increase of the surface/volume ratio of the photobioreactor is a variable enabling culture volume productivity due to the shortening of the light path (Figure 11) [84]. From the process point of view, PBRs can be divided into completely stirred tank reactors (CSTR) for the pond, column, and flat panel type, and as Plug Flow Tubular Reactor (PFTR) for the tubular one [85]. Typically, photobioreactors are operated in batch or semi-batch mode.

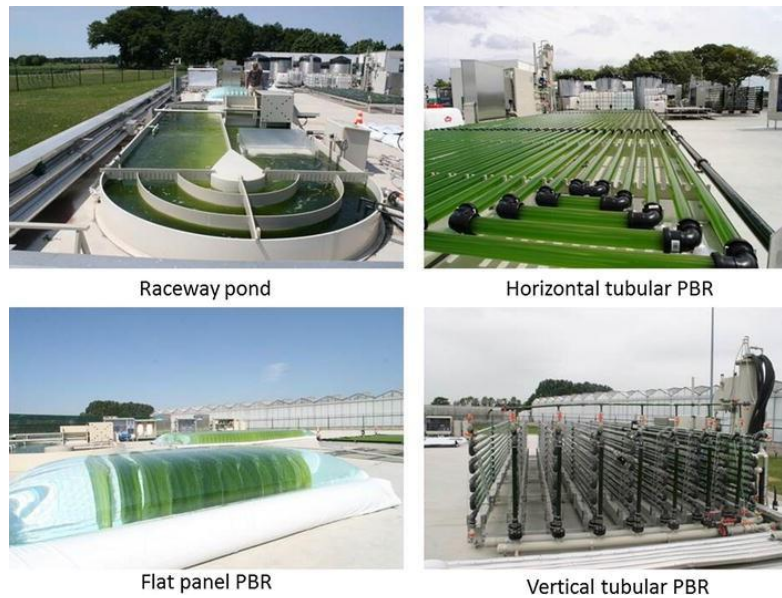


Figure 11 Semi-Pilot PBRs in Wageningen, Netherlands, reproduced from [86]

Ideally, PBRs must have the following devices: an aeration system, which can also serve as mixing device, this element can be a mechanic agitator or a bubbling pipe, and a pH controller element, allowing for the addition of an acid or a base to regulate pH to its optimal level. Light can be supplemented artificially, by a group of LEDs or other kind of lamps, or naturally with the sunlight.

1.3.4 Environmental Parameters Influencing *Arthrospira platensis* Growth

As a photosynthetic microorganism, AP growth in phototropic conditions depends largely on the physicochemical conditions of the process. The following section of the manuscript lists the main conditions affecting biomass development.

1.3.4.1 Light parameter

As microalgae and cyanobacteria are photosynthetic microorganisms, the culture in PBRs is a processes highly impacted by light, which can be provided by manmade sources like incandescent lamps or LEDs or by natural sunlight. Only a fraction of the solar spectra is available for photosynthesis, this range is within 400-700 nm and this fraction is known as photosynthetic active radiation (PAR). Light quality and quantity modification not only affect the culture productivity but also have an impact on the biomass composition of AP affecting mainly pigment concentrations [87]. One of the main challenges of microalgae and cyanobacteria culture is to maintain the cultures in optimal light. Some authors consider the light as the 4th phase of a PBR, the liquid phase is the media, the solid phase is the biomass and the gaseous phase is considered as the third one [88]. Light can be optimized regarding light availability in the PBR, light quality, light intensity, and photoperiod.

Chapter I : State of the art

The light availability optimization can be achieved through 3 strategies: (1) reducing the light transmittance pathway (short depths), (2) increasing culture circulation through mixing to ensure the microalgal cells move within the saturation zone and (3) maximizing the surface to volume ratio to ensure that sufficient light reaches the culture surface [89], and (4) regulating the culture cell density, controlling the cell availability per cell. Items (1) and (3) are related and can be reached one through the other. These strategies affect directly the light penetration.

Three cases can be established to conceptualize the light penetration: γ is defined as the working illuminated fraction (1) The PBR works at a higher light intensity than the one that the cell culture can efficiently convert by photosynthesis ($\gamma > 1$), causing light energy loss and potentially also cell damage, (2) the PBR works at lower light energy than the one that cell culture needs ($\gamma < 1$), so the PBR will have an excess of dark zones, with low photosynthesis efficiency and high respiration zones, with biomass consumption and (3) where the light flux is optimally harvested by the photosystems ($\gamma = 1$), having an efficient energy conversion [85]. Figure 12 shows schematically the concept of light availability for photosynthesis in a PBR.

To define γ , it is important to know the radiative properties of the microorganism, or to establish them empirically by varying the residence time in the PBR, finding the optimal biomass concentration enabling a $\gamma \sim 1$ [85].

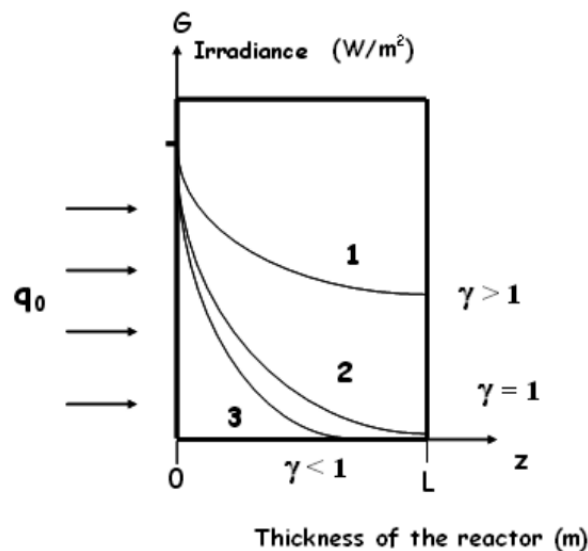


Figure 12 Definition of the working illuminated fraction in a plane PBR (γ). Where G represents the irradiance profiles; q_0 represents the incident hemispherical light flux, reproduced from [85]

The light quality refers to the light wavelength of the light provided to the cell culture. Previous studies suggest that the modification of the light spectrum enables the direction of the microorganism metabolisms to produce a certain type of metabolite, such as the pigments [90]

[91] [92]. The study of Kilimtzidi *et al.*, 2019 [93], states that the application of red light to the cultures promotes the accumulation of phycobiliproteins under different light intensities. Moreover, the study by Markou, 2014 [94], shows that the higher culture productivities of AP are obtained with red and pink light, while the blue one provokes a decrease in biomass productivity. These studies show light wavelength that could potentially be used as a tool for modifying the metabolic paths of AP. However, the application of this technique increases the energetic cost of production and limits it to high-value molecule applications [90].

Light intensity plays an important role in the cyanobacteria and microalgae culture, and has especially to be controlled as a function of the culture density and PBR depth [95]. As for the light quality, light intensity plays a role in the metabolism of the microorganism, changing its biomass composition [90]. The study by Olaizola and Duerr, 1990 [87] reveals that the maximum total carotenoid productivity was increased at a light intensity of 432 $\mu\text{mol}/\text{m}^2/\text{s}$, while photoinhibition was observed at a light intensity superior to 1500 $\mu\text{mol}/\text{m}^2/\text{s}$ under white light. Moreover, a recent study by Yang *et al.*, 2022, confirmed that the pigment content in AP biomass was decreased under high-intensity light, around 1700 $\mu\text{mol}/\text{m}^2/\text{s}$. According to Xie *et al.*, 2015 [60], the higher phycocyanin concentrations in AP were obtained when applying a light intensity of 300 $\mu\text{mol}/\text{m}^2/\text{s}$ with an initial biomass of 0.24 g/L in a 1 L PBR (15.5 cm in length and 9.5 cm in diameter).

Concerning the photoperiod impact on AP biomass productivity and composition, very little information is available. However, the study by Buso *et al.*, 2021 [96] of AP biomass, states that a photoperiod of 8h of light and 16 hours of darkness and a light intensity of 160 $\mu\text{mol}/\text{m}^2/\text{s}$ enhance pigment and biomass productivity. This experiment was made in 25 L cylindrical PBRs under photoautotrophic conditions with Zarrouk medium at 28°C, illuminated by LED lamps.

1.3.4.2 pH Medium

The control of this parameter is crucial for ensuring biomass development, as it regulates the nutrient chemical dissociation and cell physiology [97]. As mentioned before, cyanobacteria can easily metabolize HCO_3^- , which is the predominant inorganic carbon compound at pH between 8.5 and 9 in pure water. It is important to take into account the salinity of the medium to have an idea of the pH that will favor the apparition of bicarbonate ions [98]. Previous studies [99] [100] [101] have demonstrated that the best pH range for AP culture is around 8.5-9.5.

It is important to note that the pH increases during the cultivation process due to the release of OH^- ions during the NO_3^- metabolism [102]. However, when the nitrogen source is provided by ammonia its assimilation releases a H^+ proton, decreasing the pH medium. At the optimal pH, AP utilizes NH_4^+ rather than NO_3^- since the presence of NH_4^+ represses nitrate utilization.

Chapter I : State of the art

Furthermore, the NH_4^+ does not require nitrate reductase and its consumption results in energy saving compared with nitrate [71] [103].

Typically, this parameter is followed by a pH meter sensor, and can be regulated to a certain extent by injecting CO_2 or carbonated salts to the culture when the pH is not optimal for the culture development.

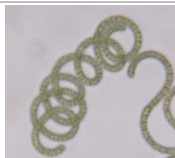
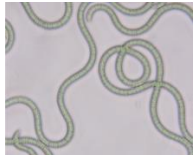
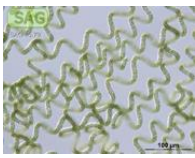


1.3.4.3 Temperature

After the light availability, this parameter is one of the most important parameters to track on microalgae and cyanobacteria culture [88]. It also affects cell metabolism nutrient availability and element speciation in the medium. As AP comes from countries of the globe with high temperatures and radiation, the microorganism can develop at a maximum temperature of 40°C and a minimum of 20°C . Previous studies [104] [105] [106] agree that 35°C is the optimal temperature for AP culture and pigment productivity optimization.

1.3.5 *Arthrospira platensis* strains

The AP strain choice can be a determinant step in the feasibility of the whole process to obtain the desired products. As this microorganism is quite well studied, there are many varieties of it, the most known are cited in Table 2. As can be observed, the trichome pattern varies from one species to another; however, it should be considered that the environmental conditions of the culture have an important influence on the trichome shape. Moreover, *Spirulina* is different from *Arthrospira* [107]. However, *Spirulina* is the commercial name for AP. One of the most prominent morphological features of the genus *Arthrospira* is the spiral coiling of multicellular trichomes [108].

Table 2 Different *Arthrospira platensis* strains

Variety name	Origin	Photography (Objective 40X)
NIES-46.	NIES Microbial Culture Collection isolated at Texcoco Lake, Mexico.	
SAG 21.99	Culture Collection of Algae at the University of Göttingen, Germany (SAG), isolated in Namibia.	
SAG 85.79	Culture Collection of Algae at the University of Göttingen, Germany (SAG), isolated in Chad.	
UTEX 3086	University of Texas at Austin, isolated at Chad.	
Paracas	Strain no. 14067 from Limnologic, Rennes, France Isolated in Peru	

Chapter I : State of the art

1.4 *Arthrospira platensis* culture monitoring parameters

As reviewed during this chapter, the culture of AP implies the balance of a variety of physicochemical factors. To ensure the proper development of the culture, it is advisable to follow continuously the parameters cited in Table 3. These parameters can be easily followed by sensors and simple samplings during the culture. To fully optimize the culture, other important factors such as the photoperiods, initial biomass characteristics, and light wavelength can be taken into account.

Table 3 Primary parameters to run an *Arthrospira platensis* culture

Parameter	Range	Source
Temperature	33-37°C	[104]
pH	8.5-9.5	[99]
Light intensity	<1700 $\mu\text{mol}/\text{m}^2/\text{s}$	[60]
Carbon source	>360 $\text{mg}_\text{C}/\text{L}$	[62]
Nitrogen source	>1.1 $\text{mg}_\text{N}/\text{L}$	[109]
Phosphorus source	>0.8 $\text{mg}_\text{P}/\text{L}$	[77]

1.5 Downstream processing of *Arthrospira platensis* for pigment industrial applications

Once the culture quality has been ensured, the biomass can be harvested and processed. As AP is a source of numerous high-value molecules, it is essential to optimize the downstream processing as much as possible to avoid the degradation of the biomass. Downstream processing is the key step to maintaining the quality of the products [110]. For that reason, this part of the document aims to give an overview of the downstream processing for the biomolecules and pigment production.

1.5.1 Harvest methods

This process involves separating the biomass from the liquid medium. At a large scale, this operation is energy-intensive and typically constitutes 20-30% of the total production costs for microalgae and cyanobacteria biomass [111]. Biomass is concentrated between 5-25% w/v [112]. It is often necessary to do this operation under a multistep scheme to warrant the optimal water content for the following process operations. Many processes can be employed to separate the biomass from the medium. The selection of the harvesting method has to be done as a function of the biomass purpose. The harvesting methods can be classified according to the action principle generating the separation; the upcoming paragraphs will discuss the most commonly utilized methods in AP processing (Figure 13).

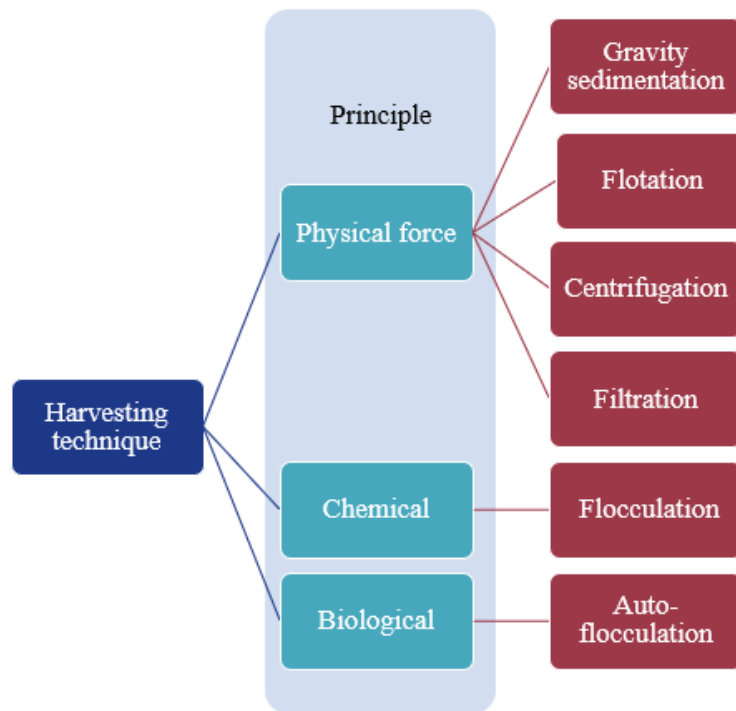


Figure 13 Classification of the harvesting methods as a function of their action principle

1.5.1.1 Physical harvesting methods

1.5.1.1.1 Gravity sedimentation

This technique is one of the cheapest ones for solid-liquid separation, it is frequently enhanced by the addition of flocculants. It is a method based on a physical principle that takes advantage of the gravity. This technique results in the formation of two distinct phases: a liquid phase at the top and a solid phase at the bottom, owing to its typically higher density. Right after the separation, the higher-density phase can be easily recovered using a decanter. As AP is a large microorganism this technique is suitable for its separation, however, in terms of time this technique is not well suited for continuous processes or high-temperature conditions, because of the risk of degradation of the biomass. Depending on the growth conditions, the biomass can sometimes float, therefore leading to different harvesting strategy. Nonetheless, this technique can be complemented with other methods, such as sun drying or filtration [113].

1.5.1.1.2 Centrifugation

This is one of the most robust techniques for biomass harvesting, commonly used during the research and development stages [113]. This technique has important advantages compared to the others, notably the fact that it requires no addition of reagents and reduces biomass volume by around 30% w/v, recovering between 80-90% of the biomass in a short time. However, the energy consumption of this unit operation is considerable compared to the other techniques, and its application at a large scale is economically unfeasible. Nonetheless, its

Chapter I : State of the art

utilization can be interesting when the produced target molecules are considered as high value. As mentioned, the principle of this method is purely physical, depending on the centrifugal force that accelerates the separation of particles as a function of the difference in density between the particle and the medium surrounding it. The denser particles will be pushed outwards, while the less dense ones will be pushed inwards. It is very important to adapt the rotational speed to the biomass conditions, to keep the integrity of the cells and avoid cell disruption [114].

1.5.1.1.3 Filtration

The principle of filtration relies on the retention of the biomass by a semi-permeable physical barrier that allows the suspending fluid to pass through [112]. This method is one of the most applied to AP culture in semi-industrial scale cultures, taking advantage of the AP filament size to ease the separation [11]. The product of the filtration operation is known as retentate, for the biomass, and permeate for the medium that passes through. Various kinds of filtration can be applied to harvest the biomass, notably, magnetic filtration, vacuum filtration, pressure filtration, and cross-flow (or tangential flow), the chosen process has to be adapted to the biomass characteristics and target product [113]. When dealing with AP, it is crucial to consider the quick occurrence of fouling due to the cells' considerable size. This amplifies resistance to fluid flow as the pressure differential across the “cake” intensifies. Moreover, the presence of EPS in the medium can accelerate membrane fouling [115].

1.5.1.1.4 Flotation

Flotation consists of the attachment of small air bubbles to destabilize cells, provoking the rise and concentration of the biomass to the surface of the reservoir where the separation occurs. This separation technique is often combined with flocculation, it is one of the most economical harvesting techniques [116]. According to previous studies [117], the separation efficiency obtained by the application of this technique is better than the one obtained by sedimentation. It can be a quite interesting harvesting technique when the microorganism has a tendency to float spontaneously, which is the case of some AP strains. Moreover, reports on the economic feasibility of this technique show that it can easily be adapted to low operating costs, decreasing the energy inputs of the process [116].

1.5.1.2 Chemical harvesting methods

1.5.1.2.1 Flocculation

This technique is based on a physicochemical principle of surface charge modification. It is necessary to add a flocculent to the culture that can be considered as a suspension, composed by the microorganisms and the culture medium [111]. The principle of this technique is based

on the action of the flocculent that has a destabilizing effect on the biomass ionic charges as illustrated in Figure 14. The flocculent favors the formation of larger aggregates by changing the charge on the cell surface and media; the produced aggregates have larger density and thus increase separation efficiency. This technique is often combined with gravity sedimentation to maximize the efficiency of the process. The technique is influenced by cell concentration, pH of the environment, medium ionic strength, type of mixing, and type and dosage of flocculent. The choice of the right flocculent and its dose are essential to avoid the modifications of the nutritional values and organoleptic properties of the biomass.

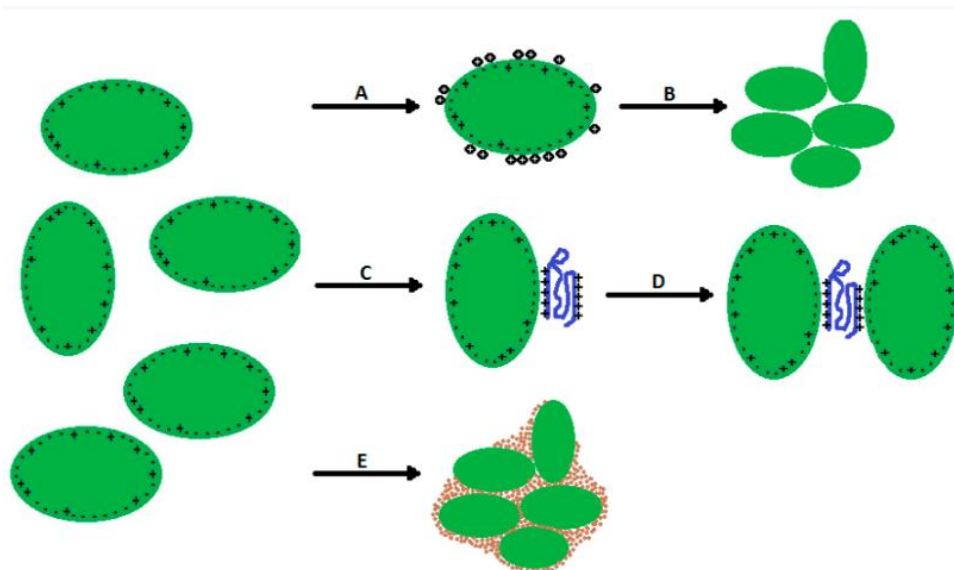


Figure 14 Basic flocculation mechanisms: A—canceling the negative surface charge of microalgae by ion, polymer, or colloidal absorption; B—interaction of surface neutral microalgal cells based on the thermodynamic balance of interaction energies; C—charged polymer, reproduced from [118].

The most common flocculating agents include cationic polymers and biopolymers like polyacrylamide and chitosan, which interact with cell surfaces, inducing flocculation through charge neutralization and bridging. Additionally, metallic salts such as aluminum and ferric Chloride can also cause flocculation by charge neutralization mediated by metal ions. The efficiency of the flocculants depends largely on the cell surface properties, type of media, and presence of exopolysaccharides in the media. The presence of the last ones can negatively influence the separation efficiency, increasing the dose needed for an efficient separation.

1.5.1.3 Biological harvesting methods

1.5.1.3.1 Auto-flocculation

As the name suggests, this technique consists of the spontaneous flocculation of the cells. This flocculation is caused by the presence of specific metabolites produced by the cells, such as exopolysaccharides (EPS), that modify the global charge of the media. The work principle

Chapter I : State of the art

of this technique is quite similar to the one described in the previous paragraph, however, the interactions between cell surface and metabolites that provoke auto-flocculation are not yet well understood. The main interest of applying the auto-flocculation approach is avoiding the addition of chemical agents., which is particularly interesting in terms of life cycle analysis (LCA).

1.5.1.4 Harvesting method recap

This section summarizes the previously discussed harvest methods for *Arthrospira platensis* (AP) processing. Adapting the method to the characteristics of the biomass and its intended applications is crucial. Table 4 resumes the most important parameters to take into account when choosing the harvest technique.

Table 4 Harvest methods applicable to *Arthrospira platensis* production

Drying technique	Final solid contents (%)	Recovery rate (%)	Energy usage (kWh/m³)	Advantages	Drawbacks	Source
Gravity sedimentation	20-30	10-50	0	-Low energy consumption	-Slow process -Not adapted for low-density biomass	[112]
Flocculation	>30	50-90	0.15	-Low energy and handling	-Biomass might be contaminated by the flocculent	[119]
Auto-flocculation	>30	50-90	0.1	-Low energy consumption -No chemical agents needed	-Time consuming -EPS presence	[120]
Flotation	>10	70-95	>10	-Good efficiency -Easy handling and operation -Easy to scale-up	-High energy consumption -High shear stress	[117]
Centrifugation	10-22	>90	1.43-2.16	-Suitable for all strains -Time saving	-High energy consumption	[121]
Filtration	10-20	20-87	1.22	-Efficient	-High maintenance	[115]

1.5.2 Biomass drying methods

AP biomass is usually marketed as a dry product to better preserve its component quality and preserve biomass decomposition. As it is known, this operation unit is a key component of the process and one of the most energetically demanding. It accounts for 75% of the energy costs of the downstream processes [122]. It has been reported that the thermal drying of microalgae represents 0.98 kWh/kg of water [123]. This is the reason why efficient drying techniques are needed to develop more sustainable processes for AP production. Maintaining high-quality biomass requires strict avoidance of exposing it to temperatures exceeding 60°C.

Chapter I : State of the art

[124]. The following section will give a detailed description of the drying methods applied to AP processing.

1.5.2.1 Solar drying

This technique is considered the most sustainable one, using sunlight as the heat source. It can be divided into two types, direct and solar heating methods. Despite its cost-effectiveness, direct sun radiation might provoke the degradation of photosynthetic pigments, such as Chl, carotenoids and PBP. The best alternative is the use of solar energy to dry indirectly the biomass (Figure 15). Solar heat can be utilized to directly warm a fluid such as water or air, which can then be circulated through a system to indirectly facilitate biomass moisture evaporation through convection. Various configurations can be implemented for this purpose [125]. This technique is commonly used in semi-industrial AP farms.

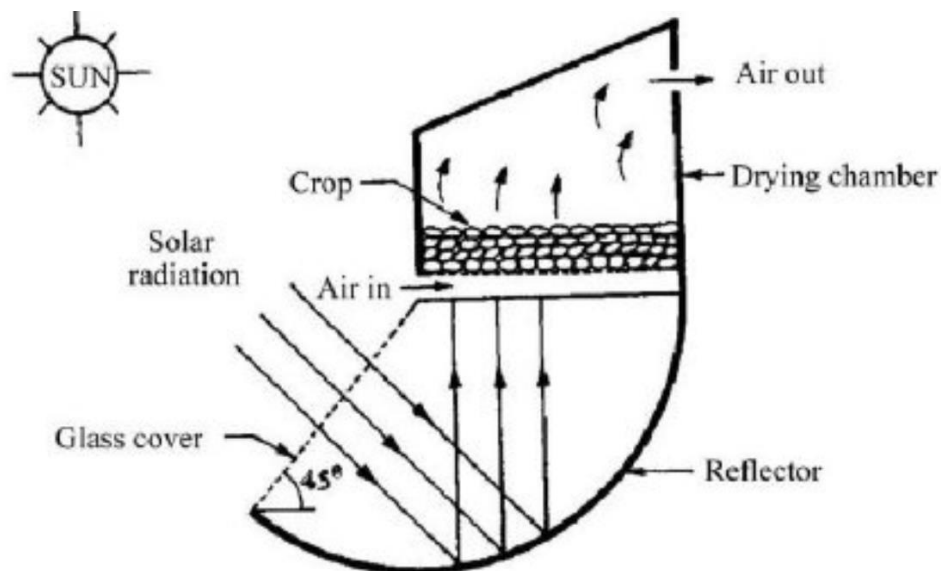


Figure 15 Schematic view of single tray reverse absorber cabinet biomass dryer, reproduced from [126]

1.5.2.2 Convective drying/Air-flow

This technique is one of the most used in AP processing. It consists of spreading the biomass in thin layers in a flat surface chamber, oven, or tunnel-type dryer, to then supply convective hot air to provoke dehydration. This technique is typically applied within a temperature range of 20-60°C, usually during 24 hours. To optimize the technique, the biomass moisture after the harvest, the thickness of the biomass, and the air temperature must be controlled. One of the drawbacks of this technique is that when the thickness of the layer is not well controlled a risk of decomposition of the biomass should be considered.

1.5.2.3 Spray-drying

A biomass feed, in a solution, suspension, or paste form is sprayed into a perpendicular tower and comes in contact with a hot gas steam that triggers the drying. Three principal steps are involved (1) atomization of feed into droplets, (2) contact of the droplets with the hot gas to evaporate the biomass moisture, and (3) dry powder separation from the gas steam, and collection. This technique is known for its high efficiency, easy scale-up, and short-time effectiveness. However, there is a possibility of degradation of the high-value molecules in the biomass because of the combined effect of the pressure (20 bar) and temperatures in the process [127]. Mouahid *et al.*'s study in 2020 [128] indicates that a temperature of 80°C and a biomass exposure time of less than 30 seconds did not result in the degradation of *Nannochloropsis maritima* biomass. Finally, the operating and maintenance costs of this technique are also important, around 0.5 euro/ kg of dry biomass. In terms of energy, this technique consumes around 1.09 kWh/ kg of evaporated water [129].

1.5.2.4 Freeze-drying/lyophilization

In the food industry, freeze-drying is widely applied to preserve high-quality products, such as microalgae and cyanobacteria biomass. Globally, it consists of the water removal from a completely frozen sample, water passes from the solid to vapor phase without passing through its liquid state. This process is called sublimation. This technique consists of three steps: (1) Pre-freezing the biomass and transportation to the vacuum chamber, (2) Primary drying by water sublimation, and (3) Secondary drying, also called “Water desorption”, during which the last water molecules from the sample are released (Figure 16). To perform this process, the following devices are needed: (a) A collector coil between 15-20°C colder than the freezing point of the sample, to trap the released water vapor, and (b) a vacuum pump, reaching at least 0.02 mbar (2 Pa), and (c) a drying chamber to keep the samples isolated from air moisture. It is very important to make sure that the sample is completely frozen, to avoid sample degradation. The freezing speed of the sample is a parameter to take into account, slow freezing can provoke the formation of large crystals, damaging the cell's wall and degrading the sample. It is known that this technique preserves the bioactive properties of the molecules present in the biomass. Nonetheless, the operating costs, energy inputs, low scalability, and time efficiency of this technology are important drawbacks.

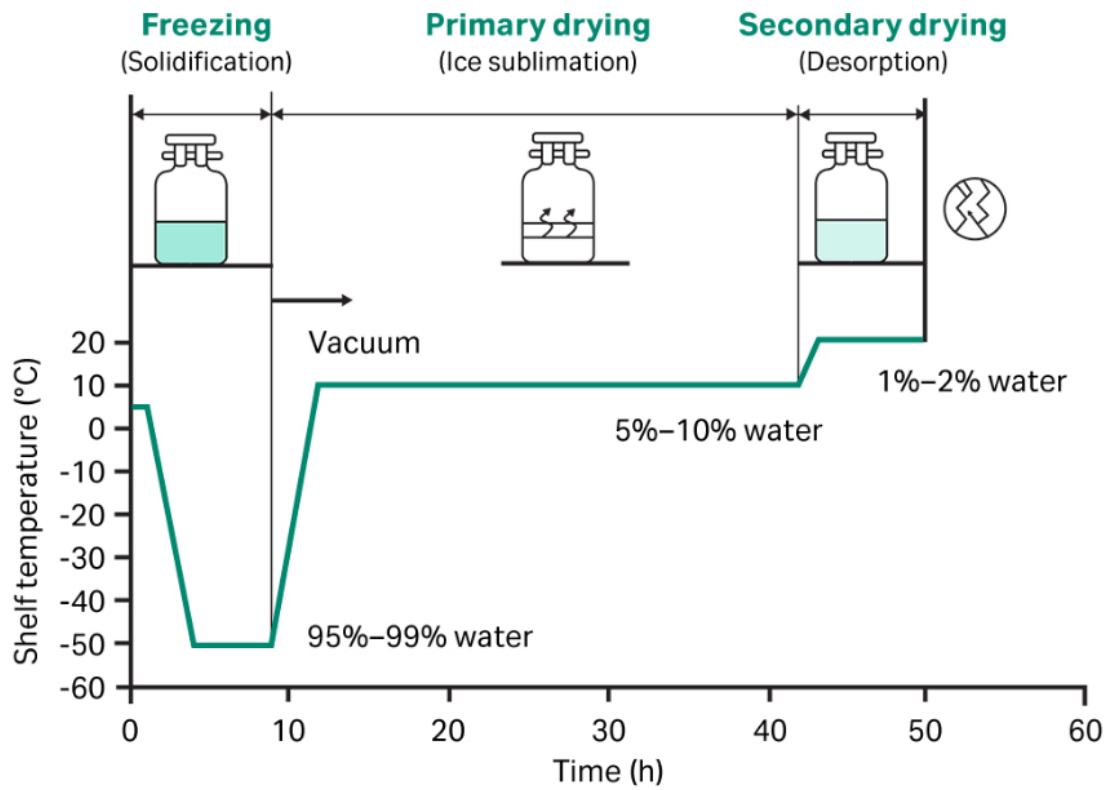


Figure 16 Freeze-drying process stages, reproduced from [130]

1.5.2.5 Drying method recap

The following table shows the general principles of the main drying techniques applied to AP processing:

Table 5 Overview of the drying methods applicable to *Arthrospira platensis* [122]

Drying technique	Principle	Advantages	Drawbacks	Source	kWh/kg water	Source
Solar drying + air-flow	Radiation	-Easy operation	-Time consuming -Biomass degradation	[125]	1.17	[131]
		-Low-cost				
Convective-drying	Convection by hot air	-Easy operation	-Multiple variables to control -Biomass degradation	[132]	0.77	[133]
		-Low-cost				
Spray-drying	Convection High-pressure atomization	-Time saving	-High energy consumption	[129]	1.35	[134]
		-Good scalability				
Freeze-drying	Water sublimation	-High efficiency -Preserves bioactive properties	-High energy consumption -Batch process	[135]	2.3	[136]

1.5.3 Cell-disruption techniques

This unit operation is applicable only when the recovery of a biomolecule is needed. As its name indicates, its main objective is to break the cell wall to ease the release or the extraction of bioactive molecules, such as pigments, proteins, lipids, etc. This operation must not be considered as an isolated process, it affects directly the further characteristics of the biomass. Notably, AP cells lack cellulose, making them particularly susceptible to breakage under mechanical forces. Thus the biomass disruption techniques might be applied as an extraction technique. The cell wall of AP primarily comprises multilayered structures consisting of glucan and peptidoglycan polymers. These polymers create a network of sugars and/or amino acids interconnected by robust covalent bonds [137]. A large number of cell-wall disruption methods have been reported to maximize the extraction efficiency of bioactive molecules (Figure 17). Nonetheless, the cell disruption method has to be adapted to the cell wall characteristics and the target molecule. The efficiency of the cell disruption method is largely affected by the operating conditions, such as the temperature, pressure, pH, cell characteristics [138].

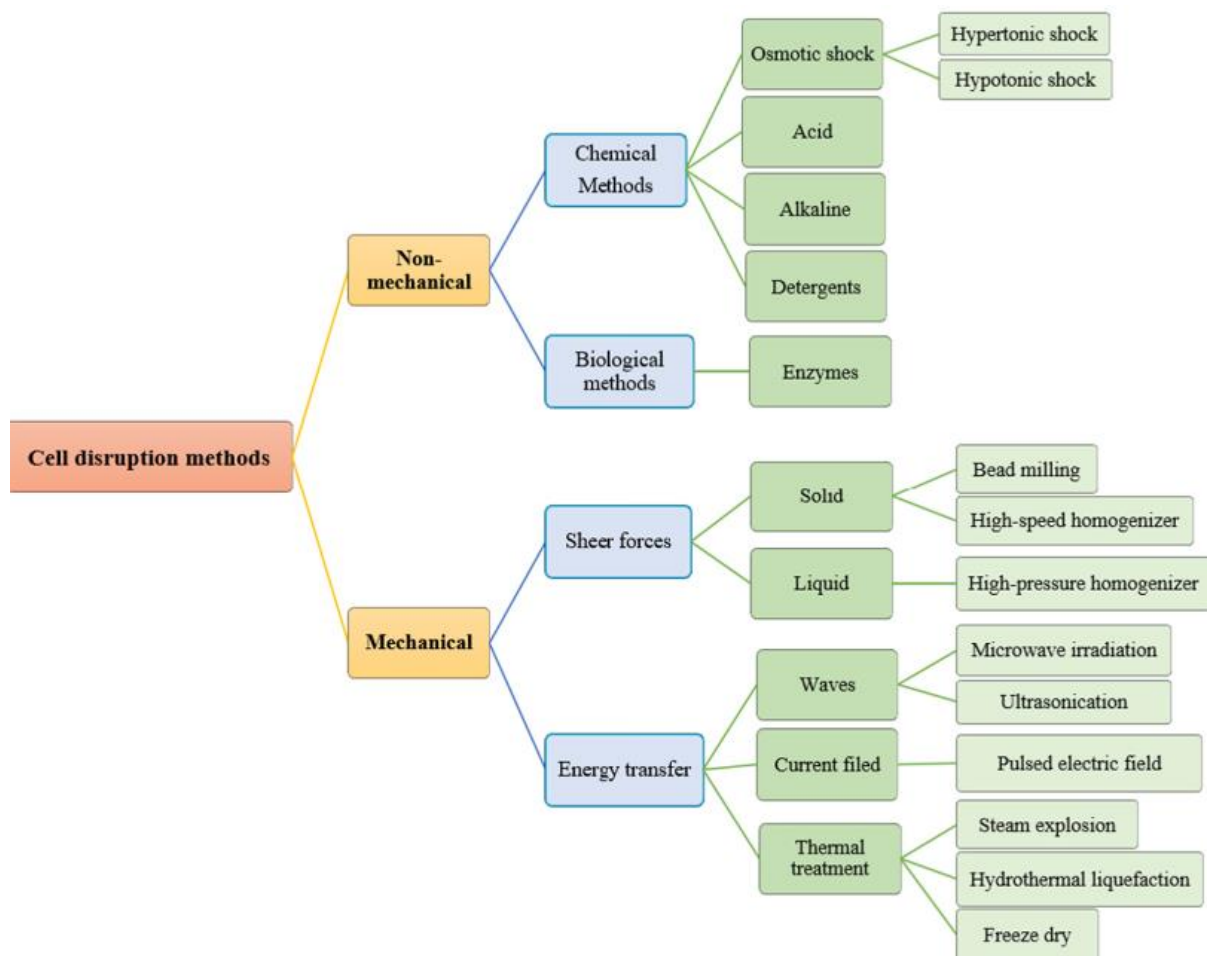


Figure 17 Cell-disruption techniques classification reproduced from [139]

Chapter I : State of the art

1.5.3.1 Mechanical cell-disruption techniques

These techniques are purely based on the application of physical forces, and can be applied to a liquid biomass (in suspension) or a solid biomass (dry biomass). The main asset of this kind of technique is the absence of by-products during the process. While biomass remains uncontaminated by other types of molecules, it's crucial to consider the energy consumption when employing this technique [133]. In the case of AP, it's notable that the cell-disruption technique can serve as an extraction method for membrane pigments, such as PBP.

1.5.3.1.1 Bead milling

The principle of this technique is very simple, it relies on the mechanical forces that the beads apply to the cells to break them down, causing complete cell damage in the case of AP [140]. Beads collide with each other and with the biomass. The bead size and weight affect largely the efficiency of the operation. The increased bead number increases the efficiency of the operation, increasing the number of collisions. The mechanic agitators run at a speed of 1500-2250 rpm. The process variables are agitator speed, proportion of the bead, bead size, suspension concentration (if applicable), and cell suspension flow rate [141].

1.5.3.1.2 Pulsed electric field (PEF)

This technique primarily involves exposing the biomass to a specific electric field for brief periods, typically ranging from seconds to milliseconds. This electric field provokes the cell wall to create temporal pores or ruptures, this technique enables ease of access to intracellular biomolecules such as lipids and carbohydrates [142]. Recent research has proved that this technique also enables access to biomolecules in the cell wall as pigments. This technique has been applied to the extraction of PC in AP biomass. The study by Käferböck *et al.*, 2020 [143], shows that the PEF application enhances PC extraction by 90% compared to what is obtained with bead milling and that the application of PEF treatment at lab-scale enabled to obtain higher purity of PC [143].

1.5.3.2 Non-mechanical methods

This kind of method does not apply shear stress forces or energy transfer to the cells but creates and modifies the cell's chemical environment, provoking a rupture of the cell wall. Globally, these methods are less energy intensive; however, the presence of other reagents may modify the cell composition or the biomolecule structure. The biomass has to be in solution to apply any of these methods.

1.5.3.2.1 Osmotic shock

This method relies on the addition of a reactive, such as a salt, an alkali, or polyethylene glycol to reduce the osmotic pressure of the solution. This change in the medium equilibria can lead to damage in the cell wall, provoking the release of the cell content to the medium. A complete cell rupture is not attainable by this technique ; this is positive because the selectivity of the technique is increased [139]. This method is widely applied in the PC extraction from AP biomass, using a phosphate buffer to create the phenomena mentioned above [140].

1.6 Extraction techniques applied to *Arthrospira platensis* valorization

The biorefinery scheme aims to maximize the use of the overall content of AP biomass for various applications. Similar to the petroleum biorefinery, different molecules can be extracted from AP biomass applying the appropriate operation conditions [144]. Notably, by the application of an adapted extraction scheme the integrality of the high-value molecules can be valorized. In a circular economy the carbohydrates that are left as bottom products, can be inserted as carbon sources in a fermentation process or even for energy production processes, such as hydrothermal liquefaction or methane production process. Figure 18 shows clearly the full process to accomplish the biorefinery process in aquatic biomass [145]. It is worth noting that the reduction of operation processes is one of the main goals of the biorefinery scheme.

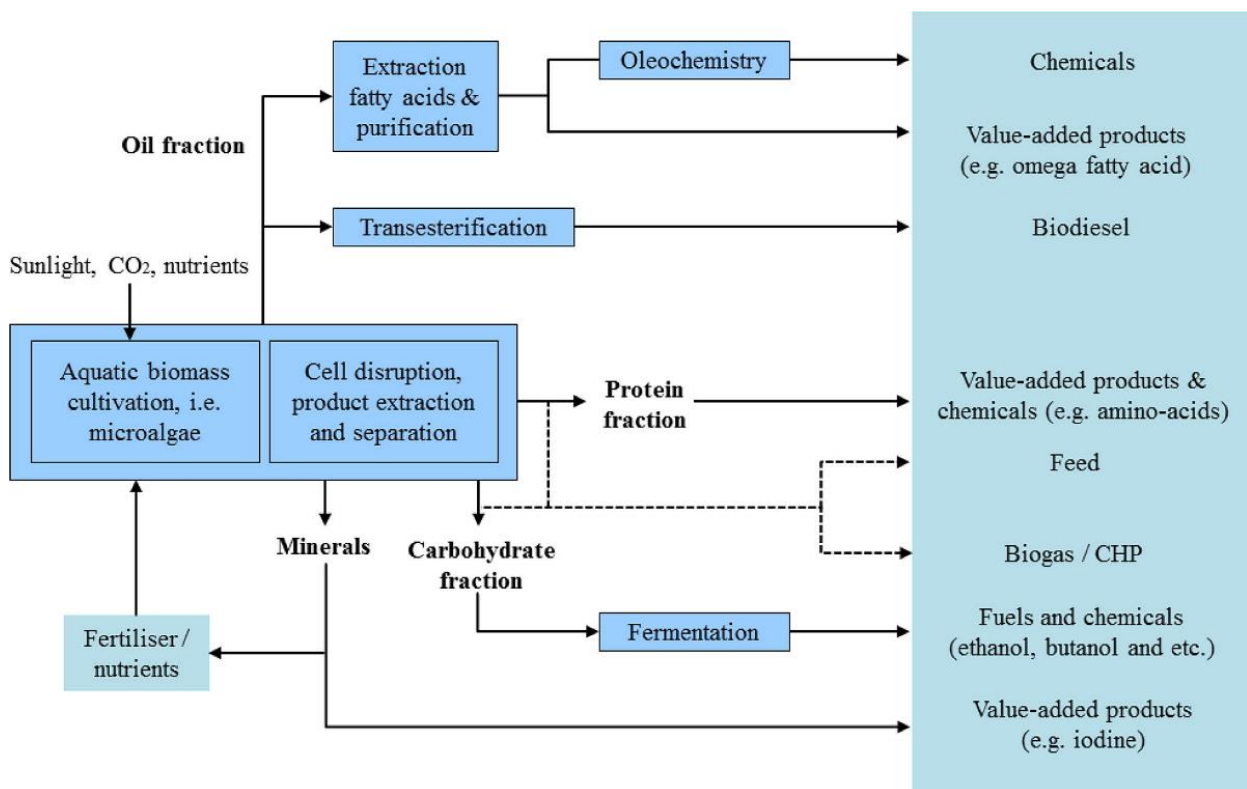


Figure 18 Applied biorefinery concept to aquatic biomass, reproduced from [118]

Chapter I : State of the art

Successive selective extractions are suitable to minimize waste production and valorize the global AP biomass content. To optimize the biorefinery process it is crucial to choose the adapted type of solvent and operation conditions that will enable to perform a selective extraction. The extractable high-value compounds from AP biomass can be classified as (A) polar or hydrophilic fraction, which are the protein-pigments, as the PBP, the non-pigmented proteins, the amino acids, and the carbohydrates, and (B) low-polarity and non-polar, which are the Chl a, carotenoids, and the lipids. Unlike hydrophobic compounds, the compounds classified as polar or hydrophilic are more susceptible to denaturalize, precipitate, or degrade under harsh conditions ($T > 45^{\circ}\text{C}$) [146]. As argued in previous studies, the easiest way to recover each fraction is to adapt the type of solvent to the target molecule, to obtain high-purity products [147]. Many techniques have been explored to optimize the high-value product extraction from aquatic biomass, In the following section of the document, these techniques will be explored.

1.6.1 Organic solvent extractions

These kinds of solvents are well adapted for the extraction of the hydrophobic fraction of the biomass, such as lipids and carotenoids. Various organic solvents and mixtures have been proposed to selectively extract the lipidic fraction of microalgal or cyanobacterial biomass [148]. The Soxhlet technique is the reference method for analytic extraction of lipids from solid materials. It is often taken as reference technique with reliable efficiency for alternative extraction techniques. Soxhlet technique has been modified and enhanced to be scaled up to industrial applications, notably, the microwave-assisted Soxhlet extraction, ultrasound-assisted Soxhlet extraction, and high-pressure Soxhlet extraction [149] are modifications that enhance the extraction efficiency of the whole process. The efficiency will depend on the affinity of the analyte to the solvent, extraction time, and the working temperature. Commonly, n-hexane stands out as the most frequently used solvent, even if it extracts either neutral lipids or polar lipids, which can be a drawback according to the application. Nevertheless, it is a flammable solvent classified as a hazardous substance due to its potential health impact [150]. Earlier research has shown that n-hexane mixture with methanol prove to be effective solvents for extracting lipids from AP biomass [150] [151] [152]. Additionally, other solvents, like blends of chloroform with methanol, demonstrate competitive extraction efficiencies [153]. Nevertheless, it's worth noting that chloroform and methanol display significant levels of toxicity. Other extraction techniques like maceration have displayed good extraction efficiencies coupled with cell disruption methods such as ultrasound, giving a name to ultrasound-assisted extraction (UAE) or microwave-assisted extraction (MAE) to enhance the

extraction [154]. These modifications permit the avoidance of heat use and thus preserve the bioactive properties of the extracted molecules.

1.6.1 Maceration

This technique is one of the simplest extraction methods, and its appeal lies in its low energy demand and versatility. It involves immersing solid plant material in a solvent, such as ethanol, water, oil, etc. The soaking time induces the extraction of the molecules contained in the plant material. The selectivity of the extraction can be regulated by the accurate choice of the solvent type, process temperature, process agitation and residence time of the biomass into the maceration tank. This technique is quite interesting for the extraction of labile compounds because of the minimum exposure of the compound with air. After the extraction is completed, the extract is separated from the solid material by physical means, like filters and sieves. Subsequently, the solid material is pressed, to obtain a maximum of extract. Finally, the extract is concentrated [155]. Maceration is widely applied for the extraction of thermolabile compounds like, the phenolic compounds present in plant material [156] [157] [158]. Notably, this technique is applied industrially to extract PBP from wet AP biomass, employing a pH 6.4 Phosphate buffer at 4°C, for 24h [159] [160]. This technique can be assisted by microwaves or ultrasounds to facilitate the cell wall disruption [161].

1.6.2 Green solvent extractions

To avoid the use of organic solvents, that represent a potential risk to the environment, health, and safety, the use of Generally Recognized As Safe (GRAS) solvents has been recommended [28]. These solvents should not present flammability or toxicity, a high selectivity is preferred to obtain high-purity extracts. Previous studies, such as the one of Pinto *et al.*, 2022 [150], have shown that the use of supercritical CO₂ (scCO₂) displays a higher selectivity for neutral lipid content than other explored techniques. Other viable alternatives for extracting polar and mid-polar molecules from AP biomass include non-toxic solvents like water and ethanol. Ethanol and water are not adapted to extract non-polar molecules. It is crucial to highlight that ethanol is both flammable and irritant. It is a combustible liquid that can be ignited by potential sources of ignition. The utilization of ethanol must adhere to the ATEX European directive [162]. The following paragraphs illustrate the different possibilities in terms of extraction techniques applying green solvents.

1.6.3 Pressurized Liquid Extraction (PLE)

This technique is based on the modification of the properties of solvents like water, by the viscosity decrease and diffusion rate increase. These modifications are reached by the application of elevated temperatures and pressures high enough to keep the solvent in its liquid

Chapter I : State of the art

state during the whole extraction procedure. The temperature and pressure are therefore kept below their critical point (Figure 19). Different liquid solvents and mixtures are then used to extract solutes from a fixed bed solid matrix.

This technique is often referred as Accelerated Solvent Extraction (ASE), when employed at a laboratory scale, in batch mode and most of time for analytical purposes. Pressurized Liquid Extraction (PLE) is generally employed for describing a semi-continuous process, when a continuous flow rate of liquid solvent is used. PLE is easily scalable while ASE is not adapted to a utilization at large-scale.

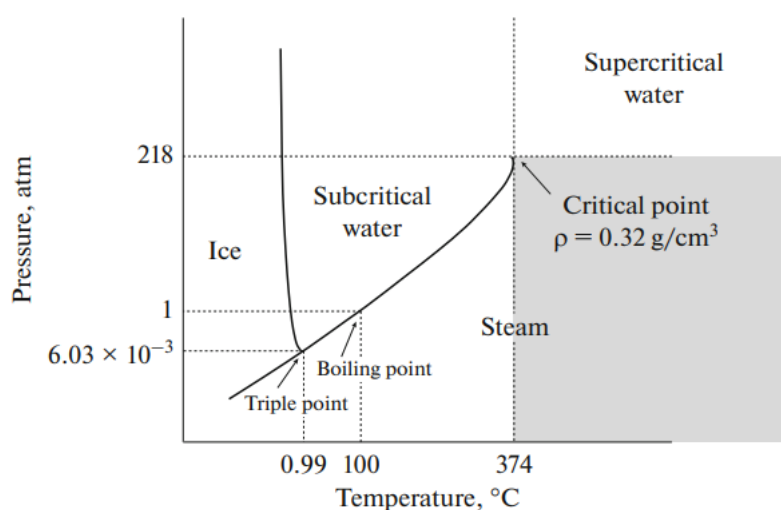


Figure 19 Water phase diagram, reproduced from [172]

For the valorization of AP, PLE can be employed to extract High-Value Molecules (HVM) from the biomass, such as phycobiliproteins (PBP) and carotenoids. These extracted compounds find applications in the food, cosmetic, and nutraceutical industries. Notably, the ethanol-water solution has proved to give interesting results in terms of AP valorization [173] [174]. Under standard room conditions, the water-ethanol solution exhibits polar characteristics. However, modifying the temperature and pressure leads to changes in the dielectric constant of the solvent. More particularly, the dielectric constant decreases significantly when the temperature increases. Consequently, as the temperature increases, the solvent affinity for molecules with lower polarities can be enhanced while increasing the temperature, allowing for the adjustment of the solvent affinity to the analyte through modifications in pressure and temperature [175]. The study published by Herrero *et al.*, 2005 [175] with AP biomass, compared the extraction yields and antioxidant activity obtained by the employ of different solvents, such as ethanol, petroleum ether, water, and hexane, in batch mode at 103 bar, 115 and 170°C and 9 and 11 minutes of extraction. The greater extraction yields were 4.30, 3.60, 19.94, and 9.86% from the total weight, for hexane, petroleum ether, ethanol

and water, respectively. This study concludes that the critical factor to consider for enhancing extraction yield in this process is temperature. The highest temperature (170°C), regardless the solvents, consistently provided the optimal extraction yield. The solvent giving the best extraction yield was ethanol, however, the antioxidant activity was slightly best preserved by hexane and worst preserved by water. Finally, this study demonstrated that the extraction time proved to be the less influential parameter in this process. The paper by Zhou *et al.*, 2021 [174] tested PLE at 103 bar in AP biomass and concluded that the best extraction conditions for valorizing the biomass using deionized water were 40°C, 10 minutes, and pH 4 water. The obtained yields in this study were protein yield ($46.8 \pm 3.1\%$), Chl a (1.46 ± 0.04 mg/g), carotenoids (0.12 ± 0.01 mg/g), total polyphenols (11.49 ± 0.04 mg/g) and carbohydrates content (78.42 ± 1.40 mg/g) of the extracts compared with non-pressurized extraction. It is noteworthy that according to some authors [140] [176] [177] the pH of the solvent has an impact on the solubility of the PC due to the solvent ionic strength influence on the protein structure. The best pH extraction conditions were reported at slightly acidic pH.

The main challenge of this technique is to control the temperature, to lead to a selective extraction. When the temperature is not a regulated parameter, the extraction is not selective and thus less interesting in terms of scalability. The parameters regulating the extraction efficiency are the extraction temperature, the solvent nature, the biomass particle diameter (d_p), the extraction time, and the fixed bed characteristics, like the void fraction (ϵ), the tortuosity (τ) and the solvent flux, when the process is performed in continue or semi-continuous mode. The tortuosity is defined as the ratio of lengths (L/L_0) (Figure 20), L being the preferential fluid pathway in a porous matrix [178]. Where, L_0 and L constitute Euclidean and geodesic distance between its two extremities, respectively. It is not necessary to vary the pressure since a variation of pressure will not influence significantly the liquid solvent density. That's the reason why the pressure used for PLE is often about 100 bar [179] [165].

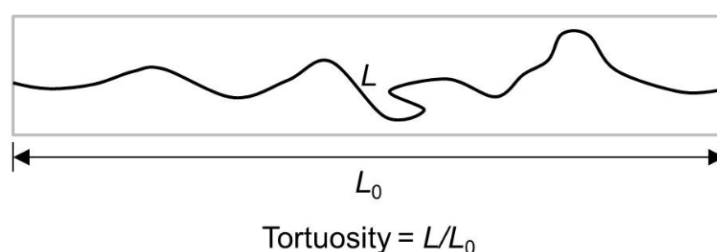


Figure 20 Schematic representation of tortuosity definition reproduced from [180]

Chapter I : State of the art

1.6.3.1 Pressurized Liquid Extraction applications

Depending on the selected solvent and operating conditions, this technique is applicable across various industries:

Food and beverages industry, for the extraction of flavors, fragrances, and other volatile compounds from plant materials, spices, and herbs [163]. Determination of pesticide residues and contaminants in food samples [164] [165].

Pharmaceutical industry, for the extraction of active pharmaceutical ingredients (APIs) from solid dosage forms or natural products. Determination of impurities and contaminants in pharmaceutical formulations [166] [167].

Polymers and plastics industry, for the analysis of additives, stabilizers, and contaminants in polymer samples [168].

Cosmetics industry, for the extraction of natural compounds for the formulation of cosmetic products [169] [170].

Environmental technologies, for the extraction of environmental contaminants from soil, sediment, and plant samples for analysis of pesticides, polycyclic aromatic hydrocarbons (PAHs), and other pollutant [171].

1.6.4 Supercritical CO₂(scCO₂) extraction

This technique is largely applied in the solid-supercritical extraction of high-value molecules from biomass. Its safety and high selectivity for the extraction of molecules with low molecular weight, neutral charges, and low volatility is one of the main assets of this solvent application [181]. This technology is well adapted for molecules susceptible to thermal degradation. Furthermore, this scCO₂ is non-toxic, cost-effective, non-flammable, has low critical temperature, and can be recycled during the process to avoid greenhouse effects [182] [183]. ScCO₂ extraction offers significant advantages, such as ensuring a clean and pure end product by leaving no residual solvents in the extracted material. Additionally, the reuse of an industry by-product like CO₂, aligns with environmental and safety considerations. Furthermore, the process facilitates efficient spontaneous separation of CO₂ from the extract by simple depressurization. Since CO₂ is gaseous at ambient conditions of pressure and temperature.

The term “supercritical” refers to the fact that CO₂ reaches the region beyond its critical point of temperature and pressure, respectively 31.1°C and 73.8 bar (Figure 21). In this domain, CO₂ presents high density, increasing the fluid compressibility and its solvent capacity, low viscosity, improving mass transfer, thus decreasing the energetic cost of the operation; high

diffusivity and gas-like low surface tensions, enhancing the solute extraction in porous materials and solid matrixes.

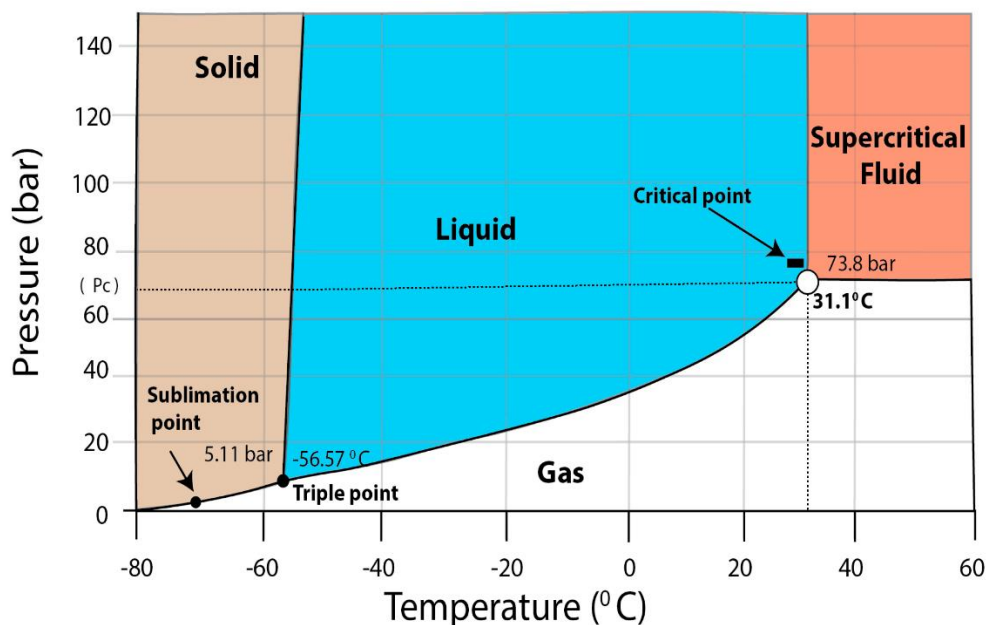


Figure 21 CO₂ Phase diagram representation reproduced from [182]

High pressure and temperature play important roles in scCO₂ extraction. The first one is linked to density increase, leading to an enhanced specific interaction between solute and solvent molecules, increasing the solute solubility. While temperature has a direct impact on viscosity, reducing it while increased. Reduced viscosity allows scCO₂ to easily penetrate in solid materials, and improves the extraction of target molecules [194]. Yet, it is essential to carefully control the thermodynamic properties of CO₂ during supercritical extractions to enhance the desired solvent characteristics. In this regard, introducing the concept of the "Widom line" becomes essential, offering valuable insights into determining the specific temperature and pressure range at which CO₂ presents significant modifications in its properties, displaying characteristics close to either a gas or a liquid [195]. The Widom line can be interpreted as an extension of the vapor-liquid equilibrium line in the supercritical region (Figure 22). It is important to keep in mind this concept when optimizing the extraction process to control the solvent properties, and phase behavior of the solvent. These properties have been identified for different fluids, like water, nitrogen, argon, and organic compounds. Along the Widom line, different fluid characteristics (heat capacity, compressibility, enthalpy,...) undergo significant modifications for very small variations of pressure and temperature [196].

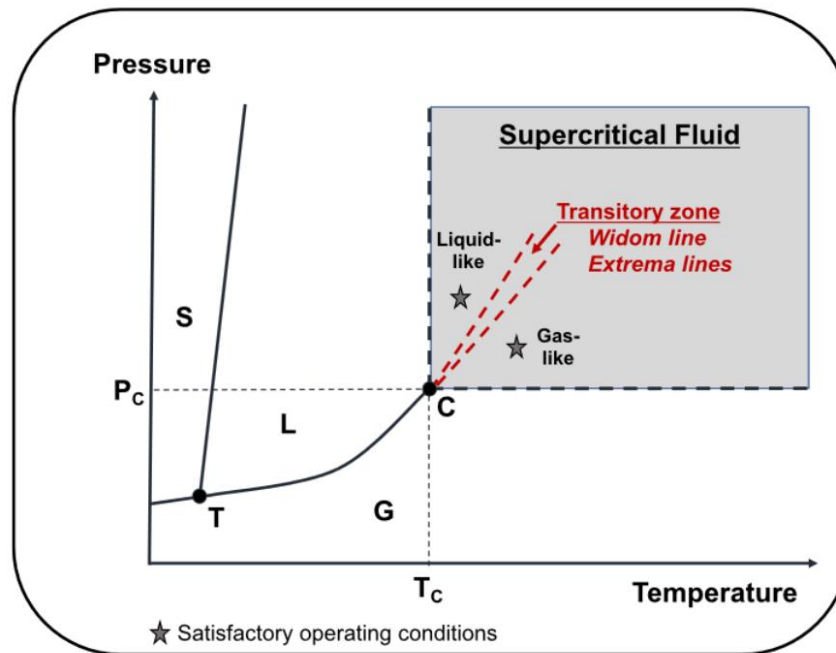


Figure 22 Widom line, reproduced from [196]

The research conducted by Di Sanzo *et al.* in 2018 [197] assesses the impact of pressure and temperature variations on the extraction of astaxanthin and lutein from *Haematococcus pluvialis* using supercritical carbon dioxide (scCO₂). This work investigates the pressure and temperature influence (100, 400, and 550 bar), and (50, 65, and 80 °C) respectively, claiming a maximum extraction of astaxanthin and lutein of 98.6% and 52.3%, respectively, at 50 °C and 550 bar. The study highlights that an increase in pressure enhances the extraction of mid-polarity molecules. Notably, Tippelt *et al.*, 2019 [198] and Cyanotech, Hawaii, USA, report extraction yields larger than 90% of astaxanthin at work pressures ≥ 800 bar and a temperature range from 60 to 80 °C, at industrial scale. The use of scCO₂ is quite attractive for the extraction of HVM [199]. The use of large-scale extraction units is a good alternative to offset the operating costs, increasing the scCO₂ competitiveness compared to traditional extraction processes [200].

ScCO₂ extraction of mid-polarity molecules can be enhanced by incorporating co-solvents such as ethanol, DMSO, or acetone. This addition aims to modify/increase the polarity of the CO₂-rich phase, subsequently boosting extraction yields [201]. The utilization of co-solvents is suggested to enhance solubility and selectivity during operations at lower pressure for molecules with larger polarity. Yet, the co-solvent use implies a further step in the process to eliminate the co-solvent traces from the extract.

Lipids and pigments extraction from microalgae and cyanobacteria has been widely studied in the last decade for food, cosmetic, and energy applications. The paper from Tabernero *et al.*,

[202] explores the different patents linked to microalgae valorization by scCO₂. Up to the year 2016, there were 150 recorded patents, with 43% of them focusing on pigments. Among these, 84% pertained to carotenoids, 13% to Chl. Additionally, 29% of the total patents were related to the extraction of lipids from microalgae [182].

The biomass from AP is scCO₂ valorized due to its content in γ -linolenic acid and carotenoids. In the study of Valderrama *et al.*, 2003, the lipid extraction yield reached 3% from 3.7% wt, using 10% mass of ethanol as a co-solvent at 300 bar and 60°C [203]. The study of Sajilata *et al.*, 2008 reports the complete extraction of γ -linolenic acid from AP biomass at 40°C, 400 bar, and 0.7 L/min scCO₂ flow rate, while the study of Golmakani *et al.*, 2012 [204] reports an extraction efficiency of 24.7% at 40 °C and 300 bar with 50% v/v ethanol as co-solvent. Table 6 displays the optimal conditions reported by previous studies for the valorization of AP biomass by scCO₂. Finally, the paper published by Careri *et al.*, 2001 states that to obtain an extract rich in β -carotene it is necessary to work at 350 bar, 40°C and 15 wt of ethanol [205]. Little information is available on the effect of supercritical conditions on the antioxidant activity of the extracts. According to Herrero *et al.*, 2004, the compounds mostly contributing to antioxidant activity are non-polar compounds [206].

Table 6 CO₂ Optimal extraction conditions for AP biomass valorization

Target molecule	Drying technique	Temperature (°C)	Pressure (bar)	Main result	Reference
Lipids	stove	60	300	81% lipid extracted	[203]
γ -linolenic	Freeze-drying	40	400	Recovery of 100% GLA	[207]
β -carotene	air-dried	55	320	Best antioxidant extract	[208]
Vitamin E	air-dried	83.3	361	29.4 mg vitamin e/g extract	[209]
Neutral lipids, carotenoids, and Chl a	air-dried	45	460	Average mass loss 11.6 \pm 0.3%	[28]

Concerning the major disadvantages of scCO₂, the hazards linked to the high pressures might be considered. Appropriate equipment, including relief systems, proper isolation, and storage tanks, should be incorporated into the process design. Regarding the economic considerations of the extraction process, energy, manpower, plant capacity, and cleaning have been identified as the most critical operating costs [194]. Nevertheless, since industrial units of supercritical extraction exist for more than 40 years now in a wide range of sectors (perfumes,

Chapter I : State of the art

aroma, food products, nutraceuticals, drug,...), and since their number is constantly increasing, the use of this technology at industrial scale is economically viable [200].

1.6.4.1 Supercritical CO₂ applications

Supercritical CO₂ finds diverse applications across several industries due to its unique properties in the supercritical domain [184]. As discussed in the previous paragraph, one significant application is in the extraction of essential oils from plants, herbs, and spices, providing a cleaner and more efficient alternative to traditional extraction methods [155] [185]. Moreover, in the pharmaceutical industry, scCO₂ is utilized for drug delivery and the production of pharmaceutical formulations [186] [187]. Additionally, it plays a crucial role in the food industry, where it is employed to extract flavors, fragrances, and natural colorants [188]. This versatile substance is also applied in decaffeinating coffee and tea [189]. Beyond that, scCO₂ is utilized in polymer processing and sterilization, environmental applications for pollutant removal [190] [191], and serves as a mobile phase in Supercritical Fluid Chromatography (SFC) [192]. Its ability to create nanostructures and nanoparticles further expands its applications [193], showcasing the broad spectrum of uses for supercritical CO₂ across various fields.

1.6.5 Pressurized Fluid Extraction (PFE) Scale-up

To industrialize a PFE, it is essential to replicate this method from laboratory-scale to pilot-scale and ultimately to industrial scale. At the laboratory scale, the identification of phase equilibria and mass transfer coefficients for the studied system is possible. The initial phase of scaling up includes modeling the extraction process, focusing on the parameters of limiting transfer. It also involves identifying the CO₂/biomass ratio, a key parameter in the scaling-up process. These parameters can be external, influenced by the solubility of the target molecule, or internal, governed by the diffusion of the target molecule within the solid matrix. The solubility controls the ideal extraction conditions and sets the minimum amount of solvent necessary to complete the extraction [210]. When the extraction is limited by the external mass transfer, the flow-rate increase might have a positive impact on the extraction. Conversely, when the extraction is limited by the internal mass transfer the increase of the flow-rate is expected to have little impact on the extraction rate of the solute. Once the limiting mass transfer has been identified the impact of the material properties can be addressed; it is known that the particle size reduction increases the solute extraction kinetics [211]. Moreover, larger particles induce potential mass transfer limitations, slow diffusion of the solvent and of the solute inside the particles. However, this size reduction may prone the void reduction and hinder the flow of the solvent through the extraction vessel, creating channeling. A well controlled particle size can lead to the cease of internal diffusion limitations, and increase the solute mass transfer from

the solute to the solvent-rich. Finally, the autoclave length to diameter ratio must be kept constant to lead a successful scale-up, this parameter is a very important consideration when designing an extraction vessel. According to previous studies [212] [213], it is recommended to maintain the cross section velocity, bulk density and porosity of the scaled-up operation [185]. The main scale-up issues in PFE extractions are the material aggregation, pressure drop, fluid channeling and the inability to keep the CO₂ plug flow [211].

1.7 High-value molecule quantification techniques for biomass extracts

The molecules present in the obtained extracts can be characterized by various physicochemical techniques, the characterization technique needs to be chosen as a function of the properties of the extract and the applications of the final product. This step is crucial to identify the extract value in terms of purity, it gives important information about the whole process.

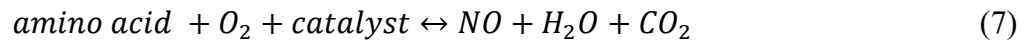
1.7.1 Protein quantification

The quantification of these molecules can be accomplished by several methods. The most known methods for protein quantification are ion-exchange chromatography [214], catalytic combustion [215] for total nitrogen, and colorimetric measurements, such as Kjeldahl and Lowry methods [216], and phosphate buffer method [217]. The chosen identification technique must answer to the final application of the extracted molecules.

1.7.1.1 Nitrogen catalytic combustion (Total protein content)

The total nitrogen measurement is a technique that can enable to estimate of the protein content in a simple and fast way. Moreover, when the standard of the target molecule is available, it is possible to generate a calibration curve permitting the identification of the desired molecule. Nitrogen is a fundamental component of amino acids which are the building blocks of proteins. Nitrogen commonly occurs in organic and inorganic forms. In this approach, high temperatures coupled with chemiluminescence detection are applied to the detection of organic and inorganic nitrogen. The principle of this technique is based on the decomposition of proteins into nitrogen monoxide at 720°C by combustion. The thermoelectrically cooled and dehumidified gas passes through a chemiluminescence analyzer, where it reacts with ozone and forms excited NO₂*. When excited NO₂* returns to the ground state, it emits radiation and this radiation is measured photoelectrically, generating a signal that can be measured. The reactions involved in the process are the reactions (7), (8), (9) and (10). The main drawback of this technique is the equipment cost and maintenance [218].

Chapter I : State of the art



1.7.1.2 Phosphate buffer method (for PBP quantification)

This method is applied to extract and quantify PBP in cyanobacteria biomass. The process involves initially rupturing the cell wall through a freeze-thaw cycle, with cells frozen at -20°C for a minimum of 12 hours. Subsequently, a 4-hour extraction of the PBP is carried out using a phosphate buffer (pH: 7.4) to maintain the ionic strength of the extraction solution, preventing protein denaturation. The extraction must be performed at a temperature between $4-20^\circ\text{C}$ [217]. After the extraction, the samples must be centrifuged and the supernatant should be measured at 720, 652, and 615 nm to determine the PBP concentration [219]. This method is quite simple and efficient, the main drawback is that the biomass characteristics must meet the requirements to avoid the extraction of other pigments slightly soluble in water, such as Chl. To avoid this, the culture growth and freeze-thawing steps must be well controlled.

1.7.2 Total sugars

1.7.2.1 Dubois method

In the case of biomass, one of the most employed techniques is the Dubois technique, which is based on a colorimetric principle [220]. This method is widely used for total sugar determination in aqueous solutions. The basic principle of this method is that carbohydrates, when dehydrated by reaction with concentrated sulfuric acid, produce furfural derivatives. The further reaction between furfural derivatives and phenol develops a detectible color. The main drawback of this technique is the use of hazardous substances, like sulphuric acid and phenol. Another drawback of this technique is that the result is obtained as a glucose-equivalent concentration that may have potential limitations, especially when the examined carbohydrates are not hexoses [221] making the result analysis less accurate. Other methods as DNS and Anthrone have been developed for the same purposes. The paper of Depraetere *et al.*, [222] states that the application of the Dubois method is effective in quantifying the extracellular polysaccharides in AP culture.

1.7.3 Lipids

The lipid quantification in cyanobacteria and microalgae biomass is one of the most important topics in renewable energy and food technology research. However, this process represents a bottleneck, due to the time and expertise that this technique demands to obtain reliable results [223].

Gravimetric methods, gas chromatography, and staining with lipophilic fluorescent dye for quantitative spectrophotometry are widely used to determine the lipid content in vegetal cells [223] [224] [225].

The gravimetric methods usually need the previous extraction of the lipids from a known quantity of dry biomass applying hexane and chloroform to evaporate the solvents and deduce the number of lipids per gram of dry biomass. The major downsides of these techniques are they employ large quantities of biomass, time-consuming techniques, and the need for previous expertise of the method. The Bligh and Dyer technique is used for the extraction of total intracellular lipids. This method is based on the permeability that this solvent mixture has to recover the total lipids in the cell, the solutes are found on the chloroform phase [226].

Once the lipids are extracted, the sample containing the lipids must go through transesterification to identify biomass fatty acids. This procedure involves the reaction between a triglyceride (oil/wax) and an alcohol, resulting in the formation of glycerol and alkyl esters. A successful transesterification consists in separating the glycerol and methyl ester layers, this reaction can be performed in acidic or basic conditions as showed in Figure 23.

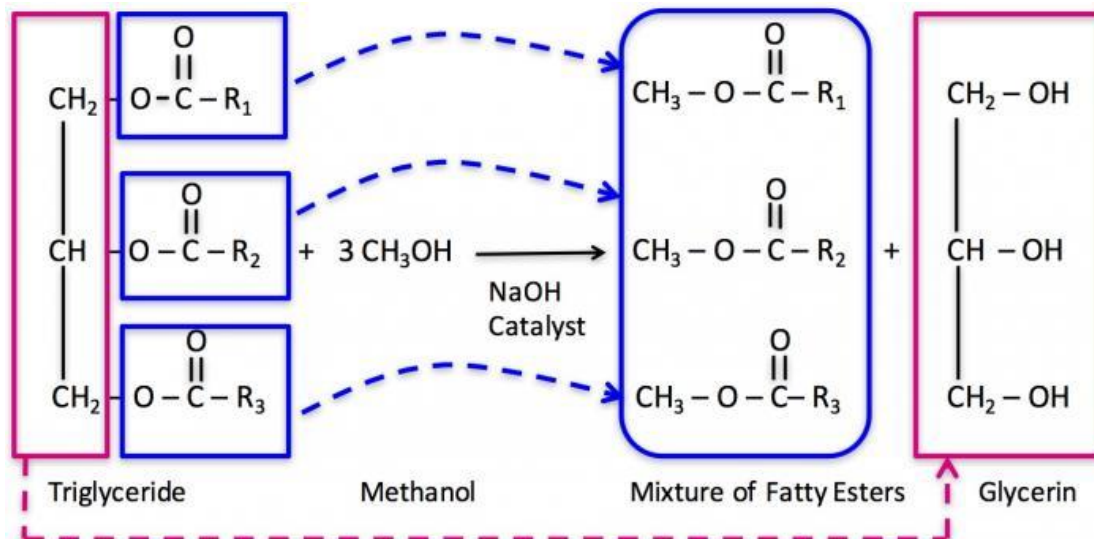


Figure 23 Transesterification in presence of an acidic catalysts, reproduced from [227].

Chapter I : State of the art

Resulting fatty acid methyl esters FAMES could be analyzed using various analytical methods such as gas chromatography equipped with mass spectrometry (GC/MS) or Flame Ionization Detector (GC-FID), or high-performance liquid chromatography (HPLC) [223].

An alternative to these methods is the application of Nile red or BODIPY techniques, their principle is to dye the lipids present in the biomass with the aid of a pigment carrier, like DMSO. However, this method is qualitative and is only effective when the cell wall is not thick [228].

1.7.4 Chlorophylls and carotenoids

Carotenoids are molecules from the terpenoids family and are biosynthetically related to other secondary metabolites such as tocopherols and ubiquinone [55]. The most applied technique for their identification is the HPLC method, which can separate and quantify individual carotenoids [229]. However, other competitive alternatives such as the spectrophotometer and near-infrared spectroscopy are reliable for determining carotenoids concentration in vegetal material. The spectrophotometer is widely used in routine tests for microalgae and cyanobacteria. Carotenoids are extracted from the biomass using an adapted solvent, and the absorbance at a specific wavelength corresponding to the target carotenoid is subsequently measured. Similar to carotenoids, Chl a can be quantified by spectrophotometer techniques and HPLC [49] [90].

1.7.5 Antioxidant properties of the extracts

The subsequent step in the AP valorization chain involves characterizing the antioxidant activity of the obtained extracts. As previously discussed, some molecules within AP biomass exhibit bioactive properties. Beyond the extraction efficiency of the employed technique, it is interesting to identify the antioxidant properties of the extracts and distinguish if they are keen to inhibit oxidative stress.

Oxidative stress is related to an imbalance between the reactive oxygen species (ROS), these species in the body are responsible for the development of many diseases [230]. The antioxidants present in vegetal extracts as the ones obtained from AP valorization can inhibit this activity and prevent cell damage. The antioxidant molecules can donate electrons to the oxidant or target molecules.

The antioxidant activity is generally associated with the ability of a compound to neutralize ROS or inhibit oxidative processes. It can be used to express the chemical reactivity of the antioxidants present in the extract under the specific conditions [231].

1.7.5.1 Total phenolic compounds (TPC)

This assay is also known as the Follin-Ciocalteu assay (FC) and employs an FC reagent to oxidize phenolic content in the sample. It has been widely applied in the determination of the total phenol/polyphenol content of plant-derived food and biological samples [233]. The reaction relies upon the spectrophotometric determination that takes place in a Na_2CO_3 solution. The reaction involves the oxidation of phenolic compounds by a mixture of phosphomolybdic and phosphotungstic acids in the presence of alkali (sodium carbonate or sodium hydroxide). A calibration curve is plotted using a standard aromatic acid, like gallic acid, comprising a phenolic ring. A blue complex with maximum absorption at 765 nm is generated during the reaction. The regression equation is employed to determine the total phenolic content in the sample [232].

1.7.5.2 Antioxidant activity (%antioxidant activity)

The antioxidant activity is the capacity of a molecule to catch free radicals and prevent their harmful effect in living environments. This process can be stimulated by various substances, including phenolic compounds, carotenoids, tocopherols, flavonoids, and ascorbic acids, among others. The antioxidant activity can be measured as a percentage of decrease of the initial activity of the oxidant at a definite time. In methods like DPPH or ABTS, the absorbance measurement can be used as an indicator of the percentage of antioxidant activity. The antioxidant activity percentage can be estimated by measuring the absorbance of the sample after the reaction by applying the following equation:

$$\% \text{ antioxidant activity} = \left(\frac{A_{\text{control}} - A_{\text{sample}}}{A_{\text{control}}} \right) \times 100 \quad (11)$$

Where;

	Definition	Unit
%antioxidant activity	Inhibition percentage	%
A_{sample}	Absorbance of the sample after the reaction	a.u.
A_{control}	Absorbance of negative control	a.u.

a.u.: Arbitrary unit

Chapter I : State of the art

The antioxidant percentage can range from 0-100%, this can vary according to the physicochemical conditions of the reaction. The higher the percentage, the greater the antioxidant activity [233]. An antioxidant activity percentage greater than 90% can be indicative of an error probably caused by the lack of a linear relationship between the measured properties and concentration of the antioxidant [230]. This method can be used to compare the antioxidant activity of extracts and mixtures under the same reaction conditions.

1.7.5.3 DPPH

This assay enables the evaluation of the antioxidant activity of extracts reacting with a stable radical (DPPH) in a methanol or ethanol solution. The DPPH reduction is monitored by following the absorbance decrease at 517 nm. In its radical form, DPPH absorbs at this wavelength. But upon reduction by an antioxidant (AH) or a radical species (R), absorption disappears as shown in equations (12) and (13) [234].



The 2,2,1-diphenyl-1-picrylhydrazyl (DPPH) possesses a radical that can be neutralized by an antioxidant and is active in different solvent mixtures (i.e., methanol, methanol/water). The antioxidant mechanism is defined as the -H transfer from the antioxidant to break oxidative chain reactions caused by free radicals. In the presence of antioxidant species, the radical is neutralized and the absorbance of the sample decreases [235].

This radical is selective and does not react with aromatic acids containing only one OH group. The main disadvantage of this technique relies on the fact that the small molecules have better access to the radical site and can show higher apparent antioxidant activity. This assay is typically compared to an antioxidant standard, such as the butylated hydroxytoluene (BHT) or vitamin E [205]

1.7.5.4 ABTS

The (2,2'-Azinobis-(3-Ethylbenzthiazolin-6-Sulfonic Acid)) (ABTS) is a molecule that easily forms a cation radical chromophore when subject to strong oxidant (such as potassium persulfate). The ABTS assay assesses the antioxidant activity within the sample indicating its ability to stabilize a green-colored cation radical. This reaction can occur in water soluble or liquid soluble environments. Similarly to DPPH, this assay is also compared to the antioxidant activity of BHT or vitamin E [236]. The formed ABTS cation radical is a stable chromophore compound in a wide pH range. This chromophore has three absorption maxima at wavelengths

of 645, 734, and 815 nm [237]. Its radical is soluble in aqueous and organic media, therefore antioxidant activity can be determined in water-soluble and fat-soluble samples [238]. Antioxidants interact with ABTS cation radical by neutralization of the chromophore. The discoloration of the blue-green sample is an indicator of the antioxidant activity of the tested sample [235].

1.8 Integral valorization of *Arthrospira platensis* biomass in a biorefinery approach

After the bioactive molecules from AP biomass have been extracted by the green extraction techniques reviewed in this chapter, the depleted biomass can be introduced into several processes to minimize waste generation and favor a multi-product bio-refinery approach. The residual biomass can be valorized into different applications that will be reviewed in this part of the document.

1.8.1 Vegan proteins

Nowadays, the demand for plant/non-animal-based proteins is increasing, due to the consumer's awareness in terms of environment and climate change. Previous studies demonstrate that AP biomass is an excellent source of leucine, valine, isoleucine, lysine, glutamic acid, aspartic acid, alanine, and arginine [239]. Its protein content is around 460–630 g/kg in dry weight and can be compared with the one of meat and soybeans, being 710–760 and 400 g/kg in dry weight, respectively [13]. Moreover, the studies of Bashir *et al.*, 2016 [239], Silva *et al.*, 2022 and [240] Ramirez-Rodriguez *et al.*, 2021 [241] demonstrate the beneficial applications of protein isolates in food technology, particularly as effective emulsifiers. Consequently, prioritizing the valorization of proteins after the extraction of bioactive molecules becomes crucial for achieving a comprehensive and integral valorization of cyanobacteria. The study of Balti *et al.*, [242] reports a method that enables to separate efficiently the proteins through membrane diafiltration. This technique enables to fractionate the AP proteins from 50-300 kDa to obtain high-purity protein extracts with nutraceutical interests. The selective extraction of these proteins enhances the sensory acceptance of *Arthrospira platensis* (AP) biomass for consumers. This is because the aromatic compounds in the biomass contribute a strong flavor that diminishes the overall acceptability of AP biomass for human consumption [33]. Further development needs to be done to optimize the protein separation without damaging the bioactive properties of the target molecules.

1.8.2 Aquaculture feed

Theoretically, the sugars contained in the residual biomass can be employed as aquaculture feed. No information is available on the use as a fish food source of AP biomass depleted from

Chapter I : State of the art

its bioactive molecules. Nonetheless, it is interesting to consider this alternative, as previous studies have shown that AP biomass has potential benefits in aquaculture [243] [244] [245]. The paper of Abdel-Latif *et al.*, [243] shows that the inclusion of 1.25, 2.5, and 5.0 g *Spirulina platensis* (SP) / kg diet biomass in the fish diet is correlated to an increase in the white and red blood cells in *Clarias gariepinus* facing environmental stress, such as food shortages and UV exposition. Similar results were observed by including AP biomass in the diet of other organisms facing stressing conditions, like the increase of immunoglobulin M in Nile tilapia (*Oreochromis niloticus*) under hypoxia conditions [246].

1.8.3 Bioplastics

Another possible use of the AP biomass depleted of bioactive molecules is the valorization of the residual sugars for bioplastic production. Polyhydroxyalkanoates (PHAs) are polyesters produced by a variety of microorganisms, these polymers can be employed for bioplastic production. The PHAs have similar thermal and mechanical characteristics to the ones of petroleum-derived plastics [247].

Polyhydroxybutyrate (PHBs) are a type of homopolymeric PHA [248], that can also be produced directly by cyanobacteria. The supplementation of short-chain carbon sources, like acetate, can lead to an increase in PHB accumulation when compared to growth under strictly photoautotrophic conditions [249]. According to Hajar *et al.*, [248] a co-production of PC and polyhydroxybutyrate (PHB) is a viable alternative to valorize AP biomass, producing cultures with a PHB content between (4-8%) using acetate, oxalate, glycerol as carbon source combinations. The study by Mei-Hui Jau *et al.*, [249] reports an accumulation of 10% wt of PHB in AP biomass cultivated under mixotrophic culture conditions.

1.8.4 Bioethanol

The potential of microalgae and cyanobacteria biomass as an energy source has been largely studied [16] [250] [251] [252]. The application of carbohydrates such as starch, glycogen, and cellulose present in microalgae and cyanobacteria as feedstock for bioethanol has shown economic viability [251] [252]. The paper of Rempel *et al.*, [253] explores the potential of AP biomass to produce bioethanol, and the wastes were employed to produce biomethane by fermentation. According to the paper, the enzymatic hydrolysis of the microalgae polysaccharides and the fermentation process presented efficiencies above 80%. The direct conversion of hydrolyzed AP biomass into ethanol presented an energy potential of 4,664 kJ/kg of biomass, while the methanisation process had an energy potential of 16,770 kJ/kg of biomass. Moreover, the study conducted by Markou *et al.*, [16] reports a bioethanol yield of $16.32\% \pm 0.90\%$ ($\text{g}_{\text{EtOH}}/\text{g}_{\text{Biomass}}$) with AP biomass hydrolyzed by a strong acid. However, little information

is found concerning the use of algae, microalgae, and cyanobacteria biomass waste for bioethanol production [254]. The valorization of the AP biomass after high-value molecule extraction for this use might bring interesting economic and energetic outcomes.

1.8.5 Biogas

As a subproduct of the fermentation for bioethanol production, the biogas obtention is relatively simple and low-cost [255]. Biogas is produced under anaerobic digestion of different biomass and waste. The paper of Hawrot-Paw *et al.*, 2023 [255] determines the potential of AP biomass as a source of biogas produced under anaerobic digestion. This study demonstrates the potential use of AP biomass as a biogas feedstock, showing a composition containing 67.32% methane. Moreover, the paper of Sumprasit *et al.*, 2017 [256] reports a methane yield of 290 mL/g of volatile solids. The introduction of AP biomass in an anaerobic digestion process after the extraction of proteins and high-value molecules can be an interesting option, due to the adequacy of the high C/N ratio to the anaerobic fermentation conditions hindering ammonia production [257].

1.9 Aims and objectives

The work presented in this thesis was carried out in the framework of two complementary approaches. The first one, the optimization of AP culture, focused on the application of sustainable alternatives, to increase the bioactive pigment (PBP, Chl a, and carotenoids) content, and the productivity in the culture biomass. The second one is the valorization of biomass bioactive compounds like pigments and lipids, by the application of green solvent technologies.

The general objective of this work is to propose a sustainable production chain of bioactive pigments from AP biomass (Figure 24).

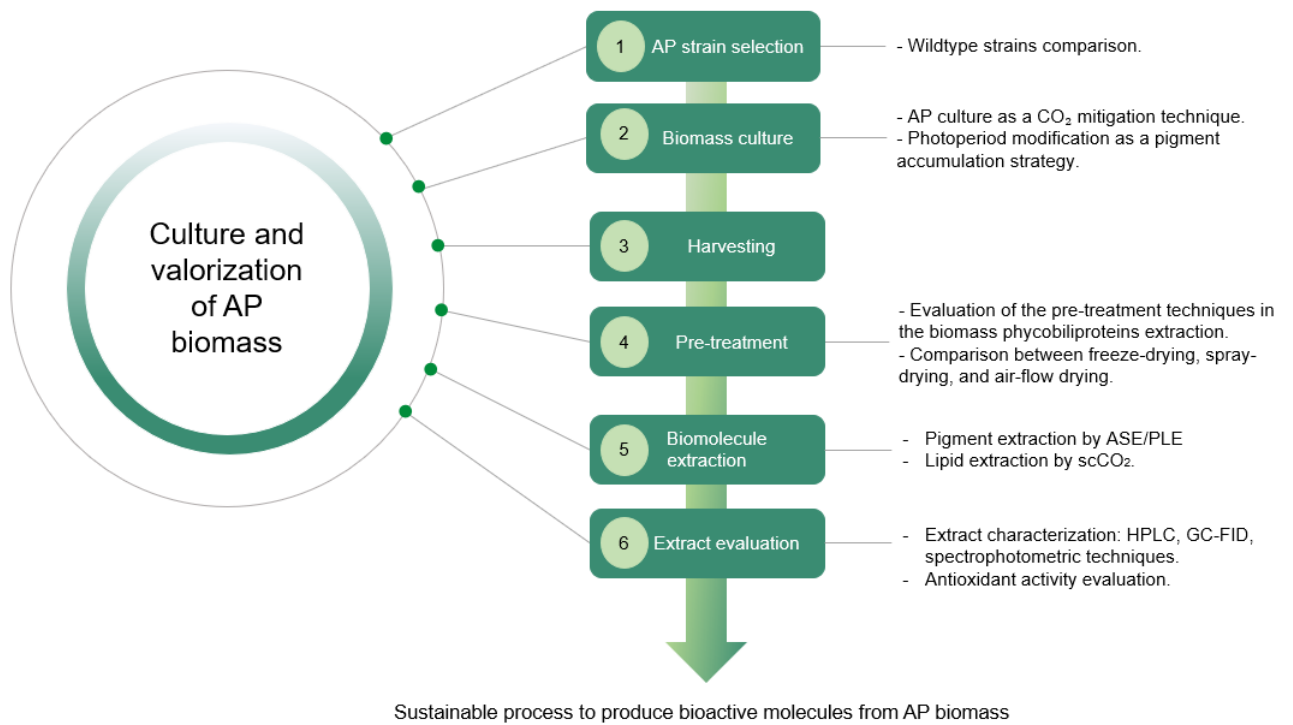


Figure 24 Project Optimization approaches for *Arthrospira platensis* culture and valorization. 1 and 2 are part of the 1st approach, while 4,5, and 6 are part of the 2nd approach.

Phase I: Development of sustainable AP culture techniques to increase the culture productivity and biomass pigment accumulation

General objective:

To study the impact of the carbon source and photoperiod duration in biomass bioactive pigment accumulation and culture productivities. To propose a culture strategy that increases the biomass and pigment productivities without compromising the energetic and environmental feasibility of the process.

Specific objectives

To evaluate the potential of AP culture as a carbon mitigation technology by integrating gaseous CO₂ as the principal carbon source in the perspective of circular economy.

To identify the principal physicochemical parameters that intensify the carbon assimilation in the culture medium.

To assess the impact of the photoperiod on the bioactive pigment accumulation in the biomass.

2nd phase: Bioactive pigment extraction by green-solvent technologies

General objective:

To develop and apply an integrated green extraction strategy to valorize the bioactive pigments and lipids present in the AP biomass cultured during the first approach experiments, to obtain extracts with competitive antioxidant activities.

Specific objectives

To perform extensive bibliographical research to identify the ASE and scCO₂ optimal operation conditions (solvent proportions, temperature, pressure, extraction time, and particle size) to extract the bioactive pigments and lipids from AP biomass.

To assess the impact of the biomass pretreatment on the extraction efficiency by comparing the effect of different drying (freeze-drying, spray-drying, air-flow drying) on the extract properties, keeping the PBP content in the biomass as main indicator.

To optimize the ASE extraction yields applying a reduced range of the optimal operation conditions (temperature and green solvent proportion) employing the central composite experiment design.

Chapter I : State of the art

To evaluate the scCO₂ extraction yields in the biomass produced during the first part of the project to compare the extraction yields with the reported values in the bibliography, and model the extraction process to facilitate further scale-up of the operation.

To accomplish a chemical characterization of the extracts employing analytic techniques (HPLC and gas chromatography).

To characterize the impact of the operation conditions on the antioxidant activity of the extract.

Chapter 2 Materials and methods

Considering the previously reviewed state of the art and the objectives described in the previous section of this document, this Ph.D. project has been developed in two main phases.

Phase I: In the initial stage of this research, an investigation was conducted on the culture of AP as a gaseous CO₂ mitigation technique from laboratory to semi-pilot scale. This was based on its ability to sequester and utilize CO₂ as a key input for biomass production. This phase of the project will allow the evaluation of AP cultivation potential to implement CO₂ as a carbon source, replacing Na₂CO₃, the conventional carbon source for AP culture.

Moreover, the optimization of biomass and bioactive pigment productivity was developed, based on the photoperiod modification, comparing two approaches: photoperiod modification at the laboratory scale, applying only artificial light, and photoperiod modification, integrating sunlight at greenhouse conditions as seen in Figure 25.

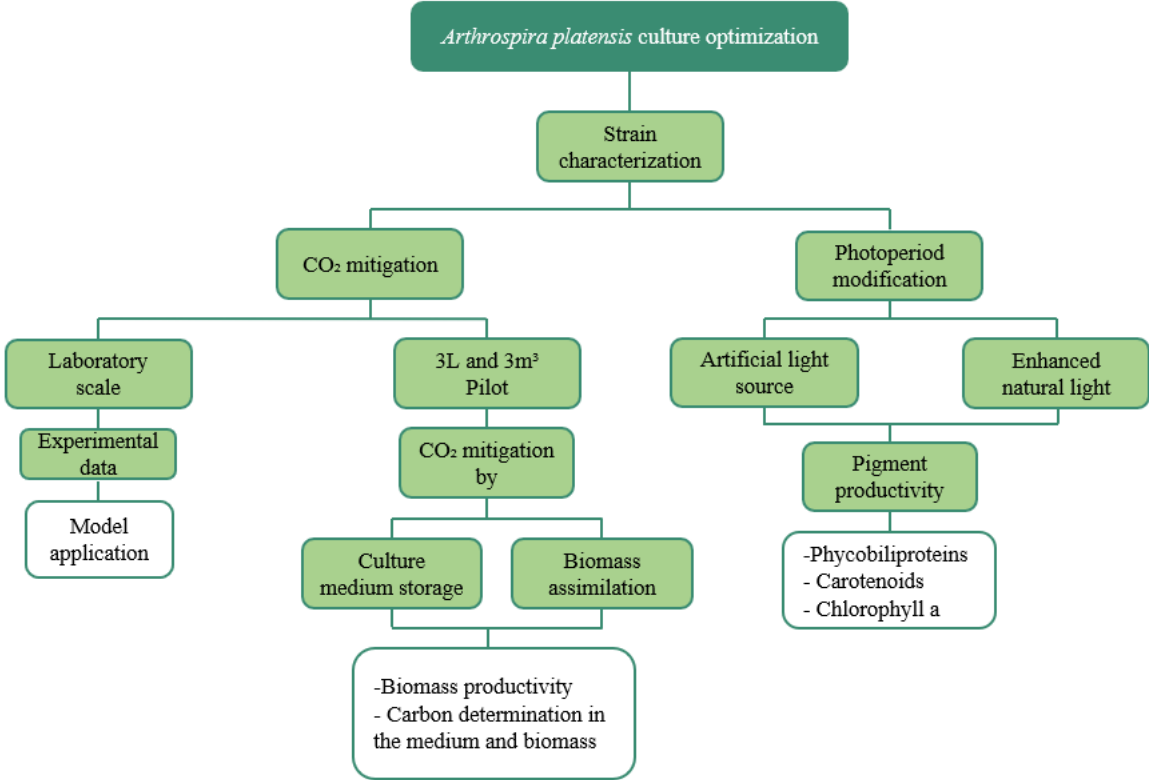


Figure 25 Structure of the culture optimization (Phase I)

Chapter II : Materials and methods

Phase II: The focus was on the sustainable valorization of the biomass generated in the initial project phase. This involved the application of green solvent technologies, including pressurized liquid solvent and supercritical CO₂ extractions (Figure 26). Initially, the optimal conditions to maximize the pigment extraction yields, and the antioxidant activities of the extracts were studied by Accelerated Solvent Extraction (ASE), a laboratory scale device used to test Pressurized Liquid Extraction (PLE) conditions. This experiment was developed following the Central Composite Design (CCD). CCD results generated contour plot responses determining the optimal operatory conditions to enhance the pigment extraction yields, the extract total phenolic compounds (TPC) concentrations, and the antioxidant activities of the obtained extracts. These optimal operatory conditions were defined as a function of the applied solvent concentration and process temperature. This experiment was carried out on two types of AP biomass; Set A) *Raw biomass*: AP biomass without any previous extraction and Set B) *PBP-free biomass*: AP biomass after PBP extraction. To understand the impact of a previous extraction process on the ASE extraction efficiency and the antioxidant activities of the extracts.

Likewise, bibliographical research was performed to identify the optimal operation conditions to valorize the lipophilic fraction of AP biomass applying scCO₂.

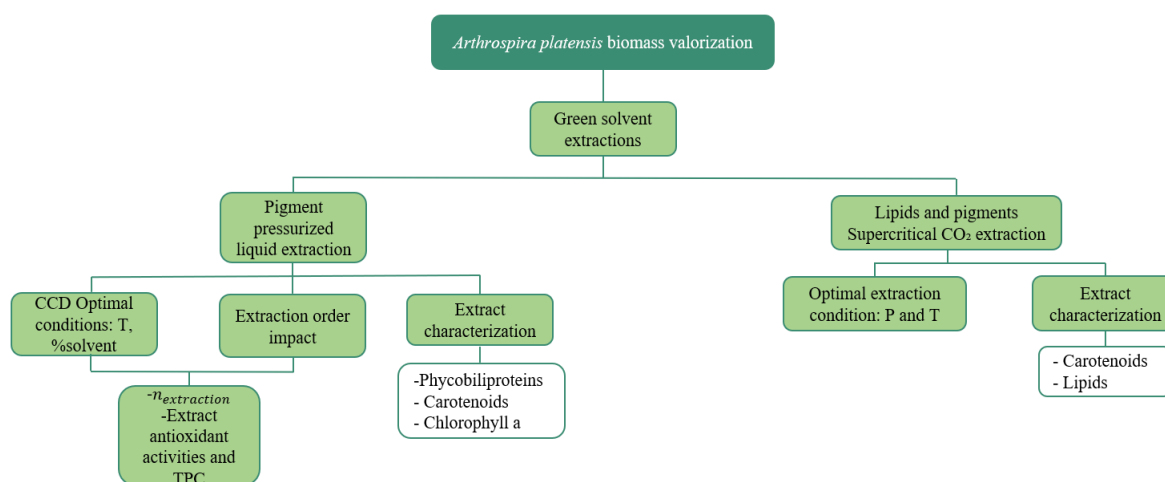


Figure 26 Structure of the biomass valorization (Phase II)

2.1 Phase I: Biomass culture optimization

2.1.1 *Arthrospira platensis* culture as a CO₂ mitigation technique

This section discusses the experimental setup to characterize physicochemical and biological phenomena related to carbon mitigation by AP culture. It also explores the impact of PBR configuration on CO₂ assimilation by the culture medium and biomass. The experiment development is schematized in Figure 27. The first stage of the experiment consisted of the strain choice, selecting the strain with desirable characteristics, like, an adequate growth rate, pigment (PBP, Chl a, and carotenoids) content, and satisfactory downstream (harvesting, drying, pigment extractability). Once the work strain was chosen, the CO₂ assimilation in the medium and culture was studied on a laboratory scale, employing a carbon-free (CFZM) culture medium, with the same composition as the Zarrouk medium (ZM) (Annex: Table 57), except for the NaHCO₃ concentration, that is absent in CFZM employed for the CO₂ assimilation study at laboratory scale. This part of the research aims to answer the following questions, *is AP culture a suitable technique to store and extenuate CO₂? If this is the case, how to implement the technology?*

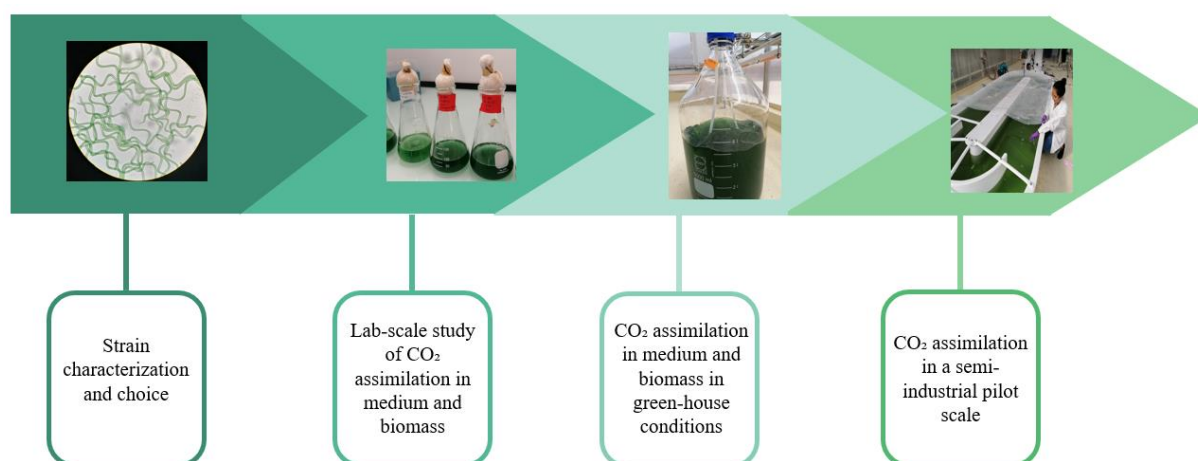


Figure 27 Experimental campaign to identify the potential of *A. platensis* as a CO₂ mitigation technique

Chapter II : Materials and methods

2.1.2 Project strain choice

Three of the wild-type strains displayed in Table 2 p. 36: SAG-21.99, NIES-46, and PARACAS were studied, comparing their productivities, pigment content, and downstream features at the laboratory scale. The strains chosen for this study are based on their proven use in practical AP exploitation. The strains were cultivated using the classic culture medium for AP: Zarrouk medium (ZM), its composition is displayed in Table 57 (See Annex p.225), applying the optimal conditions reported by the literature displayed in Table 7 p.73. The three studied cultures are pictured in Figure 28.



Figure 28 A) SAG 21 B) NIES 46 C) PARACAS taken on the 4th day of the culture
16/04/21

2.1.3 Culture conditions for project strain choice

The three strains were cultured in triplicate in incubator conditions (See Table 7) for 16 days, using conical flasks of 125 mL with a culture volume of 50 mL. The initial pH of the medium was adjusted to 8.8 prior to placement in the incubator. The seed cultures, used for inoculation, were grown under identical conditions for one week preceding the start of the experiment to prevent the cells from undergoing an adaptation phase during the kinetic study. The cultures were conducted in batch mode in an incubator (INFORS Multitron, Bottmingen, Switzerland).

Table 7 Culture conditions for the growth comparison of different *A. platensis* strains
[12] [225].

%CO₂ (v/v)	2%
Temperature	35 ° C
Agitation (RPM)	130
Photon Flux density (PFD)	100 $\mu\text{mol}/\text{m}^2/\text{s}$
Photoperiod (Light/Dark)	20 h/4 h
Initial biomass (g/L)	0.3 \pm 0.1
Light source	White fluorescent tube

The fluorescent light source light spectrum is displayed in Figure 29.

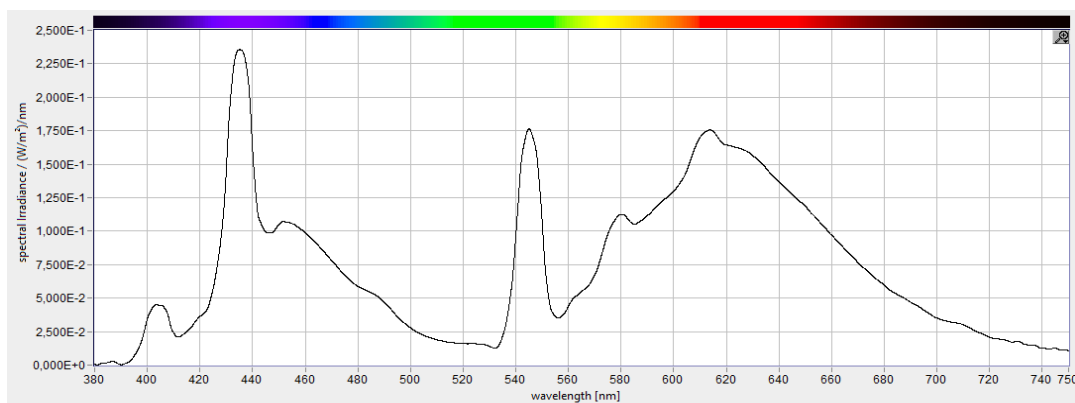


Figure 29 Fluorescent light spectrum in the incubator.

2.1.4 Dry weight determination for project strain choice

The dry weight was determined daily until the 10th culture day to follow up the biomass development in the flasks shown in Figure 28 p. 73, this process was made by filtration by triplicate. Culture sampling was performed every 24 hours \pm 4 hours, under sterile conditions. One sample of 2 mL was filtered with a pre-weighed paper filter of 20 μ m particle filtration size (Reference: 1442-055, Whatman, Buckinghamshire, United Kingdom). The retained biomass was rinsed with 20 mL of ammonia formate 0.5 M, to wash away the salts present in the culture medium. The filters with the retained biomass were placed into a stove at 100°C \pm 4°C for 24h \pm 4 hours, to evaporate the water and then weighed. Dry weight was obtained by weight difference. This determination was made in this way because some strains did not sedimented, so the filter was the most appropriate option.

2.1.5 Generic dry weight determination

Once the project strain was chosen this protocol was employed. A culture sample containing a minimum of 300 mg of dry biomass was collected and subjected to centrifugation using a Coulter Beckman Allegra X-12 centrifuge equipped with an SX4750A swinging bucket rotor. The centrifugation was carried out at 4500 RPM for 5 minutes at 4°C to precipitate the biomass in suspension. The resulting pellet was rinsed twice with deionized water to eliminate medium salts. Subsequently, the pellet was resuspended in water and transferred to a pre-weighed aluminum boat. The sample in the aluminum boat was then placed in an oven at 100°C for 12 hours to evaporate the water content. The aluminum boat containing the dry sample was weighed once the sample reached a constant temperature, and the dry weight of the biomass was determined by the difference in weight. This determination was performed by triplicate.

2.1.6 Growth and productivity calculations

The exponential growth rates (14) and productivity (15) were estimated by applying the following equations in all the performed analyses.

Chapter II : Materials and methods

$$\mu = \frac{\ln X_f - \ln X_0}{\Delta t} \quad (14)$$

Where ;

μ : exponential growth rate (d^{-1})

X_f : final biomass concentration when $t = t_f$ (g/L)

X_0 : beginning biomass concentration when $t = 0$ (g/L)

Δt : culture duration in day (d)

The biomass productivities were calculated as follows:

$$P_{biomass} = \frac{\Delta X}{\Delta t} \quad (15)$$

Where ;

$P_{biomass}$: biomass productivity (g_{DW}/L/d)

ΔX : biomass density variation (in dry weight) from the start to the end of the culture (g/L)

The values were expressed as the mean \pm standard deviation. Error bars in the figures in Chapter 3 are standard deviations of triplicate measurements.

2.1.7 Lipophilic pigments (Chl and carotenoids)

This characterization was made at the end of the experiment, 2 mL of sample were taken and centrifuged in a falcon tube of 15 mL (Coulter Beckman, Model Allegra X-12, rotor model: SX4750A, Brea, CA, USA) at 4500 RPM for 10 minutes at 4°C.

The pellet was stored and frozen at -20°C, and after 24 hours \pm 4 hours it was defrosted with a water bath at room temperature. The falcon tube containing the pellet was wrapped with foil paper, to avoid the degradation of the pigments by the light. 4.5 mL of methanol HPLC grade was added to the falcon tube and vortexed for 10 seconds, in the case of the pigment extraction for strain choice 2.1.2. The other lipophilic pigment extractions described in this document were made with 4.5 mL of ethanol HPLC grade. It was decided to switch to ethanol because of health and security reasons. The samples were agitated for 4 hours at 60 RPM. Each hour the samples were vortexed for 10 s. The pellet has to be blue/purple, without any trace of green color at the end of the extraction phase. This determination was performed by triplicate.

2.1.8 Chl a and carotenoids spectrophotometer quantification

The falcon tubes containing the extract were centrifugated (Coulter Beckman, Model Allegra X-12, rotor model: SX4750A, Brea, CA, USA) at 4500 RPM for 10 minutes at 4°C, to sediment the biomass in suspension. A volume of 2 mL of the supernatant, was placed in an optical glass cuvette. Pure solvent is used as a blank, according to the case. The absorbance of the sample and blank were measured at 470 nm, 665 nm, and 720 nm, the carotenoids, Chl a and subtraction of blank respectively.

The Chl a and carotenoids were quantified using the following equations: the Chl a and carotenoids were quantified applying equations (16) and (17) for the extractions with methanol, and Chl a was quantified with equation (18) for ethanol extraction. The subtraction of the absorbance at 720 nm was systematically performed to neglect the solvent absorbance.

$$\text{Chl a } [\mu\text{g/mL}] = 12.9447 (A_{665} - A_{720}) \text{ for methanol [258]} \quad (16)$$

$$\text{Carotenoids } [\mu\text{g/mL}] = [1000 (A_{470} - A_{720}) - 2.86 (\text{Chl a } [\mu\text{g/mL}])] / 221 \text{ for methanol [258]} \quad (17)$$

$$\text{Chl a } [\mu\text{g/mL}] = 11.9035 (A_{665} - A_{720}) \text{ for ethanol [258]} \quad (18)$$

Both equations give the concentrations of pigments in the solvent. To obtain the Chl a and carotenoids content in ($\mu\text{g/mL}$ of sample). This essay provided an estimation for the pigment content, which was subsequently validated through HPLC analysis. The values are presented as the mean \pm standard deviation, and the error bars in the Chapter 3 figures represent standard deviations from triplicate measurements.

2.1.9 HPLC Chlorophyll a and carotenoids quantification

The fraction extracted by pure ethanol was filtered by a 0.22 μm polar filter (Reference: WH10462945, Whatman, Buckinghamshire, United Kingdom) and analyzed by the following HPLC method:

The characterization and quantification of Chl a, β -Carotene, Zeaxanthin and, myxoxanthophyll were performed with a 1260 Infinity II- Ultra-High Performance Liquid Chromatography (UHPLC) system from Agilent, equipped with quaternary pumps (model Flexible pump), online degasser, and injection valve with a 20 μL loop. Separation was carried using Poroshell 120 EC-C18 (100x3 mm, 2.7 μm) column from Agilent, a gradient of elution was used at a flow rate of 0.5 mL/min and the column temperature was maintained at 25°C. The gradient of elution consists of a binary solvent mixture system. Solvent A consists of Ethyl acetate and solvent B of Acetonitrile/water (90:10) completed of 0.1% Triethylamine (TEA),

Chapter II : Materials and methods

using a linear gradient program as follows: 100% de A to 100% of B in 20 minutes. The initial conditions are maintained for 5 minutes for stabilization. The autosampler temperature is maintained at 4°C.

After separation, Chl a and carotenoids are detected by a Diod Array Detector at a wavelength of 445nm, and acquisition was further performed between 200 and 700 nm to extract absorption spectra of all the detected compounds. Quantification was performed by external calibration using standard solutions injected in the same conditions. The pigment injections were performed by duplicate.

2.1.10 Phycobiliproteins extraction

A volume equivalent to at least 200 mg of the sample was taken on the last day of the culture and centrifuged in a falcon tube of 15 mL for 10 minutes \pm 2 minutes at 4°C. The supernatant was put apart to be further analyzed and the sample was washed twice with deionized water, to wash away the salts of the pellet. The pellets were rinsed with deionized water to avoid a possible osmotic shock producing an unvoluntary extraction. The pellet was stored and frozen at -20°C, after 24 hours it was defrosted in a water bath at room temperature 25°C \pm 5°C. This procedure is followed when it comes to fresh biomass analysis. In the case of the analysis of harvested biomass a known mass of dry and homogenous samples was put into a falcon tube.

The falcon tube containing the pellet was wrapped with foil paper, to avoid the degradation of the pigments by the room light. 8 mL of phosphate buffer pH 7 (Table 8) was added to the falcon tube and vortexed for 10 seconds.

The samples were placed for 4 hours \pm 0.5 hours at 60 RPM on agitation rollers. For each hour the samples were vortexed for 10 s. This determination was performed by triplicate.

Table 8 Composition of the extraction phosphate buffer pH 7

	K₂HPO₄	KH₂PO₄	NaCl
g/L	2.7868	1.3609	8.766
mol/L	0.016	0.01	0.15

2.1.11 Dry biomass phycobiliproteins extraction

Approximately 0.5 grams of dry biomass were placed in a 50 mL Falcon tube. Subsequently, 20 mL of pH 7.4 phosphate buffer solution (refer to Table 8) were introduced, and the tube was vortexed for 10 seconds. Following this, the tube underwent maceration and gentle mixing for 4 hours at room temperature. Afterward, centrifugation was performed using a Coulter Beckman Model Allegra X-12, rotor model SX4750A, at 4500 RPM for 10 minutes

at 4°C. The process was repeated until no blue traces were left in the biomass pellet. Glass beads were added to the tubes, in order to facilitate the extraction.

2.1.12 Phycobiliproteins spectrophotometer quantification

The falcon tubes containing the extracts were centrifugated (Coulter Beckman, Model Allegra X-12, rotor model: SX4750A, Brea, CA, USA) at 4500 RPM for 10 minutes at 4°C, to sediment the biomass in suspension. 2 mL of the supernatant, were placed in a plastic cuvette. The spectrophotometer was calibrated using the phosphate buffer was used as a blank. The absorbance of the sampled and blank were measured at 562nm, 615nm, and 652nm [219]. The values are presented as the mean \pm standard deviation, and the error bars in the Chapter 3 figures represent standard deviations from triplicate measurements.

The phycocyanin was determined using the following equations from [219];

$$\text{Phycocyanin [g/L]} = (A_{615\text{nm}} - 0.474 \times A_{652\text{nm}}) / 5.34 \quad (19)$$

$$\text{Allophycocyanin [g/L]} = (A_{652\text{nm}} - 0.208 \times A_{615\text{nm}}) / 5.09 \quad (20)$$

$$\text{Phycoerythrin [g/L]} = (A_{562\text{nm}} - 2.41 \times \text{Phycocyanin} - 0.849 \times \text{Allophycocyanin}) / 9.62 \quad (21)$$

2.1.13 Laboratory scale *Arthrospira platensis* CO₂ mitigation characterization

The cyanobacterial strain used in this study was AP SAG-21.99 [1], obtained from The University of Göttingen, Germany culture collection. Except during the maintenance of the inoculum phase, the microorganism was cultivated in a modified ZM, called CFZM in the rest of the document for “Carbonate-Free Zarrouk Medium”. The usual carbon source (NaHCO₃) was omitted from its composition. The mineral carbon of the medium was obtained by the dissolution of the CO₂ from the enriched atmosphere at 5% v/v. The CFZM has the composition displayed in Table 57 Annex p. 225, except for the NaHCO₃ concentration, which was absent in CFZM. In this experiment, the carbon source for biomass development came only from the gas phase. To increase the dissolution of the mineral carbon, the pH of the CFZM was initially set at 9.2 by the addition of 10 mL of NaOH 1M per liter of medium.

2.1.14 Cultivation conditions for the laboratory scale CO₂ mitigation characterization

The inoculum for this experiment was maintained as it follows: Routinely maintained in classical ZM, the studied strain was gently centrifuged (Coulter Beckman, Model Allegra X-12, rotor model: SX4750A, Brea, CA, USA) at 4500 RPM for 5 minutes at 4°C, then rinsed and transferred to the CFZM 72h before the start of each experiment. On the first day of the experiment, 30 mg of biomass were gently separated by centrifugation, from the supernatant and resuspended in 100 mL of the medium for the assays.

Chapter II : Materials and methods

The assays were conducted for 8 days in sterile conditions. Three photoperiod conditions (light/dark) were tested: 12h/12h, 20h/4h, and 24h (continuous light). The cultures were conducted in batch mode in an incubator (INFORS Multitron, Bottmingen, Switzerland) in 250 mL conical flasks under the conditions cited in Table 9.

Table 9 Culture conditions for the laboratory scale CO₂ mitigation characterization

%CO₂ (v/v)	5%
Temperature	35 ° C
Agitation (RPM)	130
Photon Flux density (PFD)	100 μmol/m ² /s
Photoperiod (Light/Dark)	12h/12h 20 h/4 h 24h
Light source	White fluorescent tube (wavelength: 400-700 nm)
Initial pH	9.2
Culture volume	100 mL

The light intensity was measured by a light meter (WALZ, Model ULM-500 equipped with a cosine corrected mini quantum sensor MQS-B, Effeltrich, Germany), the light source was provided by fluorescent light tube (OSRAM, Model Fluora L36W/77, Munich, Germany). Each assay was performed in triplicate, and a flask of CFZM without inoculum (control with neat cultivation medium) was systematically included to have a reference of the CO₂ mitigation phenomena without biological activity.

2.1.15 Sampling for Analytical determinations in the laboratory scale CO₂ mitigation characterization

A culture sample was taken every working day right after the end of the photoperiod light time. The sample was centrifuged (Coulter Beckman, Model Allegra X-12, rotor model: SX4750A, Brea, CA, USA) at 4500 RPM for 5 minutes at 4°C. The supernatant was separated and filtered by a membrane with a pore diameter of 0.22 μm, while the pellet was washed twice with deionized water to remove the salts of the medium. The cell's integrity after the rinsing step was checked visually and under an optical microscope and no cell disruption by osmotic shock was observed.

The pH, Dissolved Inorganic Carbon (DIC), and nitrate concentration were measured from the supernatant, whereas the pellet was used to determine Total Carbon (TC) and biomass dry weight.

2.1.16 Supernatant analysis

2.1.16.1 pH

The pH was measured with a pH meter (Hannah instruments, HI-2020-02, Limena, Italy) calibrated to pH 4, 7, and 10 before each measurement.

2.1.16.2 Dissolved Inorganic Carbon (DIC)

The DIC was determined with a TOC-LCSH system (Shimadzu, Japan) equipped with an 8-channel OCT-L autosampler. Briefly, after a reaction at low pH (<3) in H₃PO₄ 25% (obtained by dilution of the commercial solution 695017 of Sigma-Aldrich, Saint Louis, USA) the carrier gas (Alphagaz Air 1 provided by Air Liquide, Paris, France), is dried and driven to the infrared detection (NDIR) at 65°C. The flow is set at 150 NmL/min. The signal was then compared with the corresponding DIC standards (laboratory-made mix of Na₂CO₃ and NaHCO₃, provided by SIGMA-Aldrich, Saint-Louis, USA, of respective references S7795 and S5761) in the range of 0-100 mgC/L. A dilution was applied to each sample to stay in this calibration range.

2.1.16.3 Nitrate content in the supernatant by Ionic Chromatography (IC)

The nitrate concentration was measured with an ion chromatography (Metrohm, 940 Professional IC Vario, Herisau, Switzerland) equipped with conductivity detection with Metrohm Suppressor Module (MSM) and a Metrosep A Supp 7 column (dimensions: 250 × 4.0 mm, 5.0 μm particle size). The flow rate of the elution solution (Na₂CO₃ 3.6 mM) was set at 0.7 ml/min. and the run time was 35 min. The standard curve was made with a nitrate standard (ref. 74246 provided by Sigma-Aldrich, Buchs, Switzerland) in the range of 1-40 mg/L. Each sample was diluted with deionized water to stay in the calibration range.

2.1.17 Biomass analysis

2.1.17.1 Total Carbon (TC)

To evaluate the total carbon (TC) and total nitrogen (TN) in the biomass, around 50 mg of dry biomass were sampled in the liquid culture, centrifuged, and washed as described in the previous paragraph. The obtained pellet was freeze-dried, and the dry pellet was manually ground with a mortar, to homogenize the particle size. The dry biomass was then suspended in 50 ml of deionized water to be analyzed by the catalytic oxidation method for the total carbon of the instrument (TOC-LCSH Shimadzu, Kyoto, Japan). Briefly, the sample was brought in a combustion chamber maintained at 720°C and the carrier gas (Alphagaz Air 1 provided by Air Liquide, Paris, France) leads the produced CO₂ to a dryer and then the infrared detector (NDIR) heated at 65°C. The flow was set at 150mL_n/min. The standard curve was prepared with potassium hydrogen phthalate (ref. P1088 from Sigma-Aldrich, Saint-Louis, USA) in the range of 0-100 mg/L.

Chapter II : Materials and methods

2.1.17.2 Total Nitrogen (TN)

Regarding TN, the method principle was introduced in the 1.7th paragraph of this document's 1st chapter p.58.

2.1.18 Kinetic parameters and CO₂ fixation rate

The CO₂ fixation rate F_{CO_2} ($mg_{CO_2}/L/d$) is defined as:

$$F_{CO_2} = P_{\text{biomass}} TC \left(\frac{M(CO_2)}{M(C)} \right) \times 1000 \quad (22)$$

Where:

TC: Total Carbon content in the biomass (mc/ m_{DW})

M(CO₂): CO₂ molar mass (g/mol)

M(C): Carbon molar mass (g/mol)

P_{biomass} Biomass productivity ($g_{DW}/L/d$) was determined as (15) in p.75

2.1.19 Statistical Analysis of the determinations in the Laboratory Scale CO₂ mitigation characterization

The values were expressed as the mean \pm standard deviation. Error bars in the figures are standard deviations of triplicate measurements. The data were analyzed by one-way ANOVA. A value of $p < 0.05$ was considered to denote a statistically significant difference. The analyzed variables were the pH, dissolved inorganic carbon (DIC), nitrate uptake, biomass content, and the carbon content in the biomass.

2.1.20 Numerical modeling of *Arthrospira platensis* culture CO₂ mitigation at laboratory scale

As developed in section 1.3 of Chapter 1 p. 27, it is possible to correlate pH, temperature, salinity, and CO₂ partial pressure (ρCO_2) to estimate the carbon speciation and the DIC concentration in a culture medium for a well-mixed culture.

To emphasize the advantages and drawbacks of the culture conditions of AP as a carbon capture technique, a comparison between the DIC species promoted in pure water at 20°C and in CFZM medium of *A. platensis* at 35°C was made. The temperature, salinity, and CO₂ partial pressure were considered for these comparisons are the conditions described for AP culture.

To theoretically estimate the CO₂ uptake in the medium, it was assumed that the cultures were homogeneous and in equilibrium with the incubator atmosphere. The CO₂ dissolution in

water is considered a complex mechanism [259]. This mechanism involves the three concurrent reversible reactions described in equations (23) to (25) below:



In all the above reactions the equilibrium constants K_0 , K_1 and K_2 are typically functions of the temperature and salinity of the medium. The salt concentration in the medium negatively affects the CO_2 solubility because of the ion complex formation between the carbonic ions and the salt ions [59][1]. Thus, the ionization constant of the carbon fractions must be considered. The equations reported by [68] were taken as references for the estimation of pK_0 , pK_1 , and pK_2 , in the cases of pure water at 20°C and CFZM at 35°C (which is close to the usual optimal growth temperature of AP). The considered salinities were 3.54 g of salt per kg of water for the CFZM and 0 g of salt per kg of water for the pure water. To determine the value of each equilibrium constant, equation (26) was applied:

$$K_i = 10^{-pK_i} \text{ for } i \in [0,1,2] \quad (26)$$

By the application of equation (26) to the values of pK_0 , pK_1 , and pK_2 given in [68], the equilibrium constants can be estimated as a function of the temperature and salinity, see Table 10.

Table 10 Equilibrium constants estimated by the equations proposed by [68] temperature and salinity of 20°C and 0 g/kg for pure water and 35°C and 3.54 g/kg for CFZM.

	K_0 (mol/L/atm)	K_1 (mol/L/atm)	K_2 (mol/L/atm)
Pure water at 20°C	0.3916	4.29×10^{-7}	4.29×10^{-11}
CFZM at 35°C	0.0456	1.23×10^{-6}	5.76×10^{-10}

Chapter II : Materials and methods

The CO₂ solubility [H_2CO_3] (mol/L) in the aqueous phase is well described as a function of the CO₂ partial pressure ρCO_2 (atm) in the atmosphere and Henry's constant K_0 (atm L/mol):

$$[H_2CO_3] = \frac{[HCO_3^-][H^+]}{[K_1]} \quad (27)$$

$$[HCO_3^-] = \frac{[CO_3^{2-}][H^+]}{[K_2]} \quad (28)$$

$$[H^+] = 10^{-pH} \quad (29)$$

$$\rho CO_2 = K_0 [H_2CO_3] \quad (30)$$

Knowing the CO₂ partial pressure in the atmosphere of the incubator ($\rho CO_2=0.05$ atm) and the equilibrium constants, the equations (27) to (30) represent a set of 4 equations and 5 unknown variables. A solution is nevertheless possible if the pH of the studied solution is fixed. This condition is experimentally realized through pH measurement. At a given pH and CO₂ partial pressure, the model calculates the concentration of the different carbon species. The total inorganic carbon in the medium phase, DIC (mgC/L), is estimated as follows:

$$DIC = [H_2CO_3] + [HCO_3^-] + [CO_3^{2-}] \quad (31)$$

The equations system was solved using the Matlab R2022a with the Symbolic Math toolbox.

2.1.21 *Arthrospira platensis* CO₂ mitigation in a 3 L system

To characterize the AP biomass culture as a CO₂ mitigation technique, the microorganism was cultivated in the experimental device pictured in Figure 30 for 8 days, under greenhouse conditions. Enriched CO₂ air was employed as the sole carbon source, and CFZM was adopted as a culture medium. CO₂ enriched air was supplied every 3-4 days when pH was greater than 10 and DIC concentration below 350 mgC/L. Adopting a semi-continuous CO₂ approach to compensate for pH increase during the culture. The cultures were continuously bubbled by compressed air. This experiment was made by duplicate.



Figure 30 Experimental device to characterize the CO₂ assimilation in a 3 L system

The carbon assimilation was characterized by employing the following procedure: Before the inoculation, the CFZM pH was set from 7.5 ± 0.5 to 9.2 ± 0.2 by the addition of NaOH 1M, and a 4% CO₂ v/v gas flux was delivered into the medium at 2.5 NL/min until a pH of around 8.3. The concentration of the DIC in the medium was determined by the inorganic carbon method of the TOC-L Series Shimadzu analyzer, the procedure is well described 2.1.16 p. 80 of this document. The CFZM DIC after CO₂ delivery was close to 600 ± 30 mgC/L, this stage in the process ensures no carbon limitation in the culture. Lastly, the pH of the medium was set to 9.2 by basic solution addition to it, and the medium was ready for the inoculation. The initial biomass of the cultures was $0.5 \text{ g/L} \pm 0.08 \text{ g/L}$. The biomass dry weight, pH, and DIC were followed each 24 hours by the methods described in 2.1.5 p.74, 2.1.16.1 p.80, and 2.1.16.2 p.80, respectively. When the DIC in the medium was below 300 ± 50 mgC/L, the enriched CO₂ gas was supplied to the medium bringing pH down to 9.2 ± 0.2 and DIC around to the initial one, 600 mgC/L. The culture conditions of this experiment are displayed in Table 11.

Chapter II : Materials and methods

Table 11 Culture conditions of the experiment characterize the CO₂ assimilation in a 3 L system

Greenhouse conditions	
Type of photobioreactor	5 L transparent glass bottle
Culture volume	3 L
Mean temperature	37 ° C
Agitation	Bubbling
Feed flux (NL/min)	4
Gas	CO ₂ 4% v/v
Average Photon Flux density (PFD)	640 μmol/m ²
Photoperiod (D/N)	15h/9h
Light source	Natural sunlight
Strain	SAG-21.99
Culture medium	Zarrouk medium without initial carbonates
Culture period	8 d
Initial biomass concentration	0.53 g/L

The specific photon flux density (φ) received by the PBR was also considered an influent factor that indirectly affects the carbon mitigation by its impact on the biomass growth, and thus the carbon assimilation in the biomass. This parameter is estimated as shown in (32), it allows to compare the light received by cell in different PBR sizes and configurations. Aiding the culture scale-up, by keeping the light received by cell, thus enabling the approximation of the growth parameters in different PBRs.

$$\varphi = \frac{PFD \times S}{X \times V} \quad (32)$$

Where:

Parameter	Meaning	Unit
φ	Specific photon flux density	μmol/g/s
PFD	Photon flux density	μmol/m ² /s
S	Illuminated surface of the PBR	m ²
X	Biomass concentration	g/L
V	Volume	L

The PFD inside the culture was measured using a spherical quantum sensor (WALZ, Model ULM-500 equipped with a cosine-corrected mini quantum sensor MQS-B, Effeltrich, Germany), the sensor was introduced to the culture, always 5 cm away from the surface, and attached to the bottle glass wall, hypothetically reproducing the light received by the cells when they are directly exposed to light in the limits of the bottle. The bottle dimensions were the following: diameter of 1.82×10^{-1} m and a culture height of 3.15×10^{-1} m, giving a

lightened surface of $1.78 \times 10^{-1} \text{m}^2$. The lightened surface of the bottle was calculated only considering the curved surface.

2.1.22 *Arthrospira platensis* CO₂ mitigation in a 3 m³ system

Photobioreactor description

To characterize the AP CO₂ mitigation potential in a semi-industrial indoor PBR, the pilot system manufactured by Coldep, Montpellier, France, was employed for this experiment, see Figure 31.



Figure 31 3 m³ Raceway Coldep system

This system consists of an 11m² (H×W= 5.5 m × 2 m) raceway photobioreactor coupled to an airlift column. The airlift column comprises an inner tube enveloped by an outer tube. The liquid medium ascends through the inner tube (indicated by blue arrows), facilitated by a vacuum pump operated with air. Once the liquid finds its higher point, thanks to gravity it goes down through the exterior tube (red arrows). Subsequently, the medium is bubbled by CO₂ enriched air at the column output, and it leaves the column. The medium initiates its route through the raceway. The medium then traverses the raceway. It is hypothesized that the CO₂ bubbles travel several meters in the raceway, prolonging their stay within the culture medium. This extended retention time is expected to enhance the assimilation of gas into the medium and promote biomass growth.

Chapter II : Materials and methods

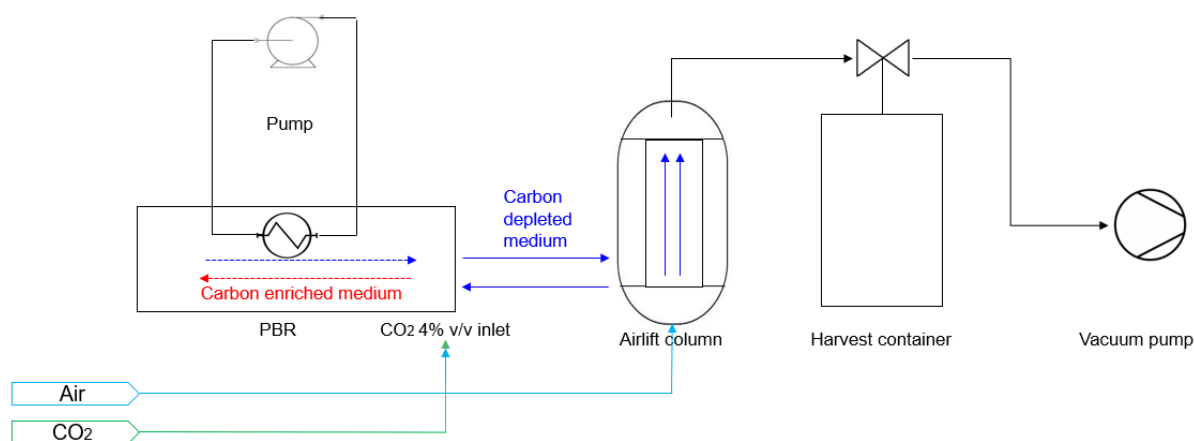


Figure 32 Coldep system diagram; CO₂ feed was performed from the output of the column. The blue arrows represent the inner tube, and the red arrows represent the exterior tube.

The main role of the column in the system is to assure the homogeneity of the nutrients in the medium, to compensate for the excess of certain dissolved gasses such as O₂, and to create the height difference that moves the culture inside the raceway. The column can also be employed for preconcentration of the biomass during the harvest.

2.1.23 3 m³ culture conditions

The culture was developed by employing a modified ZM, with a carbon concentration 7 times lower than the one in ZM, as shown in Table 12. The initial carbonate salts had a main role in maintaining the culture's pH without employing a strong base solution. A CO₂ enriched gas was supplied to the medium once the DIC concentration in the medium was below 0.3 g/L, aided by the column of the Coldep system. Each injection was of 2.6 NL CO₂/min and performed for 1 hour 30 minutes under greenhouse conditions during October and November 2021 at Saint-Paul-lez-Durance in Bouches-du-Rhône, France.

Table 12 Culture medium composition for the 3 m³ culture compared to the Zarrouk medium composition

Nutrient	Modified ZM (mg/L)	ZM Standard reference (mg/L)
CO ₃ ²⁻	2500	12000
C	500	8800
NO ₃ ²⁻	125	1824
PO ₄ ³⁻	52	273

The culture was performed for 50 days in green-house conditions, temperature was kept at 33°C ± 5°C thanks to a heat exchanger installed inside the Raceway. The culture conditions are

displayed in Table 13. The mean PAR was estimated considering the average PAR received for 24h, night included.

Table 13 Greenhouse culture conditions for the gaseous carbon input experiment in the 3 m³ system

Strain	SAG-21.99
V_{total}	3 m ³
Agitation speed	22 m/min
Mean temperature	28-38°C
Gas	CO ₂ 4% v/v
Photoperiod (D/N)	10 h /14 h
Light source	sunlight
Mean PAR over 24 hours (μmol/m²/s)	<100
Initial biomass concentration	0.3 g/L
Initial pH	8
Culture period (day)	50

2.1.24 3 m³ culture sampling

One sample was taken at three different spots of the raceway before and after each injection at the output of the column (Red arrow in Figure 32 p.87), to follow the following parameters: ΔDIC (Dissolved inorganic carbon differential), ΔDOC (Dissolved organic carbon differential), dry weight, NO₃²⁻ and PO₄³⁻. The DIC and DOC were determined by the total carbon method of the TOC-L Series Shimadzu analyzer, described in 2.1.16.2 p.80, the dry weight was determined by the method described in 2.1.5 p.74, and the NO₃²⁻ by ion chromatography, as described in section 2.1.16.3 p.80. The pH, temperature, dissolved oxygen, and conductivity were tracked every 15 minutes by online sensors (SC1000 Probe Module, 4 Sensors with Conduits, Prognosys, Modbus RS485, 110-240VAC with Conduits, Lange HACH, Ames, Iowa, USA). The photosynthetic active radiation (PAR) in the photobioreactor was measured with a spherical quantum sensor (WALZ, Model ULM-500 equipped with a cosine-corrected mini quantum sensor MQS-B, Effeltrich, Germany).

2.1.25 Carbon mass balance for culture CO₂ assimilation

The assessment of CO₂ mitigation through AP cultivation considered two pathways of carbon integration: chemical absorption and biological assimilation facilitated by AP. To facilitate the characterization of this phenomenon, four carbon mass balances were suggested. These include, a global carbon mass balance, one specifically addressing chemical absorption,

Chapter II : Materials and methods

one addressing the integration of the CO₂ in the biomass, and another exclusively focused on the Dissolved Inorganic Carbon (DIC) biological assimilation. The initial carbon conditions were measured experimentally: an initial DIC from the carbonated salts in the culture medium, an initial Dissolved Organic Carbon concentration (DOC) resulting from biomass metabolism in the culture medium, and an initial carbon content derived from the biomass constituting the present biomass in the medium, estimated as proposed by [260]. These three parameters comprise the total carbon (TC) measured. The injected CO₂ is assumed to undergo transformation in the medium, giving rise DIC, which serves as the available carbon source for biomass development. Additionally, it can result in the production of DOC, representing organic molecules excreted by the biomass metabolism, or the biomass itself, including AP cells. It is hypothesized that the PBR is perfectly homogeneous, and in stationary regime. These carbon mass balances are only valid for the moment right after the CO₂ injection into the PBR. The global process is schematized in Figure 33.

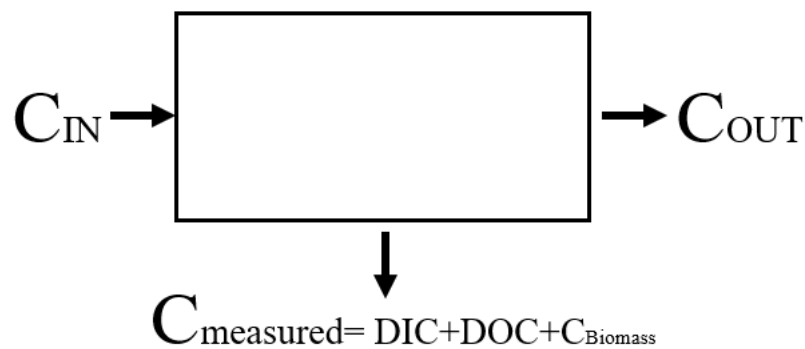


Figure 33 Schematic representation of the global carbon mass balance. The rectangle represents the photobioreactor content.

To track the changes in these parameters after CO₂ injection, the measured values were consistently subtracted from their respective initial conditions. The DIC and DOC were measured exclusively from the filtered medium, employing the technique described in 2.1.16.2 p.80. The DOC concentration was systematically neglected in the estimations due to its low value compared to the other carbonated species. The biomass carbon content was estimated by determining the dry biomass of the culture, as described in section 2.1.17.1 in p.80. The following equation was applied, considering that 50% of the dry biomass is constituted by carbon.

$$C_{biomass} = X_{biomass} \times V_{sample} \times \left(\frac{0.5}{M(C)} \right) \quad (33)$$

Where,

Variable	Meaning	Units
$C_{biomass}$	Carbon content produced in the biomass between 2 injections	mol
$X_{biomass}$	Biomass content	g/L
V_{sample}	Sample volume	L
$M(C)$	C molar mass	g/mol

For the global carbon mass balance it was considered that the measured DIC, DOC and $C_{biomass}$, constitute $C_{measured}$.

$$C_{measured} = DIC + DOC + C_{biomass} \quad (34)$$

So the following equation can be applied:

$$C_{IN} = C_{measured} + C_{out} \quad (35)$$

Where,

Variable	Meaning	Units
C_{IN}	Carbon introduced by the CO ₂ injection	mol
C_{OUT}	Desorbed or sedimented carbon	mol

The term C_{OUT} represents the carbon that was not measured due to desorption into the atmosphere or sedimentation in form of non-soluble salts, as seen in Figure 33 from p.89. The global CO₂ fixation efficiency is defined as:

$$\eta_{global} = \frac{C_{measured}}{C_{IN}} \quad (36)$$

Regarding the mass balance for evaluating CO₂ chemical absorption exclusively in the culture medium, it is assumed that the injected CO₂ is entirely fixed as DIC and DOC in the medium. Any remaining CO₂ is either desorbed into the atmosphere or sedimented as insoluble carbon forms resembling salts. So absorbed carbon is defined like:

$$C_{absorbed} = DIC + DOC \quad (37)$$

Chapter II : Materials and methods

DIC and DOC are measurable parameters, and their initial values are consistently subtracted from the values measured after CO₂ injection into the medium. The CO₂ chemical absorption mass balance is established as follows:

$$C_{IN} = C_{absorbed} + C_{out}^{lost} \quad (38)$$

$$\eta_{medium} = \frac{C_{absorbed}}{C_{IN}} \quad (39)$$

Where,

Variable	Meaning	Units
C_{out}^{lost}	Carbon desorbed or in sedimented salt form	mol

Regarding the carbon mass balance to assess CO₂ assimilation in biomass, it was assumed that injected CO₂ is fully incorporated into the biomass, with any excess being released into the atmosphere. The mass balance is established as follows:

$$C_{IN} = C_{biomass} + C_{out}^{lost} \quad (40)$$

$$\eta_{assimilation} = \frac{C_{biomass}}{C_{IN}} \quad (41)$$

In concluding the assessment of AP growth's contribution to CO₂ fixation in the medium, we consider an ideal scenario where DIC is entirely converted into biomass through the photosynthetic efficiency of AP cells. Any remaining DIC concentration in the medium is not utilized for biomass formation. The initial DIC condition was systematically subtracted from the measured value after the CO₂ injection. Thus, the following term is defined:

$$DIC_{ideal} = DIC + C_{biomass} \quad (42)$$

$$\eta_{biomass} = \frac{C_{biomass}}{DIC_{ideal}} \quad (43)$$

2.2 Phase I: Enhancement of pigment productivity in *Arthrospira platensis* cultures by photoperiod modification

This section outlines the methodology used to assess the influence of photoperiod on biomass growth and pigment content under controlled and natural conditions. Initially, the strain's response to photoperiod variations was examined at the laboratory scale. The most favorable photoperiod, determined based on pigment content, was then replicated in greenhouse conditions using LED lighting. Finally, this optimized photoperiod was implemented in a 300L PBR for the production of AP biomass in preparation for the next project stage, valorization (Figure 34). This experiment aims to respond to the following questions: *What is the influence of the photoperiod in biomass growth and pigment accumulation?*

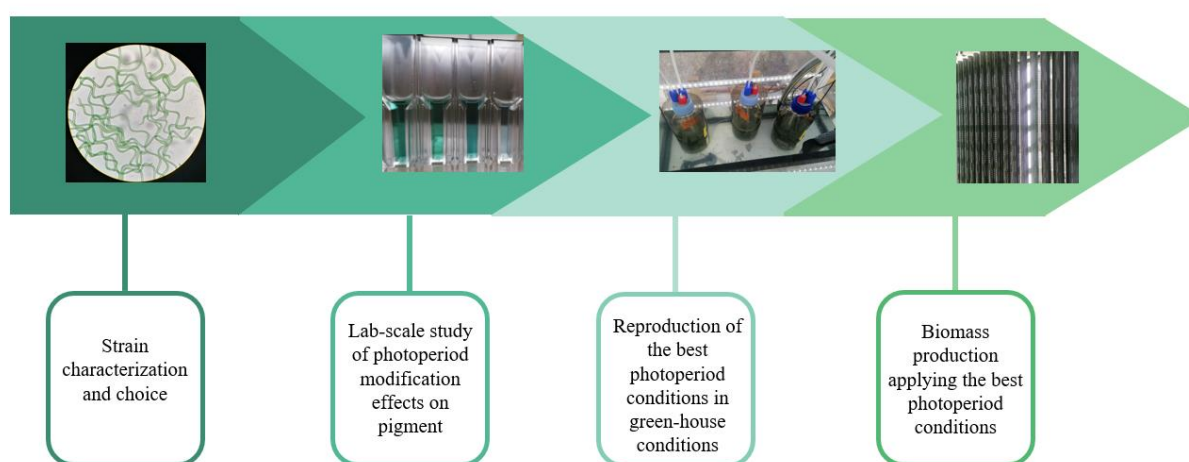


Figure 34 Experimental strategy to optimize the pigment productivity in *A. platensis* culture

2.2.1 Artificial light conditions seed culture for the photoperiod modification experiment

The selected work conditions for this part of the experiment are the same described in section 2.1.14, p.78.

2.2.2 Artificial light culture conditions

The growth kinetics with CFZM and ZM media were performed in parallel. The cultures were followed for 8 days for each studied photoperiod at the same incubator conditions of the seed culture. Each culture condition was made in triplicate.

2.2.3 Artificial light conditions sampling

One sample of the cultures was taken daily from each triplicate after the end of the light period and the beginning of the dark period. The evaporated and lost volume was compensated by the addition of distilled water. The sampling schedules are shown in Table 14.

Chapter II : Materials and methods

Table 14 Photoperiod experiment sampling schedule

Photoperiod (light/dark) *	Day starts (time: h)	Day ends (time: h)	Sampling (time: h)
12h / 12h	21	9	9
16h / 08h	16	8	9
20h / 04h	14	10	9
24h / 0h	/	/	9

(d/n) *: Day/night

2.2.4 Natural light conditions experimental set-up

The experimental set-up to compare the photoperiod effects under natural light with the artificial light complement was developed under two small-scale greenhouses for 8 days. One greenhouse was intended for the control group and the other one for the test group. The control group was exposed to only natural light with a natural photoperiod of 12h/12h. The test group was constantly illuminated by LED lights which complemented the natural sunlight during the daytime.

Both greenhouses were placed one next to each other orientated to the southeast as shown in the diagram in Figure 35. Enough space was left between both of the greenhouses to avoid unintended light from the LEDs to the control greenhouse.



Figure 35 Small-scale greenhouses position diagram. The two yellow dots represent the position of both of the systems. Natural light conditions seed culture

Both of the greenhouses were composed of the following elements (See Figure 36): 1) 1L glass square bottle by triplicate (photobioreactor), 2) Air inlet, 3) Water bath, 4) Heating resistance, 5) Inlet and outlet of the cooling system, 6) Temperature sensor, 7) PAR sensor, 8)

LED lights, 9) Shading bottle, 10) Plastic greenhouse. This experiment was done by triplicate. A control system with the without light complement was followed in parallel.

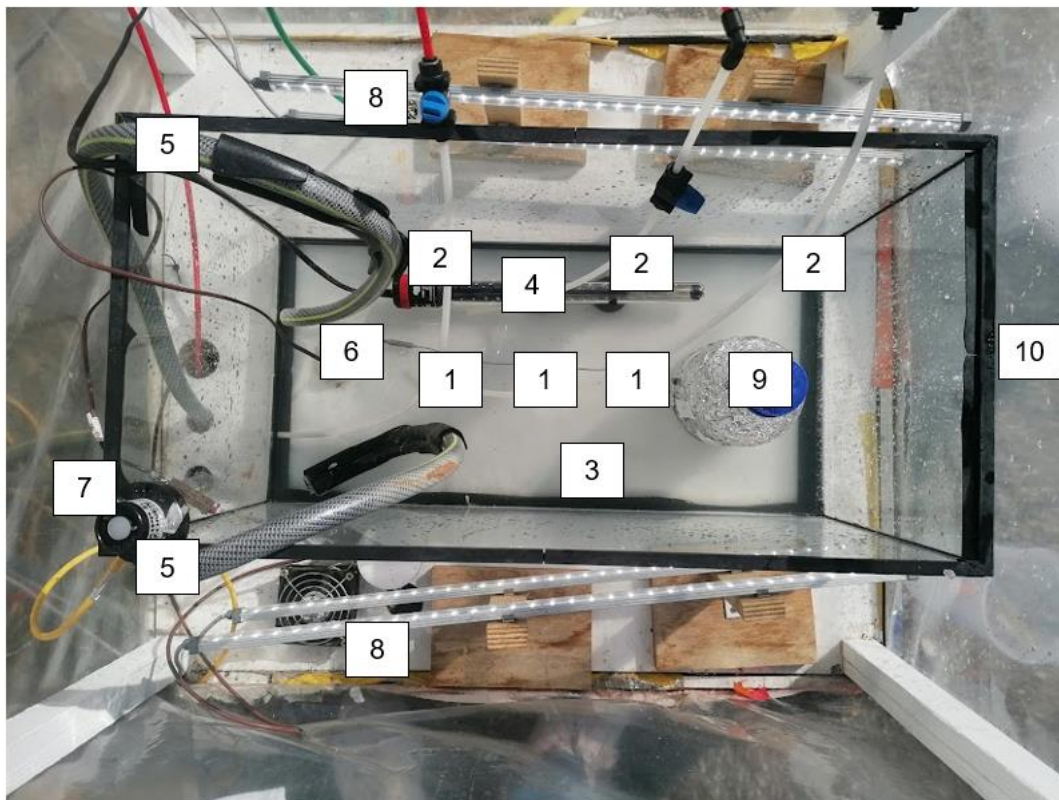


Figure 36 Small-scale greenhouse system for the evaluation of photoperiods in natural light conditions

The cultures were performed on identical square 1L glass bottles with the following dimensions: 222 mm in height, and 94 mm side, a culture volume of 900 mL, an illuminated culture surface of 0.06m², leading to a surface volume ratio (S/V) of 25. The cultures were constantly agitated by an airflow of 5 mL/min at the air inlet. The temperature in the system was maintained at a maximum temperature of 38°C during the daytime and a minimum temperature of 32 °C ± 5°C during the nighttime by the cooling system and heating resistance. The temperature evolution was recorded in each bottle by a thermocouple every 30 seconds during the experiment.

The continuous light cultures were exposed to 24 hours of natural light complemented by artificial light provided by a group of LEDs placed at each side of the cultures. The PAR evolution was recorded every 30 seconds by the PAR sensor. The light spectrum is shown in Figure 37. The continuous light system received a mean PAR of 1200 μmol/m² s during the daytime and a PAR of 200 μmol/m² s during the nighttime. On the other hand, the control system received only natural light, during the 12 natural daytime hours. The mean PAR received by the cultures in control conditions during the daytime was 900 μmol/m² s, whereas the PAR

Chapter II : Materials and methods

during the nighttime was $50 \mu\text{mol}/\text{m}^2 \text{ s}$, coming from different artificial light sources around. Both experiments were developed in parallel during September 2022 in Saint-Paul-Lez-Durance, Bouches-du-Rhône, Provence-Alpes-Côte d'Azur, 43.6977730503322, 5.734236734420879.

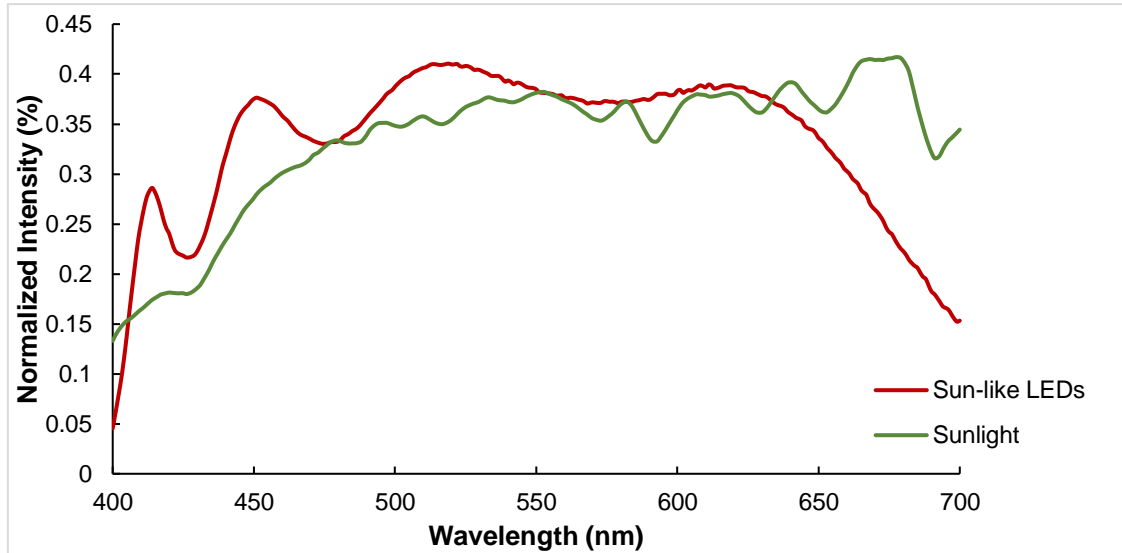


Figure 37 Natural Light spectrum of the light received by the small-scale greenhouses

2.2.5 Natural light conditions seed culture

Two seed cultures were prepared for this experiment, one for the control and one for the test conditions. Both of the seed cultures were put into the experiment conditions which are displayed in Table 15 for one week during September 2022. Once the culture was in the exponential phase, experiment cultures for each triplicate were started at an initial biomass content of 0.3 g/L .

Table 15 Natural light conditions seed culture parameters

Culture medium	Zarrouk medium
Agitation Air flux (mL/min)	5
%CO₂	1
Temperature (°C)	30-38
Mean PAR daytime ($\mu\text{mol}/\text{m}^2 \text{ s}$)	900 (Natural light)
	200 (Artificial light)
Photoperiod (light /day)	Control: 12 h/12 h
	Test: 24 h/0 h
Initial pH	9.2

2.2.6 Sampling and analysis

A sample of 10 mL of previously homogenized culture was taken daily during the 8 days of this experiment, to analyze the biomass and supernatant of the samples separately. The biomass growth was followed as described in sections 2.1.6 p. 74, and the PBP content, as described sections in 2.1.10 and 2.1.12, in p.77 and 78, respectively.

Concerning the supernatant characterization, pH was tracked as described in section 2.1.16.1 p. 80. DIC and NO_3^{2-} were followed by applying the protocols defined in paragraph 2.1.16.2 p. 80 of this chapter.

The evaporated water volume was replaced daily with distilled water.

Chapter II : Materials and methods

2.3 Phase II: *Arthrospira platensis* production for green solvent extractions

This section outlines the experimental setup used to cultivate biomass for green solvent extractions. After identifying optimal culture conditions for maximizing AP culture in terms of biomass and pigment productivity, the SAG-21.99 strain was grown in a closed tubular photobioreactor of 285 L. This cultivation aimed to produce sufficient biomass for subsequent valorization in the project's next stage.

2.3.1 *Arthrospira platensis* culture for application of biomass valorization techniques

This culture system was completely automated, with regulated temperature, photoperiod, light intensity, pH, and agitation. The reactor was composed of a series of interconnected tubes mixed by an airlift system that favored the mixing and push of the culture through the tubes. The PBR is pictured in Figure 38.



Figure 38 Tubular photobioreactor (JUMBO, Synoxis Algae, France) employed for the biomass production for extraction tests

The biomass was cultivated for 15 days, the culture conditions of this experiment are displayed in Table 16.

Table 16 *Arthrospira platensis* culture conditions for project biomass valorization

Strain	SAG-21.99
Medium	Zarrouk medium/4
V_{total}	270 L
Type of agitation	Airlift
Mean temperature	35°C ± 5°C
Photoperiod (Light/Dark)	24 h (Continuous)
Light source	Sunlight + LED lamps
Mean PAR (μmol/m²/s)	300-600
Initial biomass concentration	0.3 g/L
pH	9.5-10
Culture period (day)	15

The biomass and medium composition were monitored by applying the protocols described in paragraphs 2.1.16 p.80, 2.1.5 p.74, and 2.1.10 p.77, for NO₃²⁻ in supernatant, biomass development, and PBP analysis, respectively. When the culture reached 3 g/L, half of the culture was harvested, and the other half was completed with new medium, to harvest a 2nd time one week later.

2.3.2 *Arthrospira platensis* biomass harvesting for biomass extraction

The biomass volume was reduced by 80% wt through a pre-harvesting step, by pumping it into the membrane filter with a pore diameter of 0.2 μm (Vibro-I, Sani Membranes, Farum, Denmark) at an operator pressure of 0.2 bar and a culture flow of 0.7 L/min. The culture was transported with the aid of a sanitary pump Tapflo, Kungälv, Sweden at 10 L/min. Once the biomass was concentrated, the biomass was centrifuged in a centrifuge Coulter Beckman, Model Avanti J-26S, rotor model JLA-8.1000, Brea, CA, USA) at the following conditions 7000 RPM for 20 minutes, speed increase slow and speed decrease fast. After centrifugation, the biomass water content was 20 wt/v.

2.3.3 *Arthrospira platensis* biomass drying for biomass extraction

2.3.4 Drying efficiency test

The drying technique choice was made by comparing 3 drying methods: lyophilization, spray drying, and convection hot-air drying (Air-flow). The efficiency of each process was verified by weighting the biomass mass before and after the applied drying technique, and equation (44) was applied. This experiment was performed in triplicate.

$$\eta_{drying} = \frac{m_{initial} - m_{out}}{m_{initial}} \times 100 \quad (44)$$

Chapter II : Materials and methods

Where;

Variable	Meaning	Unit
η_{drying}	Drying efficiency	%
$m_{initial}$	Biomass mass before the drying process	g
m_{out}	Biomass mass after drying process	g

The drying method choice was also made as a function of its impact on the PBP content in the sample. After the drying process, the PBP protocol described in 2.1.10 p.77 and 2.1.12 p. 78 was applied to a dry biomass of 100 mg. This experiment was performed in triplicate.

2.3.5 Lyophilization

Around 4 g of biomass was frozen at -20°C for at least 24 hours \pm 6 hours, the frozen biomass was introduced into the freeze-dryer (Cosmos, Cryotech, Saint-Gély-du-Fesc, France) with a cold-trap at -80°C and a depressurization of around 0.07 mbar in a plastic plate, as shown in Figure 39. The biomass mass before the freeze-dryer and after it was registered to characterize the drying efficiency of the process. This experiment was performed in triplicate.

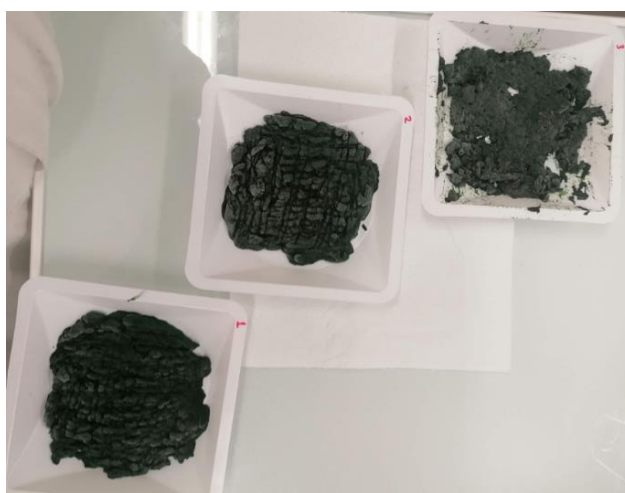


Figure 39 Frozen biomass for freeze-drying process test

2.3.6 Spray-dryer

The biomass after centrifuge was brought to a concentration of 170 g/L by adding biomass water to the sludge. The concentrated biomass was then introduced into the spray-drying equipment Mini Spray Dryer B-290 (BÜCHI, Flawil, Switzerland), at the operation conditions displayed in Table 17. The biomass water content was verified after the process to know the efficiency of the process. This experiment was performed in triplicate.

Table 17 Spray-dryer operation conditions

Parameter	Value
Inlet air temperature (°C)	100
Outlet air temperature (°C)	54
Air flow rate (L/h)	138
Aspirator output in % max. of its aspiration rate	70
Pump speed in % of its aspiration rate	100
Nozzle cleaner rate	2

2.3.7 Air-flow drying

The equivalent to $2 \text{ g} \pm 0.14 \text{ g}$ of biomass sludge after centrifuge was put into a mass-known pierced plastic cup. The plastic cup openings permitted the airflow to pass through the sample. The device's hot-air temperature was set to 50°C . The airflow parameter (Homday food dehydrator, Bordeaux, France), could not be changed in this model. The process was stopped until the 5th hour. The biomass was weighted and registered. This experiment was performed in triplicate.

2.4 Phase II: Biomass characterization

This section describes the methodology used to characterize the biomass composition.

The dry biomass was homogenized by mortar and sieved into particle diameter fractions of 300-500 μm , to then characterize its biochemical composition, PBP was characterized as described in section 2.1.10 p. 77, Chl a, and carotenoids as described in section 2.1.7 p.75, proteins as described in section 2.1.17 p.80, applying the nitrogen-protein conversion factor of 6.25 reported in [261]. The methods employed to determine the biomass moisture, total lipids, sugars, and ashes are reported in the following paragraphs.

2.4.1 Biomass moisture

A determined mass of biomass after drying was disposed into a mass-known aluminum cup. The cup with the biomass was introduced into an oven at 100°C for 20 hours \pm 4 hours. The cup with the biomass was weighted and the mass difference was registered. The moisture fraction was determined by weight difference. As it follows, the essay was performed in triplicate.

$$x_{water} = \frac{m_0 - m_1}{m_0} \quad (45)$$

Where;

Variable	Meaning	Unit
x_{water}	Water fraction	
m_0	Biomass mass before the oven	g
m_1	Biomass mass after the oven	g

2.4.2 Total lipids

This method was adapted from the one reported in [262]. 20-50 mg of dry and homogenized biomass was put into a glass tube, and 3 mL of Hydrogen Chloride solution 3 M in methanol (transesterification agent) was added to the tube with 0.2 ml of the standard fatty acid 3 mg/mL TAG-C15 (Sigma T4257, tripentadecanoin) in methanol. The tube was put into a water bath at 85°C for 1 hour. The sample was chilled and 3 mL of pure hexane were added, the tube was vortexed for 10 seconds and 1 mL of pure water was added before being vortexed again. Finally, the tubes were centrifuged for 5 minutes at 1500 RPM. Hexane clarity is crucial, as it must be free of biomass. The upper phase of the supernatant (hexane) was transferred to a vial to be then analyzed by GC-FID (GC-2010 Pro AOC-20i/AOC-20s, Shimadzu, Kyoto, Japan. The reaction is shown in Figure 40. This test was made in triplicate in each sample. A blank test with no biomass was conducted systematically. The total lipid concentration was determined by the addition of the peak areas detected and correlated to the area of the known concentration of the chosen internal standard TAG-C15 in all the samples.

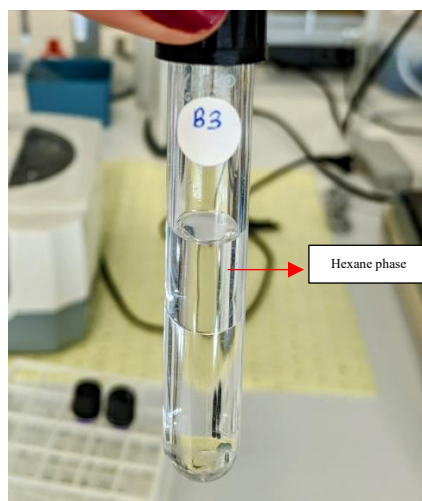


Figure 40 Lipid extraction method reaction

2.4.3 Sugars

This method was adapted from the one developed by [220]. Between 3-5 mg of biomass was put in solution with H_2SO_4 1.25M to achieve a concentration of 0.5 mg biomass/mL. The solution was then vortexed for 10 seconds and placed into a block heater at 100°C for 3 hours, to accomplish the hydrolysis of the sample. The samples were chilled, and filtered through a membrane of $0.22\ \mu\text{m}$ porosity. $50\ \mu\text{L}$ of the permeate was mixed with $450\ \mu\text{L}$ of pure water into clean glass tubes. A positive sample was made with a glucose concentration of $0.5\ \text{mg}_{\text{glucose}}/\text{mL}$.

A glucose calibration curve from 0.02 - $1\ \text{mg}_{\text{glucose}}/\text{mL}$ was prepared with pure water. $500\ \mu\text{L}$ of the sample was mixed with $500\ \mu\text{L}$ of phenol aqueous solution at 5% wt/v, and 2.5 mL of concentrated sulfuric acid was added directly to the liquid surface. The reaction was incubated for 10 minutes at room temperature and for 30 minutes at 35°C in a water bath. The reaction was vortexed every 5 seconds for 5 minutes. 1 mL of the reaction was transferred to a 24-well plate. The reactions were read at 483 nm in a spectrophotometer (Epoch 2, Biotek, Winooski, USA), and the absorbance co-related to the calibration curve. The result of the reaction is shown in Figure 41. Each measurement was made in triplicate.

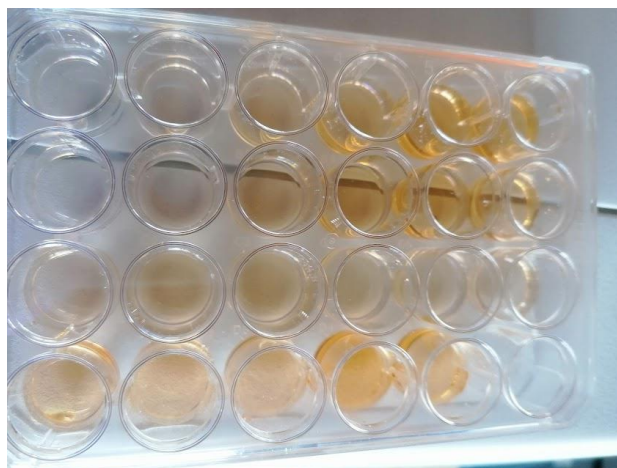


Figure 41 Sugar quantification in biomass reaction

2.4.4 Ashes

Previously dried and homogenized biomass was weighed and put into the furnace in a porcelain cup of known mass. The furnace ramping program was turned on to a target temperature of $575^{\circ}\text{C} \pm 25^{\circ}\text{C}$ for 24 ± 6 hours. The ramping program consisted of ramping from room temperature to 105°C , hold for 12 minutes, ramping to 250°C at 10°C per minute, hold for 30 minutes, ramping to 575°C at 20°C per minute, hold for 180 minutes, allow temperature to drop to 105°C and hold until samples are removed. After furnace removal, the ashed samples were introduced carefully in a desiccator for at least 3 hours ± 0.5 hours. The new weight, corresponding to the ashes proportion was recorded. The measurements were made in triplicate.

$$x_{ashes} = \frac{m_{ashes}}{m_{biomass}} \quad (46)$$

Where;

Variable	Meaning	Unit
x_{ashes}	Ashes fraction in biomass	
$m_{biomass}$	Biomass weight	g
m_{ashes}	Ashes	g

The values were expressed as the mean \pm standard deviation. Error bars are standard deviations of triplicate measurement.

2.5 Phase II: Green solvent *Arthrospira platensis* valorization

2.5.1 Valorization of hydrophilic pigments in *Arthrospira platensis* biomass

This section outlines strategies for achieving a project goal: enhancing extraction efficiency, preserving antioxidant properties in obtained extracts, and employing sustainable techniques such as green solvent extraction. In this stage, an exploratory test at 40°C and 50% ethanol v/v was performed to characterize the extraction with the laboratory scale pressurized liquid extractor Accelerated Solvent Extractor (ASE) 350 (Dionex Thermo Scientific Waltham, Massachusetts), was employed to explore pigment extraction. Then the target pigments were PBP, Chl a, and carotenoids (especially β -carotene, and zeaxanthin) employing ASE in a large temperature range, from 60-120°C, and a solvent mixture of ethanol/water from 80-100% v/v to target the condition range where the process favors high the extraction efficiency and antioxidant activity of the extracts. This strategy to use first the ASE apparatus has been adopted because this method requires less biomass quantity and allow performing automated and rapid assays. The process is schematized in Figure 42.

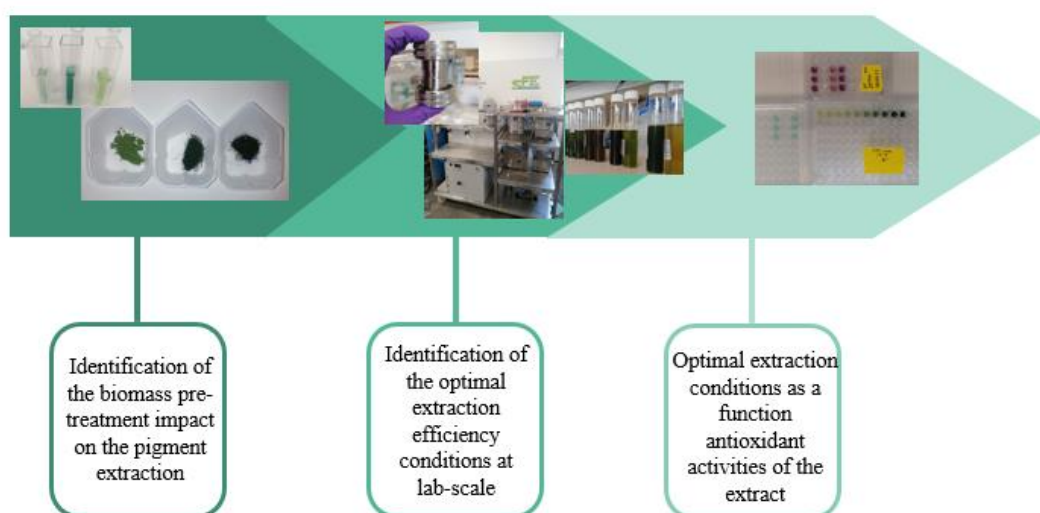


Figure 42 Experimental campaign to valorize *Arthrospira platensis* biomass by pressurized liquids.

Two separate sets of experiments were conducted, sets A and B. In set A the biomass was first valorized by ASE (raw-biomass), secondly, the PBP present in the residual biomass were extracted as described in section 2.1.10. In set B, biomass was first treated using the PBP selective extraction method previously mentioned, to secondly extract the left pigments by ASE (*PBP-free biomass*). Antioxidant activities were quantified from the ASE extracts in both of the sets as shown in Figure 43. This experiment seeks to answer the following questions: *what are the optimal temperature and solvent to boost the extraction efficiency keeping a satisfactory antioxidant activity? Towards a biomass biorefinery, what is the optimal extraction order to upgrade the valorization AP HVM like the pigments, lipids and antioxidant molecules?*

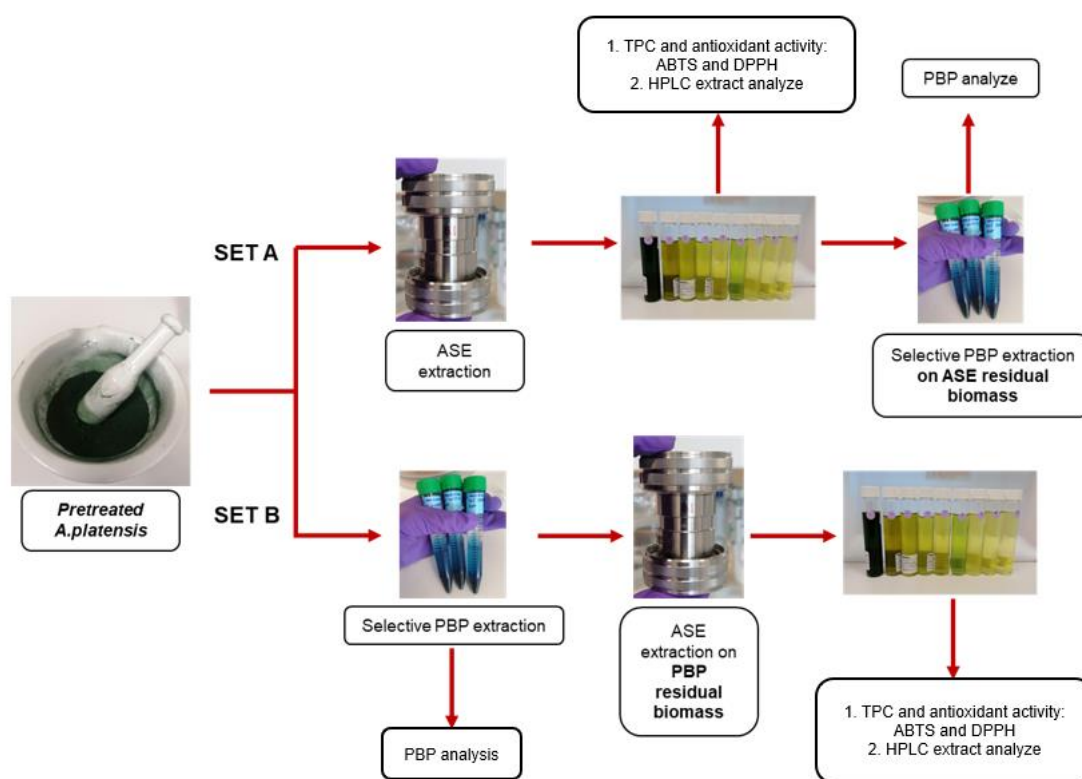


Figure 43 Illustration of set A and B strategies operated with Accelerated Solvent Extraction method

2.5.2 Configuration of ASE extraction cells

The AP biomass used for the extraction was cultivated as described in section 2.3.1 p. 97. The obtained biomass was characterized employing the methodology described in section 2.4 p. 100. The biomass was harvested as described in the section 2.3.2 in p. 98, and dried by lyophilization as described in the section 2.3.5 in p.99. The treated biomass was disposed into a stainless steel extraction cell of 22 mL. The cell was filled under the following proportions: 0.5g of dry biomass mixed with 1.5g of silica beads, and a final layer of 1g of diatomite followed by a paper filter of 50 μm , as reported in [174]. The silica served as filler while the diatomite acted as a protection layer between the biomass and the membrane at the bottom of the cell (Figure 44). It can be highlighted here that the use of such a high proportion of filler and of diatomite as a protection layer is specific to ASE being a method employed for analytical purposes. When PLE is used in semi-continuous mode as an extraction method, the filler proportion is more about 5-10 wt% and a protection layer is not required.

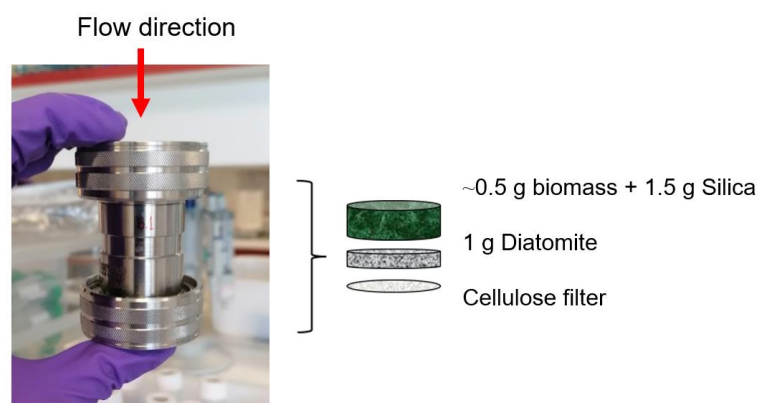


Figure 44 ASE Extraction cell disposition

2.5.3 Phycobiliprotein extraction before ASE

The analytical extraction of PBP was carried out on the biomass before ASE extraction for set B, and post-ASE extraction for set A. This essay was conducted in the following way: 0.5 ± 0.08 g of dry biomass, combined with 1.5 ± 0.02 g of silica beads, was placed into a 50 mL Falcon tube and mixed with 20 mL of phosphate buffer solution at pH 7.4 (Table 9). The biomass:solvent proportion was 1:40, after solvent addition the mixture was macerated and gently mixed for 4h at room temperature. The tubes were centrifuged (Coulter Beckman, Model Allegra X-12, rotor model: SX4750A, Brea, CA, USA) at 4500 RPM for 10 minutes at 4°C. The extract was placed in a plastic cuvette (1 cm optical path). The supernatant containing the pigments was collected and diluted with phosphate buffer to achieve an absorption measure lower than 0.9 at 562 nm. The spectrophotometer was calibrated using the phosphate buffer as a blank. The PBP content in the samples was quantified as described in section 2.1.12 in p.78.

2.5.4 Selective lipophilic pigment extraction of the initial biomass

This aspect of the experiment primarily aimed to establish a reference concentration for the carotenoids and Chl a extractable from the biomass. The values obtained in this experiment are regarded as the maximum reference pigment concentrations. The extraction methods for Chl a and carotenoids described in 2.1.7 were reproduced.

2.5.5 Accelerated Solvent Extraction (ASE) device

The extractions were performed in the Dionex ASE 350 Accelerated Solvent Extractor illustrated in Figure 45. The work pressure was 103 bar for all the performed extractions. The solvent employed for the extractions was an ethanol/water solution with ethanol concentration in the range of 50-100% v/v. In the first place, 40°C extractions were performed to explore the pigment extractability at this temperature. Secondly, a central composite experiment was performed in a temperature range between 60-120°C, with a selected extraction time of 30 minutes, and a standard extraction mode in the extractor settings. This mode performs a unique

Chapter II : Materials and methods

batch extraction that delivers a volume of 20 mL for the first extraction, 15 mL of rinsing solvent, giving a total sample volume of 35 mL. The standard extraction mode consists of the following steps: 1) oven preheating to the selected temperature, 2) load of the collection vial, 3) the oven reaches the set point, the cell is moved into the oven and the pump fills the cell with solvent. 4) The static valve remains closed, and the pump continues pumping until the pressure reaches 10 MPa. 5) 5-minute heat step occurs, followed by the first 30-minute static step. 6) After the static step, the static valve opens, the extract is expelled and the pump rinses with 12 mL of fresh solvent through the cell. 7) The method ends with a 60-second nitrogen purge step.

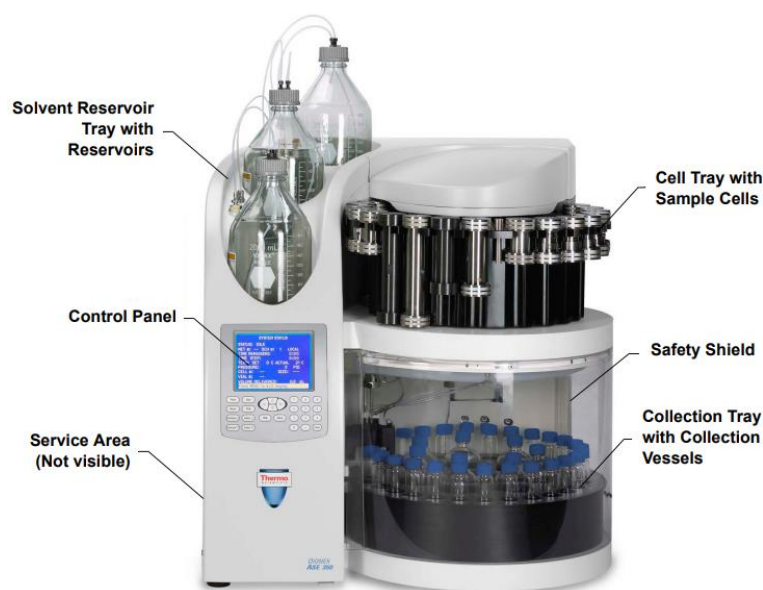


Figure 45 Accelerated Solvent Extraction device, reproduced from [263]

2.5.6 Central composite design (CCD)

The CCD was applied to optimize pigment extraction from the biomass and the antioxidant activity of the obtained extract. The CCD was applied to a solvent concentration between 80-100% ethanol v/v and temperature between 60-100°C. The function parameters applied for the CCD were defined as reported in Table 18. The statistical analysis of the responses was performed by calculating the central point standard deviation. This standard deviation was applied to the rest of the responses.

Table 18 Azurad inputs for Central Composite Design study

Parameter	Definition
Domain shape	Cubic
Function	2 nd -degree polynomial function
Matrix	Composite
No. center points	3

For this study two factors were evaluated, temperature and solvent concentration, as displayed in Table 19.

Table 19 Domain definition for Central Composite Design study

	Factor 1	Factor 2
Factor name	Temperature (°C)	Ethanol concentration v/v (%)
Domain center	75	90
Variation step	15	10
Studied responses	<ul style="list-style-type: none"> • Total pigment extraction yield (%) • Chlorophyll, Zeaxanthin, and β-carotene extraction yields (%) • Total Phenolic Compounds (GAE/g_{extract}) • Antioxidant activity: ABTS • Antioxidant activity: DPPH 	

The experimental points generated by the CCD are shown in Table 20, the central points No. 9, 10, and 11 are considered as an experimental triplicate.

Chapter II : Materials and methods

Table 20 Tested extraction conditions for the Central Composite Design (CDD) study
(P=103 bar)

Experimental point	Temperatures (°C)	%Ethanol/water (v/v)
1	60	80
2	60	100
3	120	80
4	120	100
5	90	80
6	90	100
7	60	90
8	120	90
9	90	90
10	90	90
11	90	90
12	82.5	85.7
13	82.5	94.3
14	105	90

The experimental conditions of points 12 and 13 were established by the CCD methodology to efficiently explore the relationship between the input variables (Temperature and ethanol concentration) and the response of interest (Studied responses in Table 19 in p.108).

2.5.7 ASE extract characterization

2.5.7.1 Sample preparation

To determine the concentration of total phenolic compounds (TPC) and assess the antioxidant activities (DPPH and ABTS) of the ASE extracts, 5 mL of the extracts were placed in a 50 mL Falcon tube and subsequently centrifuged (Coulter Beckman, Model Allegra X-12, rotor model: SX4750A, Brea, CA, USA) at 4500 RPM for 10 minutes at 4°C. The resulting supernatant was filtered through a 0.2µm filter, and the filtered extract was then transferred into a preweighed 10 mL glass tube. For TPC estimation in solid samples such as commercial AP biomass and phycocyanin (PC) provided by Ecosynia, 100 mg of dry samples were mixed with 4 mL of pure ethanol. After maceration in dim light conditions for 4 hours, the extract was centrifuged and filtered as described previously in this paragraph, before to introduce it into a preweighed 10 mL glass tube. The test tube with the extract was inserted into the vacuum concentrator (ThermoFisher Scientific SpeedVac SPD300DDA, Waltham, Massachusetts, USA) to evaporate the solvent from the extract at the conditions from Table 21. The vacuum concentrator was associated to a rotary vane pump (Edwards RV8, Stockholm, Sweden).

Table 21 SpeedVac solvent evaporator parameters

Parameter	
Temperature	45°C
Heat time	1 hour
Vacum level (mbar)*	26.33
Ramp	5 (50 mbar/min)
Mode	Manual

*The level is expressed in absolute pressure.

In the case of the extracts with a greater water proportion like 50 and 80% ethanol v/v, the remaining water in the extract was frozen and lyophilized for at least 16 hours \pm 2 hours to separate the extract from the water. Once the extracts were completely isolated from the solvent phase as shown in Figure 46, the tubes were introduced into a desiccator to maintain the samples dry. The dry tubes with extract were finally weighted, to estimate the obtained extract mass.



Figure 46 Tubes with dry extract after treatment

Once the mass from the extract was estimated the dry extracts were diluted to a concentration of 100 mg/mL adding pure methanol to the tubes and mixing gently.

2.5.7.2 Total Phenolic Compounds (TPC)

A volume of 5 μ L of the diluted sample was mixed with 100 μ L of ten-fold diluted Folin-Ciocalteu solution [264], the mixture was incubated for 10 minutes at room temperature under modest irradiance to prevent the sample degradation. 100 μ L of 0.01M Na₂CO₃ solution was added to the sample, then incubated for 90 minutes under dim light conditions, and finally the sample absorbance was read at 765 nm.

The TPC concentration was estimated by performing the reaction described in the previous paragraph to a Gallic Acid Equivalent (GAE) calibration curve ranging from 0-10 mg GAE/mL.

Chapter II : Materials and methods

The TPC concentrations were estimated by applying the equation obtained from the linear regression plotted in Figure 47.

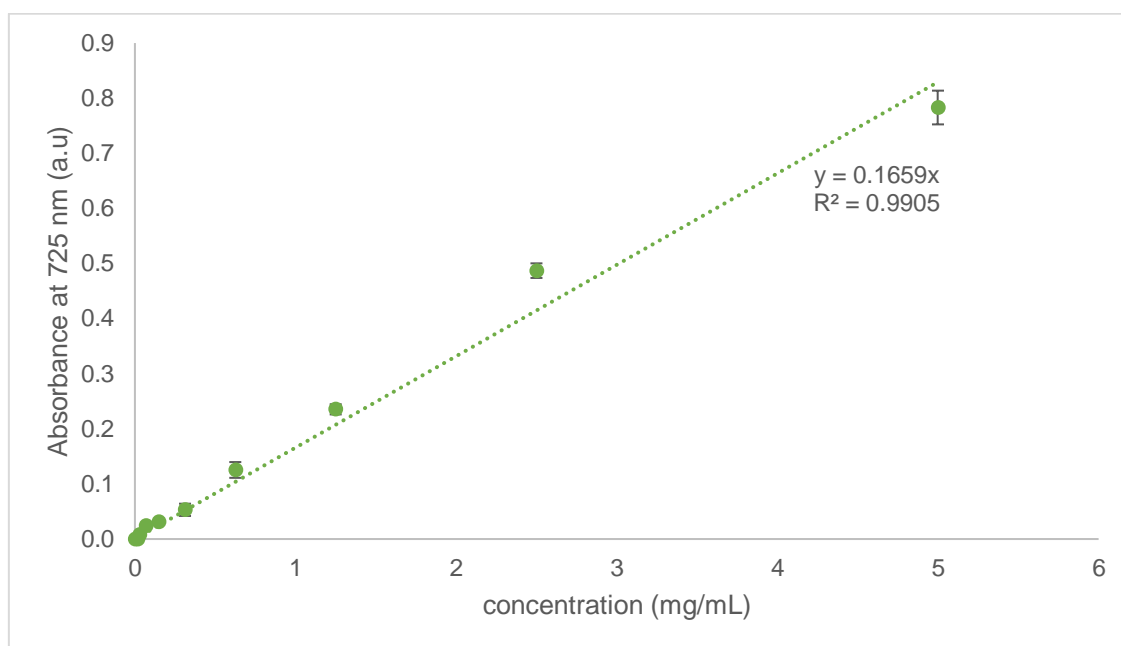


Figure 47 Gallic Acid calibration curve for Total Phenolic Compounds estimation. a.u., stands for arbitrary units

2.5.7.3 Antioxidant activity assessment: ABTS

The assay principle is described in 1.7.5.4 in p. 63. The negative control maintained the blue-green color of the ABTS radical, whereas samples exhibiting positive antioxidant activity displayed a change in color, as shown in Figure 48.

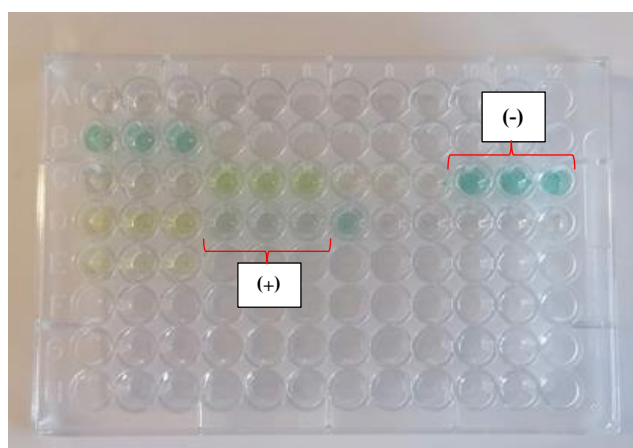


Figure 48 ABTS reaction, in this reaction wells exhibiting a blue coloration represent a negative control, whereas those remaining uncolored signify a positive sample where antioxidant activity is detected.

In dim light conditions, 10 μ l of the treated extract was mixed with 190 μ L ABTS solution 7 mM in an aqueous solution of potassium persulfate 2.5 mM. The reaction was incubated at room temperature for 6 minutes and read at 734 nm. As some of the extracts were colored, 10

μL of the treated extract was mixed with $190 \mu\text{L}$ of methanol, and the absorbance of the mixture without reaction was read at 734 nm . This absorbance was subtracted from the reaction one to obtain a net one. The % ABTS antioxidant activity was estimated by applying equation (47).

$$\%ABTS \text{ antioxidant activity} = \frac{A_c - A_s}{A_c} \times 100 \quad (47)$$

A_s = Absorbance of the tested sample (Arbitrary unit)

A_c = Absorbance of the negative control sample (Arbitrary unit)

The negative control sample in this test is analytic grade DMSO, while the positive one is pure Butylated Hydroxytoluene (BHT), the process described in the previous paragraph was reproduced in $10 \mu\text{L}$ of both controls. Positive control permits to compare the obtained antioxidant activities to a reference compound. BHT is a widely used synthetic antioxidant, having the capacity to neutralize free radicals.

2.5.7.4 Antioxidant activity assessment: DPPH

For this test, $22 \mu\text{L}$ of the treated sample was mixed with $200 \mu\text{L}$ of DPPH solution $120 \mu\text{M}$ in 96% ethanol, the reaction was incubated for 30 minutes at room temperature in dim light conditions. The sample absorbance was read at 517 nm . The reaction is shown in Figure 49.

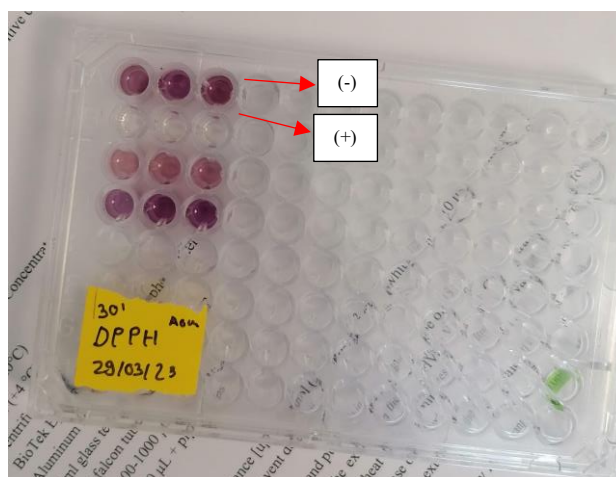


Figure 49 DPPH reaction

The negative control sample in this test is analytic grade DMSO, while the positive one is Butylated Hydroxytoluene (BHT), the process described for the samples was reproduced in $22 \mu\text{L}$ of both controls. The % DPPH antioxidant activity was estimated by applying equation (48).

Chapter II : Materials and methods

$$\%DPPH \text{ antioxidant activity} = \frac{A_c - A_s}{A_c} \times 100 \quad (48)$$

A_s = Absorbance of the tested sample (a.u)

A_c = Absorbance of the negative control sample (a.u)

a.u: Arbitrary unit

2.5.7.5 ABTS and DPPH analysis

In order to ease the data analysis of both tests, the responses were normalized relating the obtained responses to a BHT equivalent. The following equation was applied.

$$\mu g \text{ BHT}_{\text{equivalent}} = \frac{m_{\text{BHT}} \times (\text{sample}_{\% \text{antioxidant activity}})}{\text{BHT}_{\% \text{antioxidant activity}}} \times 100 \quad (49)$$

Where;

$\mu g \text{ BHT}_{\text{equivalent}}$	BHT equivalent mass	μg
$\text{sample}_{\% \text{antioxidant activity}}$	Sample antioxidant activity	%
$\text{BHT}_{\% \text{antioxidant activity}}$	BHT antioxidant activity	%

The $\mu g \text{ BHT}_{\text{equivalent}}$ value was divided by the sample's mass in mg, to obtain a result in $\mu g \text{ BHT}_{\text{equivalent}} / \text{mg sample}$.

2.5.7.6 Pigments analysis with HPLC

The protocol for this analysis is described in 2.1.9 in p. 76. The pigments analyzed from the extracts were Chl a, β -carotene, zeaxanthin, and myxoxanthophyll.

The pigment concentration per gram of biomass was quantified correlating the HPLC detected concentration to the biomass dry weight employed during the essay. The ASE concentrations were compared to the ones obtained by the selective method reported in 2.1.7 in p. 75, to estimate the extraction yields. Considering the selective method concentration as the 100%. The extraction yields were calculated as follows (48):

$$\eta_x = [C_{\text{ASE}} / C_{\text{reference}}] \times 100 \quad (50)$$

Where,

η_x	Pigment extraction efficiency	%
C_r	Reference concentration	mg/g biomass
C_{ASE}	ASE concentration	mg/g biomass

Myxoxanthophyll was omitted from this quantification due to its relatively small proportion compared to the other analyzed pigments. Including it would introduce additional complexity to the analysis. The total pigment content was estimated as follows:

$$\sum C_{total\ lipophilic\ pigments} = C_{chlorophyll\ a} + C_{zeaxanthin} + C_{beta-carotene} \quad (51)$$

Where,

$C_{chlorophyll\ a}$	Chl a concentration	mg/g biomass
$C_{zeaxanthin}$	Zeaxanthin concentration	mg/g biomass
$C_{beta-carotene}$	β -carotene concentration	mg/g biomass

The values were expressed as the mean \pm standard deviation. Error bars in the Chapter 3 figures are standard deviations of triplicate measurements.

2.6 Phase II: Valorization of lipophilic fraction in *Arthrospira platensis* biomass

This document section describes the experimental approach to valorize the lipophilic fraction of the biomass produced during the 1st stage of the project (in paragraph 2.3 in p. 97). The initial step included employing the reported optimal extraction conditions [203] [208] to characterize the supercritical carbon dioxide (scCO₂) extractions carried out in a 20 mL semi-continuous extractor (Separex, Champigneulle, France). The study of the extraction kinetics were conducted using a specified particle size range [300-500 μm] in a previously characterized biomass. The performed extractions allowed the modeling of the extraction process using Sovová's model equations. The extracts were characterized to identify the extract's lipidic and pigment profile, as pictured in Figure 50. This experiment aims to answer the following questions: *What is the mass proportion that can be extracted using scCO₂, and what are the key parameters for optimizing scCO₂ extractions of AP biomass?*

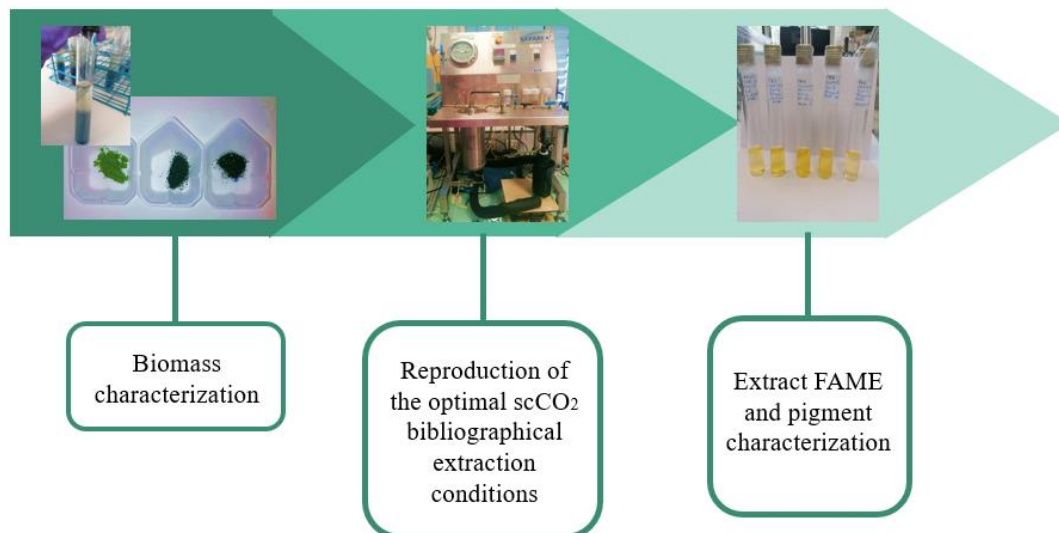


Figure 50 Experimental campaign to valorize the *A. platensis* biomass by Supercritical CO₂

2.6.1 Studied biomass for scCO₂ extraction

The biomass used during this experiment was cultivated and harvested as described in section 2.3 p. 97. After harvesting, the biomass was freeze-dried as described in section 2.3.5 p. 99, manually homogenized by mortar, and sieved; the biomass fraction employed for this study has a particle diameter (d_p) 300-500 μm.

2.6.2 20 mL semi-continuous extractor

The extraction unit consisted of 1) a CO₂ reservoir, 2) a chiller, decreasing the temperature to -6°C, 3) a piston pump (GILSON 307 5SC type, Gilson Inc., Middletown, Wisconsin, USA), 4) Manometer 5) a jacketed vessel, 6) an extraction autoclave with a capacity of 20 mL, 7)

extract receptacle, 8) CO₂ output, 9) cleaning solvent bottle, and 10) cleaning solvent pump, see Figure 51.

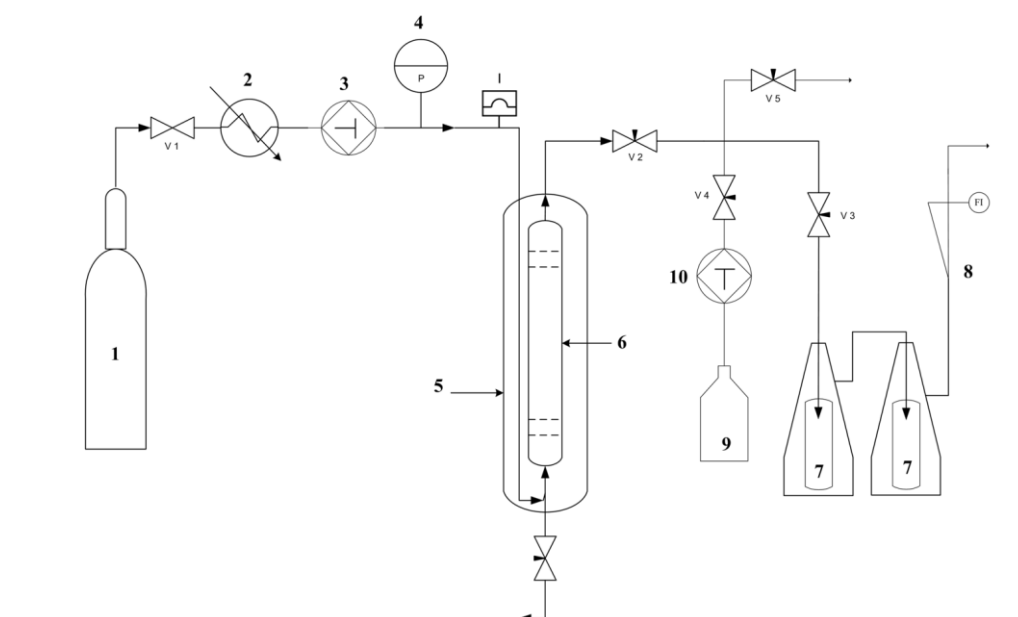


Figure 51 Semi-continuous CO₂ extraction unit Piping and Instrumentation Diagram (P&ID), reproduced from [265]

2.6.3 Supercritical CO₂ extraction conditions for extraction kinetics

After the study of the optimal parameters (Table 6 p.56) to valorize AP biomass, the extraction kinetics were determined by applying the operating parameters in Table 22. The biomass studied for these extractions was pretreated as described in section 2.3.5 The extraction autoclave was always filled 80% of its total capacity. The extraction column parameters were a length of 18 cm and exterior diameter 1.5 cm.

Table 22 Kinetics Extraction parameters in 20 mL extraction unit

Parameter	
Solvent	Pure CO ₂
Temperature (°C)	60
Pressure (bar)	300 ± 5
CO₂ flow (kg/h) at 20°C and 1 atm	0.2 ± 0.025
Biomass in extractor (g)	4.4 ± 0.2
Particle diameter (µm)	300-500
% biomass moisture	3
Drying method	Freeze-drying
Milling method	Ceramic mortar

Chapter II : Materials and methods

2.6.4 Extraction kinetics operating mode

The biomass previously sieved was introduced into the extraction autoclave previously cleaned and dried. The autoclave was systematically filled until 80% of its total capacity. The biomass and autoclave initial biomass were weighted by a gravimetric balance with an accuracy of 10^{-3} g. The autoclave was introduced in the extractor, previously set at the operation temperature. Once the system was completely isolated, valves 4 (V4) and 5 (V5) were closed. V1 and V2 were opened to let pass the CO₂, the CO₂ was brought to $-6^{\circ}\text{C} \pm 2^{\circ}\text{C}$ by the chiller, to then pass through the pump, and increase its pressure to $300 \text{ bar} \pm 5 \text{ bar}$, when entering the extraction autoclave the CO₂ was heated to 60°C , reaching the extraction conditions. The CO₂ flow was controlled with a micrometric valve (V3), the flow rate was measured by a flowmeter at the end of the extraction line. The extractions were performed at the conditions from Table 22 for 20-30 minutes. The vial with the extract obtained in the 7th element of Figure 51, after the end of each extraction point, was suspended in pure ethanol for further analysis. The extraction was reproduced twice to estimate its reproducibility, the reproducibility was estimated by the average deviation.

The mass loss after extraction was registered. The extraction kinetics stopped when the mass loss was negligible or none. The mass loss was estimated by calculating the difference between the sample mass before and after extraction, applying equation (52).

$$m_{extract} = \frac{m_0 - m_t}{m_0} \quad (52)$$

Where,

Variable	Meaning	Units
$m_{extract}$	Mass loss	
m_0	Autoclave+biomass before extraction	g
m_t	Autoclave+biomass after extraction	g

The extraction yield was estimated by the following equation

$$\eta_{extraction} = \frac{m_{extract}}{m_{biomass}} \quad (53)$$

Where,

Variable	Meaning	Units
$\eta_{extraction}$	Extraction yield	
$m_{extract}$	Mass of extract	g
$m_{biomass}$	Mass of introduced biomass	g

To obtain the experimental extraction curve the extraction yield was plotted as a function of the relative amount of CO₂ and the biomass, applying equation (54), where mass loss is a function of CO₂ mass per unit mass of biomass.

$$q = \frac{m_{CO_2}}{m_{biomass}} \quad (54)$$

Where,

Variable	Meaning	Units
q	Relative amount of passed solvent	g/g
m_{CO_2}	CO ₂ mass at a given time	g
$m_{biomass}$	Mass of introduced biomass	g

2.6.5 ScCO₂ extract characterization

2.6.5.1 Lipid analysis by Flame ionization detector Gaseous chromatography method for supercritical (GC-FID)

The extracts obtained at each stage of the extraction kinetics were mixed with 5 mL of pure ethanol. Subsequently, these suspensions underwent filtration through a 0.22 μm membrane (Reference: WH10462945, Whatman, Buckinghamshire, United Kingdom) and were concentrated using the ThermoFisher Scientific SpeedVac SPD300DDA vacuum concentrator, following the conditions outlined in Table 21 p.110. The resulting samples were then subjected to trans esterification, following the described procedure 2.4.2 in p.101. The procedure was performed in duplicates, the error was estimated performing the absolute difference of the obtained values.

To estimate the FAMES concentration in the extracts it was hypothesized that no extract was lost in the extractor pipelines, that all the extract was recovered in the extract receptacle, and that the only extractable fractions in the sample were lipids and lipophilic pigments except from Chl a.

The relative FAMES proportion and its concentration in the extract were estimated as it follows:

$$m_{FAMES} = \frac{FAMES\ peak\ area \times m_{IS}}{IS\ peak\ area} \quad (55)$$

$$\text{Relative FAMES proportion (\%)} = \frac{m_{FAME}}{\Sigma m_{FAME}} \times 100 \quad (56)$$

Chapter II : Materials and methods

$$\text{FAMES [mg/g extract]} = \frac{m_{\text{FAMES}}}{m_{\text{extract}}} \quad (57)$$

Where,

Variable	Meaning	Units
<i>FAMES peak area</i>	FAMES peak area	$\mu\text{V.s}$
m_{FAMES}	Fatty acid mass	mg
m_{IS}	Internal Standard TAG-C15 mass in sample	mg
<i>IS peak area</i>	Internal standard peak area	$\mu\text{V.s}$
m_{loss}	Mass loss in the extraction autoclave	g

2.6.5.2 Pigment HPLC analysis

The protocol described in 2.5.7.5 was applied to the extract suspended in 5 mL of pure ethanol. The procedure was performed in duplicates, the error was estimated performing the absolute difference of the obtained values. To calculate the pigment content in the scCO₂ extract, the mass of the dry extract at each extraction point was reported to the biomass in autoclave mass loss at each extraction point, obtained applying equation (52). The equation (58) was applied, and it was hypothesized that no pigment was lost in the extraction pipelines.

$$C_{pigment} = C_{sample} \times V_{Dilution} \times \frac{1}{m_{loss}} \quad (58)$$

Where,

Variable	Meaning	Units
$C_{pigment}$	Pigment concentration in the extract	mg of pigment/ g extract
C_{sample}	HPLC Pigment concentration in sample	mg pigment/L sample
$V_{Dilution}$	Ethanol volume for diluting the extract	L
m_{loss}	Mass loss in the extraction autoclave	g

2.6.6 Supercritical CO₂ extraction modeling

The model more adapted to represent the extraction phenomena is the one developed by Sovová [266]. This model contemplates two extraction periods, the first one governed by the phase equilibrium and the second one governed by the internal diffusion in particles. This model considers the potential modifications of the solid matrix during the pre-treatment, such as the cell rupture. The sample exhibits then intact cells and of broken cells. It also considers the transfer phenomena occurring in the solid phase: the fixed bed, and the fluid phase: the solvent/s. The phase equilibrium, mass transfer, and solvent flow effect on the extraction are considered in this model.

Phase equilibrium:

Case 1) When the concentration in the solid matrix is high, the fluid-phase concentration is independent of the matrix and equal to solubility.

Case 2) When the solute concentration is low, the equilibrium is controlled by solute-matrix interaction and the fluid-phase concentration is lower than the solubility.

The equilibrium is considered as a linear relationship between the solid and liquid phase concentration. The constant of proportionality is called the partition coefficient.

Mass transfer

During the extraction, solute diffuses to the particle surface. The internal diffusion is modeled by applying the effective diffusion coefficient or the solid mass transfer coefficient.

Chapter II : Materials and methods

The broken cell concept was introduced to describe the reduction in extraction rate after the first extraction period. Two regions are considered for the model.

Region 1) Close to the surface region, where the cells have been damaged by the mechanical pre-treatment. Region 2) The particle core, containing intact cells. There is a large difference in diffusion rates in both regions. The extraction in the first region is way faster than the one in the 2nd one. In the model, both types of equilibrium are supposed to occur simultaneously [266].

Solvent flow

The model describes a situation when the solvent flows through a homogeneous fixed bed plant material in a cylindrical extractor. and the temperature and pressure are constants.

It is assumed that the solute in the surface broken cells passes directly to the fluid phase and the solute in the core cells diffuses first to broken cells and then to the fluid phase. The fixed bed characteristics like the void fraction and surface area are not modified by the mass loss during the extraction. The fluid density is neither affected by the solute dissolved in it.

The model equations proposed for this model are converted to dimensionless form and solved numerically. The mass balance is developed in equations (59), (60), and (61)

$$\rho_f \varepsilon \left(\frac{\delta y}{\delta t} + U \frac{\delta y}{\delta h} \right) = j_f \quad (59)$$

$$r \rho_s (1 - \varepsilon) \frac{\delta x_1}{\delta t} = j_s - j_f \quad (60)$$

$$(1 - r) \rho_s (1 - \varepsilon) \frac{\delta x_2}{\delta t} = -j_s \quad (61)$$

Initial and boundary conditions are

$$\begin{aligned} y|_{t=0} &= y_0; & x_1|_{t=0} &= x_1, 0; \\ x_2|_{t=0} &= x_2, 0; & Y|_{h=0} &= 0 \end{aligned}$$

The extraction curve is estimated as follows:

$$E = \dot{Q} \int_0^t y|_{h=H} dt \quad (62)$$

The mass transfer is triggered by a modification in the phase equilibrium between the solid-phase and fluid-phase. The equilibrium discontinuity takes place at x_t , When solid concentration is lower than x_t , the solute interacts with the solvent, and the equilibrium is determined by K_x , the partition coefficient. When the solute concentration is greater than x_t , the fluid concentration in the solid matrix is equal to y_s .

$$y^*(x_1) = y_s \text{ for } x_1 > x_t$$

$$y^*(x_1) = Kx_1 \text{ for}$$

$$x_1 \leq x_t ; Kx_1 < y_s$$

The four possible cases are described by this model and the extraction cases are defined as a function of the solubilization conditions. The extraction types can be characterized by the extraction curve shape.

Where,

Variable	Meaning	Units
x_1	Concentration in broken cells	kg solute/kg biomass
x_2	Concentration in intact cells	kg solute/kg biomass
x_t	Transition concentration	kg solute/kg solvent
y	Fluid phase concentration	kg solute/kg solvent
y_0	Initial fluid phase concentration	kg solute/kg solvent
y_s	Solubility	kg solute/kg solvent
$y^*(x_1)$	Equilibrium fluid-phase concentration	kg solute/kg solvent
Y	Dimensionless fluid phase concentration y/y_0	
K	Partition coefficient	
h	Axial co-ordinate	m
H	Extraction bed-length	m
ρ_f	Solvent density	kg/m ³
ρ_s	Solid density	kg insoluble solid/m ³ of solid phase
ε	Void fraction	
j_f	Flux from broken cells to solvent	kg/m ³ /s
j_i	Flux from intact cells to solvent	kg/m ³ /s
r	Volumetric fraction cells	
\dot{Q}	Solvent flow rate	kg/s

Case A and D, represent an extraction where solute-matrix interaction is low or negligible, this extraction can be identified by the presence of a single straight section in the extraction curve. Case A and D can be differentiated by the presence of a sharp or smooth transition between the two extraction phases for the case A and D, respectively. In these cases, the interactions between the solute and the matrix start from the beginning of the process, transfer resistance in broken cells can be neglected. In case A the extraction curve slope is typically close to the value of solubility. While case D presents a curve slope minor than the solubility. In types B and C the mass transfer resistance is more important. In the C type of extraction the phenomenon is mainly governed by the solute-matrix interaction and secondly by internal

Chapter II : Materials and methods

diffusion. These cases can be differentiated by the transition between the 1st and 2nd extraction phases, in case C, the transition is well-marked, while in case D this transition is smoother.

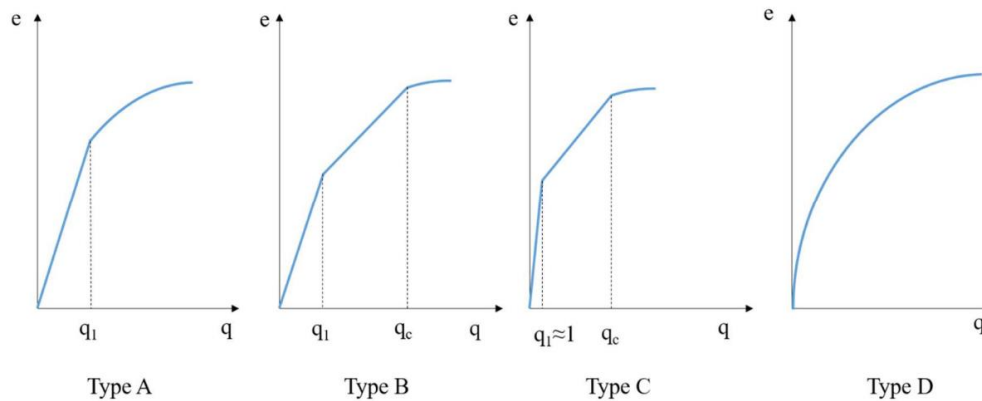


Figure 52 Extraction curve types described by Sovová's model theory, reproduced from [265]

Following the model's logic, the first part of the extraction yield and its first period can be represented by the equations (63) and (64) for curves without solute-matrix interaction.

$$e_1 = q y_s \text{ for } 0 \leq q \leq q_c \quad (63)$$

$$e = x_u [1 - C_1 \exp(-C_2 q)] \text{ for } q > q_c \quad (64)$$

The slope of y_s is fitted at the first part of the equilibrium. The second part of the extraction estimates the grinding efficiency and the solid phase mass transfer coefficients from constants C_1 and C_2 in the coordinate q_c . The $k_s a_s$ represents the intact cell diffusion.

$$r = 1 - C_1 \exp(-C_2 q_c / 2) \quad (65)$$

$$k_s a_s = (1 - r)(1 - \varepsilon \dot{Q} C_2 / N_m) \quad (66)$$

Where,

Variable	Meaning	Units
e_1	Extraction yield at the first extraction period	kg solute/kg biomass
C_1, C_2	Mass transfer Constants	
x_u	Concentration of extract in the plant before extraction	kg solute/kg solvent
N_m	Charge of insoluble solid	

q	Relative amount of passed solvent	kg/kg solute s
q_c	Value of q at the crossing point for the second part of the extraction curve	kg/kg solute s
k_s	Solid mass-transfer coefficient	m/s
a_s	Specific area between the regions of intact and broken cells	m^{-1}
r	Grinding efficiency (fraction of broken cells)	

For the model applications, the following assumptions were taken into account [267]:

The fluid flow corresponded to a laminar plug flow in a cylindrical tube through a porous medium (Biomass fixed bed).

The fluid is distributed homogeneously in the autoclave.

The solid matrix contains broken cells on the surface and intact cells in the core.

The solute from the broken cells easily gets transferred to the fluid phase by solubility.

The solute from the intact cells gets transferred to the broken cells and after to the fluid phase by diffusivity.

The fluid-phase mass transfer coefficient permits the characterization of the mass transfer from the broken cells.

The reduction of the solid matrix during the extraction does not affect the fixed bed characteristics.

The fluid density is unchanged by the extraction.

The extraction is considered analogous to the one of vegetable seeds.

The average absolute relative deviation (AARD%) was determined as follows:

$$AARD (\%) = \frac{1}{100} \sum \left| \frac{\text{experimental yield} - \text{calculated yield}}{\text{experimental yield}} \right| \quad (67)$$

The application of this methodology is intended to provide enough experimental data to evaluate the proposed strategy to optimize the culture and green solvent fractionation of AP

Chapter II : Materials and methods

biomass. The results obtained will be compared to prior research findings, facilitating a discussion on the viability of the suggested techniques for enhancing the valorization of AP biomass.

Chapter 3 Results and Discussions

3.1 Phase I: Biomass culture optimization

3.1.1 *Arthrospira platensis* culture as a CO₂ mitigation technique

Abstract

The CO₂ mitigation potential of the AP strain SAG.21-99 was tested in two approaches. Initially, at laboratory incubator conditions with all the culture parameters well controlled, to understand the role of temperature, pH, light, and CO₂% in AP growth and carbon capture. In this case, the CO₂ concentration was maintained constant during the whole experiment at 5% v/v CO₂ by the incubator atmosphere. Secondly, the CO₂ mitigation potential was tested in 3 L and 3 m³ configurations at greenhouse conditions, adding semi-continuously CO₂ enriched air at 4% v/v for periods of 1 hour ± 0.2 hours when the Dissolved Inorganic Carbon (DIC) concentration was < 300 mgC/L. The pH, DIC, and biomass development were continuously followed in the three studied cases in the supernatant and biomass of the culture, respectively. While the nitrate evolution was only measured in the laboratory conditions study. In the case of the laboratory condition experiment, DIC and pH reached equilibrium at 675 ± 44.5 mgC/L and 8.2 ± 0.06, respectively, these equilibrium values were well approached by the application of the model developed by [268]. This model approaches the DIC concentration in a saltwater sample by integrating the equilibrium temperature, pH, and salt concentration constants for saltwater developed by [68]. The biological influence in the CO₂ assimilation was observed by contrasting the observed DIC and pH in the cultures with the ones in the witness sample without biomass. In the case of the greenhouse conditions experiments, pH reached 10.35 ± 0.49, and 305 ± 7.07 mgC/L, respectively, before the carbon restock. CO₂ mitigation efficiencies by the supernatant absorption and biomass assimilation were estimated by carbon mass balances in the 3 L and 3 m³. It was observed that the 3 L system presented a better CO₂ assimilation in the biomass, compared to the 3 m³, being 39.38 ± 0.42% and 7.09 ± 2.21%, respectively. Meanwhile, the 3 m³ culture presented greater DIC absorption in medium compared to the 3 L, reaching efficiencies of 62.43 ± 9.03%, and 7.71 ± 1.06%, respectively. Finally, the global CO₂ mitigation efficiencies were of 11.37 ± 4.01%, and 67.78 ± 9.19%, for the 3 L bottle and the 3 m³ raceway, respectively. The obtained results permit to affirm that the AP culture physicochemical parameters enhance the DIC assimilation. This microorganism can be applied for mass cultivation and simultaneous biological fixation of CO₂. The pH, temperature, salt concentration, gas delivery techniques, mixing, and light availability are important parameters to warrant an efficient biological CO₂ mitigation.

Chapter III : Results and Discussions

3.1.2 Strain screening

To select the most suitable strain for the project, three commercial AP strains were compared. The strains reached a maximum biomass ($X_{biomass}$) concentration of 3.38, 3.17, and 3.47 g/L for SAG-21.99, NIES-46, and PARACAS respectively on the 8th day. The exponential growth lasted for 2 days, probably stopped due to the light limitation [85], while the linear growth lasted for the next 6 days. Finally, the stationary phase was reached after the 8th day. The dry weight measured on the 16th day was made to confirm the stationary phase of the culture.

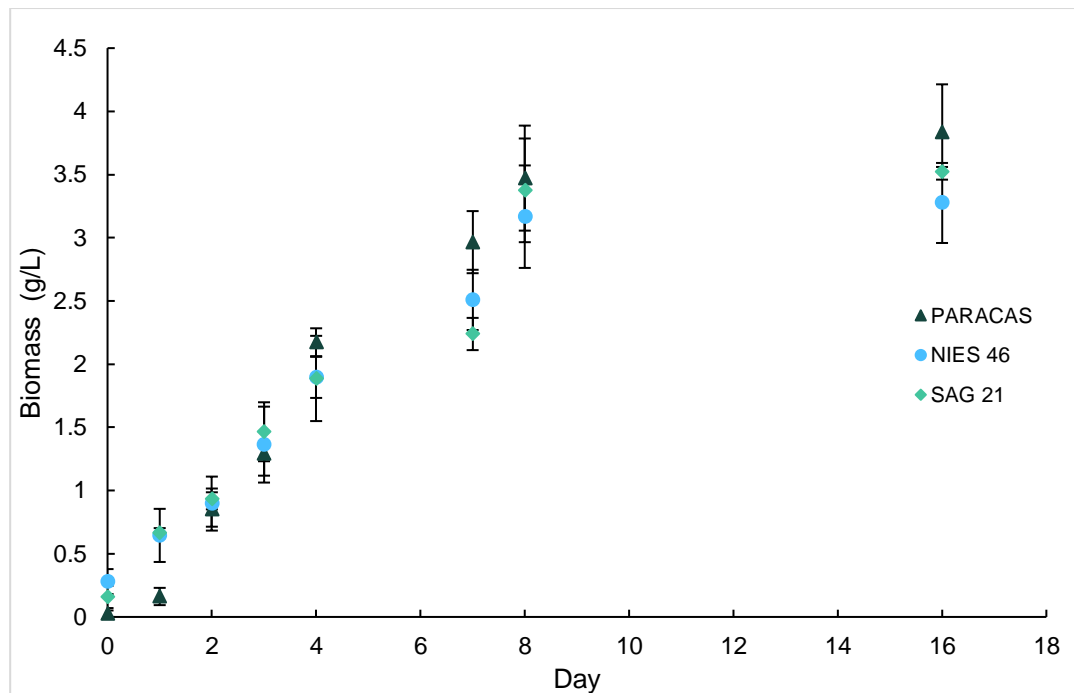


Figure 53 Growth curve of the compared *Arthrospira platensis* strains at laboratory scale conditions

The three tested strains showed their maximum growth rate (μ_{max}) during the first 24 hours of culture, which corresponds to an exponential growth phase Figure 53. Being, 1.44, 0.83, and 1.87 d⁻¹, for SAG-21.99, NIES 46, and PARACAS, respectively.

On the other hand, the mean observed growth rates (μ) between day 0 at day 8 were, 0.66, 0.46, and 1.10 d⁻¹ for SAG-21.99, NIES-46, and PARACAS respectively. The biomass productivity ($P_{biomass}$) were 0.38, 0.36, and 0.43 g/L/d for SAG-21.99, NIES-46, and PARACAS respectively. The growth kinetics results are reported in Table 23. The NIES 46 and SAG 21 mean growth rates are comparable with the one reported by [100] [269] [270]. μ_{max} and μ_{mean} were determined applying equation (14) in p. 75, the first one was the greater one registered during the whole experiment, while the second one was the average of the whole experiment growth rates.

Table 23 Growth kinetics parameters to compare three different *Arthrospira platensis* strains

	$X_{biomass}(g/L)$	$\mu_{max}(d^{-1})$	$\mu_{mean}(d^{-1})$	$P_{biomass}(g/L/d)$
SAG-21.99	3.38	1.44	0.66	0.38
NIES-46	3.17	0.83	0.46	0.36
PARACAS	3.47	1.87	1.10	0.43

Chlorophyll a and carotenoids

Concerning the pigment content calculated by applying the protocol described in 2.1.8 p.76, the strain showing a slightly higher concentration of *Chl a* and Carotenoids was NIES-46. This might be explained by the presence of biomass aggregates which exposed the culture to lower and heterogeneous light intensities, probably causing an increase in the Chl content by cell [271] [272].

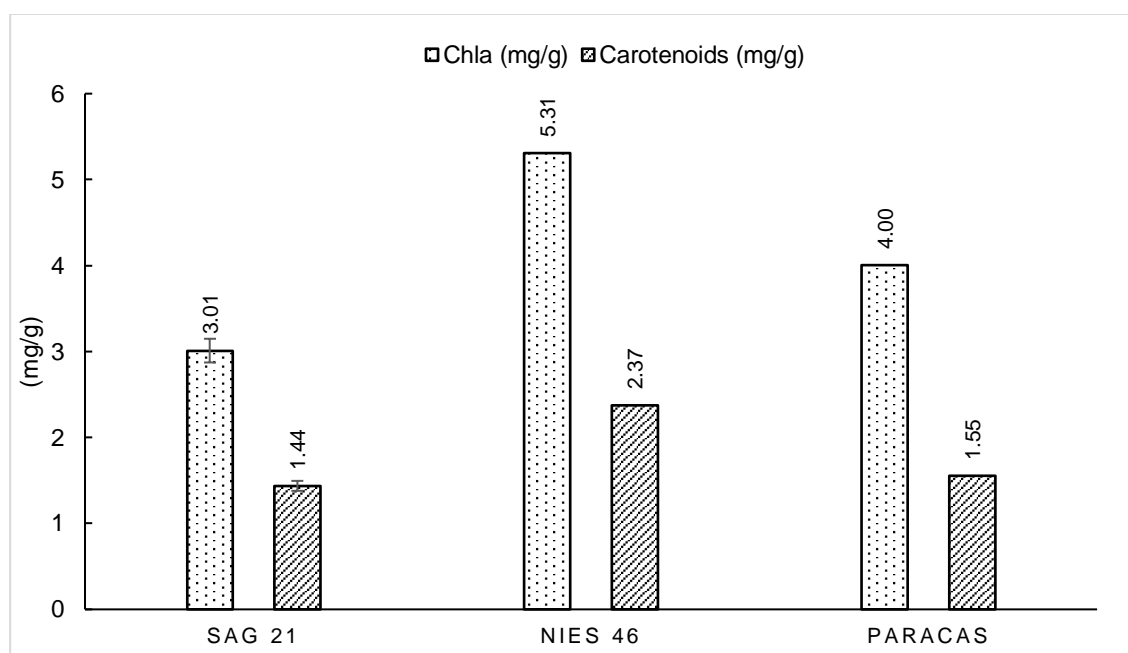


Figure 54 Chlorophyll a and pigment content comparison between different *Arthrospira platensis* strains

PARACAS and NIES 46 did not show significant differences in terms of phycocyanin (PC) concentration. However, these concentrations are low, compared to other studies, like [95] and [273], which reported a PC content close to 140 mg/g. In contrast, the SAG-21.99 PC concentration was 1.4 times higher than the other tested strains (Figure 55). This concentration is similar to that reported by other authors [60] [95].

Chapter III : Results and Discussions

The higher concentration of phycocyanin in SAG-21.99 might be explained by the fact the homogeneity of the culture enhanced a uniform light exposure for all the cells and thus a better growth and a better metabolite accumulation.

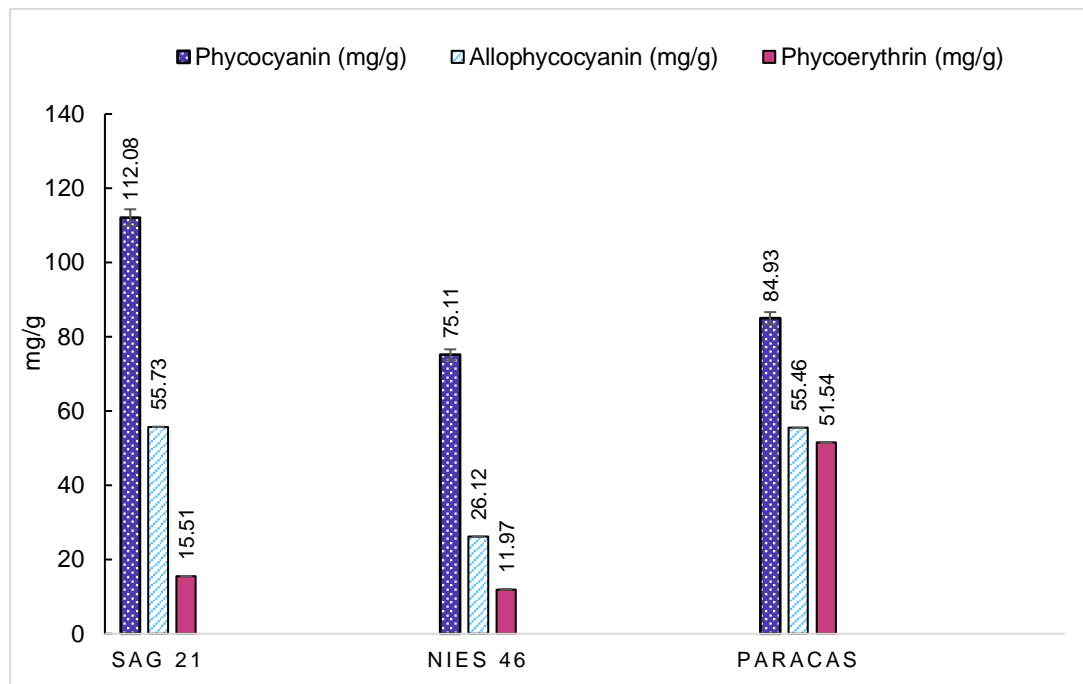


Figure 55 Phycobiliprotein content comparison between different *A. platensis* strains

As a consequence of its higher PC content, and its satisfactory growth parameters, compared to the studied organisms, SAG-21.99 was the selected microorganism to continue with the research activities developed during this Ph.D. It is worth mentioning the separation of the biomass from the culture was performed by centrifugation. This strain was completely sedimented in the bottom of the tube, while the other two studied microorganism biomass floated partially to the top of the tube.

3.1.3 Laboratory scale *Arthrospira platensis* CO₂ mitigation characterization

3.1.3.1 Effect of culture physicochemical parameters on CO₂ dissolution

The three tested photoperiods and the control (without biomass) started at an initial pH of 9.2. According to [274], a pH of around 9 is suitable for AP culture. After 2 days of the experiment, the pH of the three conditions with active AP cultures decreased and stabilized at a pH of 8.2 ± 0.06 . There were no significant differences between the photoperiods in terms of pH equilibrium ($p > 0.05$). The results shown in Figure 56 are consistent with those of [275] and [276], who studied AP in modified Zarrouk medium and municipal wastewater. On the contrary, the pH of the non-inoculated control dropped to 6.7 ± 0.1 from the second day and remained stable during the entire experiment.

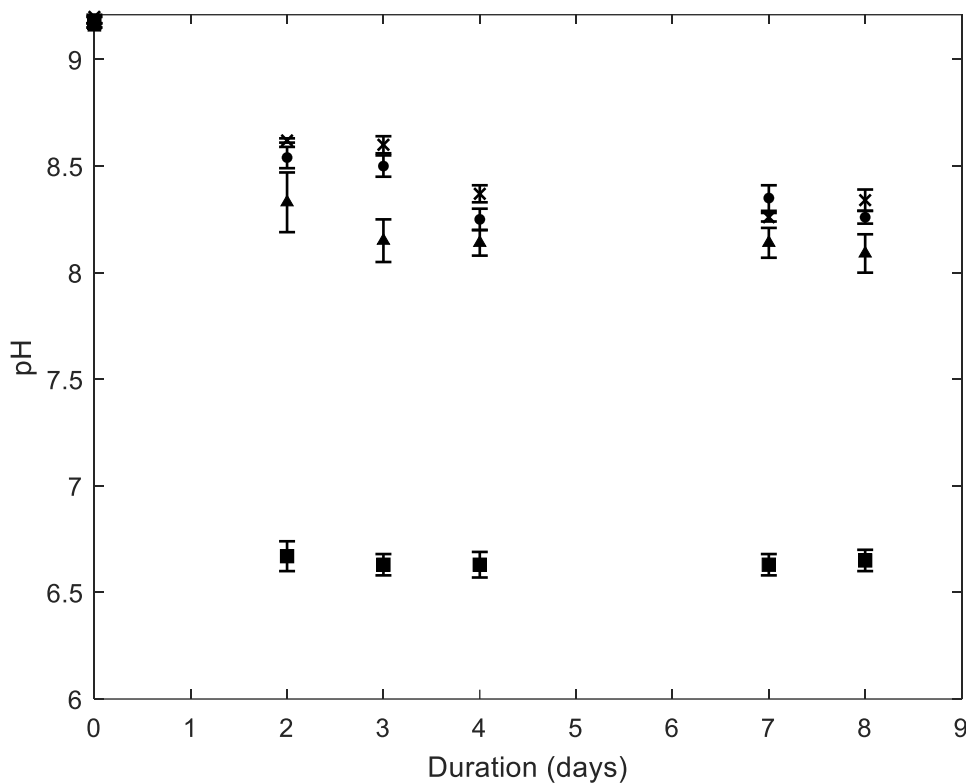


Figure 56 Evolution of the pH of *A. platensis* cultures and control neat culture medium during the growth kinetics for the three studied photoperiods (■) Control experiment without biomass, (▲) Continuous illumination 24h photoperiod, (●) 20h/04h photoperiod, (×)

As plotted in Figure 57, a higher pH in the active AP cultures was associated with an increase in DIC for the three photoperiod conditions, these results are in line with [277] with *Spirulina maxima* grown using flue gas as a carbon source for the medium. Furthermore, the availability of DIC species has a strong influence on biomass development [278]. A significant increase in the CO₂ fixation rate was reported between 360-1200 mgC/L [279] [63] in large-scale open raceway ponds with CO₂ supplementation. Similarly, in this study, the DIC reached

Chapter III : Results and Discussions

an equilibrium concentration at 675 ± 44.5 mg_C/L by the end of the batch for the flasks with live biomass inoculum in the three photoperiod conditions. Even if DIC concentration was higher in 20h/04h than in the other photoperiods, no significant differences were assessed between the three studied conditions ($p > 0.05$). In contrast, the control without live biomass reached an equilibrium concentration of 36 ± 1.07 mg_C/L.

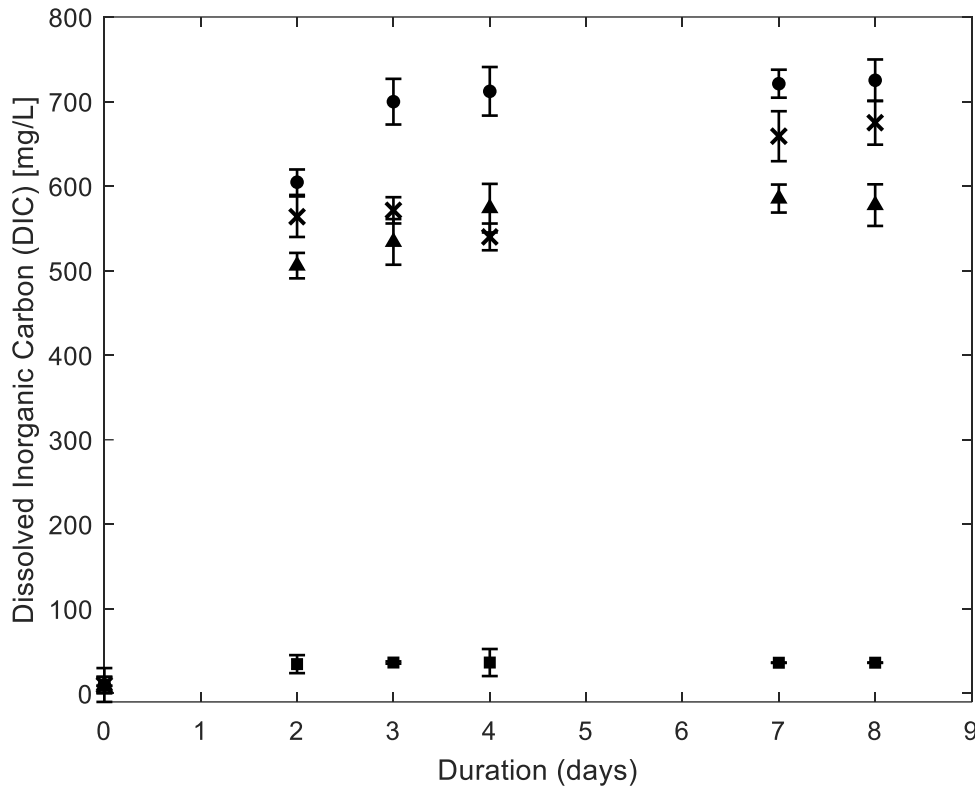


Figure 57 DIC evolution with and without inoculum of *A. platensis* for the three chosen photoperiods (■) Control experiment without biomass, (▲) Continuous illumination 24h photoperiod, (●) 20h/04h photoperiod, (×) 12h/12h photoperiod.

Light irradiance intensity and photoperiod are important factors for cell growth and CO₂ bio-mitigation [280]. Previous efforts have been made to evaluate irradiance intensity's impact on the carbon capture mechanisms of AP [281]. However, the photoperiod role in CO₂ bio-mitigation by AP has not been well defined yet. The results obtained in this study show that, although the samples with 20h/4h (day/night) photoperiod appeared with a DIC slightly higher than the other photoperiods, no significant differences were assessed between photoperiods. As for the pH, biological activity seems to be the main factor affecting DIC and its corresponding CO₂ uptake in the culture medium. The study of [103] with *Nostoc* cultivated in BG-11 medium stated that the NO₃⁻ reduction reactions play a significant role in pH increase, as the NO₃⁻ uptake is balanced by OH⁻ release, which leads to pH and alkalinity increase. In the present study, as the incubator atmosphere was enriched with CO₂, the release of alkalinity was compensated by

the increase in CO₂ absorption. As indicated in equations (23) to (25) in p.82, the dissolution of each absorbed CO₂ molecule releases one or two H⁺, this counter-mechanism leads to pH stability together with a slight increase in DIC. This mechanism is well described for instance by [102], [282], and [58]. The Figure 58 plot of nitrates consumption makes possible the calculation of mean nitrate consumption. Nitrate uptake in 12h/12h and 20h/04h batches presented slight differences, being 0.37 ±0.04 and 0.35 ±0.02 g/L respectively, whereas the nitrate uptake during the 24h condition was 0.45 ±0.01 g/L. The nitrate consumption differed significantly between photoperiods (p < 0.05). As discussed by [58] and [283] in the case of Chlorophyceae there is a link between biomass composition, O₂ production, CO₂ uptake, and nitrogen consumption in the culture. If nitrate uptake was only correlated with biomass production, we would have expected to observe an increase in nitrogen consumption in parallel with the photoperiod increase. It is possible that in this study, the photoperiods also have slightly influenced the biomass composition and therefore decreased the nitrogen uptake of the biomass for the 20h/04h photoperiod. This hypothesis is confirmed by the measurement of carbon content in the biomass that is slightly higher for 20h/04h photoperiod (0.48 ±0.03 gC/g_{biomass}) compared to 12h/12h and 24h/0h (0.43 ±0.01 and 0.45 ±0.04 gC/g_{biomass} respectively).

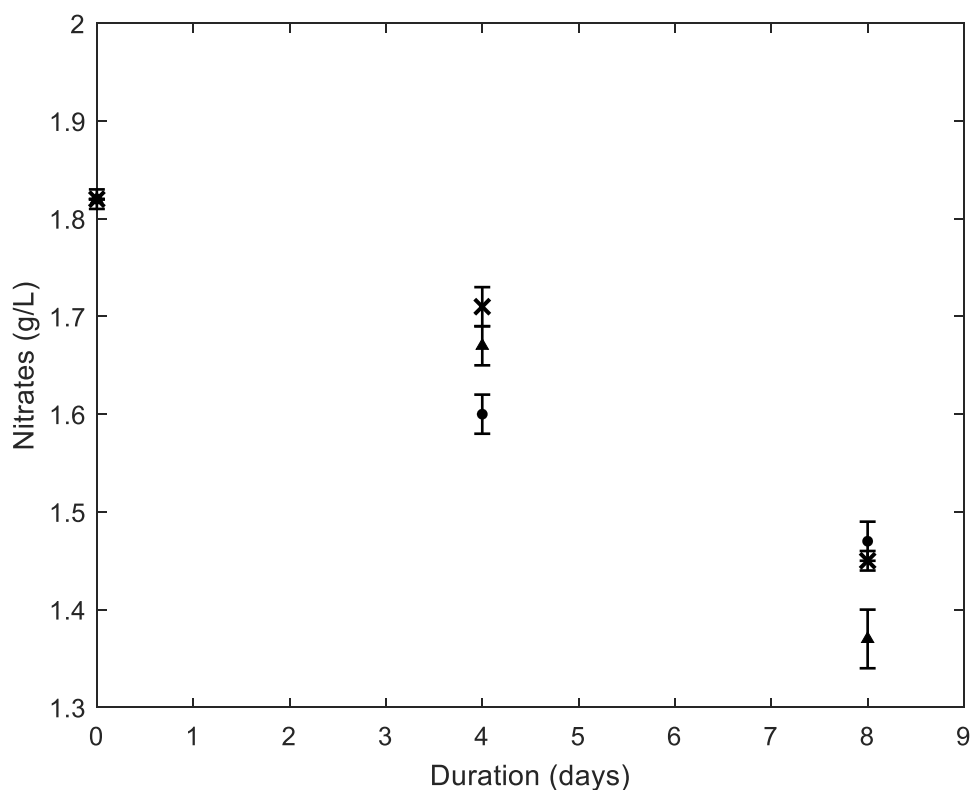


Figure 58 Nitrate consumption kinetics for the three chosen photoperiods (▲) Continuous illumination 24h photoperiod, (●) 20h/04h photoperiod, (×) 12h/12h photoperiod

Chapter III : Results and Discussions

To plot the DIC variation according to the pH, equations (26) to (31) in p.82 were applied following the resolution steps proposed. This plot is compared in Figure 59 with the experimental measurements obtained with the different photoperiods.

A good match is found between the experimental data and the numerical application of the theory, meaning that the kinetics of the carbon absorption by AP is slow enough to respect the thermodynamic equilibrium of CO_2 dissolution from the atmosphere. Moreover, the observed DIC values indicate that the carbon source was not a limiting factor for the culture development [284] indicating that the DIC limit concentration for Cyanophyceae is approximately 360-480 mg_C/L .

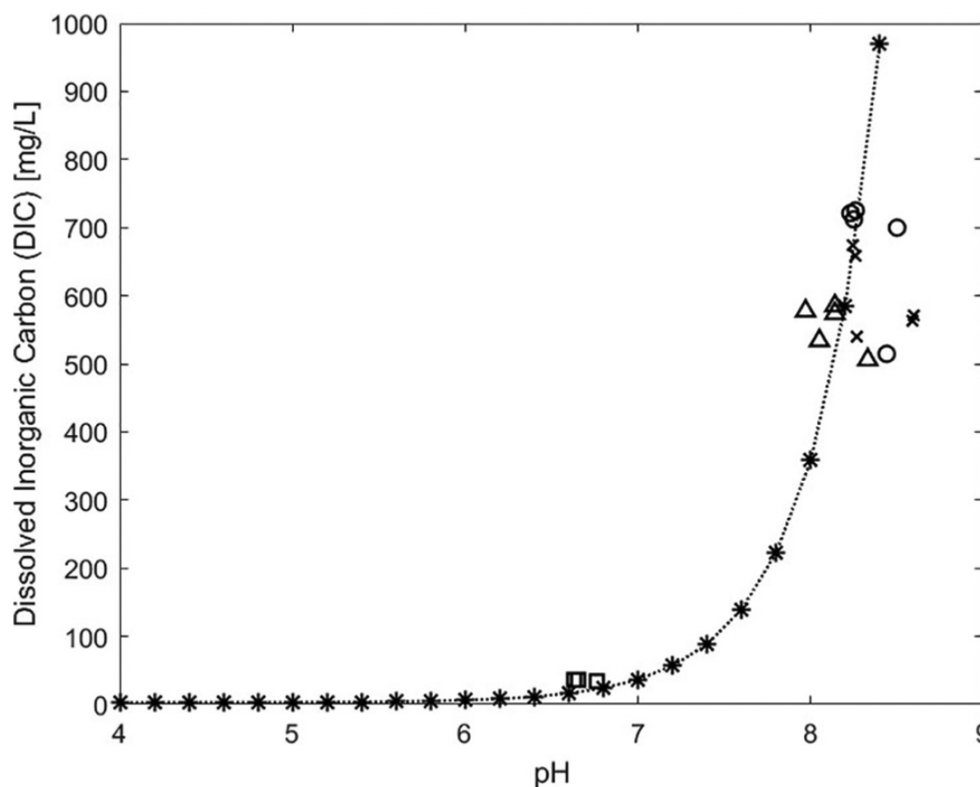


Figure 59 Dissolved Inorganic Carbon (DIC) estimated by the application of the model compared to the experimental data obtained during the *A. platensis* growth kinetics for the three chosen photoperiods. (*) Model data, (Δ) Continuous illumination 24h photoperiod, (o) 20h/04h photoperiod, and (\times) 12h/12h photoperiod

By the application of the equilibrium equations to the DIC concentration values, it was possible to estimate that HCO_3^- was the predominating carbon form in the culture medium, as illustrated in Figure 60. The HCO_3^- is known to be the accumulated carbon species during the CCM [285], serving cyanobacteria as a substrate for the carboxisomes center to increase the CO_2 concentrations around RUBISCO and enhance the carbon uptake by photosynthesis [72].

It was confirmed that the temperature and salinity of the culture play a role in carbon speciation. A reduction in bicarbonate ion proportion was observed in CFZM compared with

the one observed in the pure water at 20°C for a pH greater than 8. The culture of a photosynthetic organism growing optimally at lower temperatures, lower salinity, and higher pH could also be an attractive option for the CO₂ bio-sequestration.

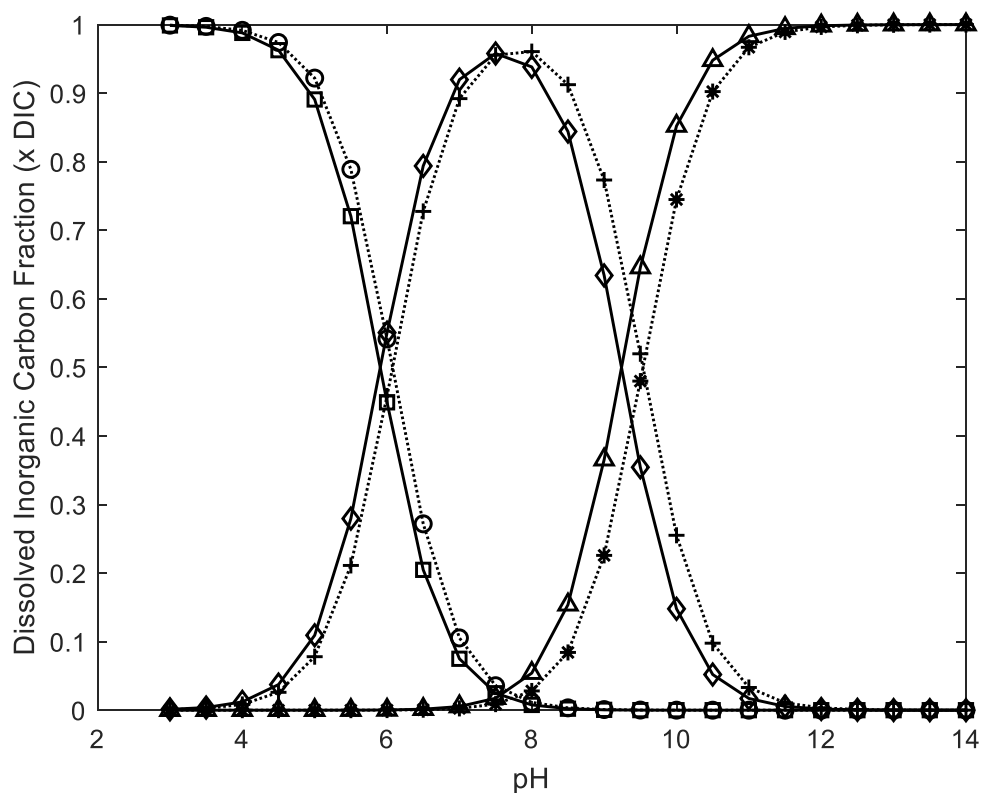


Figure 60 Carbon forms in an aqueous phase as a pH function. Plotted using Stumm and Morgan model. Solid lines for carbonate-free Zarrouk medium at 35°C and dashed lines for the pure water at 20° C, Solid line: (□) H₂CO₃, (◇) HCO₃⁻³, (△) CO₃⁻², Dashed line: (○)

3.1.3.2 Photoperiod effect on the CO₂ bio-mitigation by the *Arthrospira platensis* biomass

A difference in biomass growth kinetics was assessed for the different tested photoperiods. The continuous exposition of the cultures to the light proved to enhance the growth parameters of the cultures. As displayed in Figure 61, the biomass content reached respectively on the 8th day 0.9 ±0.03, 1.74 ±0.03, and 1.98 ±0.03 g/L for 12h/12h, 20h/04h, and 24h photoperiod conditions.

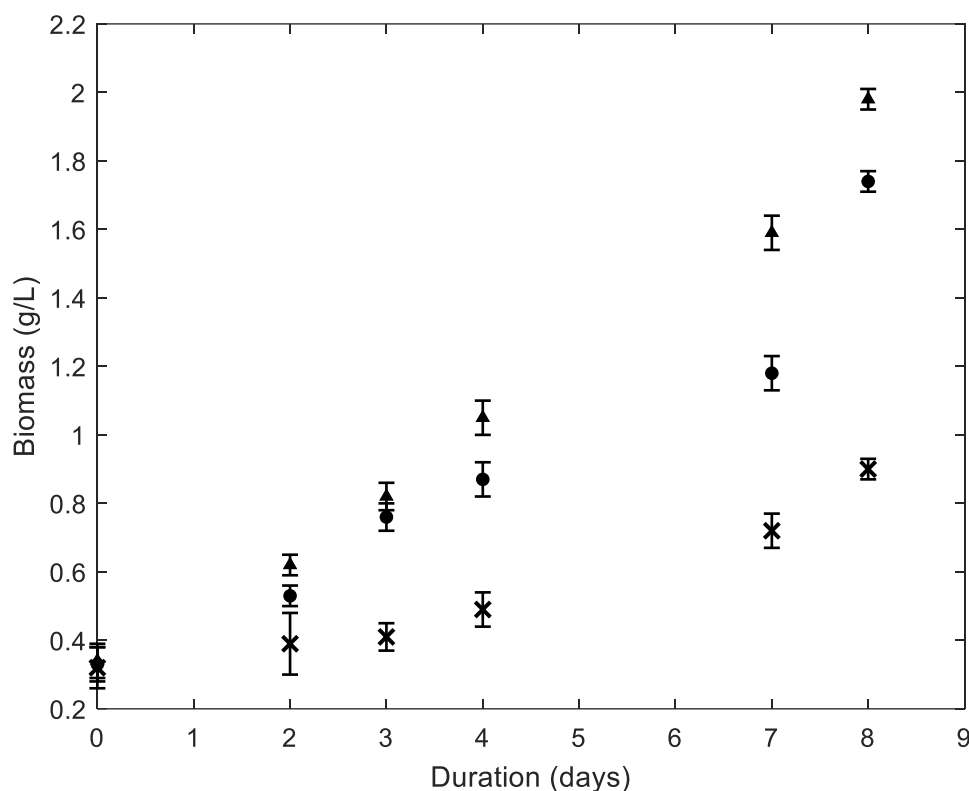


Figure 61 Biomass growth kinetics for the three chosen photoperiods (▲) Continuous illumination 24h photoperiod, (●) 20h/04h photoperiod, (×) 12h/12h photoperiod

The highest biomass content observed with the continuous light does not correspond with the highest measured DIC, confirming that the dissolved carbon concentration is higher than the need for AP. This is in coherency with the results reported by [286] for the *Spirulina sp.* culture in a carbonate-free Zarrouk medium. The biomass content measured for the 20h/04h and 24h photoperiods showed only slight differences and no sign of photoinhibition was observed in any of the conditions of this study, in line with [60] results with *A. platensis*. However, studies on other photosynthetic microorganisms state that photoperiods higher than 18 h could cause an inhibitory effect on biomass growth, such as the one reported by [287] [288] and [289] with *Scenedesmus obliquus* and *Nannochloropsis sp.*, respectively. The carbon content in the biomass did not differ significantly ($p > 0.05$) for the three tested conditions and is measured to be 0.43 ± 0.01 , 0.48 ± 0.03 , and 0.45 ± 0.04 gC/g_{biomass} for respectively the 12h/12h, 20h/04h, and 24h/0h day/night conditions. Nevertheless, the slight carbon content variations at the different conditions may be a response to the photoperiod modifications, provoking an impact on the circadian rhythm and metabolism of the cyanobacteria as reported by [290] and [291].

The photoperiods also affected the biomass productivity and CO₂ fixation rate, as displayed in Table 24. Although the 20h/04h and continuous illumination photoperiods displayed similar

performances in terms of biomass productivity and CO₂ fixation rate, the continuous light photoperiod (24h) exhibited the best performances. However, to define the best photoperiod conditions it would be necessary to evaluate the biomass quality in terms of high-value molecules content, together with the energy input needed to increase the photoperiod with artificial lighting.

Table 24 Average biomass productivity and CO₂ fixation rate as a function of the photoperiod. Average (AVR) and standard deviation (SD)

Photoperiod	12h/12h		20h/04h		24h	
	AVR	%RSD	AVR	%RSD	AVR	%RSD
Biomass productivity (g/L/d)	0.05	5.29	0.09	4.75	0.13	2.39
FCO ₂ (mgCO ₂ /L/d)	71.92	3.61	153.95	8.93	216.84	5.38

The highest biomass productivity and CO₂ fixation rate observed during this study are in line with the ones reported by (Chen *et al.*, 2013), who reported biomass productivity of 0.07 ±0.01 g/L/d and a CO₂ fixation rate of 120 ±0.01 mg (CO₂)/L/d for *S. platensis* cultivated with CO₂ concentration of 2.5% v/v.

It is important to note that one of the objectives of this work was to bring to light the roles and interconnections of different abiotic factors (temperature, photoperiod duration, salinity of the medium, availability of dissolved inorganic carbon) and their impact on the biomass growth parameters and CO₂ fixation rates. The aim was to provide information that serves a better understanding of the complex dynamics that occur in a photobioreactor to enhance the CO₂ bio-sequestration.

3.1.4 Conclusions of laboratory scale *Arthrospira platensis* CO₂ mitigation characterization

To assess the culture of AP as a CO₂ bio-sequestration technique, the DIC concentration in the supernatant, the biomass growth parameters, and the CO₂ fixation rate were evaluated at three different photoperiods. It is well known that the CO₂ dissolution reactions are functions of the physicochemical parameters of the aqueous medium. The DIC concentration did not show significant differences in the three studied photoperiods, as the mean concentration remained at 675 ± 44.5 mgC/L and pH 8.2 ± 0.06 after the first two days of culture growth. The role of AP biomass growth in the CO₂ mitigation was put in evidence, as DIC concentration in the control without biomass remained constantly lower at 36 ± 1.07 mgC/L and pH of 6.7 ±0.1. The transfer of atmospheric CO₂ into the growth medium seems to be enhanced by the

Chapter III : Results and Discussions

alkalization linked with nitrate and CO₂ bio-assimilation. An increase in biomass productivity and CO₂ fixation rate was achieved through increased exposure to light during the photoperiod. The higher biomass productivity and CO₂ fixation rates were assessed during the continuous light photoperiod being respectively 0.13 g/L/d and 216.84mg (CO₂)/L/d. AP culture has proved to be an interesting CO₂ bio-sequestration technique under the studied conditions. In any case, a screening of the high-value molecule content in the biomass, together with the evaluation of the energy consumption linked to the increase of photoperiod duration, are required to determine the interest in prioritizing the continuous light photoperiod from the other options. In addition, the alkalinity of its medium promotes the CO₂ dissolution and is a strong advantage, whereas the high optimal growing temperature and low growth rate of AP compared with other microorganisms are clear drawbacks. Nevertheless, its current market as a natural blue food dye and nutritional supplement, its filamentous structure that facilitates harvesting, and its ability to grow in relatively harsh conditions (pH and temperature) make AP culture an interesting CO₂ bio-mitigation technique.

3.1.5 *Arthrospira platensis* CO₂ mitigation in a 3 L system

CO₂ bio-mitigation by the Arthrospira platensis biomass

The initial culture conditions were the following: DIC of 700 ± 52 mgC/L, a biomass content of 0.53 ± 0.01 g/L, and an initial pH of 8.8 ± 0.3 . After 4 days of culture, the pH increased to 10.7 ± 0.5 , the DIC decreased to 300 ± 20 mgC/L, and the biomass increased to 0.96 ± 0.1 g/L. The final biomass content in the culture was 1.39 ± 0.2 g/L, with a growth rate of 0.12 ± 0.02 d⁻¹ and a productivity of 0.11 ± 0.02 g/L/d (Figure 62). The registered growth parameters were satisfactory, compared to what is reported in the study of [273], who reported a final biomass content of 1.09 g/L, and biomass productivity of 0.07 g/L/d in an AP biomass cultivated at the following conditions in a conventional flask, light intensity: 100 μmol/m²/s, light type: fluorescent, and temperature: 30°C. It was considered that the culture was not carbon-limited.

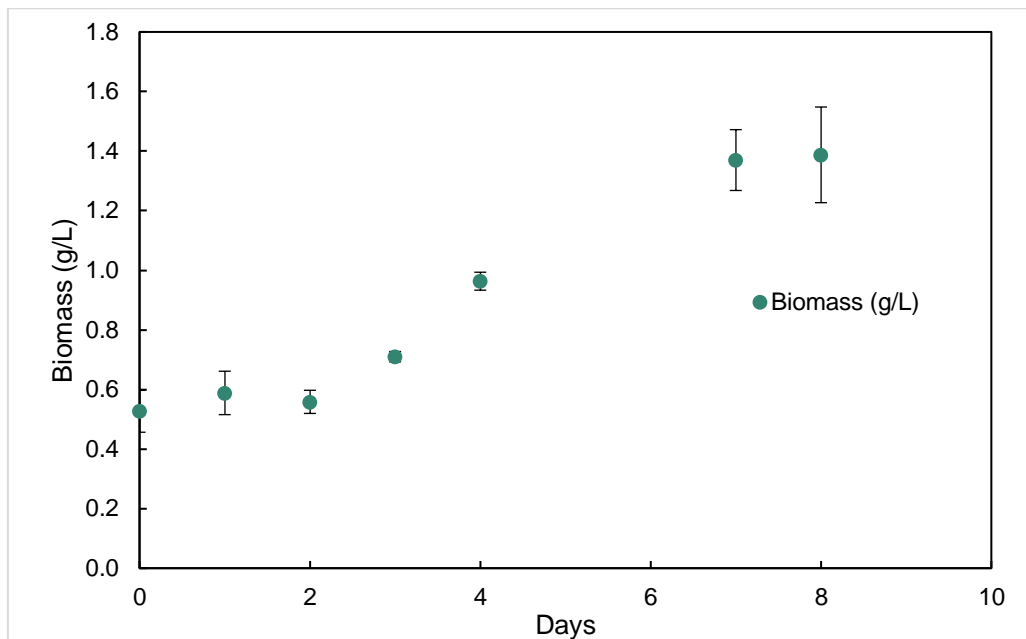


Figure 62 Biomass growth kinetics for CO₂ mitigation evaluation from *Arthrospira platensis* biomass in greenhouse conditions

The culture carbonates were restored by bubbling enriched air at 4% CO₂ v/v on the 4th and 7th days when pH was beyond 10. The DIC concentration was increased to 600 ± 80 mgC/L. Three CO₂ bubblings were performed, one at the culture start, one on the 4th day, and lastly on the 7th day, as pictured in Figure 63.

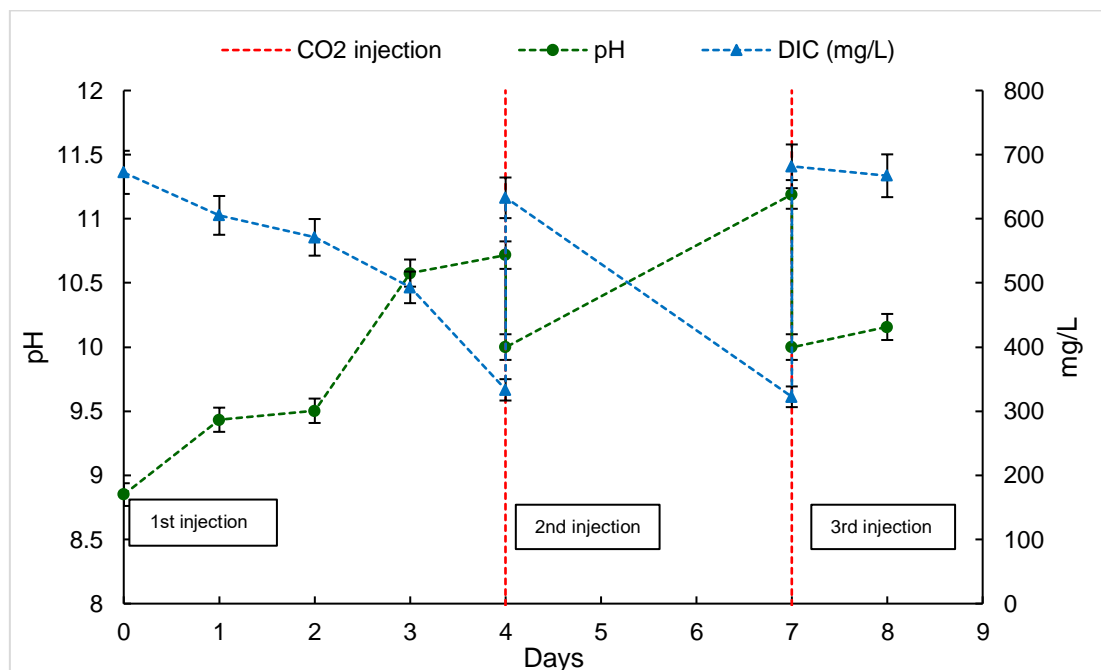


Figure 63 pH and Dissolved Inorganic Carbon (DIC) evolution for the 3 L culture. The dashed blue lines on the 4th and 7th day represent the CO₂ injection for the restoration of the carbon source

Chapter III : Results and Discussions

The absorption efficiencies of carbon mass balance for the global system, medium, assimilation, and biomass were determined using equations. (36), (39), (41), and (43) from p.90, respectively. The obtained efficiencies are displayed in Table 25.

Table 25 Carbon mass balances for the 3 L system

CO₂ injection	1ST	2ND	3RD
C_{IN} (g)	11.76	11.76	11.76
C_{MEASURED} (g)	1.67	1.54	0.8
C_{ABSORBED} (g)	1.02	0.93	0.77
C_{BIOMASS} (g)	0.65	0.61	0.03
DIC_{IDEAL} (g)	1.67	1.54	0.8
η_{global} (%)	14.22	13.10	6.77
η_{medium} (%)	8.7	7.9	6.6
η_{assimilation} (%)	5.6	5.2	0.2
η_{biomass} (%)	39.17	39.59	3.3

The decrease in the global carbon mitigation of the system in the 3rd injection can be attributed to the decrease in the biomass productivity observed in the culture, that passed from 1.37 to 1.39 g/L/d from the 7th to the 8th day of the culture. However, the obtained global carbon mitigation efficiency of the system was of 13.66% ± 1.11%. This mitigation efficiency is comparable with the one reported by [12], who cultured *Chlorella sp.* in a semicontinuous mode, injecting CO₂ 15% v/v and reported a CO₂ assimilation of 11%. The authors explain their efficiency in CO₂ assimilation as a result of a pre-adaptation of the strain and the implementation of a large inoculum.

It is known that the absorption rate in the medium depends on the physicochemical conditions reviewed in section 1.3.4 from p.32, and on the hydrodynamic conditions of the photobioreactor, such as the mixing rate, the bubble size, and the retention time of the bubble in the PBR [31][33][62]. However, it is yet needed to characterize the impact of the light exposure by cell and the PBR configuration in the CO₂ mitigation by aquatic photosynthetic microorganisms like AP. By the application of the equation (32) from p.85, the mean specific photon flux density (φ) in this culture was 1.69 μmol/g s ± 0.27 μmol/g s.

3.1.6 *Arthrospira platensis* CO₂ mitigation in a 3 m³ system

The culture's starting conditions, as outlined in Table 13 in p. 88, included an initial DIC of 500 mgC/L, a pH ranging from 9.15 ± 0.2, and an initial biomass of 0.3 g/L. Regarding the culture temperature, it's important to highlight that in the initial 30 days of cultivation, the PBR operated without a heating system. As a result, the temperature fluctuated between 20 and 30°C, hindering the biomass from achieving satisfactory productivity (See Figure 97 in Annex p.226).

The initial carbon stock maintained a DIC level above 400 mgC/L until the 20th day of cultivation, reaching 320 mgC/L, indicating proximity to carbon scarcity conditions. Until this day, the biomass content increased to 0.5 ± 0.1 g/L and reached its stationary phase. The growth rate and biomass productivity were determined by applying equations (14) and (15) from p.75, being 0.058 ± 0.001 d⁻¹ and 0.01 ± 0.0001 g/L/d, respectively. The obtained biomass productivity is comparable to the one reported by [292], where an AP strain was cultivated in a 4m² indoor raceway, with CO₂ as its principal carbon source.

The first injection was performed on the 20th day of cultivation when the temperature was 30°C, a pH of 10 ± 0.5 , and a DIC 360 ± 36 mgC/L. After 1.6 h of bubbling, the DIC increased to 470 ± 60 mgC/L and the pH decreased to 8.3 ± 0.2 . It took around 15 hours for the culture to regain the equilibrium pH of 9.4 (See Figure 64). It is important to note that the coupled column to the system played a role in the carbon desorption of the media previously injected. As seen in the figure mentioned earlier, the pH decrease corresponds to an increase in DIC concentration in the medium. The subsequent pH increase and DIC concentration decrease within a 15-hour span, without a significant increase in biomass content, suggests a carbon loss likely caused by the interaction between the airlift system and the carbon charged medium raceway. This phenomenon was not present in the 3 L system, where the pH increase and DIC decrease could be linked to a biomass increase.

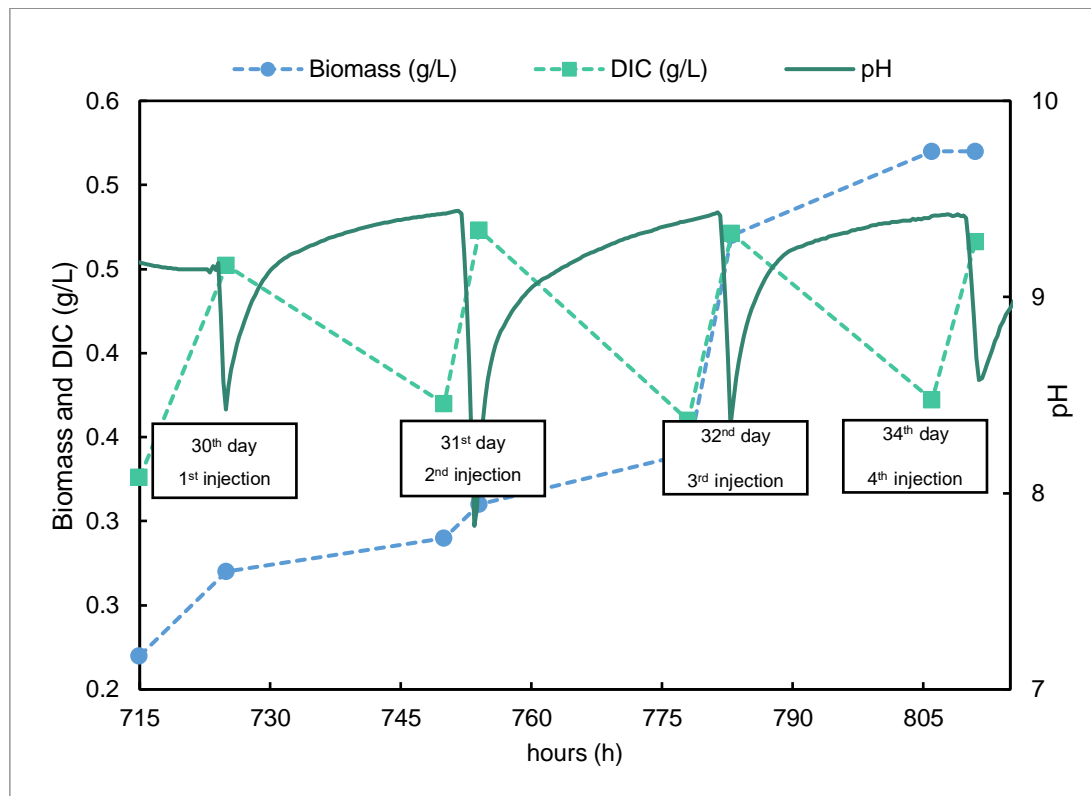


Figure 64 Biomass content, Dissolved Inorganic Carbon, and pH evolution during the 30th to 34rd culture in the 3 m³ raceway. The pH data plotted was obtained by the culture pH sensor. Each pH decrease represents a CO₂ injection to the PBR.

Eight CO₂ bubbling’s were performed on the culture during the following days to restore the carbon content for the culture development (Table 26).

Table 26 Carbon mass balances for the 3 m³PBR. The carbon mass is expressed in average values.

CO ₂ injection	1 ST	2 ND	3 RD	4 TH	5 TH	6 TH	7 TH	8 TH
C _{IN} (g)	514.74	542.48	588.72	554.81	576.39	557.90	357.55	258.91
C _{MEASURED} (g)	389.53	328.42	359.75	431.89	342.98	414.69	192.37	189.84
C _{ABSORBED} (g)	355.25	296.78	328.11	400.25	327.16	393.60	192.37	189.84
C _{BIOMASS} (g)	34.28	31.64	31.64	31.64	15.82	21.09	0	0
DIC _{IDEAL} (g)	386.43	328.42	359.75	431.89	342.98	414.69	192.37	189.84
η _{global} (%)	75.67	60.54	61.11	77.84	59.50	74.33	53.80	73.32
η _{medium} (%)	69.02	54.71	55.73	72.14	56.76	70.55	53.80	73.32
η _{assimilation} (%)	6.66	5.83	5.37	5.70	2.74	3.78	0	0
η _{biomass} (%)	8.87	9.63	8.80	7.33	4.61	5.09	0	0

The global and medium carbon absorption efficiencies averaged 65.78% ± 9.19% and 62.43% ± 9.03%, respectively. Excluding the 7TH and 8TH injections, the biomass exhibited an average efficiency of 7.09% ± 2.21%. These findings demonstrate the potential of cultivating AP biomass in this PBR setup for CO₂ storage and utilization. However, it was noted that the primary factor in CO₂ absorption from the medium was chemical absorption, overshadowing

the contribution of biomass growth to CO₂ mitigation. This may be attributed to limited light availability, with PAR < 100 μmol/m²/s (refer to Table 13, p.88), hampering biomass development in this system. Moreover, the utilization of the column prevented the accumulation of Dissolved Inorganic Carbon (DIC) in the system. The carbon accumulation in the PBR was not evident, as the contact of the culture medium with the air used for column operation induced gas desorption, inhibiting observable carbon accumulation. To improve this process, consider the following recommendations: reduce the culture level to shorten the light path and increase the light availability, cover the raceway surface to prevent CO₂ loss, and operate the column with enriched CO₂ rather than air to avoid carbon desorption.

To estimate the biomass's CO₂ fixation rate, the theoretical productivity for indoor raceways proposed by Muller-Feuga, 2003 [49] was considered at 25 g/m² per day. Accounting for the surface and volume of the studied system and applying the CO₂ mitigation efficiency in equation (22), the calculated value was 168.05 mg CO₂/L/day. This aligns closely with the value reported by [1], which was 169.26 mg CO₂/L/day for *Spirulina sp.* cultivated in a columnar photobioreactor with 10% CO₂, under LED illumination of 56–63 μmol/m²/s in a 12:12 h dark-light (D:L) photoperiod. Nonetheless, the same study reports CO₂ mitigation efficiencies from different strains ranging from 55.20 to 414.15 mg CO₂/L/day. The study argues that the CO₂ fixation rate of a strain not only relies on the culture parameters, but also on the strain tolerance to a certain condition, like high CO₂ concentration or high temperature.

The hydrodynamic conditions of the photobioreactor affect directly the mass transfer phenomena in the PBR. When comparing the CO₂ absorption efficiency of the two evaluated systems it could be confirmed that the coupled absorption column and the micro-diffuser installed in the raceway fulfill their duty in the gas dissolution into the medium (Table 27). Concerning the utilization of dissolved CO₂ for biomass development, the bottle system demonstrates superior performance. This could be attributed to the higher light availability per gram of biomass in the bottle system, as indicated by the mean specific photon flux density, which is 2.68 times greater than the light received by the biomass in the raceway. Finally, when it comes to global CO₂ mitigation efficiency, the raceway system fulfills this function in a better way, demonstrating the importance of installing an adequate gas dissipation technology in biomass culture for CO₂ mitigation purposes. On the other hand, once the gas dissolution is warranted it is very important to provide the light conditions for the conversion of the dissolved CO₂ into biomass. It was observed that when it comes to the CO₂ assimilation by the biomass growth the bottle culture proved to have better performance, due to the light availability that this system presents, confirmed by the φ parameter.

Chapter III : Results and Discussions

Table 27 Studied photobioreactors CO₂ mitigation comparison

	3 L Bottle Culture	3 m³ Raceway with absorption column
η_{global} (%)	11.37 ± 4.01	65.78 ± 9.19
η_{medium} (%)	7.71 ± 1.06	62.43 ± 9.03
$\eta_{biomass}$ (%)	39.38 ± 0.42	7.09 ± 2.21
φ (μmol/g/s)	1.69	0.63
F_{CO_2} (mg CO ₂ /L/d)	216.84	168.05 *

* Calculated employing a productivity theoretical value.

3.1.7 Conclusions of greenhouse conditions *Arthrospira platensis* CO₂ mitigation characterization

Both evaluated systems presented similar behaviors in terms of pH and DIC equilibria, at 10.35 ± 0.49 and 305 mgC/L ± 7.07 mgC/L, respectively. The physicochemical conditions of AP culture proved to be adequate for CO₂ assimilation, according to the carbon assimilation model presented in 3.1.3 p.130. This makes AP an adequate microorganism for the biological fixation of CO₂ and the simultaneous mass cultivation, exploiting its alkali-tolerant characteristics. However, the operating conditions of both studied systems were not adequately managed provoking a CO₂ desorption potentially caused by the mixing strategies [293]. A constant CO₂ deliver approach like the one performed in the laboratory scale combined with appropriate lightening is recommended to increase the performance in both systems. Separating CO₂ absorption in the medium from biomass cultivation would allow both processes to operate optimally without compromising either the CO₂ absorption in the medium or its conversion into biomass. Furthermore, light availability proved to be a decisive parameter when it comes to CO₂ conversion into biomass affecting severely biomass productivity in the raceway and its CO₂ mitigation rate.

3.1.8 Enhancement of pigment productivity in *Arthrospira platensis* cultures

Abstract

Light availability is one of the fundamental parameters that affect the performance of a PBR, this experiment aims to characterize the impact of the photoperiod modification on the biomass growth parameters and pigment content. The photoperiod effect on biomass was tested by two approaches, fully controlled physicochemical parameters at incubator conditions, and greenhouse light conditions with artificial complementary light to reach a 24-hour photoperiod. In the incubator conditions experiment, two medium treatments were tested: Zarrouk medium (ZM) and Carbon Free Zarrouk medium (CFZM). The results of this test showed that the differences in terms of growth parameters and pigment content of the produced biomass are not significant between medium treatments. Nonetheless, when modifying photoperiods at incubator conditions from 12h/12h to 24 h (continuous light) an increase of $74.07 \pm 3.76\%$ and $80 \pm 1.8\%$ in the global productivity for ZM and CFZM, respectively was registered. Concerning the PBP content in the biomass an increase of $35.34 \pm 5.04\%$ and $36.84 \pm 3.5\%$ was registered when increasing the photoperiod from 12h/12h to 24 h (continuous light) in both medium treatments. Regarding the Chl a and carotenoids profile in the biomass, a reduction of these molecules in the biomass was measured parallelly to a PBP increase in the different tested photoperiods at incubator conditions. Carotenoids like, β -carotene, zeaxanthin, and myxoxanthophyll were identified in the produced biomass. Finally, the 24-hour photoperiod was conducted under greenhouse light conditions supplemented with artificial light. A control experiment under sunlight conditions was conducted. No significant differences were observed between the experiments in terms of growth parameters, however, the PBP content was reduced by $30\% \pm 12\%$ under the 24-hour photoperiod, this change in the biomass pigment profile might be triggered by the sunlight intensity modification compared to the incubator conditions experiment.

Chapter III : Results and Discussions

3.1.8.1 Artificial light photoperiod modification in incubator conditions

The increase in the photoperiod daytime showed a positive effect on the biomass content, productivity, and growth rate of the biomass in the cultures. In the experiment performed with the Zarrouk Medium (ZM) the final biomass content X_{\max} (g/L) showed an increase from 0.73 ± 0.05 to 2.17 ± 0.07 g/L in the photoperiod of 12h/12h and 24h, respectively (See Figure 65).

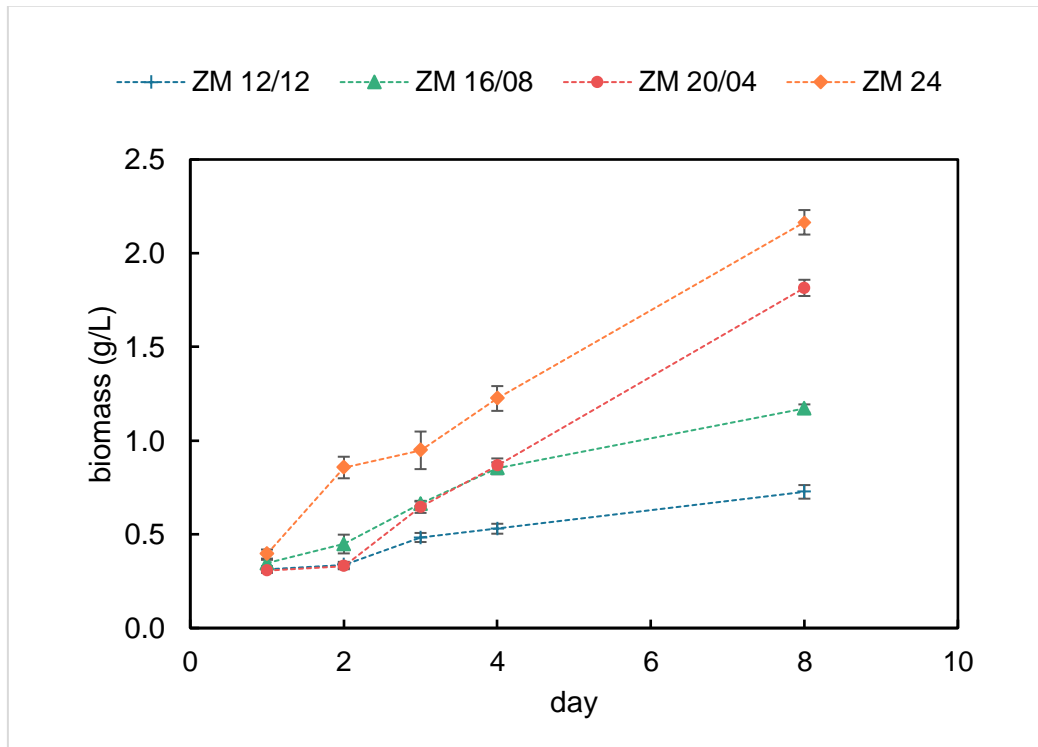


Figure 65 Biomass growth at different photoperiods in incubator conditions using the Zarrouk Medium treatment

The productivities were and growth rates of the 3rd culture day being these the higher registered values for this parameter (See Table 28).

Meanwhile, in the experiment performed with the CFZM the final biomass content increased from 0.9 ± 0.03 to 1.98 ± 0.18 g/L in the photoperiods of 12h/12h and 24h, respectively (See Figure 66).

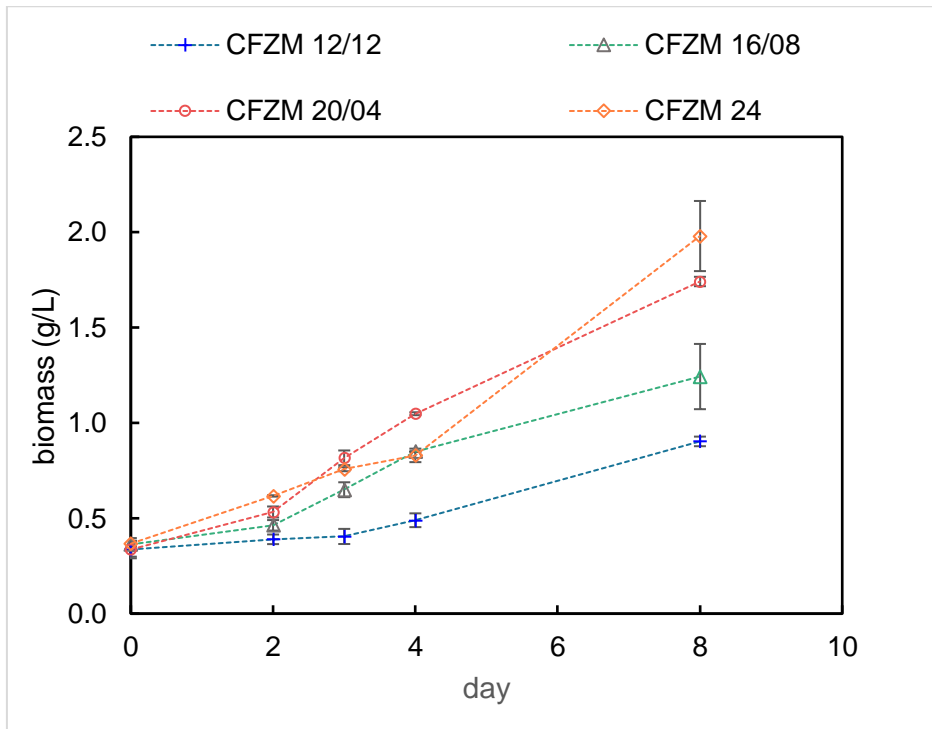


Figure 66 Biomass growth at different photoperiods with the CFZM treatment

The differences between parameters for the two medium treatments CFZM and ZM can be considered negligible (See Table 28).

Table 28 Biomass productivity and growth rate comparison at different photoperiods and media carbon source

	$P_{\text{biomass}}(\text{g/L/d})$ 12h/12h	$P_{\text{biomass}}(\text{g/L/d})$ 16h/08h	$P_{\text{biomass}}(\text{g/L/d})$ 20h/4h	$P_{\text{biomass}}(\text{g/L/d})$ 24h (continuous)
ZM	0.07 ± 0.01	0.15 ± 0.01	0.23 ± 0.01	0.27 ± 0.01
CFZM	0.05 ± 0.01	0.16 ± 0.01	0.22 ± 0.01	0.25 ± 0.04

The positive effect of photoperiod increase has been described previously with other photosynthetic microorganisms [14][15][16]. Different species respond differently to the photoperiods and light intensity variation [17] [18], see Table 29.

Chapter III : Results and Discussions

Table 29 Growth rate response to 24h photoperiod from different photosynthetic microorganisms

Strain	Photoperiod	μ (d ⁻¹)	Reference
<i>A.platensis</i>	24h	0.77	This study, ZM, continuous artificial light
<i>B. braunii</i>	24h	0.66	[294]
<i>S. obliquus</i>	24h	0.71	[294]
<i>A.platensis</i>	24h	0.13	[96]
<i>T. chui</i>	24h	0.61	[295]

Globally, the photoperiod increase has a positive effect on the biomass growth. Nonetheless, the mass density increase in the culture affects the cell's the light availability. Extending the photoperiod in artificial light conditions positively increased the photosynthetic pigment content in the cultivated biomass. This effect was also discussed by [296]. The studies made by Danesi, 2014 [271] and Olaizola, 1990 [87] have demonstrated the ability of microalgae to photo-acclimate changing the size of their thylakoid number and photosynthetic pigments.

Phycocyanin was the primary produced phycobiliprotein (PBP) across the four tested photoperiods, with its content increasing at each condition (refer to Figure 67). Conversely, both allophycocyanin and phycoerythrin content remained stable throughout the experimentation (see Figure 30).

Table 30 Incubator conditions phycobiliproteins content in biomass cultivated at different photoperiods employing ZM

	12h/12h	16h/08h	20h/04h	24h
Phycocyanin (%)	9.11 ± 0.3	10.3 ± 0.13	17 ± 0.24	16.6 ± 0.07
Allophycocyanin (%)	6.9 ± 0.34	6.8 ± 0.14	5.7 ± 0.22	7.9 ± 0.15
Phycoerythrin (%)	1.2 ± 0.21	1.5 ± 0.12	1.2 ± 0.17	1.3 ± 0.03

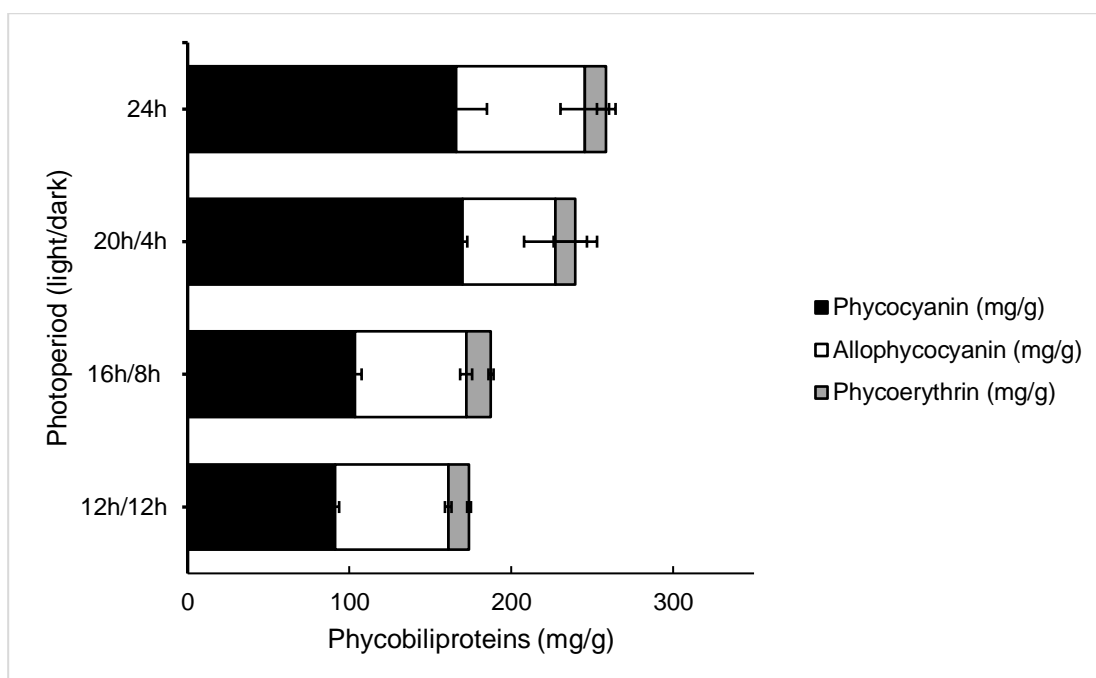


Figure 67 Phycobiliproteins content in the biomass at different photoperiods with the Zarruk Medium treatment in incubator conditions.

Similarly, in the CFZM treatment, the PBP content increased from 17.75 ± 0.56 % wt PBP in the 12h/12h photoperiod to $28.1 \pm 0.05 \pm 0.56$ % wt PBP in the 24h/0h photoperiod (Figure 68), this value is similar to the one reported by [40] [273]. Phycocyanin, the primary phycobiliprotein (PBP) in the biomass, remained stable across 12h/12h, 16h/08h, and 20h/04h photoperiods. However, during the 24h photoperiod, phycocyanin content increased by 24%. Allophycocyanin exhibited a similar trend, while phycoerythrin content in the biomass varied without a clear pattern across different photoperiods (Refer to Table 31).

Table 31 Incubator conditions phycobiliproteins content in biomass cultivated at different photoperiods employing CFZM

	12h/12h	16h/08h	20h/04h	24h/0h
Phycocyanin (%)	11.1 ± 0.24	11.2 ± 0.4	11.6 ± 0.24	14.6 ± 0.02
Allophycocyanin (%)	6.1 ± 0.2	6.7 ± 0.37	4.6 ± 1.94	10.1 ± 0.02
Phycoerythrin (%)	4.4 ± 0.11	2.2 ± 0.37	5.7 ± 0.13	3.2 ± 0.04

Chapter III : Results and Discussions

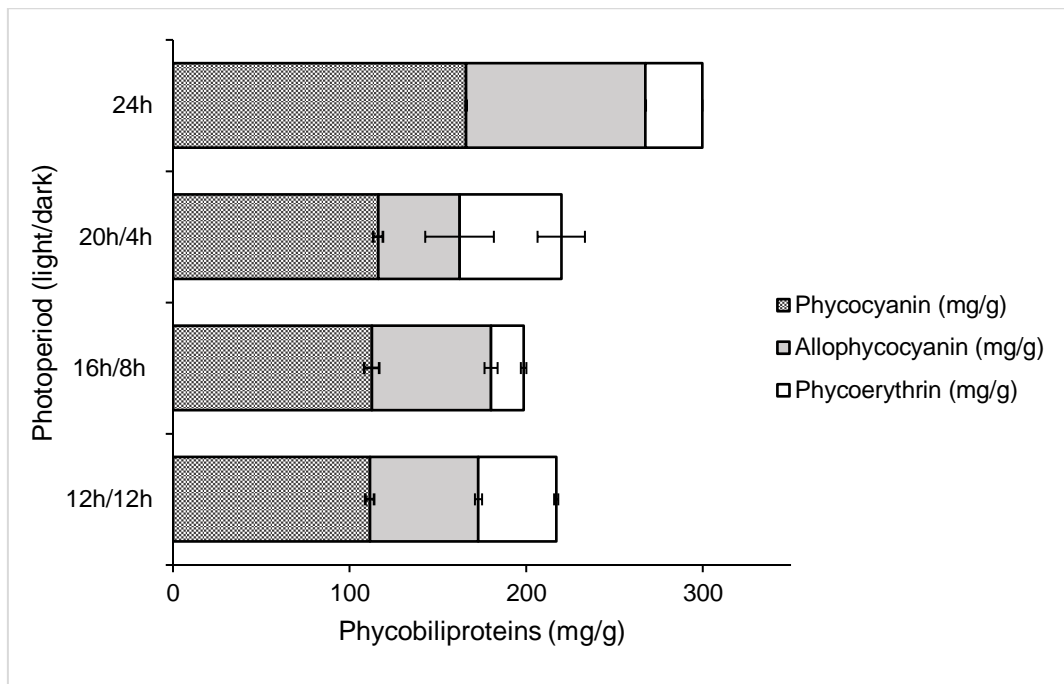


Figure 68 Phycobiliproteins content in the biomass at different photoperiods with the CFZM treatment

In both treatments biomass increase enhanced the production of PBP in AP cells, increasing the PBP content in cells to increase their photosynthetic efficiency. The obtained results in this work are similar to the ones obtained by Kilimtzi, 2019 [93], who assessed an increase in the phycocyanin and protein content by the shading effect of the culture.

The obtained phycocyanin content is consistent with the results obtained by other studies where the light was attenuated or modified (See Table 32).

Table 32 Biomass phycocyanin content comparison

Microorganism	Phycocyanin (mg/g biomass)	Light type	Light intensity ($\mu\text{mol}/\text{m}^2 \text{ s}$)	Photoperiod I/D (h/h)	Ref.
<i>S. platensis</i> (ATCC 29408)	152	Red LED	750	NR	[90]
<i>A. platensis</i> (SAG 21.99)	134.71	Red LED	100	16/08	[93]
<i>Spirulina sp.</i> (LEB 18)	126	Green Fluorescent lamp Green LED	F: 3200 L: 500	12F/06L/12 D	[291]
<i>S. platensis</i>	148.1	Silver light reflector	92	NR	[95]
<i>A. platensis</i> (SAG 21.99)	166	White LED	100	24/0	This study, ZM, continuous artificial light

NR: Not reported; F: Fluorescent tube; L: LED; D: Dark, l: light

Globally, extending the photoperiod had a decreasing effect on the Chl a and carotenoid content in the biomass for both treatments. These results are consistent with the results reported by Seyfabadi, 2011 [297], who noticed a significant variation in the biochemical composition of the biomass linked to the irradiance exposure. Bouterfas *et al.* [298] and Hobson, 1979 [299], reported a Chl a decrease associated with the daylight increase.

In the ZM treatment, there was an observed increase in Chl a, rising from 2.23 ± 0.39 $\text{mg}_{\text{Chla}}/\text{g}_{\text{DW}}$ in the 24h photoperiod to 8.87 ± 0.53 $\text{mg}_{\text{Chla}}/\text{g}_{\text{DW}}$ in the 12h/12h photoperiod (Figure 69). A decreasing trend in the Chl a concentration was observed with the increase of the photoperiod, while the carotenoid content in the biomass stayed nearly stable during the photoperiods of 12h/12h, 16h/08h, and 20h/04h. Nevertheless, during the 12h/12h photoperiod, the carotenoid content was 8.87 ± 0.02 mg of carotenoids g of biomass (See Table 33)

Table 33 Incubator conditions carotenoids and chlorophyll a content in biomass cultivated at different photoperiods employing ZM

	12h/12h	16h/08h	20h/04h	24h/0h
Chl a (%)	0.88 ± 0.05	0.3 ± 0.07	0.35 ± 0.03	0.22 ± 0.04
carotenoid (%)	0.88 ± 0.02	0.27 ± 0.08	0.25 ± 0.37	0.21 ± 0.04

Chapter III : Results and Discussions

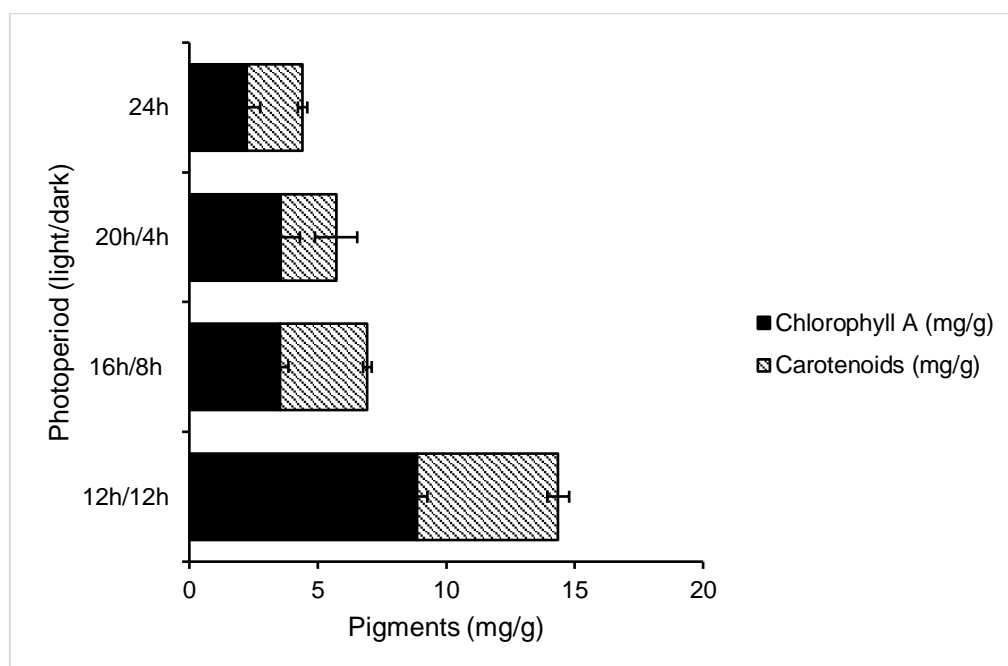


Figure 69 Chl a and carotenoids content at different photoperiods with Zarrouk Medium treatment

Comparably, during the treatment with CFZM, the Chl a concentration in the biomass showed a similar tendency to the one observed in the ZM treatment (Table 35). Carotenoid content showed a slight variation during the photoperiods of 16h/08h, 20h/04h and 24h, respectively. While, the biomass grown during the 12h/12h showed a carotenoid concentration of $4.44 \pm 0.02 \text{ mg}_{\text{Carotenoid}}/\text{g}_{\text{DW}}$ (Figure 70).

Table 34 Incubator conditions carotenoids and chlorophyll a content in biomass cultivated at different photoperiods employing CFZM

	12h/12h	16h/08h	20h/04h	24h/0h
Chl a (%)	0.79 ± 0.02	0.64 ± 0.08	0.51 ± 0.05	0.32 ± 0.04
Carotenoid (%)	0.44 ± 0.01	0.33 ± 0.03	0.21 ± 0.01	0.24 ± 0.03

Chen, 2010 [90] and Kilimtzidi, 2019 [93] reported a decrease in the Chl with an increase in the light intensity. According to Lönneborg, 1985 [25] Chl and PBP can work as complementary light-harvesting systems. According to this author Chl a accumulation stops when PBP production increases in the cell.

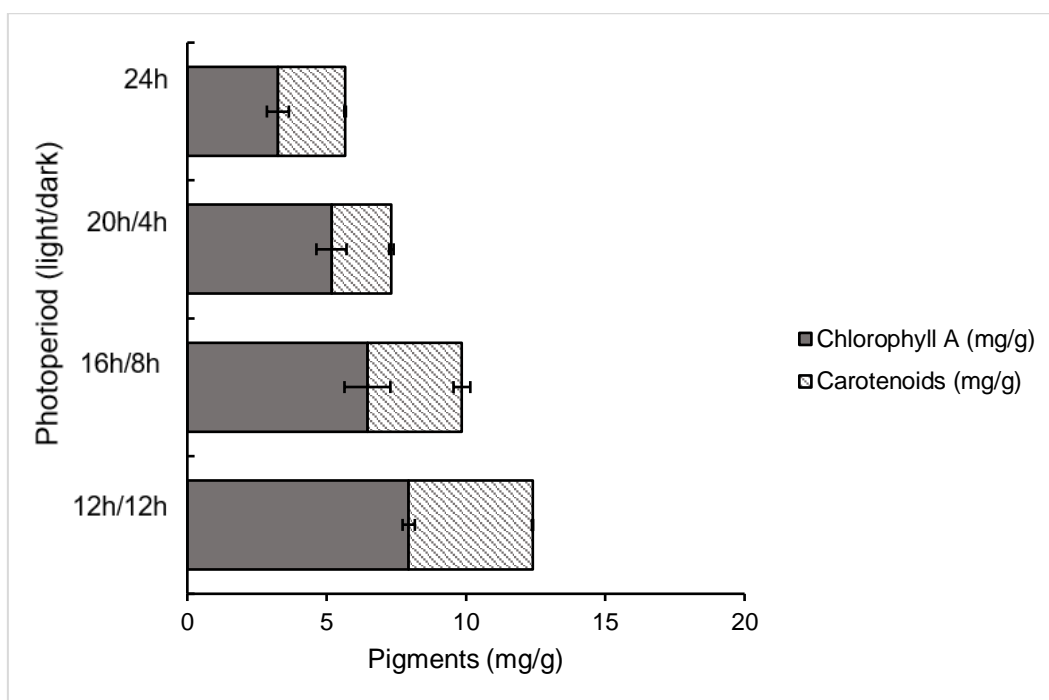


Figure 70 Chl a and carotenoids content at different photoperiods with CFZM treatment

3.1.8.2 High Liquid Pressure Chromatography lipophilic pigment analysis

The pigments present in the biomass at different photoperiods were analyzed parallelly by the HPLC method described in 2.1.9 in p.76, to identify all the carotenoid types present in the extracts, and confirm the Chl a presence. This essay confirmed the existence of the following carotenoids in the analyzed biomass: myxoxanthophyll, zeaxanthin, and β -carotene were present in all the samples. Moreover, when comparing the pigment concentration obtained by the spectrophotometric and HPLC methods, an error of $\pm 0.16\%$ wt biomass for all the samples.

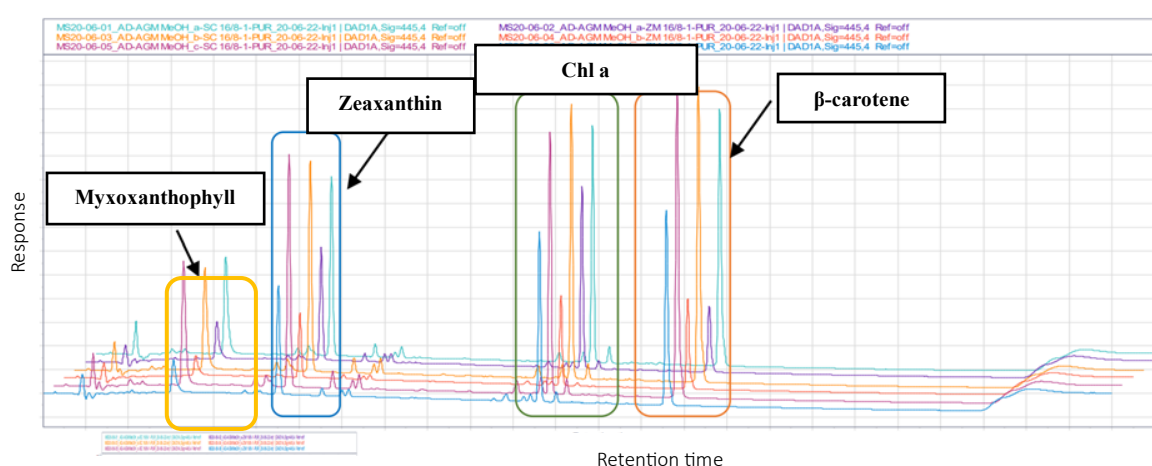


Figure 71 HPLC chromatogram of the extracted polar pigments in the biomass of the 16h/08h photoperiods of both of the given treatments.

When analyzing the carotenoid concentrations in the samples, the profiles described in Table 35 were found. β -carotene emerged as the dominant carotenoid in the examined biomass,

Chapter III : Results and Discussions

with its concentration significantly elevated under the 12-hour light photoperiod. This notable increase can be attributed to the lower biomass content generated under this light condition, exposing the cells to higher light intensity compared to conditions with higher biomass content. This higher light intensity may enhance the carotenoid metabolism in cells. Carotenoids are known to be a group of pigments with a functional and structural role in the cell. The β -carotene is the only carotenoid localized in the PSII [300]. According to Zakar *et al.* 2016 [300] carotenoids are indispensable for photosynthesis not only because they are involved in the photoprotective role of the cell but for the productive synthesis and accumulation of photosynthetic proteins especially.

Table 35 HPLC Carotenoid concentrations found in the biomass studied from the different photoperiods at laboratory conditions.

Medium treatment	Photoperiods	β -carotene (mg/g)	Zeaxanthin (mg/g)	Myxoxanthophyll (mg/g)
ZM	12h/12h	5.93 \pm 1.64	1.15 \pm 0.14	-
	16h/08h	2.37 \pm 0.75	0.90 \pm 0.15	0.42 \pm 0.1
	20h/04h	2.22 \pm 0.18	0.47 \pm 0.09	-
	24h	2.10 \pm 0.01	0.25 \pm 0.05	-
CFZM	12h/12h	3.02 \pm 1.51	0.89 \pm 0.12	-
	16h/08h	2.77 \pm 0.08	0.37 \pm 0.08	0.25 \pm 0.1
	20h/04h	2.04 \pm 0.14	0.62 \pm 0.02	-
	24h	2.07 \pm 0.01	0.29 \pm 0.02	-

*The myxoxanthophyll was not quantified in the 12h/12h, 20h/04h, and 24h conditions, due to the low content of this molecule in the biomass.

3.1.8.3 Natural light conditions

The obtained results from the 24-hour photoperiod at incubator conditions produced a higher PC content and boosted the growth parameters of the culture. Thus, this photoperiod was selected to be replicated in natural light conditions complemented by LED lamps at greenhouse conditions as pictured in Figure 36 p.94, a control with only natural light was followed in parallel to contrast the photoperiod effects in the biomass growth parameters and PBP profile. In these experiments, PAR ranged from 30-2025 $\mu\text{mol}/\text{m}^2/\text{s}$ (Figure 72), for the control experiment and 220-2025 $\mu\text{mol}/\text{m}^2/\text{s}$ for the continuous light experiment. In the continuous light experiment, the temperature ranged from 30-40°C, whereas in the control group, it varied between 25-35°C, see Figure 98 in Annex p.189.

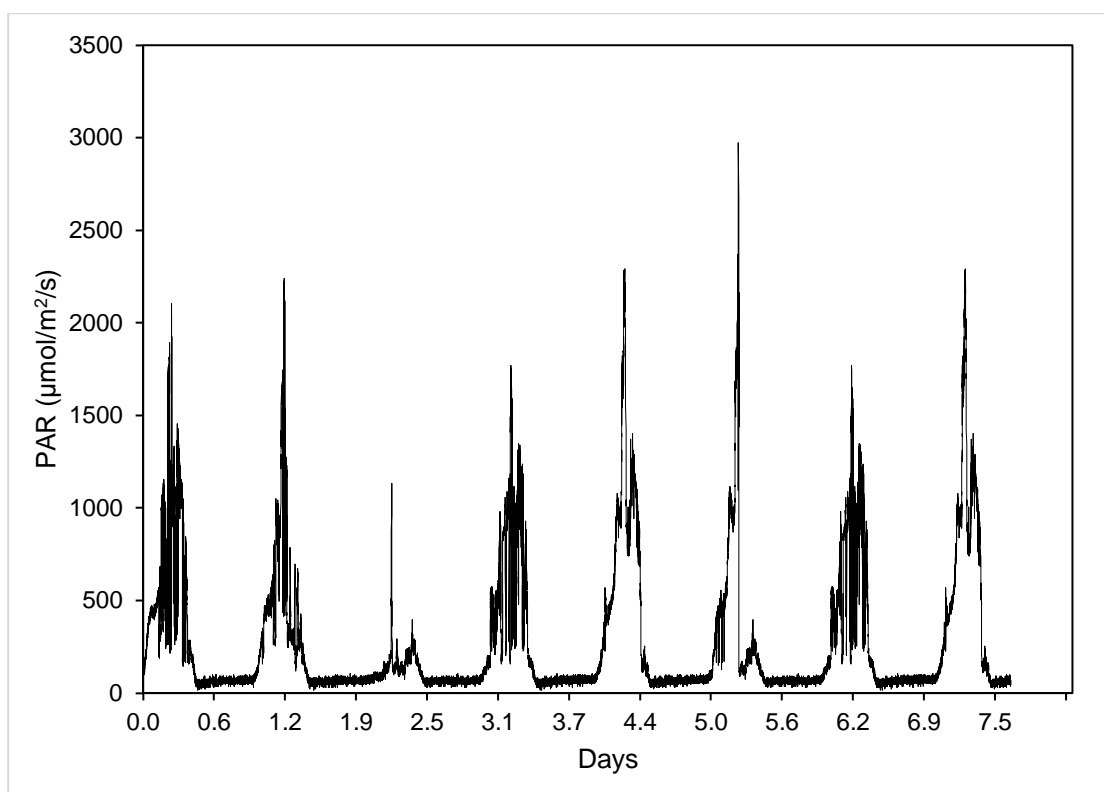


Figure 72 Photosynthetic Active Radiation (PAR) received by the control experiment in greenhouse conditions.

No significant differences were observed in the assessed growth parameters between the control group and the continuous light experiment. This indicates that the supplementary light in natural conditions does not yield significant variations in culture productivities, unlike the outcomes obtained in laboratory settings (Refer to Table 36).

Table 36 Growth rate parameters obtained during the experiments with natural light

	$X_{\text{biomass}}(\text{g/L})$	$P_{\text{biomass}}(\text{g/L/d})$	$\mu(\text{d}^{-1})$
Continuous light	1.20 ± 0.06	0.15 ± 0.01	0.25 ± 0.01
Control	1.02 ± 0.05	0.12 ± 0.01	0.27 ± 0.01

Similarly, the temperature difference between the control and light supplemented system did not proved to have a significant influence on the biomass growth. This suggests that the light apported by the LED group was not adapted to reproduce the light conditions tested in the laboratory. It is important to note that the PAR in laboratory conditions was constant during the 24h. While the PAR in the greenhouse conditions did varied along the day (Figure 72). Moreover, the light spectrum of both experiments was different one from each other (Refer to Figure 29 and Figure 37 in p.74 and p.95, respectively). To replicate the laboratory results in natural light conditions, it is recommended to supplement sunlight with an additional LED group featuring higher light intensity. This approach aims to achieve a consistent PAR comparable to the levels obtained in the controlled laboratory environment.

Chapter III : Results and Discussions

To evaluate the influence of light on the phycobiliprotein (PBP) content in the cultivated biomass, phycocyanin was consistently monitored throughout the entire experiment as a reference pigment. The phycocyanin concentration in biomass evolved similarly in the light-supplemented and control experiments (Figure 73).

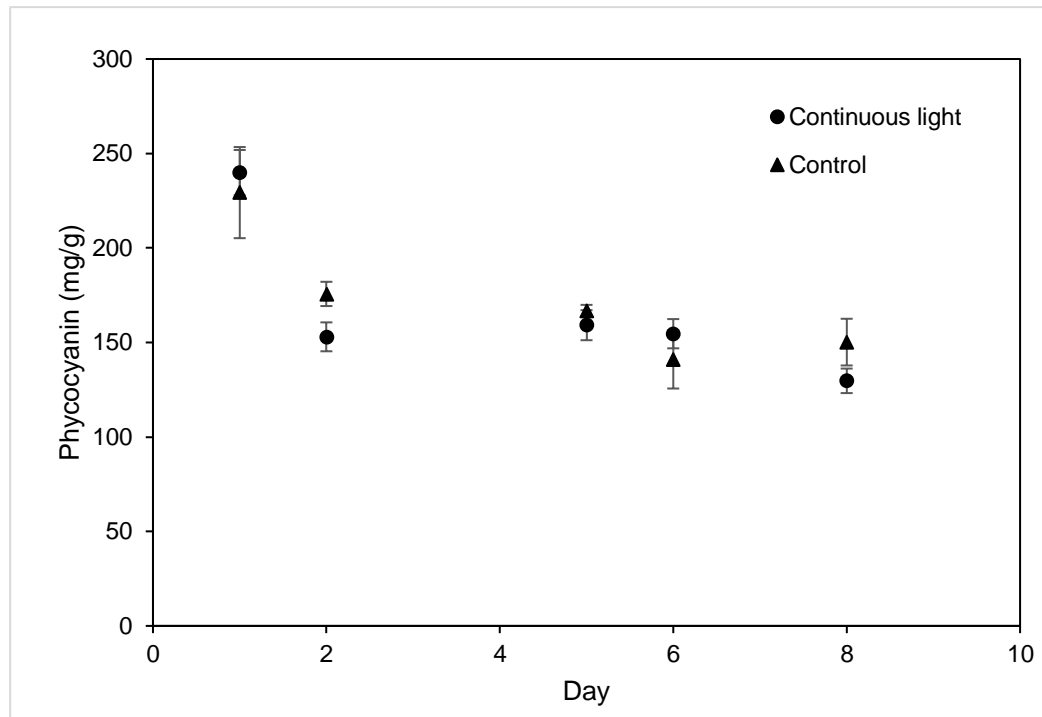


Figure 73 Phycocyanin evolution during the greenhouse conditions photoperiod experiment

A decrease of $37.39\% \pm 1.25\%$ in the phycocyanin concentration was observed by the end of the experiment. This might be enhanced by the increase in the light intensity received by the cultures Figure 72, hindering the need to produce antenna pigments like PBP. It's crucial to highlight that the cultures exposed to natural light experienced a maximum PAR of $2025 \mu\text{mol}/\text{m}^2/\text{s}$, which is 20 times higher than the conditions inside the incubator.

Concerning the PBP profile of the produced biomass on the 8th day of the experiment, it was observed that the biomass from the control experiment contained $30\% \pm 12\%$ more PBP than the continuous light experiment (Figure 74). Significant differences ($p > 0.05$) were observed in the PBP content of the biomass cultivated by both experiments. These differences can be attributed to the fact that the biomass cultivated under natural light complemented with LED was less stimulated to metabolize PBP. This is a result of the continuous light delivery to the cultures. This can lead to the conclusion that in order to increase the biomass and pigment productivity in AP culture, the photoperiod and the PAR need to be considered. In this case it can be supposed that the sunlight and natural photoperiod (12h/12h) are more suitable to accumulate PBP). In order to confirm this theory it is advisable to reproduce this experiment

adding a more intense light source to complete the sunlight, to provide a constant PAR to the cultures, as made in the laboratory conditions experiment.

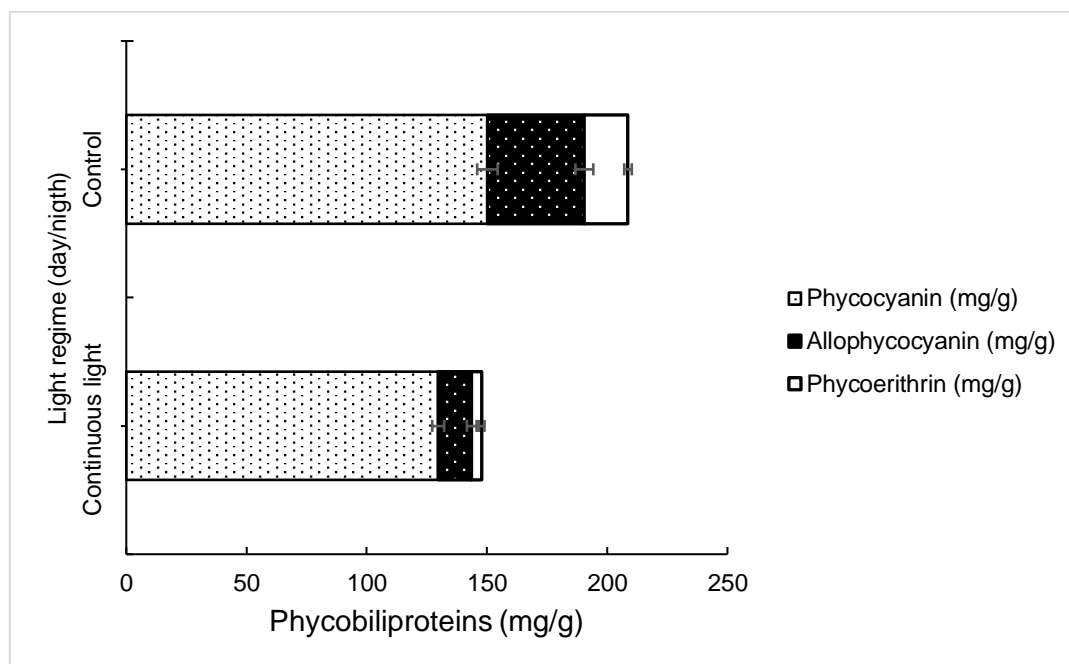


Figure 74 Greenhouse photoperiod biomass phycobiliprotein profile

3.1.9 Conclusions of the enhancement of pigment productivity in *Arthrospira platensis* cultures

Modifying the photoperiod emerged as a crucial factor for improving biomass growth parameters and photosynthetic pigments in well-controlled laboratory conditions. In laboratory conditions the continuous light (24 h) proved to be the best culture condition. This condition was brought to natural light conditions in a greenhouse. In the case of the greenhouse condition experiment, it was observed that the photoperiod modification did not significantly increase the biomass growth parameters of the studied biomass, however, the pigment profile was affected by the photoperiod modification in this condition, decreasing the PBP concentration in biomass $30\% \pm 12\%$. It was inferred that the PAR provided to the cultures play an important role in the biomass and pigment accumulation in the PBR as the photoperiod does.

3.2 Phase II: *Arthrospira platensis* production for the application of biomass valorization techniques

Abstract

The drying process is known to be a bottleneck in the microalgae and cyanobacteria valorization, because of its energetic cost. Nonetheless, this operation impacts the biomass quality, and its choice has to be made taking into account the modifications that it can imply for the interest molecules present in *Arthrospira platensis* biomass. Three different drying techniques were compared to characterize the impact of their operation conditions on the biomass quality. The PBP content in the dry biomass was taken as a quality indicator parameter. Lyophilization, spray-dry, and air-flow drying performances were assessed. The three assessed techniques demonstrated comparable drying efficiencies. However, regarding PBP degradation, the convection air-flow drying technique yielded the least favorable outcomes with a PBP degradation of $57.38 \pm 8.9\%$. In contrast, the spray-drying technique exhibited a PBP degradation of $11.23 \pm 3.8\%$, relative to the PBP concentration obtained through extraction in fresh biomass. Ultimately, lyophilization demonstrated its ability to preserve the PBP concentration in the biomass, with no PBP degradation. This is why the lyophilization was chosen as drying technology for this study. The dry biomass profile was characterized by its valorization by green solvents.

3.2.1 Drying techniques comparison

The three compared techniques presented similar drying efficiencies (Table 37). The drying efficiencies were estimated by applying equation (44) in p. 98. While the electric consumption of each process was estimated multiplying the equipment power in kilowatts (kW) by the process duration in hours to obtain the electric consumption in kWh. The spray-dryer technique presented a drying efficiency slightly superior to the other techniques at the chosen process conditions.

Table 37 Drying Techniques Comparison

	η_{drying} (%)	%error	Process duration (h)	Energy consumption (kWh/kg _{biomass})
Lyophilization	97	2.2	24	1150
Spray-dryer	98.2	0.4	0.3	32
Convection hot-air drying (Air-flow)	95	3.25	5	360

*The freezing step before the lyophilization was excluded from the energy consumption estimation, however the vacuum pump energy consumption and the freeze-drying sublimation was taken into account for this estimation.

A PBP extraction was performed in a sample of the dried biomass, as described in the section 2.1.11 p.77. The fresh biomass extraction was performed as indicated in section 2.1.10 p. 77. The main objective of this experiment was to characterize the impact of the drying technique on the PBP content. The effect of the drying technique on PBP concentration was correlated to a reference PBP concentration extracted from fresh biomass to estimate the pigment degradation by the applied technique.

The pigment degradation was estimated by comparing the concentration difference between the PBP concentration in fresh extract versus the one in the biomass dried at the compared techniques. A total PBP degradation of $57.38 \pm 8.9\%$, $11.23 \pm 3.8\%$, and 0% , was registered for the convection air-flow, spray-dryer, and lyophilization, respectively. The lyophilization technique proves to be the most effective technique for drying the AP biomass for PBP valorization purposes (Figure 75). The spray-dryer technique confirmed to be the most interesting in terms of time optimization, the operation took around 5 minutes per gram of dry biomass, while the lyophilization and air-flow drying took around 16 and 5 hours, respectively. This positions the spray-drying as the most interesting drying technique in terms of energy efficiency. However the PBP content experiments a degradation effect provoked by the temperature increase in the process. This effect was previously reported by [301], who compared the phycocyanin content in the AP biomass dried by spray-drying at three different inlet temperatures, 90°C , 110°C , 130°C . The 90°C inlet temperature proved to preserve better the phycocyanin content in the dried samples, showing a phycocyanin content 16% higher than the one observed in the biomass dried at 110°C and 130°C . Moreover, it is important to note that the optimal reported conditions to prevent phycocyanin degradation are temperatures lower than 55°C [302]. For this study, we hypothesize that the degradation rate of Phycobiliproteins

Chapter III : Results and Discussions

(PBP) within the biomass during spray-drying is low, considering the short contact time of the biomass with the air at 100°C at the equipment inlet. The degradation kinetics need to be taken into consideration to estimate an accurate degradation of PBP.

In the case of the air-flow drying, a greater degradation rate is seen due to the process duration, permitting the degradation of the biomass content. For this process, it is advisable to conduct a degradation kinetics study at various temperatures. This approach helps identify the optimal temperature and duration required to achieve satisfactory moisture levels and PBP content. Finally, lyophilization was chosen as the drying technique since it is well adapted to store the biomass for long periods, and it exhibited no phycobiliprotein (PBP) degradation in the biomass when compared to the extraction from fresh biomass. However, the energy consumption of this technique is 26 times higher than that achieved with convection air-flow drying. In conclusion, the spray-drying provides the best compromise between energy consumption and drying efficiency, despite the PBP degradation, which was relatively low. However, as the biomass for this project was frozen for its storage, lyophilization was the best option to dry it without provoking any degradation.

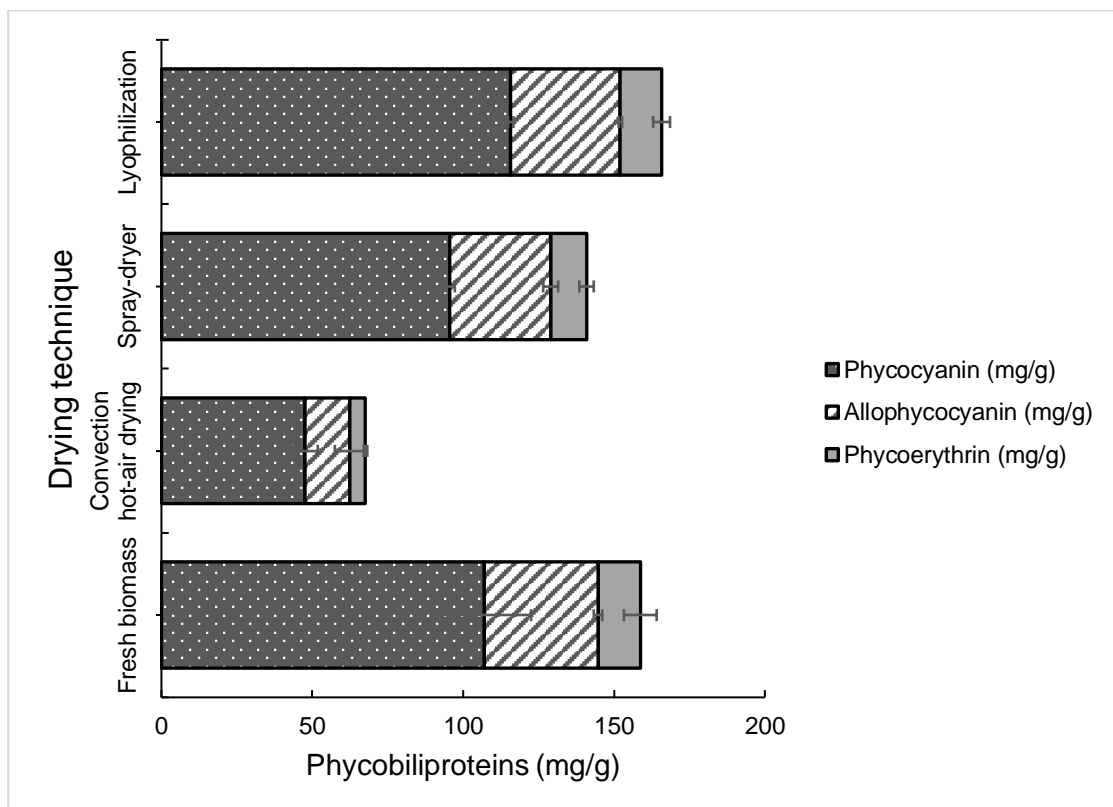


Figure 75 Drying technique comparison as a function of the phycobiliprotein content in the dried biomass

3.2.2 Biomass characterization

Around 2.5 kg of dry AP biomass were cultivated as described in 2.3.1. p. 97. The biomass was dried by lyophilization as described in the section 2.3.3 p. 98, and characterized to evaluate the biomass composition profile as described in the sections 2.1.7 p.75, 2.1.10 p.77, 2.1.17 p.80, and 2.4 p.100. The analyzed biomass presented the composition displayed in the following table (Table 38).

Table 38 Project valorized biomass composition

Component	mg/g dry biomass	± mg/g
Sugars	239.50	17.79
Phycocyanin	115.74	7.32
Allophycocyanin	36.35	2.05
Phycocerythrin	13.67	1.15
Other proteins than PBP	410.94	25.77
Lipids	57.36	7.30
Chl a	3.31	0.42
β-carotene	2.21	0.05
Zeaxanthin	0.84	0.06
Myxoxanthophyll	0.67	0.04
Ashes	75.12	2.21
Total	955.71	

From the analyzed FAMES in lipids, the following chains were characterized in the samples, C16:0, C18:0, C20:3, and C18:1[cis-11], being Palmitic acid, Stearic acid, Linoleic acid, and Oleic acid, respectively, see Table 39.

Table 39 FAMES proportions in *Arthrospira platensis* biomass cultivated for valorization

FAMES	Proportion (%) ¹	± (%)	Concentration mg/g dry biomass	± (mg/g)
Saturated Fatty Acids (SFA)				
Palmitic acid (C16)	58.2	8.5	27.57	4.04
Stearic acid (C18)	16	1	11.84	0.88
Polyunsaturated Fatty Acids (PUFA)				
Alpha linoleic acid C20:3 [cis-8,11,14]	4.1	0.01	10.25	1.59
Oleic acid C18:1[cis-11]	21.6	3.3	2.91	0.25
Total SFA	74.2	2.2	39.41	6.47
Total PUFA	25.7	5.32	13.16	3.7
Total FAMES	100	--	52.57	4.84

¹ Percent of total Fatty acids

3.3 Phase II: Green solvent *Arthrospira platensis* valorization

3.3.1 Valorization of hydrophilic pigments in *Arthrospira platensis* biomass

Abstract

This study aims to evaluate the application of pressurized solvent extractions for *Arthrospira platensis* valorization. Two kinds of biomass were studied, an untreated one (Set A), and a biomass with a previous PBP extraction (Set B). A central composite design was employed to characterize the impact of temperature and solvent concentration on pigment extraction yields, total phenolic compound concentration (TPC), and antioxidant activities in the extracts. β -carotene, zeaxanthin, Chl a, total pigments extraction yields, and total phenolic compounds were evaluated as responses. The antioxidant activity responses were assessed with ABTS and DPPH tests. By analyzing the contour plots it was observed that the temperature was a major influence parameter in the evaluated responses, while the solvent concentration effect was minor. The temperature parameter performed opposing effects on the responses increasing the extraction yields and decreasing the antioxidant activities when increased. Moreover, the two studied biomass types presented different responses to the evaluated parameters. Total pigment extraction yield was increased by 19.76% and 24.08% when increasing the extraction temperature from 80°C to 100°C in sets A and B, respectively. The desirability test was conducted to establish optimal extraction conditions, aiming for a TPC concentration of 10 mg GAE/g and extraction yields for the total lipophilic pigments of 20% and 25% for sets A and B, respectively. The determined optimal extraction parameters were 60°C with 100% ethanol in set A and 65°C with 90% ethanol (v/v) in set B.

3.3.2 Pigment Extraction by Accelerated Solvent Extraction Preliminary study

In the first place, the extraction efficiency was studied by applying the conditions displayed in 2.5.2 and 2.5.5 in p. 105 and 106, respectively. The employed solvents were: pure water, pure ethanol, and an ethanol solution of 50% v/v. The extraction efficiencies were estimated by applying (50) and (51) in p.113. The reference concentrations were estimated by applying the methodologies described in 2.1.7 and 2.1.9 in p.75 and 76, respectively. The reference pigment concentrations are displayed in Table 40. The composition displayed in Table 40 is different from the one in Table 38 p.158, because the biomass harvest batch is different. In this experiment the PBP are not quantified by HPLC because the quantification method was only available for the lipophilic pigments.

Table 40 Reference lipophilic pigments for the ASE extraction efficiency determination

Reference pigment	mg/g	± mg/g
Chl a	3.28	2.08E-03
β-carotene	1.57	3.21E-04
Zeaxanthin	0.78	2E-04

The maximum extraction efficiency for total pigments was obtained employing pure ethanol, being 19.40% ± 4.96%. The 50% v/v ethanol solution delivered the worst extraction efficiencies, showing negligible extraction for Chl a and very low extraction efficiencies for the rest of the analyzed molecules. In the case of pure solvents, the best-extracted molecule was Chl a, See (Figure 76).

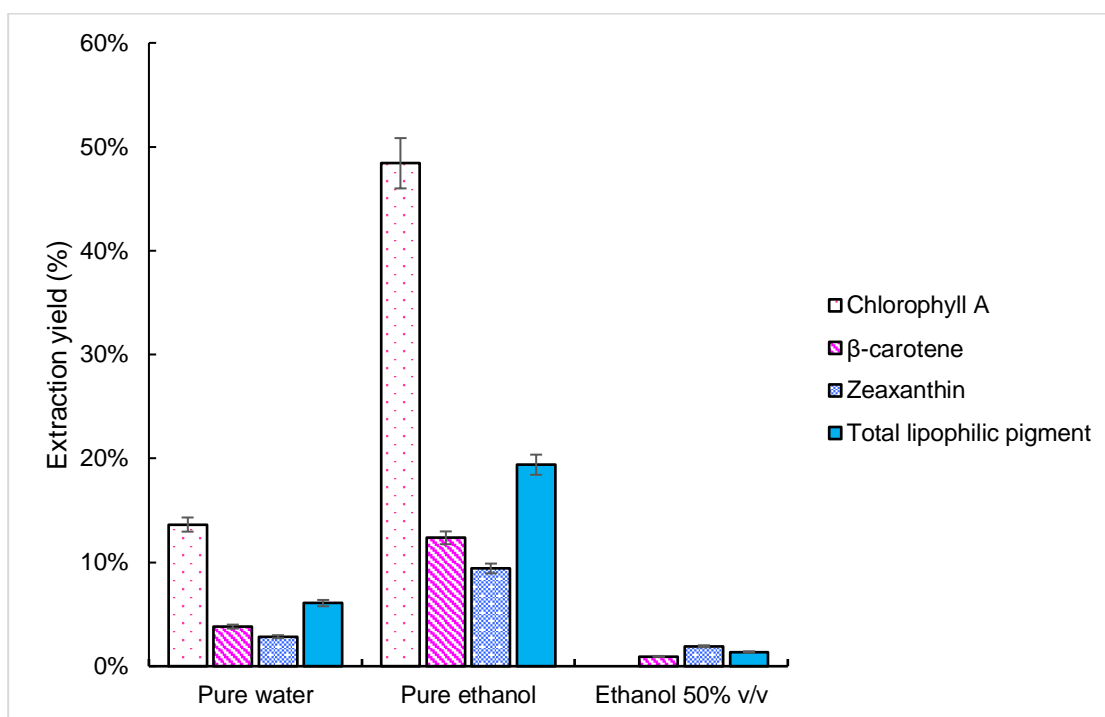


Figure 76 Preliminary study Total lipophilic pigment, Chl a, β-carotene, and zeaxanthin extraction efficiencies at 40°C.

These results set the basis for choosing the operation conditions for the CCD experiment. Temperatures higher than 40°C and ethanol concentrations higher than 50% v/v were targeted. (Refer to Table 42 in p.164). These conditions were reproduced in two experimental sets: (A) ASE with no previous PBP extraction, and (B) ASE with a previous PBP extraction (Figure 43 in p.105). The results from both experimental sets provided enough data to determine an empirical quadratic model to set the optimal extraction conditions to enhance the lipophilic pigment extraction yields and antioxidant activities from the biomass. Both responses were treated separately as a function of extraction temperature and ethanol concentration.

The quadratic model employed for the response is displayed in equations (68) and (69) for the extraction yield and the antioxidant activity, respectively. The coefficients of the empirical

Chapter III : Results and Discussions

model were estimated by multiple linear regression. The contour plots were performed by applying the fitted polynomial equation.

$$Y_i = \beta_0 + \beta_1 T + \beta_2 X + \beta_{1,1} T^2 + \beta_{2,2} X^2 + \beta_{1,2} TX + error \quad (68)$$

$$A_i = \beta_0 + \beta_1 T + \beta_2 X + \beta_{1,1} T^2 + \beta_{2,2} X^2 + \beta_{1,2} TX + error \quad (69)$$

Where;

Y	Extraction Yield	(%)
A	Antioxidant activity	(%)
T	Temperature	(°C)
X	Ethanol concentration	(%)
β_0	Intercept coefficient	
β_1, β_2	Linear coefficient (1:T, 2: X)	-
$\beta_{1,1}, \beta_{2,2}$	Quadratic coefficient (1,1:T-T ; 2,2: X-X)	-
$\beta_{1,2}$	Interaction coefficient (1,2:T-X)	-
error	Error coefficient	-

$\beta_0, \beta_1, \beta_2, \beta_{1,1}, \beta_{2,2}$ and $\beta_{1,2}$ are dimensionless as they are regression coefficients. They represent the numerical values that determine the relationship between the variables in the polynomial, but they do not have physical units. The units of the variables themselves are accounted for in the overall equation, and the coefficients are adjusted accordingly to maintain dimensionless consistency in mathematical operations

The validity of the model in the range of 60-120°C and 80-100% ethanol v/v was estimated by the error of the fit evaluation. The models were suitable enough to describe the data (error < 10%), see Table 41.

Table 41 Regression coefficients and %error for the fit for the obtained multilinear regressions for the experiments

Set	Total pigments		Chl a		β-carotene		Zeaxanthin	
	A	B	A	B	A	B	A	B
β_0	8.01	27.99	8.72	30.69	4.96	21.32	8.68	17.57
β_1	3.21	12.76	3.90	14.31	1.08	6.94	1.57	11.95
β_2	7.69	2.11	8.31	1.87	5.31	2.95	7.42	2.41
$\beta_{1,1}$	4.64	-4.74	4.53	-4.94	5.39	-6.70	3.64	2.40
$\beta_{2,2}$	8.09	-2.09	8.30	-4.13	8.61	3.22	4.72	4.99
$\beta_{1,2}$	-1.57	0.21	-2.67	-0.49	2.13	2.13	0.21	2.43
%Error	0.54	1.34	1.04	1.57	0.78	8.77	0.59	7.34

3.3.2.1 Set A ASE lipophilic pigment extraction yields

The experimental extraction yields obtained by the application of the operation conditions were applied for the construction of the contour plots showed in the next sections of this document. These responses ranged from 3.69% to 29.84% from the reference concentrations (Refer to Table 42).

Table 42 Set A Total lipophilic pigment experimental responses for the construction of the contour plots by CCD

[Ethanol] (% v/v)	Temperature (°C)	η Total lipophilic pigment (%)
80	60	9.37
100	60	10.15
80	120	23.02
100	120	24.81
80	90	11.39
100	90	22.08
90	60	8.77
90	120	29.84
90	90	4.08
90	90	3.69
90	90	4.72
85.7	82.5	6.37
94.3	82.5	7.12
90	105	20.27

Observing the highest extraction yield at 120 °C and 90% v/v of ethanol concentration, the lowest pigment extraction yield was registered at a temperature and ethanol concentration of 90°C and 90% v/v respectively. The contour plot demonstrates that the process temperature was the most influential parameter in the extractions (Figure 77). Results showed that to reach total lipophilic pigment extraction yields between 20.25-27.66% it is necessary to extract at

Chapter III : Results and Discussions

temperatures greater than 110°C. To minimize the organic solvent use it is advisable to extract with ethanol 80% v/v at 110°C to extract between 20 and 22% of total lipophilic pigments.

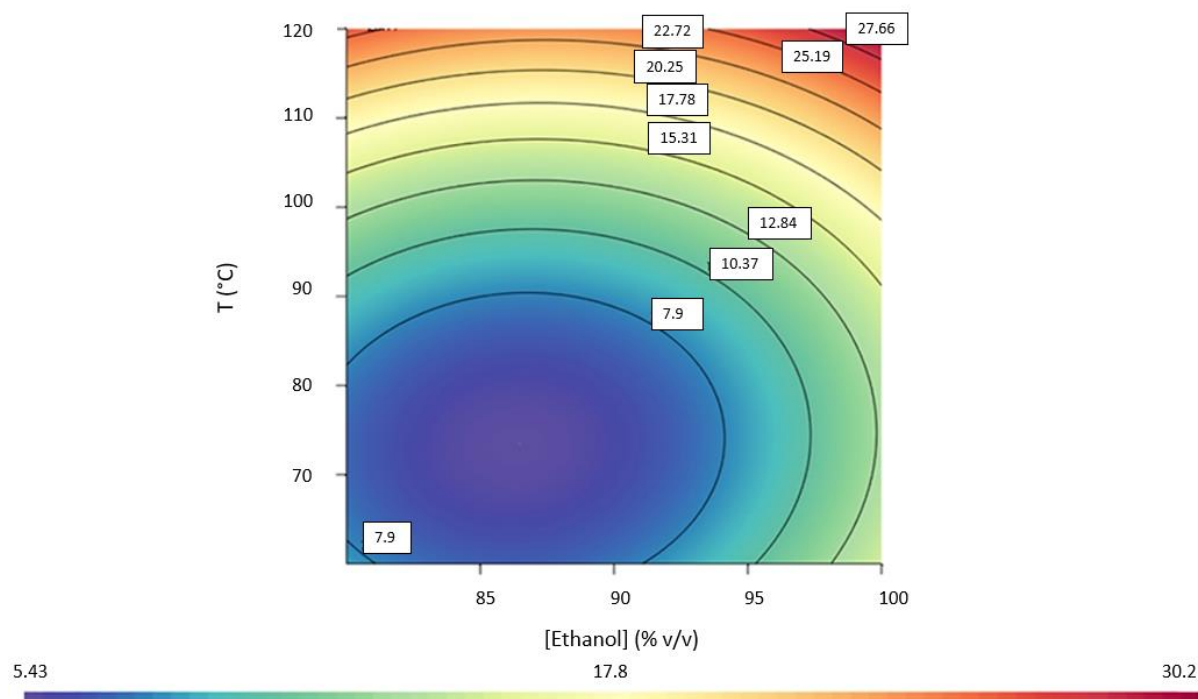


Figure 77 Set A total lipophilic pigment extraction yield. The color bar at the bottom of the figure indicates the extraction yield in %.

Concerning Chl a, the maximum experimental extraction yield was $31.7 \pm 0.72\%$, at 120°C and 90% v/v. Ethanol concentrations between 90-100% and temperatures between 110-120°C warranted to have an extraction yield greater than 20% (Refer to Table 43).

Table 43 Set A Chlorophyll a experimental responses for the construction of the contour plots by CCD

[Ethanol] (% v/v)	Temperature (°C)	η Chla (%)
80	60	7.78
100	60	8.24
80	120	5.25
100	120	25.79
80	90	10.92
100	90	23.72
90	60	8.85
90	120	31.69
90	90	5.28
90	90	4.97
90	90	5.35
86	82.5	7.68
94	82.5	8.06
90	105	21.29

Extraction yields lower than 10% were associated with ethanol concentrations and temperatures lower than 90% v/v and 90°C (Figure 78). However, the temperature increase from 80°C to 120°C proved to improve by 19.79% the extraction efficiency, while the increase from 80 to 100% ethanol v/v enhanced extraction efficiency by 4.94%.

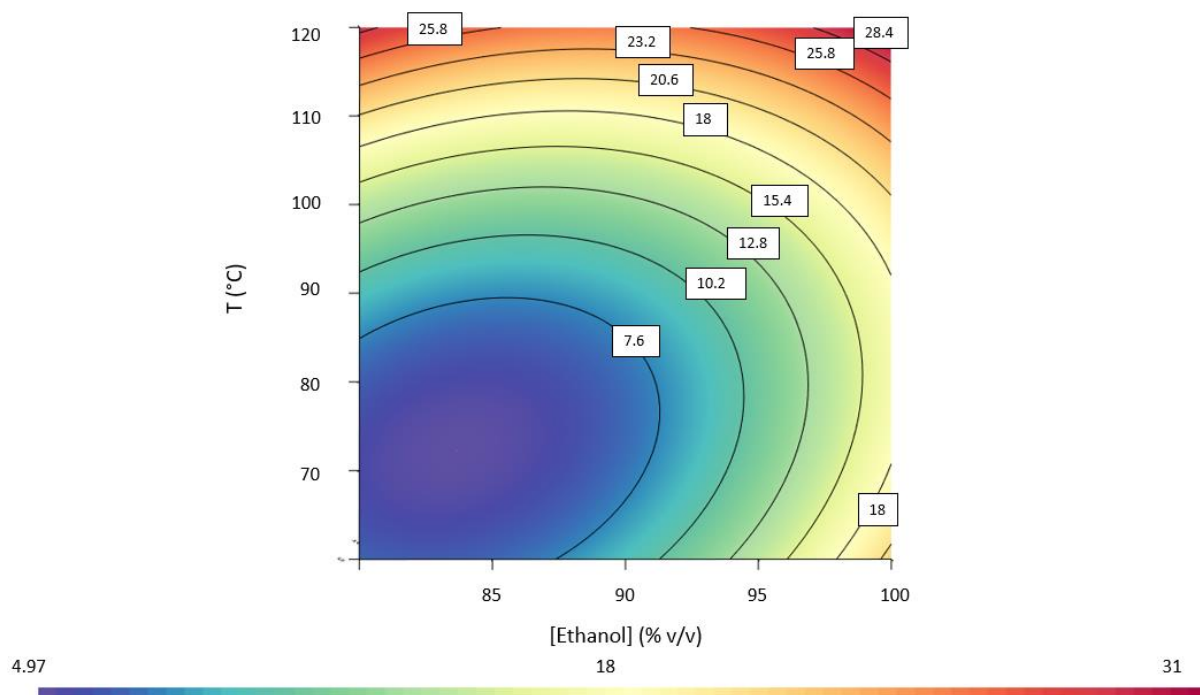


Figure 78 Set A Chlorophyll a extraction yield. The color bar at the bottom of the figure indicates the extraction yield in %

Zeaxanthin and β -carotene extraction yields were similar to the ones reported for Chl a, the solvent proportion was not an influential parameter on the extraction as the temperature proved to be (Refer to Table 44).

Chapter III : Results and Discussions

Table 44 Set A Zeaxanthin and β -carotene experimental responses for the construction of the contour plots by CCD

[Ethanol] (% v/v)	Temperature ($^{\circ}$ C)	η Zeaxanthin (%)	η β -carotene (%)
80	60	9.00	15.83
100	60	7.33	11.64
80	120	14.50	17.48
100	120	19.68	22.92
80	90	13.79	12.32
100	90	19.94	16.39
90	60	9.25	8.28
90	120	22.35	25.44
90	90	5.53	7.89
90	90	5.51	6.67
90	90	6.61	7.04
86	82.5	3.96	2.10
94	82.5	8.20	2.96
90	105	2.90	12.79

However, it was observed that a temperature decrease needed a solvent concentration increase to enhance the extraction efficiency. As displayed in Figure 79 and Figure 80 carotenoids extraction yields were lower compared to Chl a ones, being $22.35 \pm 4.24\%$, and $25.4 \pm 4.98\%$ for Zeaxanthin and β -carotene, respectively, both were obtained at 120° C and ethanol 90% v/v.

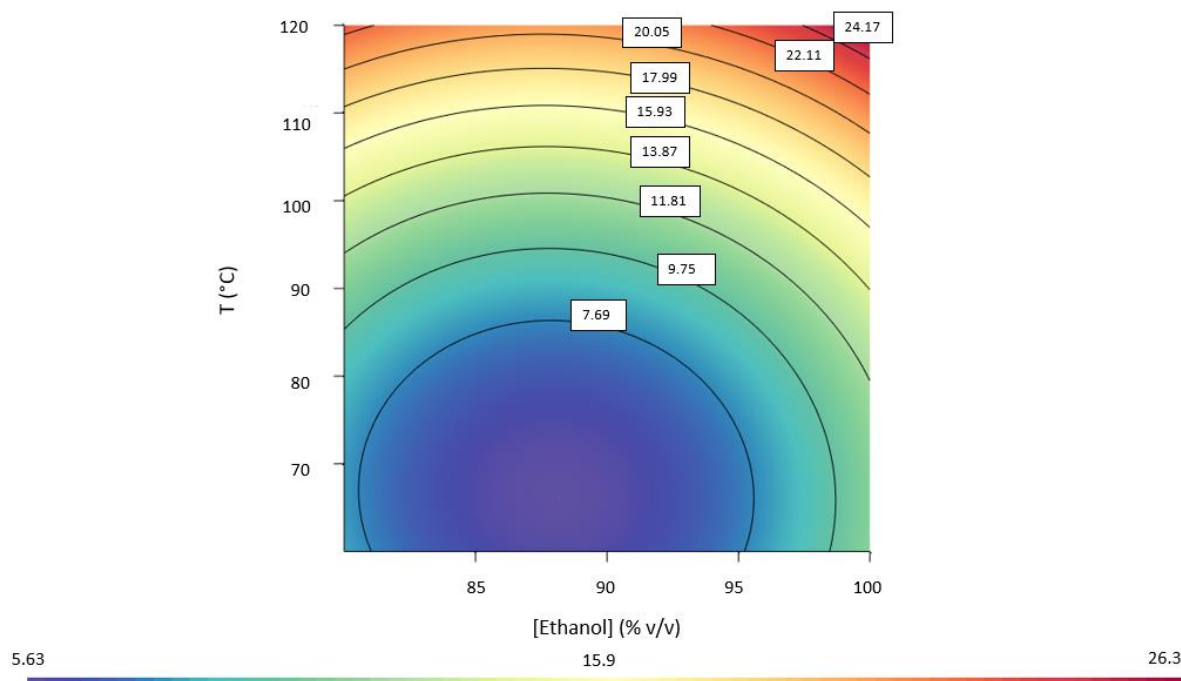
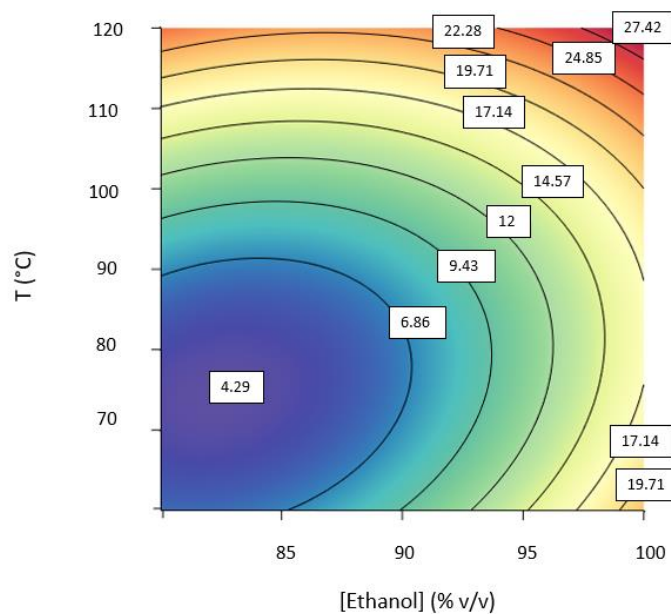


Figure 79 Set A zeaxanthin extraction yield. The color bar at the bottom of the figure indicates the extraction yield in %.



4.29

17.2

30

Figure 80 Set A β -carotene extraction yield. The color bar at the bottom of the figure indicates the extraction yield in %.

3.3.2.2 Set A phycobiliprotein content after ASE

The PBP concentrations in the biomass after ASE extraction showed that these molecules were barely present in the biomass after the ASE process. Indicating that the majority of the PBP content is extracted during the ASE (Refer to Figure 81). This result was expected, due to the affinity that PBP have towards polar solvents, like water and ethanol solutions. The PBP concentrations of the biomass in this set before the ASE extractions are the same of the biomass treated in set B (Refer to Table 45 in p.170).

Chapter III : Results and Discussions

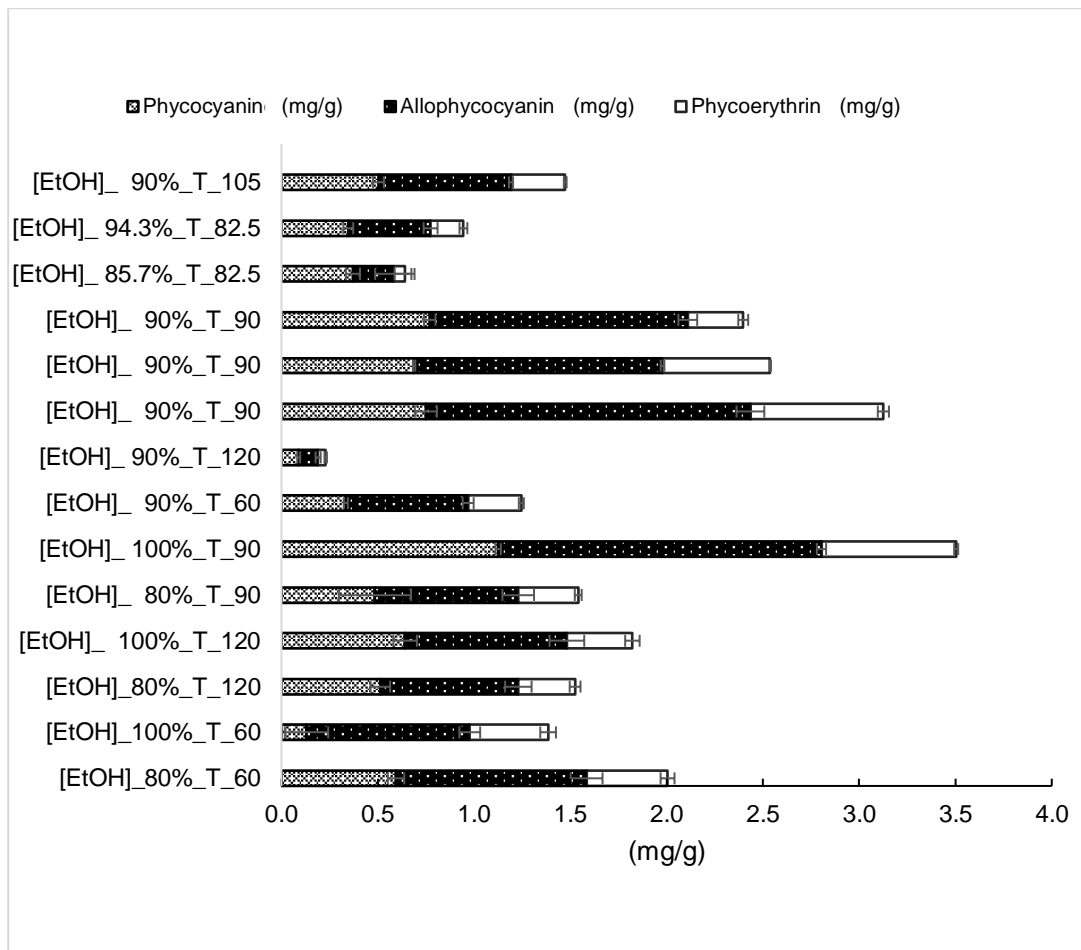


Figure 81 Set A residual biomass phycobiliprotein content after ASE extraction

3.3.2.3 Set B ASE lipophilic pigment extraction yields

The reference extract concentrations for lipophilic pigments were identical to the ones considered for set A analysis.

Given that the biomass of each condition tested in this set originates from the same batch, the protocol for PBP quantification outlined in section 2.5.3 in p.106 was applied by triplicate. It was assumed that the PBP concentration in the biomass remained uniform for each condition.

Table 45 Phycobiliprotein concentration in biomass from set B before ASE

	(mg/g)	SD
Phycocyanin	120	6.03
Allophycocyanin	42.35	3.65
Phycoerythrin	11.11	1.23

The ASE experimental results showed that the extraction yields for the total pigments ranged from $6.46 \pm 0.8\%$ to $38.07 \pm 4.58\%$ (Refer to Table 46).

Table 46 Set B Total lipophilic pigment experimental responses for the construction of the contour plots by CCD

[Ethanol] (% v/v)	Temperature (°C)	η Total lipophilic pigment (%)
80	60	6.46
100	60	8.80
80	120	35.29
100	120	38.07
80	90	18.64
100	90	27.85
90	60	10.69
90	120	31.81
90	90	25.06
90	90	29.75
90	90	29.32
86	82.5	28.57
94	82.5	26.57
90	105	31.40

The highest experimental extraction yield was obtained at 100% ethanol at 120°C, while the lowest one was obtained at 80% ethanol v/v at 60°C, respectively. Temperature increase had a positive effect on the total lipophilic pigment extraction yield. Similarly, an increase in the ethanol concentration proved to enhance the total lipophilic pigment extraction yield. However, the temperature effect displayed a greater influence on the extraction (Figure 82).

Chapter III : Results and Discussions

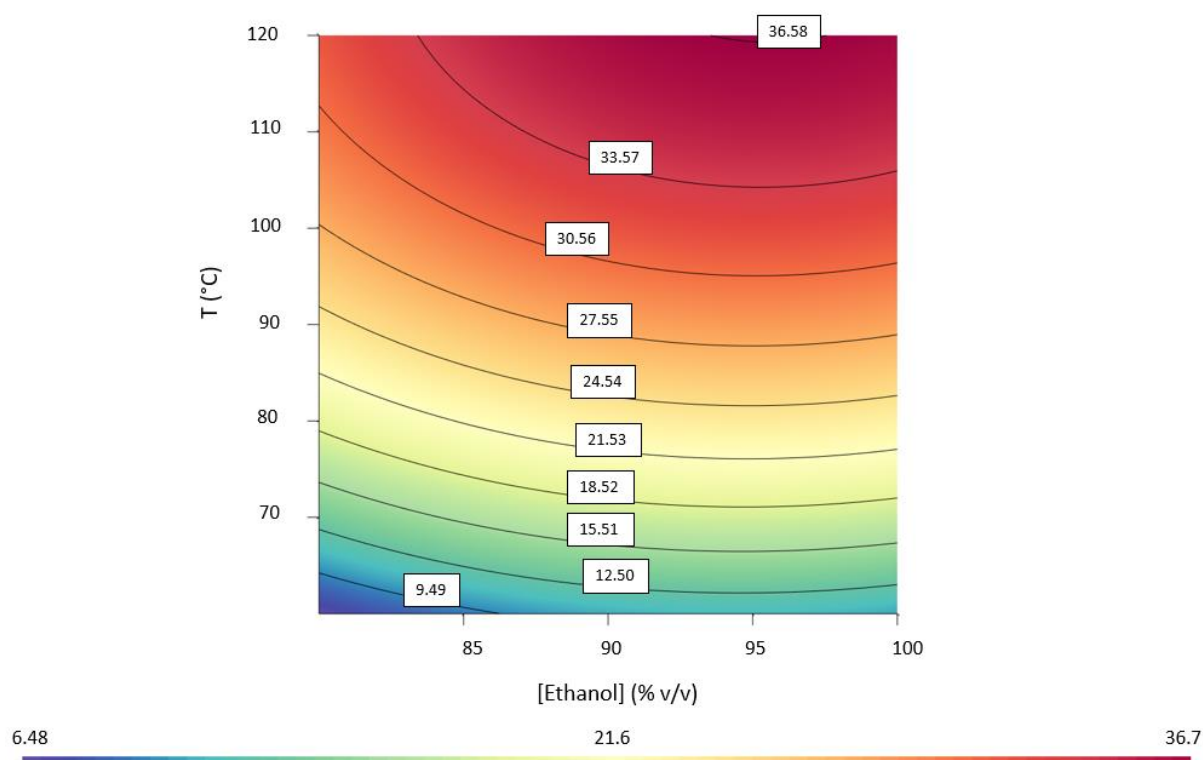


Figure 82 Set B total pigment extraction yield. The color bar at the bottom of the figure indicates the extraction yield in %.

Regarding chlorophyll a (Chl a), the maximum extraction efficiency was $39.3 \pm 4.65\%$ of the reference extraction, achieved with 90% ethanol v/v at 105°C. In contrast, the minimum extraction yield was $6.92 \pm 0.81\%$, observed with 80% ethanol v/v at 60°C, as indicated in Table 47.

Table 47 Set B Chlorophyll a experimental responses for the construction of the contour plots by CCD

[Ethanol] (% v/v)	Temperature (°C)	η Chla (%)
80	60	6.92
100	60	9.95
80	120	37.84
100	120	38.68
80	90	18.20
100	90	26.51
90	60	8.26
90	120	35.11
90	90	27.96
90	90	33.44
90	90	29.66
86	82.5	30.19
94	82.5	29.79
90	105	39.33

As showed Figure 83 the solvent concentration did not have an important effect on the extraction yield of Chl a as temperature did on.

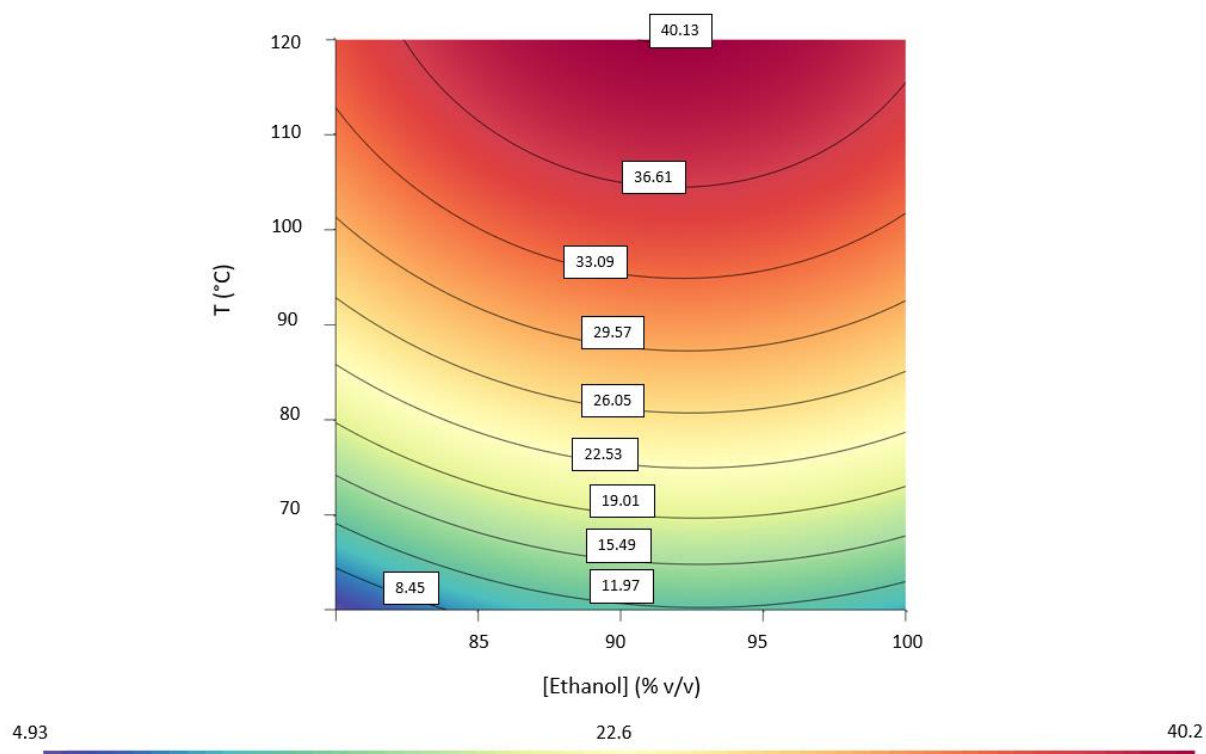


Figure 83 Set B Chlorophyll a extraction yield. The color bar at the bottom of the figure indicates the extraction yield in %

Results show that to extract at least 20% of β -carotene in the biomass it is necessary to employ temperatures higher than 90°C.

Chapter III : Results and Discussions

Table 48 Set B Zeaxanthin and β -carotene experimental responses for the construction of the contour plots by CCD

[Ethanol] (% v/v)	Temperature (°C)	η Zeaxanthin (%)	η β -carotene (%)
80	60	10.05	3.22
100	60	6.03	5.29
80	120	39.46	23.55
100	120	44.44	33.18
80	90	13.71	22.33
100	90	30.26	32.26
90	60	15.80	18.38
90	120	26.24	20.88
90	90	16.86	16.73
90	90	18.25	19.59
90	90	21.10	31.21
86	82.5	21.24	24.99
94	82.5	15.78	18
90	105	13.93	6.71

Best extraction conditions were found between 90-100% v/v and 100-120°C.

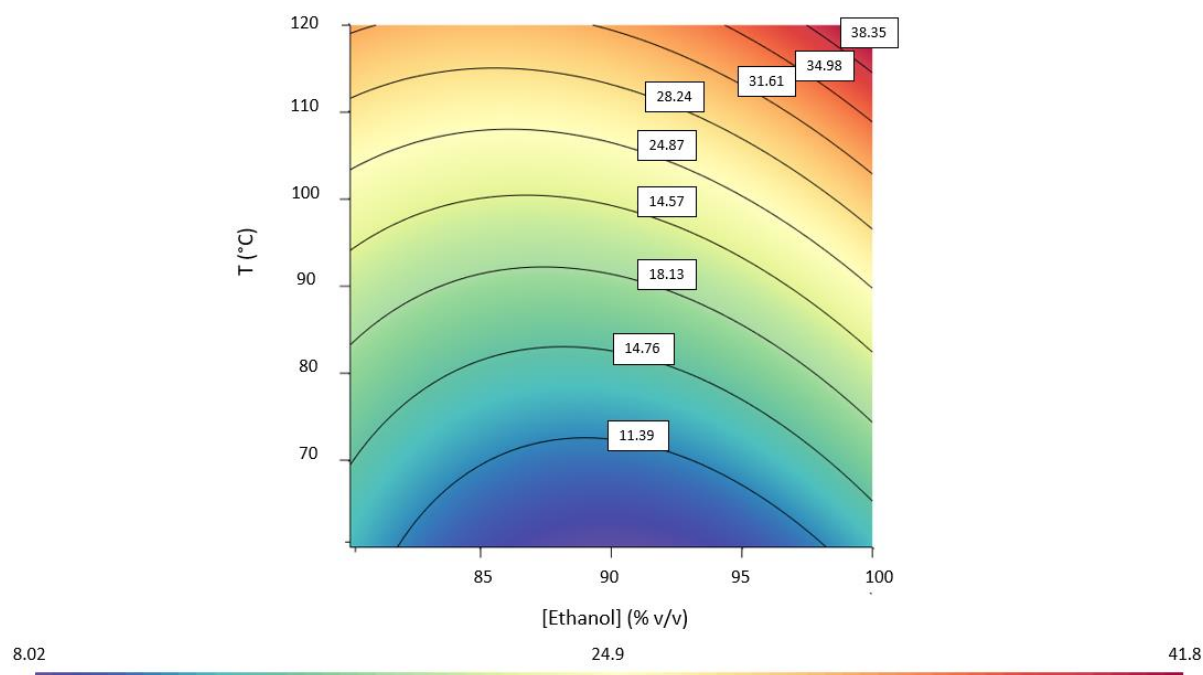


Figure 84 Set B zeaxanthin extraction yield. The color bar at the bottom of the figure indicates the extraction yield in %.

The β -carotene extraction yields ranged between $3.22\% \pm 0.3\%$ and $33.18\% \pm 4.58\%$. In the extraction of this molecule, temperature proved to be the most influential parameter, temperatures between 90-110°C proved to have a positive effect on the extraction, and the

ethanol proportion proved to be more efficient between an ethanol concentration of 95-100% v/v.

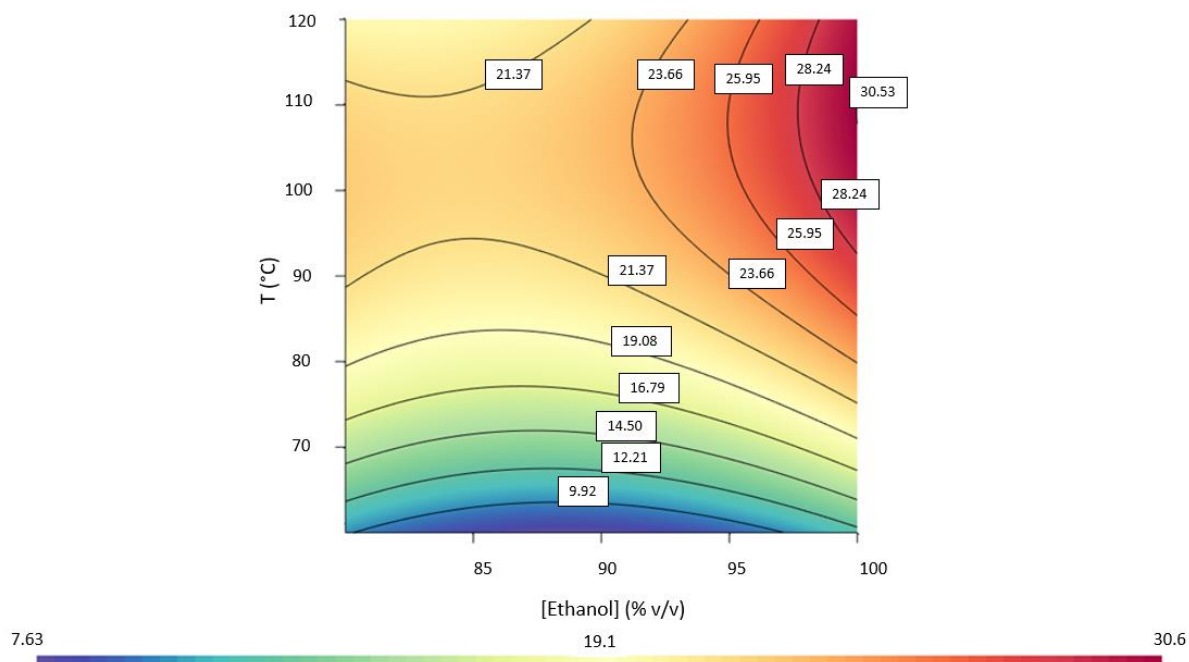


Figure 85 Set B β -carotene extraction yield. The color bar at the bottom of the figure indicates the extraction yield in %

Compared to set B, set A needed a higher process temperature to increase the extraction yield. For the analyzed pigments set B presented an extraction yield 19.4 ± 1.8 , 34.74 ± 4 , 23.33 ± 2.2 , and $21.62 \pm 1.28\%$ greater than the one presented in set A for Chl a, zeaxanthin, β -carotene, and total lipophilic pigments, respectively. This increase in the extraction yield is potentially promoted by the PBP extraction step in set B, causing a cell disruption that enhances the extraction of the non-polar pigments [303] [175]. For example, to reach a 20% extraction yield of total pigments, it was necessary to extract between 115-120°C in set A, while for set B the same extraction yield could be reached at 80°C (Refer to Figure 77 p.165 and Figure 82 p. 171). The temperature rise decreases the water polarity, increases its affinity to mean and low polarity molecules [175], and enhances the diffusion coefficient of the liquid in the solid matrix, easing the extraction.

In terms of solvent concentration, it could be observed in both sets that the increase in the ethanol concentration boosted the extraction efficiency as a result of the solvent affinity for the target molecules, especially zeaxanthin, and β -carotene. However, this effect was more evident in set A, where to obtain total pigment extraction yields between 25-28% it was necessary to extract with ethanol concentrations between 95-100% v/v, at temperatures $\geq 100^\circ\text{C}$ (Refer to Figure 77 p. 165). In set B, ethanol concentration did not represent a significant influence on the total pigment extraction yield. It is advisable to increase the extraction temperature when

Chapter III : Results and Discussions

decreasing the solvent concentration. This difference in the extractability might be justified by the increase of lipophilic pigment accessibility in set B after the PBP extraction, whereas for set A the total lipophilic pigment extraction yield could only be risen by decreasing the solvent polarity [304].

When comparing extraction yields between molecules in both sets it was registered that the pigment that relied the less on the organic solvent concentration was Chl a, followed by β -carotene and zeaxanthin, in order of solvent reliance to organic solvent concentration. Zeaxanthin and β -carotene needed a combination of high temperatures and high solvent concentrations to increase the extraction yields. This response is a result of the low polarity of carotenoids, needing a low solvent polarity to enhance the extraction [303]. The molecule that relied the most on solvent polarity was the β -carotene, displaying the optimal extraction conditions at the highest temperatures and solvent concentrations. These optimal operation conditions can be attributed to the absence of functional groups in this molecule, decreasing its polarity. [305].

3.3.2.4 Extract phenolic compounds and antioxidant activity

The total phenolic compounds (TPC) concentration, ABTS, and DPPH were evaluated to characterize the impact of the extraction conditions on phenolic compounds concentrations, and the antioxidant activity of the extracts. The contour plots were performed by the application of the multilinear regression to the experimental data, to fit the polynomial equation (69) in p.163. The applied coefficients are displayed in Table 49.

Table 49 Regression coefficients and statistics for the fit for the obtained multilinear regressions for the experiments of total phenolic compounds and antioxidant activities

Set	Total Phenolic Compounds		ABTS		DPPH	
	A	B	A	B	A	B
β_0	4.62	6.46	22.00	50.15	28.23	8.95
β_1	-1.59	-2.24	-25.27	-11.08	-9.86	-6.20
β_2	0.87	-0.14	0.69	7.93	3.13	-0.99
$\beta_{1,1}$	0.63	-1.21	19.52	-2.25	-11.26	-3.72
$\beta_{2,2}$	1.85	-1.26	10.10	1.86	4.30	4.01
$\beta_{1,2}$	0.44	-0.38	-2.11	7.54	-2.16	0.62
%Error	0.42	2.46	4.17	3.00	0.64	2.62

Both tests presented similar results for TPC concentrations. The maximum experimental TPC for sets A and B was 10.46 ± 0.79 and 10.17 ± 1.99 mg GAE/g_{extract}, obtained at 90°C and 100% ethanol, and 82.5°C and 85% ethanol v/v, respectively (See Table 50).

Table 50 Experimental Total Phenolic Compounds concentrations in set A and B

[Ethanol] (% v/v)	Temperature (°C)	GAE/g _{extract}	
		Set A	Set B
80	60	8.96	6.27
100	60	8.20	6.52
80	120	4.44	3.43
100	120	5.41	2.07
80	90	5.26	3.18
100	90	10.46	3.71
90	60	8.39	6.22
90	120	3.70	1.48
90	90	5.07	4.90
90	90	5.71	5.14
90	90	5.87	6.93
86	82.5	1.73	10.17
94	82.5	2.08	9.44
90	105	5.37	5.20

Set A exhibited greater sensitivity to temperature and ethanol concentration compared to the responses observed in set B (Refer to Figure 87 and Figure 90). Despite this, set A samples displayed a slightly higher TPC concentration than those in set B. Probably the PBP extraction prior to ASE performed in set B extracted a part of the phenolic compounds present in the AP biomass. Under optimal operating conditions for maximizing TPC concentration, set A achieved a total lipophilic pigment extraction yield of 20.15% at 60°C with 100% ethanol. In contrast, set B exhibited a total lipophilic pigment extraction yield of 12.5% under its optimal operating conditions for maximizing TPC, set at 60°C with 90% ethanol.

Chapter III : Results and Discussions

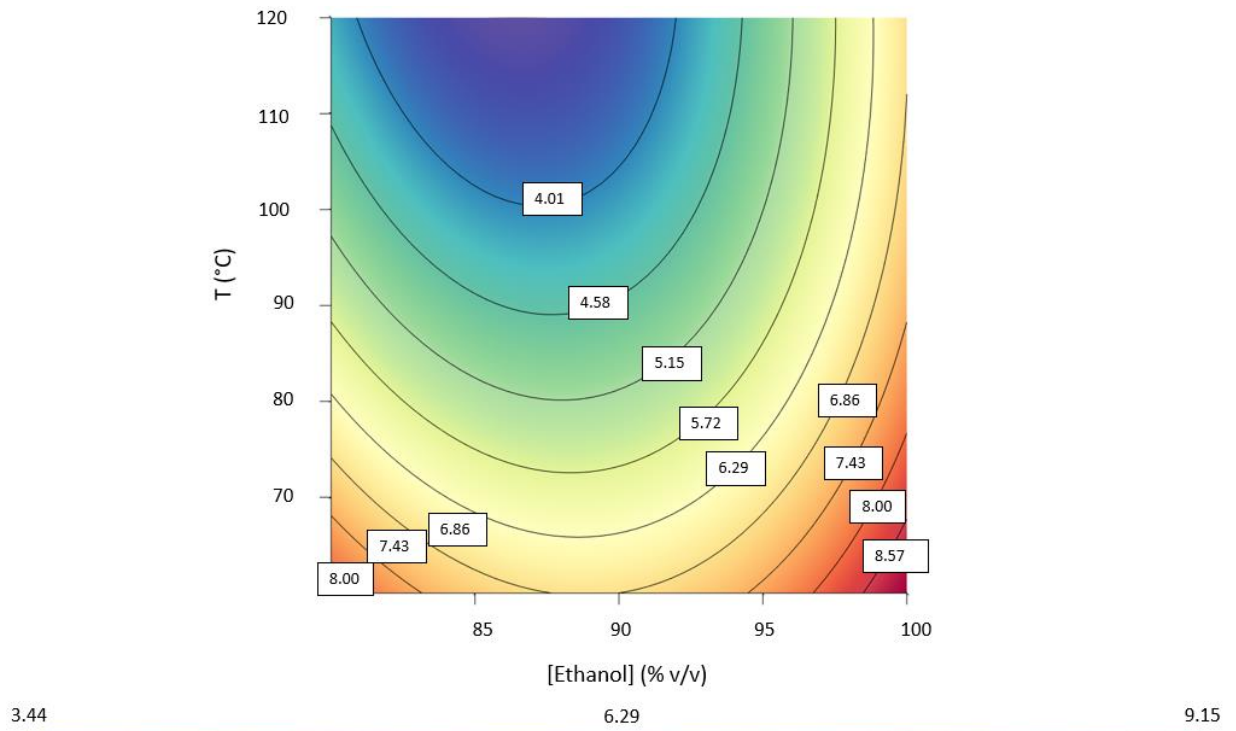


Figure 86 Set A Total Phenolic Compound concentration. The color bar at the bottom of the figure indicates TPC concentration in mg GAE/g_{extract}

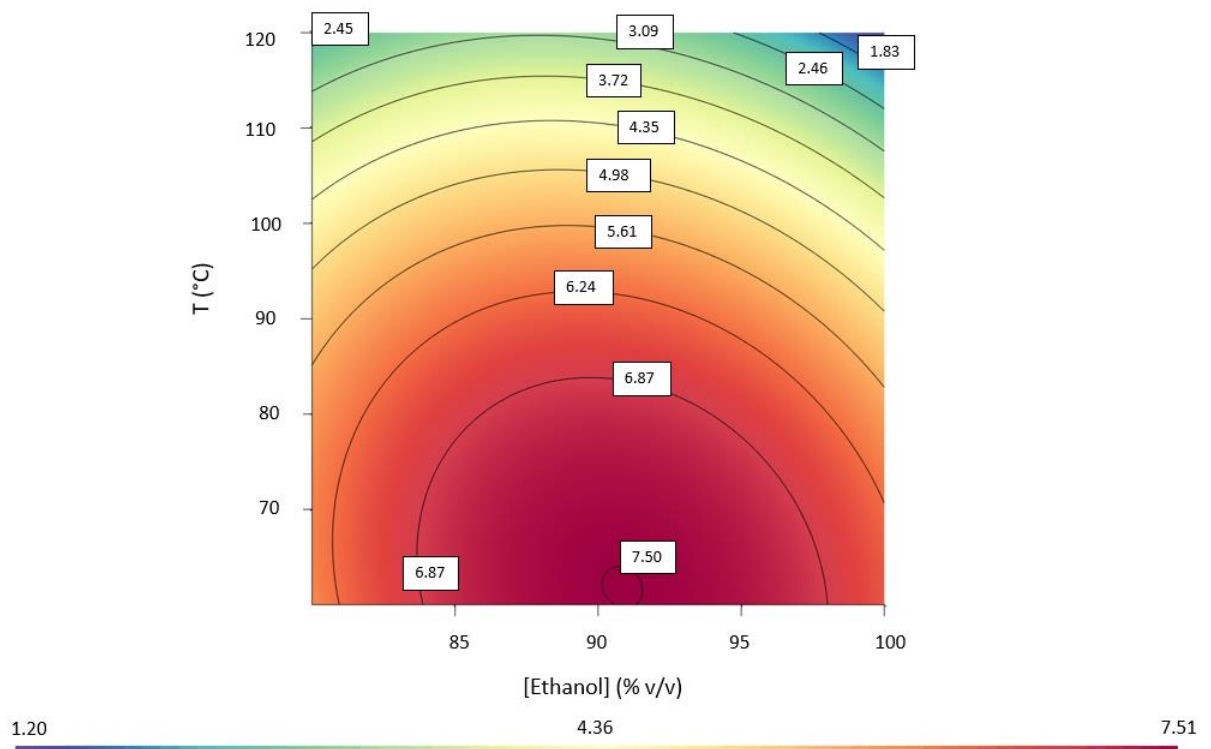


Figure 87 Set B Total Phenolic Compound concentration. The color bar at the bottom of the figure indicates TPC concentration in mg GAE/g_{extract}

Concerning the antioxidant activities, the integrated analysis ABTS and DPPH gave a clear response of the antioxidant activity of the extracts. Both analyses were performed in the same extract, to have more information about the kind of antioxidants present in the sample. The BHT gave an antioxidant activity of $86.91 \pm 3\%$ and $70 \pm 0.8\%$ for the ABTS and DPPH assays, respectively. It is noteworthy that the antioxidant activity assays assess the ability of the antioxidants in the sample to reduce free radicals or reactive oxygen species. The antioxidant molecules can be phenolic compounds, ascorbic acid, carotenoids, tocopherol, flavonoids. Notably, it is known that the ABTS assay is often conducted in both water-soluble and lipid-soluble environments, making it versatile in assessing the overall antioxidant capacity. On the other hand DPPH radical is larger and tends to be more soluble in organic solvents. This may limit its interaction with certain types of antioxidants that are not as soluble or active in organic solvents [233]. According to the literature [306] [307] [308], certain types of antioxidants show a good response to DPPH assay, like phenolic compounds, carotenoids and vitamin E.

When analyzing set A, it was observed that temperature had a strong effect on ABTS and DPPH antioxidant activity (Refer to Figure 88), increasing this response when decreasing the process temperature, (Refer to Figure 89 in p.180). The antioxidant activities ranged from 15.66-75.3% and 6.63-43.87% for ABTS and DPPH, respectively. The variation in responses between the two assays could be attributed to higher sensitivity of ABTS compared to DPPH. The greatest experimental ABTS and DPPH antioxidant activities were registered at the experimental condition of 60°C with 100% ethanol, coinciding with the TPC best extraction condition.

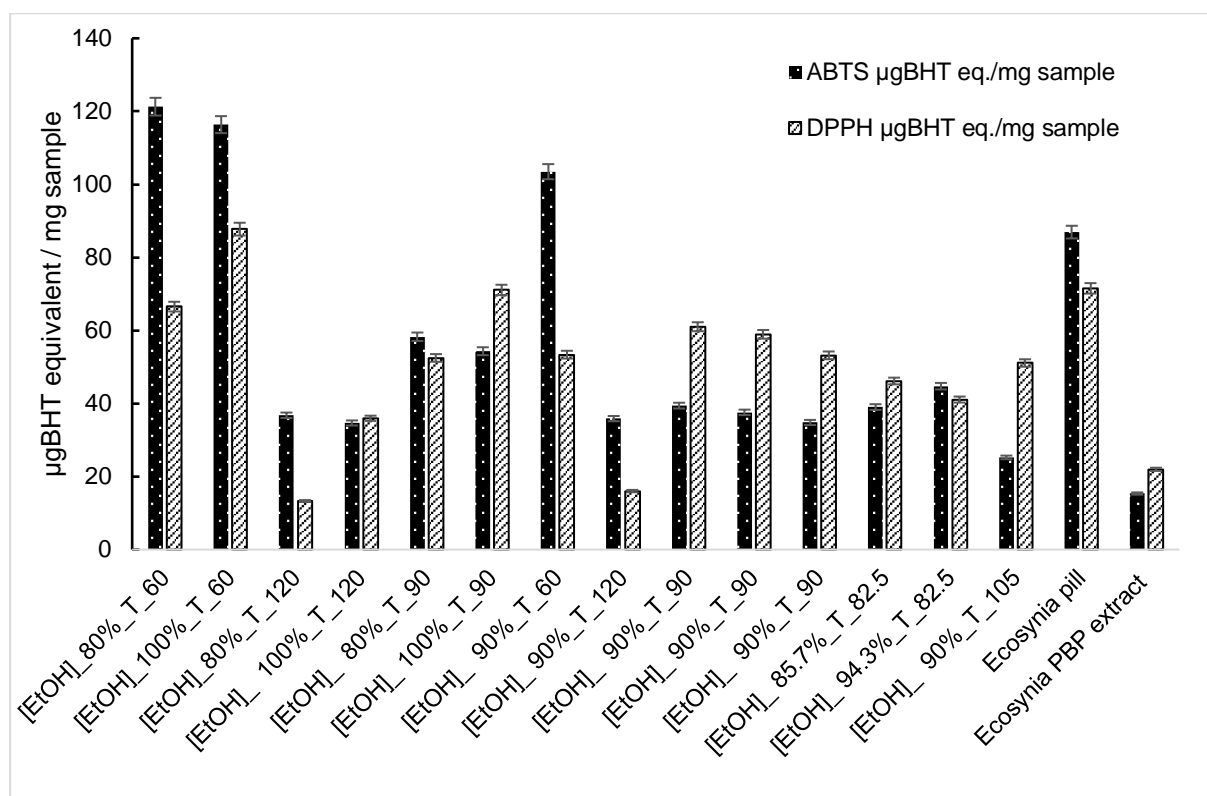


Figure 88 Experimental ABTS and DPPH antioxidant activities for set A

In the case of set B, ABTS and DPPH ranged from 14.04-65.17%, and 1.51-20.09 %, respectively, refer to Figure 89 in p.180. In both responses, the inhibition activity was boosted by temperatures lower than 80°C, ethanol concentrations did not have a strong influence on this factor. Set B exhibited a lower antioxidant activity compared to that recorded for set A, attributed to the prior PBP extraction in the biomass of set B. This assay permitted to affirm that the concentration of a compound and its functional activity, such as antioxidant properties, are not always directly proportional, and various factors can influence their relationship. These factors can include its chemical structure, the presence of co-factors, and the surrounding environment. Modifying any of these factors can potentially decrease the antioxidant activity of the pigment.

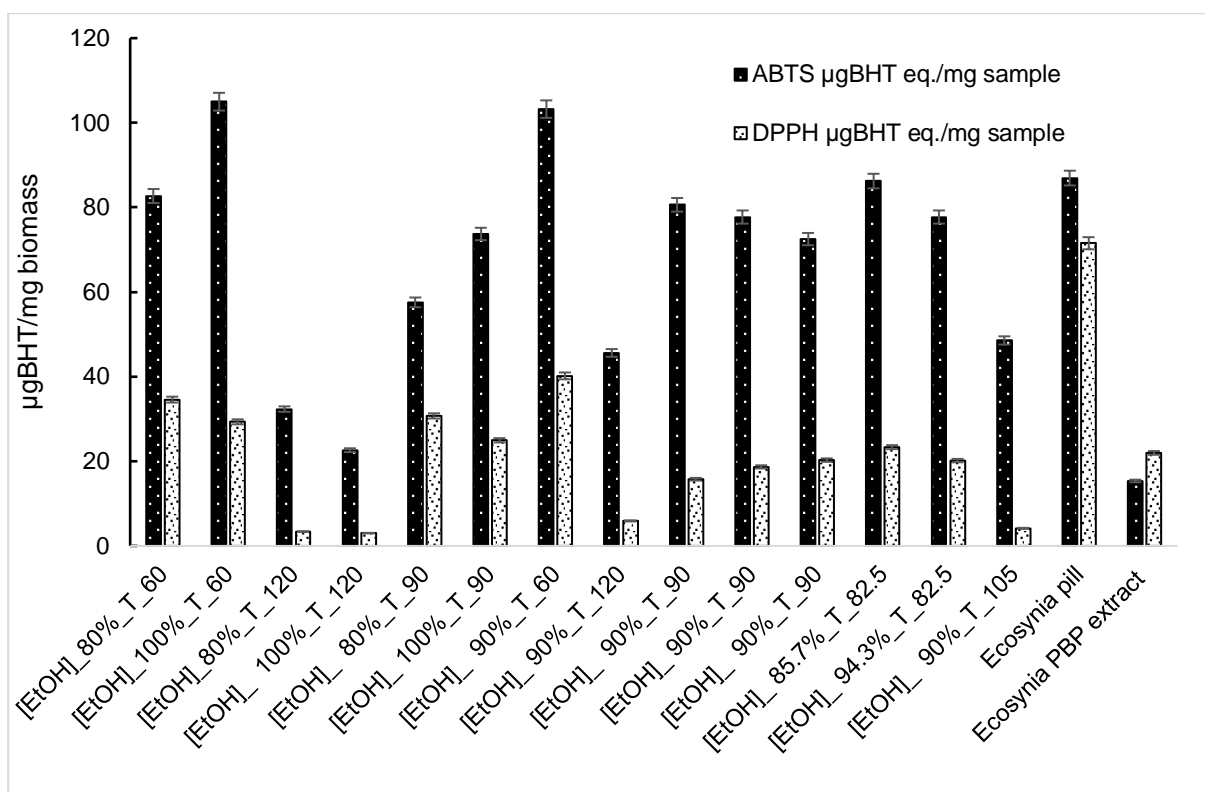


Figure 89 Experimental DPPH antioxidant activities for set B

The commercial AP biomass extract presented antioxidant activities considerably stronger than the ones presented by the phycocyanin commercial extract (Table 51). It can be theorize that the performed protocol 2.5.7 in p. 109 was principally adapted for the extraction of non-polar antioxidant molecules, giving more important antioxidant activities in samples with an important presence of these molecules. It is worth noting that the obtained antioxidants in commercial extracts by selective methods are comparable to the ones obtained by ASE.

The TPC concentrations were parallely analyzed and compared to the ones obtained from AP biomass and phycocyanin commercial extracts, being 6.92 ± 0.52 and 16.8 ± 1.28 mg GAE/ g_{extract} . The obtained TPC concentration is comparable to the one reported by [309].

Table 51 Commercial samples antioxidant activities

Sample	DPPH ($\mu\text{gBHT eq./mg sample}$)	SD	ABTS ($\mu\text{gBHT eq./mg sample}$)	SD	TPC (mg GAE/ g sample)	SD
<i>Arthrospira platensis</i> commercial biomass	71.53	8.3	86.93	11.1	14.55	1.55
Phycocyanin commercial extract	21.97	7.03	15.35	4.57	6.92	0.6

Chapter III : Results and Discussions

3.3.2.5 Desirability study of the optimal extraction conditions by ASE

Globally, the temperature increase hindered the antioxidant activity, while this parameter boosted the extraction efficiency in both of the experiments. To set the optimal extraction conditions to boost both responses a desirability evaluation was performed for both sets. The desirability parameters to find the optimal extraction conditions are displayed in Table 52, the target values were set as a function of the previously reported data [173] [310] for the TPC, and the target total pigment extraction yield was set as the high extraction efficiency obtained during the experimental sets.

Table 52 Desirability parameters

	TPC (mg GAE/g)		Total pigment Extraction yield (%)	
Set	A	B	A	B
Target value	10	10	20	25
Minimum value	3	3	10	10

It was determined that to reach 82.94% of the desirable target parameters in set A, the extraction conditions should be a temperature of 60°C and 100% ethanol. Avoiding the parameters marked by the purple zone in Figure 90.

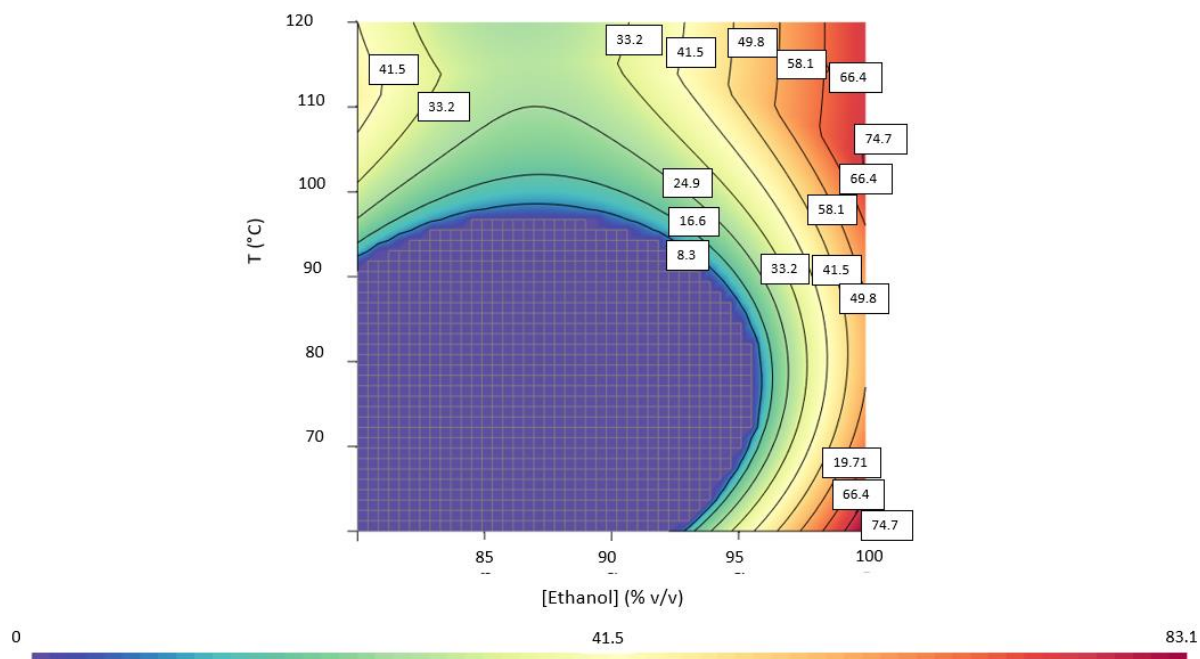


Figure 90 Desirability parameters for set A

Regarding set B, the extraction conditions to reach the target parameters listed in Table 52 are 65°C and 90% ethanol v/v, with a desirability of 79.87%, the extraction conditions in the purple zones in Figure 91 must be avoided to approach a TPC concentration of 7.46 mg GAE/g and an extraction efficiency of 25%. η Total pigments

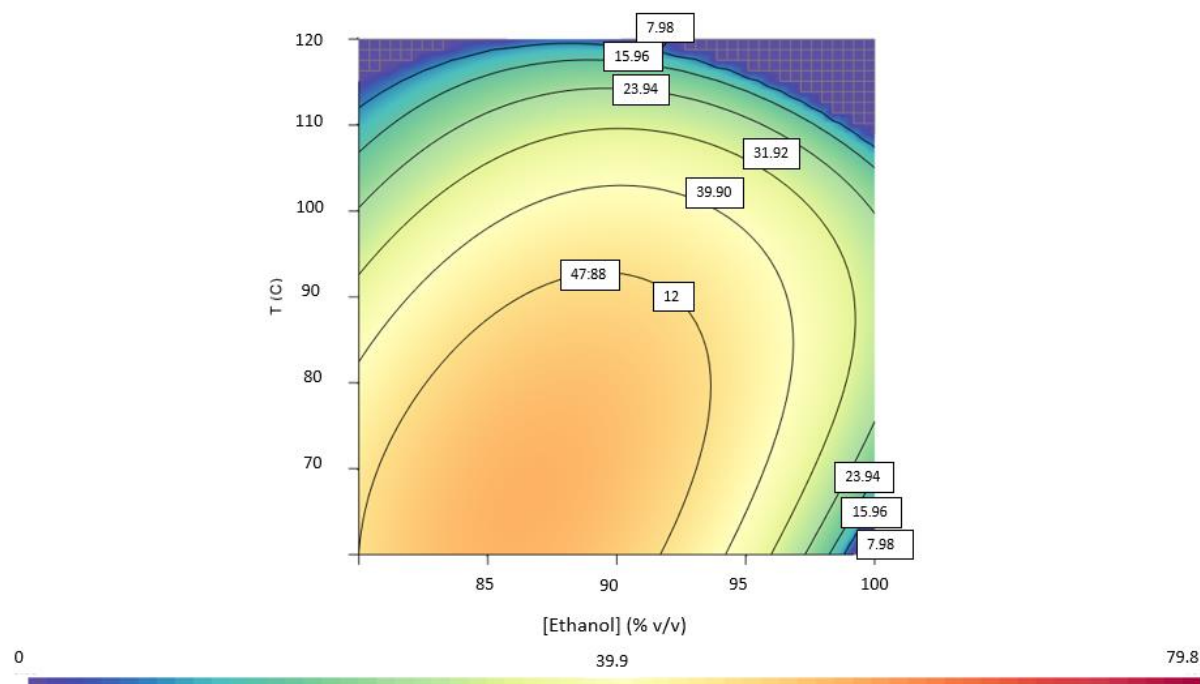


Figure 91 Desirability parameters for set B

Chapter III : Results and Discussions

3.3.3 Conclusions

In both experimental sets, Set A comprises biomass with no prior extraction, while Set B consists of biomass lacking phycobiliproteins. The chosen ranges of temperature and ethanol concentration did have an important effect on the biomass extraction yield and the extract TPC, and antioxidant activities. Temperature increase from 60°C to 120°C proved to have a strong influence on the studied responses, boosting the total pigment extraction efficiencies and hindering the antioxidant activities and TPC concentration in the extracts. Both sets presented similar extraction yields. Nonetheless, set B reached greater extraction yields, due to the previous PBP extraction, provoking a greater exposition of the target molecules to the ASE solvents. Complementary, extraction temperature increase displayed an adverse effect on TPC concentrations, ABTS, and DPPH antioxidant activities in the two studied sets. Moreover, the estimated TPC concentrations and antioxidant activities were satisfactory when compared to the performances of commercial samples and previously reported data. Finally, the desirability study provided a glimpse of the optimal extraction conditions to maximize the total lipophilic pigment extraction yield and the total phenolic compounds content. The optimal extraction conditions were 60°C/100% ethanol and 65°C/90% ethanol for the set A and B, respectively. In the perspective of the valorization of AP with a biorefinery approach it is advisable to apply set B configuration, in order to keep the PBP properties and purity, and to enhance the pressurized solvent extraction efficiency.

3.4 Phase II: Valorization of lipophilic pigments in *Arthrospira platensis* biomass

3.4.1 Supercritical CO₂ valorization of *Arthrospira platensis* biomass

Abstract

The supercritical CO₂ technique is widely recognized for its extraction selectivity and efficiency. In the high-value molecule extraction context, the application of this technique is quite attractive. This experiment has as its main purpose to characterize the scCO₂ extraction in the *Arthrospira platensis* biomass studied during this research. The optimal parameters reported by previous authors were reproduced in this work [203] [208], being 300 bar and 60°C at a granulometry of 300-500µm. Thanks to the application of Sovová's model to the experimental extraction curves it was observed that the drying method was the limiting factor in the second part of the extraction, hindering the diffusion phenomenon. The modeled experimental data permitted to set that $7.7 \pm 2.26\%$ of the dry biomass was extractable, and the extract was characterized. Zeaxanthin, β - carotene, palmitic acid, stearic acid, linoleate, and alpha-linolenic acid were detected in the extracts. Palmitic acid and linoleate were the predominant fatty acids among those identified, being $31.55 \pm 2\%$ and $32.94 \pm 1\%$ respectively. While β - carotene represented $85.56\% \pm 5.51\%$ of the total analyzed pigments.

3.4.2 Repeatability test

The AP studied biomass composition is listed in Table 38 in p.158 and Table 39 in p.160, for the FAMEs. This biomass is equivalent to the one studied in set A from the section 3.3.1, without prior extraction of PBP. The biomass composition is displayed in Table 38 p.160. The extraction kinetics were performed twice at the conditions displayed in Table 22 in p. 116. The assessed repeatability was considered satisfactory, with an error of 5.83%. In both of the performed extraction kinetics, the maximum experimental extraction yield was $6.46\% \pm 0.22\%$. The confirmation run was performed in one single step, at 60°C and 300 bar without stopping, to corroborate the extraction end assessed during the two performed extraction curves.

The scCO₂ extract constituted a higher proportion of the biomass compared to the neutral lipids and carotenoids, which collectively represented 6.11% of the biomass as determined by analytical methods Table 38 in p.160.

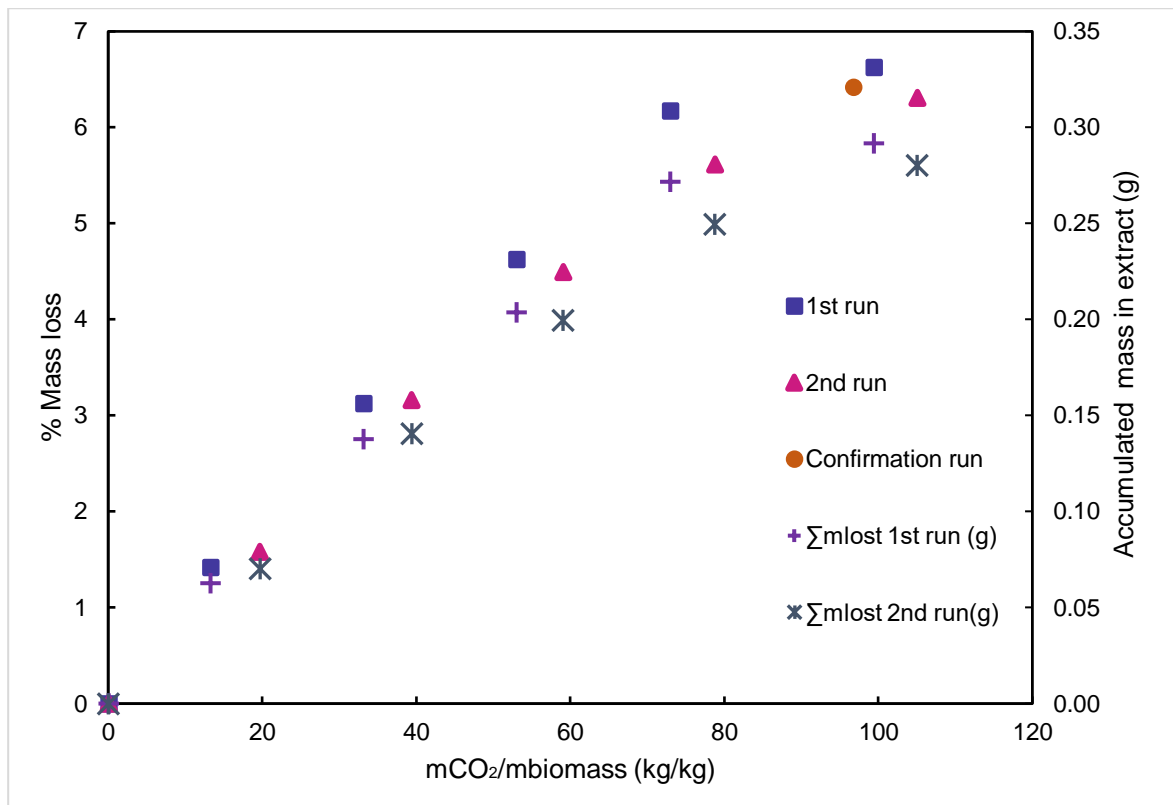


Figure 92 Supercritical CO₂ extraction kinetics at 60°C and 300 bar, performed in biomass with no prior PBP extraction. The secondary axis indicates the cumulative mass loss of the extraction autoclave throughout the entire extraction process.

The executed extractions were modeled employing Sovová's equations aborded in 2.6.6 p.120., showing a relative deviation of 2.26% between the model and the experimental data. Proving that the chosen model parameters are adapted to represent the experimental results. This model has been applied previously to model microalgae scCO₂ extractions [311] [128] [267]. The obtained extraction shape corresponds to the case A described by [266], and plotted Figure 52 p.123. This kind of extraction supposes an unimportant interaction between the fluid and the matrix. According to the modeled data, 7.7% of the biomass is extractable under the applied operation conditions. In line with the experimental data for scCO₂ extraction, the model predicts that the extractable proportion of biomass using scCO₂ surpasses the concentration of neutral lipids and carotenoids identified in the biomass experimentally. Table 53 shows that the proportion of biomass extractable by analytical methods, including neutral lipids and carotenes, is lower than the extraction results obtained through both scCO₂ experimentation and modeling. It can be theorized that the scCO₂ operation conditions boost the extraction of some components that were not completely extracted by the analytical methods described in sections 2.1.7 and 2.4.2 in p. 101 and 75, respectively for lipophilic pigments and lipids. Another theory to explain this difference might be that the biomass gained moisture during its storage, and thus molecule

solubility in CO₂ was modified by the water presence in the sample. A picture of the dry extract is shown in Annex Figure 99 p. 227.

Table 53 Comparison between the extractable lipophilic fractions of *Arthrospira platensis* biomass

	Biomass (%wt)	SD
Analytical methods	6.11	0.73
Experimental scCO₂	6.46	0.22
Model scCO₂	7.7	2.26

The extract presented an oily/pulp texture yellow-orange color, indicating the presence of carotenoids (Figure 93). A further pigment analysis was made to confirm the absence of other pigments different from carotenoids.



Figure 93 Supercritical CO₂ extraction at 300 bar and 60°C extract from *Arthrospira platensis*, suspended in 5mL of ethanol.

Moreover, it will be interesting to model this data applying a mathematical model for oil extraction from microalgae, incorporating adsorption on microalgal surfaces, like the one developed by Sovová and Stateva, 2019 [312]. This step will assess the precision of the model used in this study.

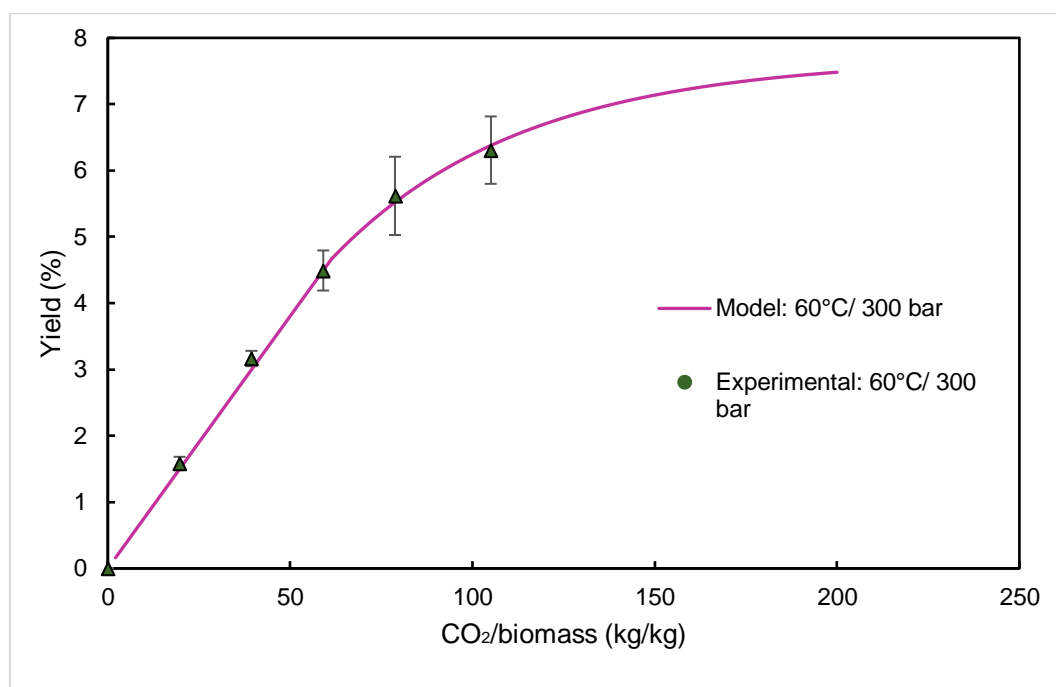


Figure 94 Experimental extraction curves modeled with Sovová's model at 60°C and 300 bar on *Arthrospira platensis* biomass

3.4.3 Evaluation of the modeled parameters

The modeled parameters gave important information about the extraction process and the effect of the biomass pre-treatment in the extraction. All the analyzed parameters are in the same order of magnitude as previously reported data for microalgae and cyanobacteria. Concerning the mass transfer parameters, the $k_s a_s$ term proves that the diffusion in the intact cells was an important parameter to take into account. This parameter can be improved in two ways, the increase of the biomass particle diameter, reducing the channeling probability, and the work pressure increase [265]. In the case of the crushed almond and *Spirulina* extract seen in Table 54, the d_p were 700 μm and 160 $< \mu\text{m}$, respectively. When it comes to the influence of the fraction between intact and broken cells, represented by r , it can be discussed that the chosen grinding and drying methods did not effectively broke the cells, hindering the mass transfer. The biomass by Mouahid *et al.*, [267] was dried by air-flow. The air-flow method enhances the cell breakage, and has an improving effect on the extractions, while the freeze-drying method conserves the cell integrity, and protects the thermolabile molecules, as PBPs. However, as the cell remains unbroken after freeze-drying the extraction of certain molecules might be hindered. This suggests that the best drying technique for PBP extraction is not the best for lipophilic molecules extraction by scCO_2 .

Table 54 Sovová equations modeled parameters

Parameters	r (%)	Biomass	Pre-treatment	y_s (g solute/ kg CO ₂)	$k_s a_s (x10^{-5})$ (s ⁻¹)	AARD (%)	Reference
300 bar / 60°C	29	<i>A. platensis</i>	L/M	0.76	5.87	2.26	This study
350 bar / 55°C	-	Chlorella	L/C	11.2	-	-	[311]
300 bar/ 60°C	-	Nannochloropsis	O/BM	10.2	-	-	[311]
300 bar/ 40°C	-	Botryococcus	L/M	8.8	-	-	[311]
350 bar / 40°C	71	Crushed almond	F/C	11	10	-	[266]
300 bar/ 40°C	9.2	Argan seed	S/G	7.08	0.465	9.59	[265]
400 bar / 60°C	41.8	Spirulina	AF/G	3.4	11.5	5.3	[267]

L=Lyophilization, O= Oven, AF= Air-Flow, S= Sun-dried, F=Fresh, M=Mortar, C=Crushed, BM= Bead-milling, G=Grinded, (-) = Not reported.

When it comes to the analysis of the solute solubility, it was observed that the biomass studied in this experiment presented a low solubility compared to the previous studies made at similar conditions. This can be explained by the lipidic profile of the extracted oil. It is worth noting that the biomass in this study was not cultivated in any lack of nutrients favoring lipid accumulation, and thus the oil composition is different from the other studies focused on microalgae and cyanobacteria valorization.

3.4.4 Extract characterization

3.4.4.1 Pigment characterization

The HPLC pigment chromatogram revealed that the predominant extractable pigments by scCO₂ were β -carotene and zeaxanthin, due to their reduced polarity compared to Chl a. The extract was predominantly composed of β -carotene, making up $76.59 \pm 5.51\%$ of the total analyzed pigments. This dominance is attributed to its strong affinity for low-polarity solvents. The obtained chromatogram is showed in Figure 100 from the Annex in p. 227. Upon analyzing the extracts obtained at each point of the extraction curve it could be observed that β -carotene and zeaxanthin were extracted during the whole process, and not predominantly in one part of the extraction curve (Figure 95).

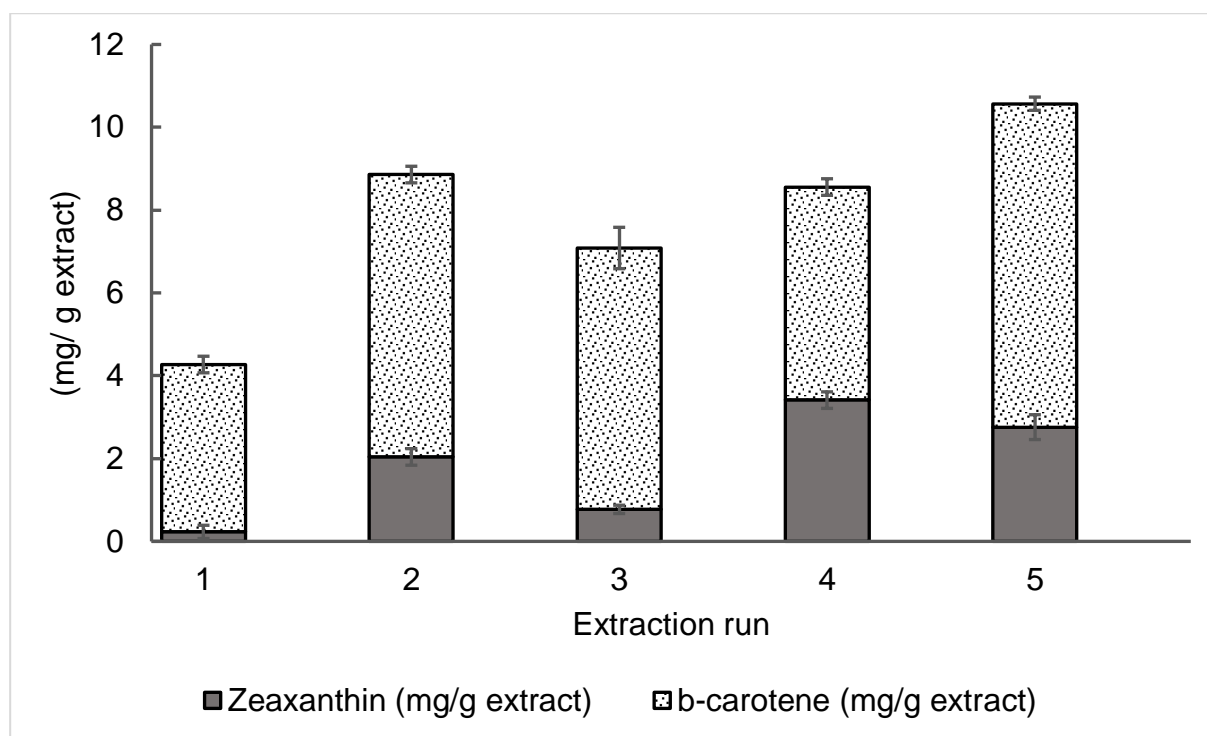


Figure 95 Extract pigment profile at each extraction point of the extraction curve

It was observed that pigment concentration obtained by scCO_2 (Table 55) is close to the zeaxanthin and β -carotene concentrations identified in the biomass characterization from Table 38 in p.160. Considering that the extract mass corresponds to 0.29 g, and that the sample biomass in the extraction autoclave was of 4.4 g.

Table 55 β -carotene and zeaxanthin concentrations obtained by scCO_2 compared to the reference biomass concentrations

	Zeaxanthin (mg/g biomass)	\pm mg/g biomass	β-carotene (mg/g biomass)	\pm mg/g biomass
scCO₂	0.61	0.09	1.99	0.1
Analytic method	0.84	0.05	2.21	0.06

3.4.4.2 Lipid characterization

Upon analyzing the extracts using GC-FID, it was noted that the extract from the initial point of the curve was the sole one containing all the identified fatty acids in the biomass (See Table 59 from the Annex in p. 228). Thus the majority of the fatty acids are extracted within the first 20 minutes of extraction. In contrast, the extracts from the subsequent four points of the curve only featured palmitic acid, which was the predominant fatty acid in the AP biomass of this study. The extract composition is showed in Table 56. The injection chromatogram is displayed in Figure 101 from the Annex in p 228.

Table 56 *Arthrospira platensis* lipid profile obtained by scCO₂

	Relative proportion (%) ¹	mg/g biomass
Saturated Fatty Acids (SFA)		
Palmitic acid (C16)	31.55 ± 2	20.09 ± 0.4
Stearic acid (C18)	20.24 ± 0.5	12.89 ± 0.64
Polyunsaturated Fatty Acids (PUFA)		
Linoleate C18:2	32.94 ± 1	20.98 ± 0.2
Alpha linoleic acid C20:3[cis-8,11,14]	15.27 ± 1	9.72 ± 0.09
Total SFA	51.79 ± 0.5	32.98 ± 1.64
Total PUFA	48.21 ± 0.5	30.70 ± 1.53

¹ Percent of total Fatty acids

The relative proportions of saturated fatty acids (SFA) and polyunsaturated fatty acids (PUFA) in the present study closely align with those documented by Crampon *et al.*, 2020 [28], wherein the reported relative proportions were 65.38% for SFA and 23.14% for PUFA. Nevertheless, the concentrations of FAMEs as documented in [28] surpass those measured in the current investigation. This divergence can be explained by the difference in nitrogen availability during the cultivation of the biomass under examination in this study. Unlike the biomass studied in [1], the biomass in our study was not cultivated under nitrogen-limited conditions, thereby mitigating lipid accumulation in cells. The palmitic acid proportions assessed during this study are in line to the ones reported by previous studies [25][313] [314].

3.4.5 Conclusions

The conducted study demonstrates that 7.7% of the analyzed biomass can be valorized through the application of supercritical CO₂. Sovová's model suggests that the drying method used induces mass transfer limitation by internal diffusion. The solute in the analyzed biomass exhibited a comparably low solubility coefficient in contrast to findings in other studies. The diffusivity phenomenon played an important role in this extraction. The chosen biomass pretreatment technique was not the optimal for supercritical CO₂ valorization. The lipid extract presented a predominant composition comprising linoleate and palmitic acid.

3.5 Proposition of a new *Arthrospira platensis* valorization scheme

After the study of the different process alternatives to optimize the valorization of AP biomass, the process in p.192 is proposed. For starters, it is proposed to cultivate the AP biomass in a covered raceway photobioreactor. This setup is optimal for preventing CO₂ loss during the flow of the medium through the raceway pond. Concerning the nutrient supplementation, a diluted carbon-free Zarrouk medium can be used to provide the cells with essential nutrients. The carbon source can be introduced semi-continuously in gas form directly into the culture. Alternatively, a separate carbon enrichment process can be conducted in the medium before inoculating the microorganisms into the PBR. Regarding photoperiod conditions, it is advisable to conduct the cultivation under continuous lighting when introducing LED-like light in controlled conditions. For the utilization of natural light, it is recommended to implement a photoperiod of 12 hours of light and 12 hours of darkness during the summer in southern Europe to achieve satisfactory productivities in controlled conditions. For biomass harvest, membrane filtration preserves the integrity of the biomass and provides a desirable water content for subsequent processes. It is advisable to verify the integrity of harvested biomass cells under a microscope once the separation process is completed. If no cell damage is identified, the valorization step can commence. It is advisable to initiate the extraction of phycobiliproteins (PBP) first, as these molecules are the most susceptible to damage and possess the highest added value. The maceration process with a buffer is an interesting option, thanks to its low energy consumption and efficiency. Once the PBP are extracted, the biomass can be separated from the extraction buffer by membrane filtration. After filtration the biomass can be inserted directly into PLE process. However, it is advisable to consider a water rinsing process to prevent interference from the buffer in the PLE process at 60°C and 90% v/v ethanol. After PLE, an antioxidant extract primarily consisting of chlorophyll, carotenoids, and phenolic compounds is obtained. The remaining biomass is then subjected to a spray-drying process to reduce the water content to values below 5% wt. It is theorized that the biomass lipids remain within the biomass since it was not subjected to low-polarity solvents. The scCO₂ process can be performed at 300 bar and 60°C to obtain the neutral lipid content in the biomass. The residual biomass is potentially rich in protein and carbohydrates with food industry applications.

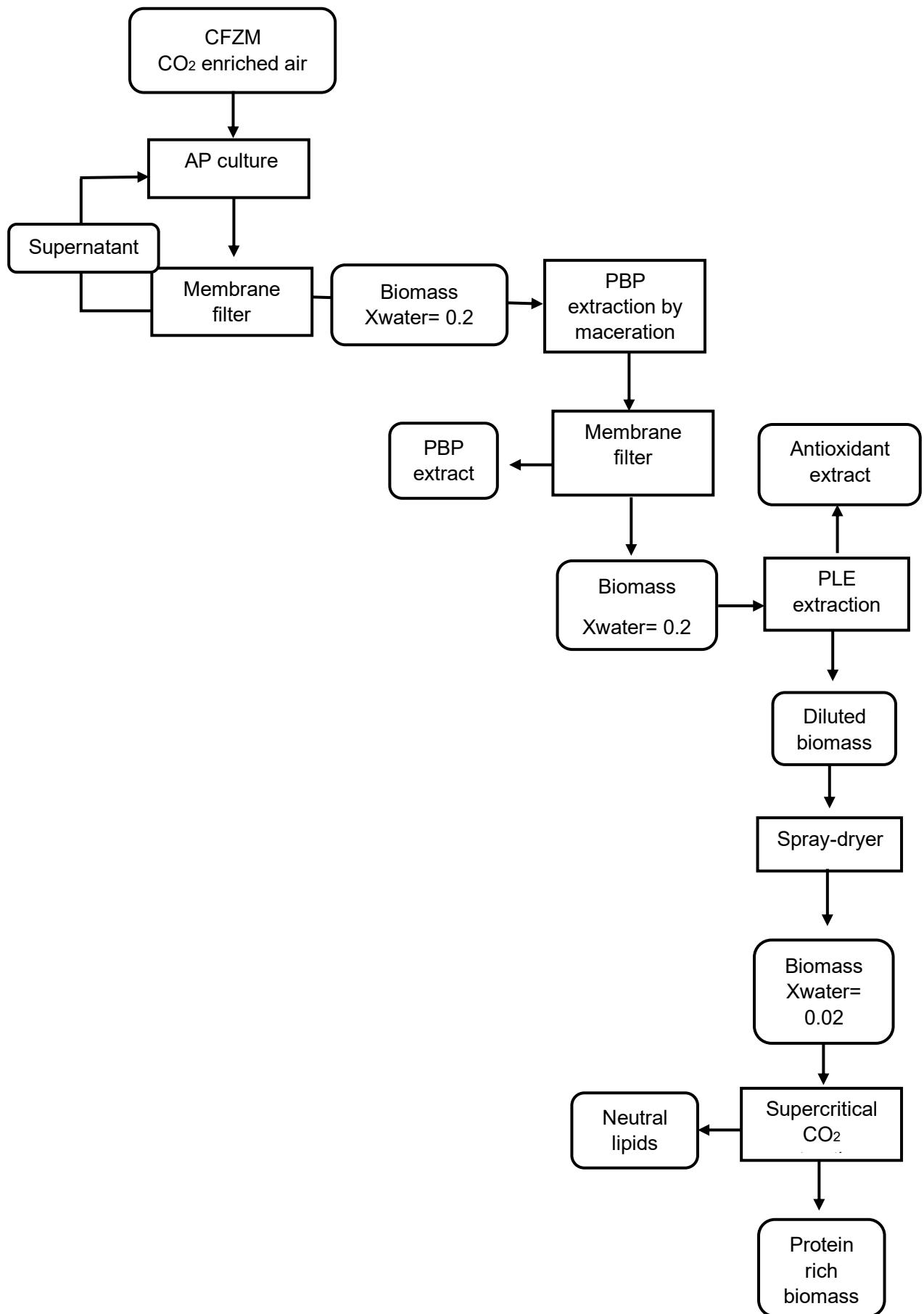


Figure 96 *Arthrospira platensis* valorization process

General Conclusions and perspectives

This chapter will wrap up by summarizing the key research findings in connection with the primary research questions, as well as the significance and contributions of the study. Additionally, it will assess the study limitations and propose opportunities for further research.

The study aimed to contribute to the AP culture and fractionation optimization by implementing sustainable cultivation and extraction approaches.

Phase I:

Concerning the culture optimization, the CO₂ mitigation potential of AP was evaluated, aiming to assess the carbonate salt substitution with CO₂. The model selected for the study of the CO₂ absorption in the medium aligns effectively with the DIC levels in the medium. The findings suggest that AP cultures exhibit notable promise as a carbon mitigation technique, especially given its preference for high pH conditions promoting optimal growth and efficient CO₂ absorption in the culture medium. The nitrate assimilation in the culture seemed to play an important role on the medium pH, affecting the CO₂ absorption in the medium. No reductions in biomass productivity were observed when cultivating AP with CO₂ as the sole carbon source in laboratory conditions. In the evaluation of CO₂ bio-mitigation within 3 L and 3 m³ PBR, the influence of light on CO₂ assimilation by biomass was analysed. A decrease in biomass productivity was observed, leading to diminished CO₂ bio-mitigation in the PBR with lower PAR, specifically the 3 m³ PBR. These results give an insight into the parameters to control when growing AP biomass as a CO₂ mitigation technique. To address study limitations, continuously record pH and nitrate evolution in the lab-scale experiment for a more comprehensive understanding of their relationship. This, in turn, could aid in developing regulatory techniques to improve CO₂ bio-mitigation. In comparing the CO₂ bio-mitigation in the 3 L and 3 m³ PBRs, two primary factors posed limitations: the size disparity between the two systems and the heterogeneous biomass density in the 3 m³ PBR, rendering the data less reliable. Incorporating an intermediate size in this study and enhancing the mixing parameters in the 3 m³ PBR would guarantee a more comprehensive investigation. Additionally, the study of the volumetric mass transfer coefficient (kL_a) would enable to have a more accurate comprehension of the physical factor effect on the CO₂ absorption in the medium.

In line with the AP culture optimization, this research aimed to characterize the influence of the photoperiod modification in biomass productivity and pigment profile with LEDs and natural light complemented by LEDs. The findings show that under LED illumination,

extending the photoperiod from 12 hours to continuous light (24 hours) resulted in a positive response in biomass productivity and pigment content. Both ZM and CFZM medium treatments exhibited comparable responses to the extension of the photoperiod in both biomass productivity and pigment content. The introduction of CO₂ as the sole carbon source did not hinder the responses assessed in this experiment. Cultures subjected to prolonged light exposure exhibited an accumulation of PBP, unlike those cultivated with shorter photoperiods, which did not show this tendency. Hypothetically, differences induced by changes in light availability provoked by the increase in the biomass density can explain these differences in the pigment composition. When transitioning this experiment from LED light to natural light supplemented with LEDs, there was a 30% reduction in PBP content compared to the control. Additionally, biomass productivity decreased from 0.27 g/L/d to 0.15 g/L/d in the natural complemented and LED light experiments, respectively. This can suggest it is needed to control light intensity along with the photoperiod. The results of this experiment contribute to the study of a little-explored abiotic parameter in the AP biomass culture. Concerning the limitations of this research, a measure of the incident light availability in the PBR at each studied photoperiod could confirm the hypothesis of its influence on the biomass pigment profile. Conducting an additional investigation to characterize how modifications in wavelength impact the pigment profile of AP can be beneficial for optimizing culture conditions. This optimization is especially relevant when aiming to produce a specific target molecule using sunlight as the light source.

Phase II:

Looking forward to the biomass valorization, an assessment of the drying method effect on the PBP content in biomass revealed that lyophilization was the most effective technique in preserving PBP content compared to other drying methods tested. Nevertheless, the utilization of the spray-drying method yields comparable outcomes in terms of process effectiveness and superior outcomes in terms of energy efficiency. After establishing the biomass drying pretreatment, the research focused on determining the optimal extraction parameters, specifically considering temperature and ethanol proportions, to enhance the PLE process via its laboratory scale ASE. The results suggest that the temperature parameter was the most influent on this process. Moreover, elevating both temperature and ethanol proportion during the extraction leads to an increased yield of the analyzed lipophilic pigments (β -carotene, zeaxanthin, and Chl a). However, the temperature increase proved to have a negative effect on the TPC concentration and antioxidant activity of the extracts for the two sets. Two types of biomass were evaluated: raw biomass and PBP-free biomass. The PBP-free biomass showed a slightly higher extraction yield compared to the raw biomass, and this outcome is likely

General Conclusions and perspectives

associated with the impact of the previous PBP extraction on the biomass surface disruption. To determine the optimal PLE extraction parameters for both types of biomass, a desirability test was conducted. The criteria set included a TPC concentration of 10 mg GAE/g_{extract} and extraction yields of 20% and 25% for raw biomass and PBP-free biomass, respectively. The identified optimal parameters were 60°C with 100% ethanol v/v for raw biomass and 65°C with 90% ethanol v/v for PBP-free biomass. The findings of this study establish the foundational temperature range and solvent proportions for developing an industrial-scale PLE process to valorize AP biomass keeping a satisfactory extract quality in terms of TPC content and antioxidant activity. However, conducting HPLC PBP characterization on the extracts obtained through ASE would be valuable for obtaining an accurate pigment profile. For future developments, scaling up this process using the defined optimal operating parameters will confirm the applicability of the results in relevant industrial domains. Comparing the proposed process with the established extraction method in terms of efficiency and energy consumption would further clarify the relevance of applying this technology.

Concerning AP valorization through scCO₂, this study aimed to identify the key drawback parameters that impact the extraction under the optimal conditions reported in the literature, 60°C and 300 bar. Additionally, the study looked forward to examining the extract profile, particularly in terms of lipids and pigments, obtained by applying the identified optimal parameters. The results revealed that 7.7% of the dry biomass could be extracted under the selected conditions, suggesting a lack of selectivity for lipids. The application of the Sovová model to the extraction curve permitted to identify a limiting factor on the diffusion phenomenon, in the second part of the extraction curve. For the studied biomass, this work highlights that the lyophilization may induce mass transfer limitation by internal diffusion. Upon characterizing the extract, a predominant presence of β -carotene, palmitic, and linoleate was observed, highlighting the nutraceutical value of the obtained extract. The results obtained in this research gave a glimpse into the scCO₂ valorization of AP biomass. Addressing the experiment limitations, a more thorough evaluation of the pretreatment influence on extraction efficiency and extract quality would provide a broader understanding of the process. Additionally, in the extraction curve experiment, analyzing the evolution of the extract mass would improve the analysis, allowing for a quantitative assessment of the obtained extract. For future advancements, it is advisable to conduct an experimental design that explores the impact of pressure and biomass pretreatment on extraction yields and extract quality. The valorization of the scCO₂ residual biomass through PLE would be a step forward for the AP biomass biorefinery. Additionally, measuring the antioxidant activity in the extract by ABTS or DPPH would be valuable for scaling up this process.

In conclusion, this research offers practical insights to enhance the sustainable cultivation and fractionation of AP biomass, particularly focusing on pigments and lipids. The results obtained can serve as a foundation for future process developments aimed at a biorefinery approach for any type of microalgae or cyanobacteria biomass.

List of tables

Table 1 Mass composition (%) of AP [62]	27
Table 2 Different <i>Arthrospira platensis</i> strains	36
Table 3 Primary parameters to run an <i>Arthrospira platensis</i> culture	37
Table 4 Harvest methods applicable to <i>Arthrospira platensis</i> production	42
Table 5 Overview of the drying methods applicable to <i>Arthrospira platensis</i> [122].....	45
Table 6 CO ₂ Optimal extraction conditions for AP biomass valorization	56
Table 7 Culture conditions for the growth comparison of different <i>A. platensis</i> strains [12] [225].	73
Table 8 Composition of the extraction phosphate buffer pH 7	77
Table 9 Culture conditions for the laboratory scale CO ₂ mitigation characterization	79
Table 10 Equilibrium constants estimated by the equations proposed by [68] temperature and salinity of 20°C and 0 g/kg for pure water and 35°C and 3.54 g/kg for CFZM.	82
Table 11 Culture conditions of the experiment characterize the CO ₂ assimilation in a 3 L system.....	85
Table 12 Culture medium composition for the 3 m ³ culture compared to the Zarrouk medium composition	87
Table 13 Greenhouse culture conditions for the gaseous carbon input experiment in the 3 m ³ system.	88
Table 14 Photoperiod experiment sampling schedule.....	93
Table 15 Natural light conditions seed culture parameters.....	96
Table 16 <i>Arthrospira platensis</i> culture conditions for project biomass valorization	98
Table 17 Spray-dryer operation conditions	100
Table 18 Azurad inputs for Central Composite Design study	108
Table 19 Domain definition for Central Composite Design study.....	108
Table 20 Tested extraction conditions for the Central Composite Design (CDD) study (P=103 bar) .	109
Table 21 SpeedVac solvent evaporator parameters	110
Table 22 Kinetics Extraction parameters in 20 mL extraction unit.....	116
Table 23 Growth kinetics parameters to compare three different <i>Arthrospira platensis</i> strains.....	128
Table 24 Average biomass productivity and CO ₂ fixation rate as a function of the photoperiod. Average (AVR) and standard deviation (SD).....	136
Table 25 Carbon mass balances for the 3 L system	139
Table 26 Carbon mass balances for the 3 m ³ PBR. The carbon mass is expressed in average values. .	141
Table 27 Studied photobioreactors CO ₂ mitigation comparison.....	143
Table 28 Biomass productivity and growth rate comparison at different photoperiods and media carbon source	146
Table 29 Growth rate response to 24h photoperiod from different photosynthetic microorganisms...	147
Table 30 Incubator conditions phycobiliproteins content in biomass cultivated at different photoperiods employing ZM	147
Table 31 Incubator conditions phycobiliproteins content in biomass cultivated at different photoperiods employing CFZM	148
Table 32 Biomass phycocyanin content comparison	150
Table 33 Incubator conditions carotenoids and chlorophyll a content in biomass cultivated at different photoperiods employing ZM	150
Table 34 Incubator conditions carotenoids and chlorophyll a content in biomass cultivated at different photoperiods employing CFZM	151
Table 35 HPLC Carotenoid concentrations found in the biomass studied from the different photoperiods at laboratory conditions.	153
Table 36 Growth rate parameters obtained during the experiments with natural light	154
Table 37 Drying Techniques Comparison	158
Table 38 Project valorized biomass composition.....	160
Table 39 FAMES proportions in <i>Arthrospira platensis</i> biomass cultivated for valorization.....	160
Table 40 Reference lipophilic pigments for the ASE extraction efficiency determination	162

Table 41 Regression coefficients and statistics for the fit for the obtained multilinear regressions for the experiments.....	164
Table 42 Set A Total lipophilic pigment experimental responses for the construction of the contour plots by CCD.....	164
Table 43 Set A Chlorophyll a experimental responses for the construction of the contour plots by CCD	165
Table 44 Set A Zeaxanthin and β -carotene experimental responses for the construction of the contour plots by CCD.....	167
Table 45 Phycobiliprotein concentration in biomass from set B before ASE	170
Table 46 Set B Total lipophilic pigment experimental responses for the construction of the contour plots by CCD.....	170
Table 47 Set B Chlorophyll a experimental responses for the construction of the contour plots by CCD	171
Table 48 Set B Zeaxanthin and β -carotene experimental responses for the construction of the contour plots by CCD.....	173
Table 49 Regression coefficients and statistics for the fit for the obtained multilinear regressions for the experiments of total phenolic compounds and antioxidant activities.....	175
Table 50 Experimental Total Phenolic Compounds concentrations in set A and B	176
Table 51 Commercial samples antioxidant activities.....	180
Table 52 Desirability parameters	181
Table 53 Comparison between the extractable lipophilic fractions of <i>Arthrospira platensis</i> biomass.	186
Table 54 Sovová equations modeled parameters	188
Table 55 β -carotene and zeaxanthin concentrations obtained by scCO ₂ compared to the reference biomass concentrations	189
Table 56 <i>Arthrospira platensis</i> lipid profile obtained by scCO ₂	190
Table 57 Zarrouk medium composition	225
Table 58 Hutner solution composition [298].....	225
Table 59 FAMES fraction of the analyzed extracts by GC-FID.....	228

List of figures

Figure 1 Project view of <i>Arthrospira platensis</i> valorization chain.....	15
Figure 2 Illustration of the Aztecs collecting <i>Arthrospira platensis</i> biomass from Texcoco Lake, reproduced from [2].....	17
Figure 3 Microscope picture (40x) of <i>Arthrospira platensis</i> SAG-21.99 from DRT MAP, Cadarache.....	18
Figure 4 Typical cyanobacterium structure reproduced from [15].....	19
Figure 5 Phycobilisome over thylakoid schematic representation for general cyanobacteria [38].....	21
Figure 6 Phycobiliprotein and Chlorophyll Absorption spectra [49].....	22
Figure 7 Allophycocyanin maximum absorption and emission wavelengths, reproduced from [45].....	23
Figure 8 Different classes of phenolic compounds with their backbone structures, reproduced from [57].....	25
Figure 9 Distribution of the dissolved inorganic carbon species as percentages of the total carbon content, C_T . The values are calculated using Henry's law for temperatures of 5 and 25°C and for salinities of 0 and 35 ‰ as a function of the pH. To illustrate the dependence of the carbon distribution on salinity, reproduced from [68]......	28
Figure 10 Schematic model for inorganic carbon transport and CO ₂ accumulation in the cyanobacterial cell, reproduced from [72].....	29
Figure 11 Semi-Pilot PBRs in Wageningen, Netherlands, reproduced from [86].....	32
Figure 12 Definition of the working illuminated fraction in a plane PBR (γ). Where G represents the irradiance profiles; q_0 represents the incident hemispherical light flux, reproduced from [85].....	33
Figure 13 Classification of the harvesting methods as a function of their action principle.....	38
Figure 14 Basic flocculation mechanisms: A—canceling the negative surface charge of microalgae by ion, polymer, or colloidal absorption; B—interaction of surface neutral microalgal cells based on the thermodynamic balance of interaction energies; C—charged polymer, reproduced from [118]......	40
Figure 15 Schematic view of single tray reverse absorber cabinet biomass dryer, reproduced from [126].....	43
Figure 16 Freeze-drying process stages, reproduced from [130].....	45
Figure 17 Cell-disruption techniques classification reproduced from [139].....	46
Figure 18 Applied biorefinery concept to aquatic biomass, reproduced from [118].....	48
Figure 19 Water phase diagram, reproduced from [163].....	51
Figure 20 Schematic representation of tortuosity definition reproduced from [172].....	52
Figure 21 CO ₂ Phase diagram representation reproduced from [174].....	54
Figure 22 Widom line, reproduced from [178].....	55
Figure 23 Transesterification in presence of an acidic catalysts, reproduced from [210]......	60
Figure 24 Project Optimization approaches for <i>Arthrospira platensis</i> culture and valorization. 1 and 2 are part of the 1 st approach, while 4,5, and 6 are part of the 2 nd approach.....	67
Figure 25 Structure of the culture optimization (Phase I).....	70
Figure 26 Structure of the biomass valorization (Phase II).....	71
Figure 27 Experimental campaign to identify the potential of <i>A.platensis</i> as a CO ₂ mitigation technique.....	72
Figure 28 A) SAG 21 B) NIES 46 C) PARACAS taken on the 4th day of the culture 16/04/21.....	73
Figure 29 Fluorescent light spectrum in the incubator.....	74
Figure 30 Experimental device to characterize the CO ₂ assimilation in a 3 L system.....	84
Figure 31 3 m ³ Raceway Coldep system.....	86
Figure 32 Coldep system diagram; CO ₂ feed was performed from the output of the column. The blue arrows represent the inner tube, and the red arrows represent the exterior tube.....	87
Figure 33 Schematic representation of the global carbon mass balance. The rectangle represents the photobioreactor content.....	89
Figure 34 Experimental strategy to optimize the pigment productivity in <i>A. platensis</i> culture.....	92
Figure 35 Small-scale greenhouses position diagram. The two yellow dots represent the position of both of the systems. Natural light conditions seed culture.....	93
Figure 36 Small-scale greenhouse system for the evaluation of photoperiods in natural light conditions.....	94

Figure 37 Natural Light spectrum of the light received by the small-scale greenhouses.....	95
Figure 38 Tubular photobioreactor (JUMBO, Synoxis Algae, France) employed for the biomass production for extraction tests	97
Figure 39 Frozen biomass for freeze-drying process test.....	99
Figure 40 Lipid extraction method reaction	102
Figure 41 Sugar quantification in biomass reaction.....	103
Figure 42 Experimental campaign to valorize <i>Arthrospira platensis</i> biomass by pressurized liquids.	104
Figure 43 Illustration of set A and B strategies operated with Accelerated Solvent Extraction method	105
Figure 44 ASE Extraction cell disposition	106
Figure 45 Accelerated Solvent Extraction device, reproduced from [246]	107
Figure 46 Tubes with dry extract after treatment.....	110
Figure 47 Gallic Acid calibration curve for Total Phenolic Compounds estimation.	111
Figure 48 ABTS reaction, in this reaction wells exhibiting a blue coloration represent a negative control, whereas those remaining uncolored signify a positive sample where antioxidant activity is detected.	111
Figure 49 DPPH reaction	112
Figure 50 Experimental campaign to valorize the <i>A. platensis</i> biomass by Supercritical CO ₂	115
Figure 51 Semi-continuous CO ₂ extraction unit Piping and Instrumentation Diagram (P&ID), reproduced from [248]	116
Figure 52 Extraction curve types described by Sovová's model theory, reproduced from [248]	123
Figure 53 Growth curve of the compared <i>Arthrospira platensis</i> strains at laboratory scale conditions	127
Figure 54 Chlorophyll a and pigment content comparison between different <i>Arthrospira platensis</i> strains	128
Figure 55 Phycobiliprotein content comparison between different <i>A. platensis</i> strains	129
Figure 56 Evolution of the pH of <i>A. platensis</i> cultures and control neat culture medium during the growth kinetics for the three studied photoperiods (■) Control experiment without biomass, (▲) Continuous illumination 24h photoperiod, (●) 20h/04h photoperiod, (×)	130
Figure 57 DIC evolution with and without inoculum of <i>A. platensis</i> for the three chosen photoperiods (■) Control experiment without biomass, (▲) Continuous illumination 24h photoperiod, (●) 20h/04h photoperiod, (×) 12h/12h photoperiod.	131
Figure 58 Nitrate consumption kinetics for the three chosen photoperiods (▲) Continuous illumination 24h photoperiod, (●) 20h/04h photoperiod, (×) 12h/12h photoperiod.....	132
Figure 59 Dissolved Inorganic Carbon (DIC) estimated by the application of the model compared to the experimental data obtained during the <i>A. platensis</i> growth kinetics for the three chosen photoperiods. (*) Model data, (Δ) Continuous illumination 24h photoperiod, (○) 20h/04h photoperiod, and (×) 12h/12h photoperiod.....	133
Figure 60 Carbon forms in an aqueous phase as a pH function. Plotted using Stumm and Morgan model. Solid lines for carbonate-free Zarrouk medium at 35°C and dashed lines for the pure water at 20° C, Solid line: (□) H ₂ CO ₃ , (◇) HCO ⁻³ , (Δ) CO ₃ ⁻² , Dashed line: (○)	134
Figure 61 Biomass growth kinetics for the three chosen photoperiods (▲) Continuous illumination 24h photoperiod, (●) 20h/04h photoperiod, (×) 12h/12h photoperiod.....	135
Figure 62 Biomass growth kinetics for CO ₂ mitigation evaluation from <i>Arthrospira platensis</i> biomass in greenhouse conditions.....	138
Figure 63 pH and Dissolved Inorganic Carbon (DIC) evolution for the 3 L culture. The dashed blue lines on the 4th and 7th day represent the CO ₂ injection for the restoration of the carbon source	138
Figure 64 Biomass content, Dissolved Inorganic Carbon, and pH evolution during the 30 th to 34 th culture in the 3 m ³ raceway. The pH data plotted was obtained by the culture pH sensor. Each pH decrease represents a CO ₂ injection to the PBR.	141
Figure 65 Biomass growth at different photoperiods in incubator conditions using the Zarrouk Medium treatment.....	145
Figure 66 Biomass growth at different photoperiods with the CFZM treatment.....	146

Figure 67 Phycobiliproteins content in the biomass at different photoperiods with the Zarrouk Medium treatment in incubator conditions.	148
Figure 68 Phycobiliproteins content in the biomass at different photoperiods with the CFZM treatment	149
Figure 69 Chl a and carotenoids content at different photoperiods with Zarrouk Medium treatment .	151
Figure 70 Chl a and carotenoids content at different photoperiods with CFZM treatment.....	152
Figure 71 HPLC chromatogram of the extracted polar pigments in the biomass of the 16h/08h photoperiods of both of the given treatments.	152
Figure 72 Photosynthetic Active Radiation (PAR) received by the control experiment in greenhouse conditions.	154
Figure 73 Phycocyanin evolution during the greenhouse conditions photoperiod experiment	155
Figure 74 Greenhouse photoperiod biomass phycobiliprotein profile.....	156
Figure 75 Drying technique comparison as a function of the phycobiliprotein content in the dried biomass	159
Figure 76 Preliminary study Total lipophilic pigment, Chl a, β -carotene, and zeaxanthin extraction efficiencies at 40°C.....	162
Figure 77 Set A total lipophilic pigment extraction yield. The color bar at the bottom of the figure indicates the extraction yield in %.....	165
Figure 78 Set A Chlorophyll a extraction yield. The color bar at the bottom of the figure indicates the extraction yield in %.....	166
Figure 79 Set A zeaxanthin extraction yield. The color bar at the bottom of the figure indicates the extraction yield in %.....	167
Figure 80 Set A β -carotene extraction yield. The color bar at the bottom of the figure indicates the extraction yield in %.....	168
Figure 81 Set A residual biomass phycobiliprotein content after ASE extraction	169
Figure 82 Set B total pigment extraction yield. The color bar at the bottom of the figure indicates the extraction yield in %.....	171
Figure 83 Set B Chlorophyll a extraction yield. The color bar at the bottom of the figure indicates the extraction yield in %.....	172
Figure 84 Set B zeaxanthin extraction yield. The color bar at the bottom of the figure indicates the extraction yield in %.....	173
Figure 85 Set B β -carotene extraction yield. The color bar at the bottom of the figure indicates the extraction yield in %.....	174
Figure 86 Set A Total Phenolic Compound concentration. The color bar at the bottom of the figure indicates TPC concentration in mg GAE/g _{extract}	177
Figure 87 Set B Total Phenolic Compound concentration. The color bar at the bottom of the figure indicates TPC concentration in mg GAE/g _{extract}	177
Figure 88 Experimental ABTS and DPPH antioxidant activities for set A	179
Figure 89 Experimental DPPH antioxidant activities for set B	180
Figure 90 Desirability parameters for set A	182
Figure 91 Desirability parameters for set B	182
Figure 92 Supercritical CO ₂ extraction kinetics at 60°C and 300 bar, performed in biomass with no prior PBP extraction. The secondary axis indicates the cumulative mass loss of the extraction autoclave throughout the entire extraction process.....	185
Figure 93 Supercritical CO ₂ extraction at 300 bar and 60°C extract from <i>Arthrospira platensis</i> , suspended in 5mL of ethanol.....	186
Figure 94 Experimental extraction curves modeled with Sovová's model at 60°C and 300 bar on <i>Arthrospira platensis</i> biomass	187
Figure 95 Extract pigment profile at each extraction point of the extraction curve	189
Figure 96 <i>Arthrospira platensis</i> valorization process	192
Figure 97 Temperature assessment in the 3 m ³ raceway.....	226
Figure 98 Temperature assessment in the natural light conditions experiment for pigment enhancement	226
Figure 99 scCO ₂ full extraction dry extract.....	227

Figure 100 ScCO ₂ extracted pigment chromatogram. Response (mA) as a function of the retention time	227
Figure 101 scCO ₂ Lipid injection chromatogram	228

Bibliography

1. Guidi F, Gojkovic Z, Venuleo M, Assunção PACJ, Portillo E (2021) Long-Term Cultivation of a Native *Arthrospira platensis* (*Spirulina*) Strain in Pozo Izquierdo (Gran Canaria, Spain): Technical Evidence for a Viable Production of Food-Grade Biomass. *Processes* 9:1333. <https://doi.org/10.3390/pr9081333>
2. Farrar WV (1966) Tecuitlatl; A Glimpse of Aztec Food Technology. *Nature* 211:341–342. <https://doi.org/10.1038/211341a0>
3. Díaz del Castillo B (2005) Historia verdadera de la conquista de la Nueva España. *Historia verdadera de la conquista de la Nueva España* 0–0
4. Powell RC, Nevels EM, McDowell ME (1961) Algae Feeding in Humans. *The Journal of Nutrition* 75:7–12. <https://doi.org/10.1093/jn/75.1.7>
5. Zarrouk C (1966) Contribution à l'étude d'une Cyanophycée, influence de divers facteurs physiques et chimiques sur la croissance et la photosynthèse de "*Spirulina maxima*" (Setch et Gardner) Geitler. S.L.N.D
6. Bortolini DG, Maciel GM, Fernandes I de AA, Pedro AC, Rubio FTV, Branco IG, Haminiuk CWI (2022) Functional properties of bioactive compounds from *Spirulina* spp.: Current status and future trends. *Food Chemistry: Molecular Sciences* 5:100134. <https://doi.org/10.1016/j.fochms.2022.100134>
7. Belay A, Ota Y, Miyakawa K, Shimamatsu H (1993) Current knowledge on potential health benefits of *Spirulina*. *J Appl Phycol* 5:235–241. <https://doi.org/10.1007/BF00004024>
8. Shiomi N, Waisundara V (2017) Superfood and Functional Food: The Development of Superfoods and Their Roles as Medicine. BoD – Books on Demand
9. Almeida LMR, Cruz LF da S, Machado BAS, Nunes IL, Costa JAV, Ferreira E de S, Lemos PVF, Druzian JI, Souza CO de (2021) Effect of the addition of *Spirulina* sp. biomass on the development and characterization of functional food. *Algal Research* 58:102387. <https://doi.org/10.1016/j.algal.2021.102387>
10. Vo T-S, Ngo D-H, Kim S-K (2015) Chapter 19 - Nutritional and Pharmaceutical Properties of Microalgal *Spirulina*. In: Kim S-K (ed) *Handbook of Marine Microalgae*. Academic Press, Boston, pp 299–308
11. Venkataraman LV (1997) *Spirulina platensis* (*Arthrospira*): Physiology, Cell Biology and Biotechnology, edited by Avigad Vonshak. *Journal of Applied Phycology* 9:295–296. <https://doi.org/10.1023/A:1007911009912>
12. Qiang H, Guterman H, Richmond A (1996) Physiological Characteristics of *Spirulina Platensis* (cyanobacteria) Cultured at Ultrahigh Cell Densities1. *Journal of Phycology* 32:1066–1073. <https://doi.org/10.1111/j.0022-3646.1996.01066.x>
13. Lupatini AL, Colla LM, Canan C, Colla E (2017) Potential application of microalga *Spirulina platensis* as a protein source. *Journal of the Science of Food and Agriculture* 97:724–732. <https://doi.org/10.1002/jsfa.7987>
14. Machu L, Misurcova L, Vavra Ambrozova J, Orsavova J, Mlcek J, Sochor J, Jurikova T (2015) Phenolic Content and Antioxidant Capacity in Algal Food Products. *Molecules* 20:1118–1133. <https://doi.org/10.3390/molecules20011118>
15. Kelvinsong (2013) English: Diagram of a cyanobacterium. Based on 1, 2 3, and 4. Designed to be viewed at 680×380 px.

16. Markou G, Angelidaki I, Nerantzis E, Georgakakis D (2013) Bioethanol Production by Carbohydrate-Enriched Biomass of *Arthrospira* (*Spirulina*) *platensis*. *Energies* 6:3937–3950. <https://doi.org/10.3390/en6083937>
17. Liu Q, Yao C, Sun Y, Chen W, Tan H, Cao X, Xue S, Yin H (2019) Production and structural characterization of a new type of polysaccharide from nitrogen-limited *Arthrospira platensis* cultivated in outdoor industrial-scale open raceway ponds. *Biotechnology for Biofuels* 12:131. <https://doi.org/10.1186/s13068-019-1470-3>
18. Hasanin M, Swielam EM, Atwa NA, Agwa MM (2022) Novel design of bandages using cotton pads, doped with chitosan, glycogen and ZnO nanoparticles, having enhanced antimicrobial and wounds healing effects. *International Journal of Biological Macromolecules* 197:121–130. <https://doi.org/10.1016/j.ijbiomac.2021.12.106>
19. Gopinath V, Saravanan S, Al-Maleki AR, Ramesh M, Vadivelu J (2018) A review of natural polysaccharides for drug delivery applications: Special focus on cellulose, starch and glycogen. *Biomedicine & Pharmacotherapy* 107:96–108. <https://doi.org/10.1016/j.biopha.2018.07.136>
20. Moon Y, Kweon M (2021) Potential application of enzymes to improve quality of dry noodles by reducing water absorption of inferior-quality flour. *Food Sci Biotechnol* 30:921–930. <https://doi.org/10.1007/s10068-021-00936-6>
21. Mathiot C, Ponge P, Gallard B, Sassi J-F, Delrue F, Le Moigne N (2019) Microalgae starch-based bioplastics: Screening of ten strains and plasticization of unfractionated microalgae by extrusion. *Carbohydr Polym* 208:142–151. <https://doi.org/10.1016/j.carbpol.2018.12.057>
22. Babadzhyanov AS, Abdusamatova N, Yusupova FM, Faizullaeva N, Mezhlumyan LG, Malikova MKh (2004) Chemical Composition of *Spirulina platensis* Cultivated in Uzbekistan. *Chemistry of Natural Compounds* 40:276–279. <https://doi.org/10.1023/B:CONC.0000039141.98247.e8>
23. Ramadan F, Asker M, Ibrahim Z (2008) Functional bioactive compounds and biological activities of *Spirulina platensis* lipids. *Czech Journal of Food Sciences* 26:211–222. <https://doi.org/10.17221/2567-CJFS>
24. Tornabene T, Bourne T, Raziuddin S, Ben-Amotz A (1985) Lipid and lipopolysaccharide constituents of cyanobacterium *Spirulina platensis* (Cyanophyceae, Nostocales). *Mar Ecol Prog Ser* 22:121–125. <https://doi.org/10.3354/meps022121>
25. Jung F, Braune S, Jung CHG, Krüger-Genge A, Waldeck P, Petrick I, Küpper J-H (2022) Lipophilic and Hydrophilic Compounds from *Arthrospira platensis* and Its Effects on Tissue and Blood Cells—An Overview. *Life* 12:. <https://doi.org/10.3390/life12101497>
26. López CVG, García M del CC, Fernández FGA, Bustos CS, Chisti Y, Sevilla JMF (2010) Protein measurements of microalgal and cyanobacterial biomass. *Bioresour Technol* 101:7587–7591. <https://doi.org/10.1016/j.biortech.2010.04.077>
27. Ahmad MU, Ali SM, Ahmad A, Sheikh S, Chen P, Ahmad I (2020) Polar Lipids: Phospholipids and Glycolipids. In: *Bailey's Industrial Oil and Fat Products*. John Wiley & Sons, Ltd, pp 1–27
28. Crampon C, Nikitine C, Zaier M, Lépine O, Tanzi CD, Vian MA, Chemat F, Badens E (2017) Oil extraction from enriched *Spirulina platensis* microalgae using supercritical carbon dioxide. *The Journal of Supercritical Fluids* 119:289–296. <https://doi.org/10.1016/j.supflu.2016.10.006>
29. Cohen Z, Vonshak A (1991) Fatty acid composition of *Spirulina* and spirulina-like cyanobacteria in relation to their chemotaxonomy. *Phytochemistry* 30:205–206. [https://doi.org/10.1016/0031-9422\(91\)84125-C](https://doi.org/10.1016/0031-9422(91)84125-C)
30. Remize M, Brunel Y, Silva JL, Berthon J-Y, Filaire E (2021) Microalgae n-3 PUFAs Production and Use in Food and Feed Industries. *Mar Drugs* 19:113. <https://doi.org/10.3390/md19020113>

31. Zhou Y, Wang T, Zhai S, Li W, Meng Q (2016) Linoleic acid and breast cancer risk: a meta-analysis. *Public Health Nutr* 19:1457–1463. <https://doi.org/10.1017/S136898001500289X>
32. Farvid MS, Ding M, Pan A, Sun Q, Chiuve SE, Steffen LM, Willett WC, Hu FB (2014) Dietary linoleic acid and risk of coronary heart disease: a systematic review and meta-analysis of prospective cohort studies. *Circulation* 130:1568–1578. <https://doi.org/10.1161/CIRCULATIONAHA.114.010236>
33. Lupatini AL, De Oliveira Bispo L, Colla LM, Costa JAV, Canan C, Colla E (2017) Protein and carbohydrate extraction from *S. platensis* biomass by ultrasound and mechanical agitation. *Food Research International* 99:1028–1035. <https://doi.org/10.1016/j.foodres.2016.11.036>
34. Volkmann H, Imianovsky U, Oliveira J, Sant’anna E (2008) Cultivation of *Arthrospira* (*Spirulina*) *platensis* in desalinator wastewater and salinated synthetic medium: protein content and amino-acid profile. *Brazilian journal of microbiology* : [publication of the Brazilian Society for Microbiology] 39:98–101. <https://doi.org/10.1590/S1517-838220080001000022>
35. Lafarga T, Fernández-Sevilla JM, González-López C, Acién-Fernández FG (2020) *Spirulina* for the food and functional food industries. *Food Res Int* 137:109356. <https://doi.org/10.1016/j.foodres.2020.109356>
36. Kirst H, Formighieri C, Melis A (2014) Maximizing photosynthetic efficiency and culture productivity in cyanobacteria upon minimizing the phycobilisome light-harvesting antenna size. *Biochimica et Biophysica Acta (BBA) - Bioenergetics* 1837:1653–1664. <https://doi.org/10.1016/j.bbabi.2014.07.009>
37. Ravelonandro PH, Ratianarivo DH, Joannis-Cassan C, Isambert A, Raherimandimby M (2008) Influence of light quality and intensity in the cultivation of *Spirulina platensis* from Toliara (Madagascar) in a closed system. *Journal of Chemical Technology & Biotechnology* 83:842–848. <https://doi.org/10.1002/jctb.1878>
38. Phycobilisome : définition et explications 🇵🇷. In: AquaPortail. <https://www.aquaportail.com/definition-1316-phycobilisome.html>. Accessed 18 Jul 2023
39. Dagnino-Leone J, Figueroa CP, Castañeda ML, Youlton AD, Vallejos-Almirall A, Agurto-Muñoz A, Pavón Pérez J, Agurto-Muñoz C (2022) Phycobiliproteins: Structural aspects, functional characteristics, and biotechnological perspectives. *Computational and Structural Biotechnology Journal* 20:1506–1527. <https://doi.org/10.1016/j.csbj.2022.02.016>
40. Wang F, Yu X, Cui Y, Xu L, Huo S, Ding Z, Hu Q, Xie W, Xiao H, Zhang D (2023) Efficient extraction of phycobiliproteins from dry biomass of *Spirulina platensis* using sodium chloride as extraction enhancer. *Food Chemistry* 406:135005. <https://doi.org/10.1016/j.foodchem.2022.135005>
41. Roy, S., Llewellyn, C., Egeland, E.S., and Johnsen, G. 2011. *Phytoplankton Pigments: Characterization, Chemotaxonomy and Applications in Oceanography*. Cambridge University Press, Cambridge, UK, 845 pp. - Welschmeyer - 2013 - *Journal of Phycology* - Wiley Online Library. <https://onlinelibrary.wiley.com/doi/10.1111/jpy.12035>. Accessed 20 Jul 2023
42. C-Phycocyanin from *Spirulina* Inhibits α -Synuclein and Amyloid- β Fibril Formation but Not Amorphous Aggregation - PubMed. <https://pubmed.ncbi.nlm.nih.gov/30620188/>. Accessed 23 May 2023
43. Palenik B (2001) Chromatic Adaptation in Marine *Synechococcus* Strains. *Appl Environ Microbiol* 67:991–994. <https://doi.org/10.1128/AEM.67.2.991-994.2001>

44. Tario JD, Wallace PK (2014) Reagents and Cell Staining for Immunophenotyping by Flow Cytometry. In: McManus LM, Mitchell RN (eds) *Pathobiology of Human Disease*. Academic Press, San Diego, pp 3678–3701
45. Jung TM, Dailey MO (1989) A novel and inexpensive source of allophycocyanin for multicolor flow cytometry. *J Immunol Methods* 121:9–18. [https://doi.org/10.1016/0022-1759\(89\)90414-6](https://doi.org/10.1016/0022-1759(89)90414-6)
46. SureLight® Allophycocyanin (APC). In: Columbia Biosciences. <https://columbiabiosciences.com/product/surelight-allophycocyanin-apc/>. Accessed 22 Nov 2023
47. Extraction and Purification of R-Phycoerythrin Alpha Subunit from the Marine Red Algae *Pyropia Yezoensis* and Its Biological Activities - PubMed. <https://pubmed.ncbi.nlm.nih.gov/34770894/>. Accessed 23 May 2023
48. Virtanen O, Constantinidou E, Tyystjärvi E (2022) Chlorophyll does not reflect green light – how to correct a misconception. *Journal of Biological Education* 56:552–559. <https://doi.org/10.1080/00219266.2020.1858930>
49. Hosikian A, Lim S, Halim R, Danquah MK (2010) Chlorophyll Extraction from Microalgae: A Review on the Process Engineering Aspects. *International Journal of Chemical Engineering* 2010:e391632. <https://doi.org/10.1155/2010/391632>
50. Ngamwonglumlert L, Devahastin S (2019) Carotenoids. In: Melton L, Shahidi F, Varelis P (eds) *Encyclopedia of Food Chemistry*. Academic Press, Oxford, pp 40–52
51. Lohr M (2009) Chapter 21 - Carotenoids. In: Harris EH, Stern DB, Witman GB (eds) *The Chlamydomonas Sourcebook (Second Edition)*. Academic Press, London, pp 799–817
52. Cazzaniga S, Bressan M, Carbonera D, Agostini A, Dall'Osto L (2016) Differential Roles of Carotenes and Xanthophylls in Photosystem I Photoprotection. *Biochemistry* 55:3636–3649. <https://doi.org/10.1021/acs.biochem.6b00425>
53. Galanakis CM (2017) Chapter 1 - Introduction. In: Galanakis CM (ed) *Nutraceutical and Functional Food Components*. Academic Press, pp 1–14
54. Park WS, Kim H-J, Li M, Lim DH, Kim J, Kwak S-S, Kang C-M, Ferruzzi MG, Ahn M-J (2018) Two Classes of Pigments, Carotenoids and C-Phycocyanin, in *Spirulina* Powder and Their Antioxidant Activities. *Molecules* 23:2065. <https://doi.org/10.3390/molecules23082065>
55. Burns J, Fraser PD, Bramley PM (2003) Identification and quantification of carotenoids, tocopherols and chlorophylls in commonly consumed fruits and vegetables. *Phytochemistry* 62:939–947. [https://doi.org/10.1016/S0031-9422\(02\)00710-0](https://doi.org/10.1016/S0031-9422(02)00710-0)
56. Cichoński J, Chrzanowski G (2022) Microalgae as a Source of Valuable Phenolic Compounds and Carotenoids. *Molecules* 27:8852. <https://doi.org/10.3390/molecules27248852>
57. Ali Redha A (2021) Review on Extraction of Phenolic Compounds from Natural Sources Using Green Deep Eutectic Solvents. *J Agric Food Chem* 69:878–912. <https://doi.org/10.1021/acs.jafc.0c06641>
58. Eriksen NT, Riisgård FK, Gunther WS, Lønsmann Iversen JJ (2007) On-line estimation of O₂ production, CO₂ uptake, and growth kinetics of microalgal cultures in a gas-tight photobioreactor. *J Appl Phycol* 19:161–174. <https://doi.org/10.1007/s10811-006-9122-y>
59. Verma R, Kumari KVLK, Srivastava A, Kumar A (2020) Photoautotrophic, mixotrophic, and heterotrophic culture media optimization for enhanced microalgae production. *Journal of Environmental Chemical Engineering* 8:104149. <https://doi.org/10.1016/j.jece.2020.104149>

60. Xie Y, Jin Y, Zeng X, Chen J, Lu Y, Jing K (2015) Fed-batch strategy for enhancing cell growth and C-phycoyanin production of *Arthrospira* (*Spirulina*) *platensis* under phototrophic cultivation. *Bioresource Technology* 180:281–287. <https://doi.org/10.1016/j.biortech.2014.12.073>
61. They NH, Amado AM, Cotner JB (2017) Redfield Ratios in Inland Waters: Higher Biological Control of C:N:P Ratios in Tropical Semi-arid High Water Residence Time Lakes. *Frontiers in Microbiology* 8:
62. Pruvost J, LEGOUIC B, CORNET J-F, LOMBARD C (2017) Biofixation du CO₂ par microalgues. In: Ref : TIP142WEB - “Chimie verte.” <https://www.techniques-ingenieur.fr/base-documentaire/procedes-chimie-bio-agro-th2/gestion-durable-des-dechets-et-des-polluants-42495210/biofixation-du-co2-par-microalgues-chv7005/>. Accessed 11 Jan 2021
63. Zhu C, Chen S, Ji Y, Schwaneberg U, Chi Z (2022) Progress toward a bicarbonate-based microalgae production system. *Trends in Biotechnology* 40:180–193. <https://doi.org/10.1016/j.tibtech.2021.06.005>
64. Valdovinos-García EM, Barajas-Fernández J, Olán-Acosta M de los Á, Petriz-Prieto MA, Guzmán-López A, Bravo-Sánchez MG (2020) Techno-Economic Study of CO₂ Capture of a Thermoelectric Plant Using Microalgae (*Chlorella vulgaris*) for Production of Feedstock for Bioenergy. *Energies* 13:413. <https://doi.org/10.3390/en13020413>
65. EU-ETS price 2022-2023. In: Statista. <https://www.statista.com/statistics/1322214/carbon-prices-european-union-emission-trading-scheme/>. Accessed 9 Dec 2023
66. Diamond LW, Akinfiyev NN (2003) Solubility of CO₂ in water from –1.5 to 100 °C and from 0.1 to 100 MPa: evaluation of literature data and thermodynamic modelling. *Fluid Phase Equilibria* 208:265–290. [https://doi.org/10.1016/S0378-3812\(03\)00041-4](https://doi.org/10.1016/S0378-3812(03)00041-4)
67. Rinberg A, Bergman AM, Schrag DP, Aziz MJ (2021) Alkalinity Concentration Swing for Direct Air Capture of Carbon Dioxide. *ChemSusChem* 14:4439–4453. <https://doi.org/10.1002/cssc.202100786>
68. Dickson A, Millero F (1987) A comparison of the equilibrium constants for the dissociation of carbonic acid in seawater media. *Deep Sea Research Part A Oceanographic Research Papers* 34:1733–1743. [https://doi.org/10.1016/0198-0149\(87\)90021-5](https://doi.org/10.1016/0198-0149(87)90021-5)
69. Agbebi TV, Ojo EO, Watson IA (2022) Towards optimal inorganic carbon delivery to microalgae culture. *Algal Research* 67:102841. <https://doi.org/10.1016/j.algal.2022.102841>
70. Ramanan R, Kannan K, Deshkar A, Yadav R, Chakrabarti T (2010) Enhanced algal CO₂ sequestration through calcite deposition by *Chlorella* sp. and *Spirulina platensis* in a mini-raceway pond. *Bioresource Technology* 101:2616–2622. <https://doi.org/10.1016/j.biortech.2009.10.061>
71. Li S, Song C, Li M, Chen Y, Lei Z, Zhang Z (2020) Effect of different nitrogen ratio on the performance of CO₂ absorption and microalgae conversion (CAMC) hybrid system. *Bioresource Technology* 306:123126. <https://doi.org/10.1016/j.biortech.2020.123126>
72. Badger MR, Price GD (2003) CO₂ concentrating mechanisms in cyanobacteria: molecular components, their diversity and evolution. *Journal of Experimental Botany* 54:609–622. <https://doi.org/10.1093/jxb/erg076>
73. Inabe K, Miichi A, Matsuda M, Yoshida T, Kato Y, Hidese R, Kondo A, Hasunuma T (2021) Nitrogen Availability Affects the Metabolic Profile in Cyanobacteria. *Metabolites* 11:867. <https://doi.org/10.3390/metabo11120867>

74. Herrero A, Muro-Pastor AM, Flores E (2001) Nitrogen Control in Cyanobacteria. *J Bacteriol* 183:411–425. <https://doi.org/10.1128/JB.183.2.411-425.2001>
75. Aikawa S, Izumi Y, Matsuda F, Hasunuma T, Chang J-S, Kondo A (2012) Synergistic enhancement of glycogen production in *Arthrospira platensis* by optimization of light intensity and nitrate supply. *Bioresour Technol* 108:211–215. <https://doi.org/10.1016/j.biortech.2012.01.004>
76. Report C (1970) CHEMISTRY OF NITROGEN AND PHOSPHORUS IN WATER. *Journal (American Water Works Association)* 62:127–140
77. Markou G, Chatzipavlidis I, Georgakakis D (2012) Effects of phosphorus concentration and light intensity on the biomass composition of *Arthrospira (Spirulina) platensis*. *World Journal of Microbiology and Biotechnology*. <https://doi.org/10.1007/s11274-012-1076-4>
78. Rueter JG, Petersen RR (1987) Micronutrient effects on cyanobacterial growth and physiology. *New Zealand Journal of Marine and Freshwater Research* 21:435–445. <https://doi.org/10.1080/00288330.1987.9516239>
79. Delrue F, Alaux E, Moudjaoui L, Gaignard C, Fleury G, Perilhou A, Richaud P, Petitjean M, Sassi J-F (2017) Optimization of *Arthrospira platensis (Spirulina)* Growth: From Laboratory Scale to Pilot Scale. *Fermentation* 3:59. <https://doi.org/10.3390/fermentation3040059>
80. Pandey J, Tiwari A, Mishra R (2010) Evaluation of Biomass Production of *Spirulina maxima* on Different Reported Media. *Journal of Algal Biomass Utilization* 2229-6905 1:70–81
81. Soni RA, Sudhakar K, Rana RS (2019) Comparative study on the growth performance of *Spirulina platensis* on modifying culture media. *Energy Reports* 5:327–336. <https://doi.org/10.1016/j.egyr.2019.02.009>
82. Vergnes JB, Gernigon V, Guiraud P, Formosa-Dague C (2019) Bicarbonate Concentration Induces Production of Exopolysaccharides by *Arthrospira platensis* That Mediate Bioflocculation and Enhance Flotation Harvesting Efficiency. *ACS Sustainable Chem Eng* 7:13796–13804. <https://doi.org/10.1021/acssuschemeng.9b01591>
83. Fuchs T, Arnold ND, Garbe D, Deimel S, Lorenzen J, Masri M, Mehlmer N, Weuster-Botz D, Brück TB (2021) A Newly Designed Automatically Controlled, Sterilizable Flat Panel Photobioreactor for Axenic Algae Culture. *Frontiers in Bioengineering and Biotechnology* 9:
84. Zou N, Zhang C, Cohen Z, Richmond A (2000) Production of cell mass and eicosapentaenoic acid (EPA) in ultrahigh cell density cultures of *Nannochloropsis* sp. (Eustigmatophyceae). *European Journal of Phycology* 35:127–133. <https://doi.org/10.1080/09670260010001735711>
85. Cornet J-F (2010) Calculation of Optimal Design and Ideal Productivities of Volumetrically-Lightened Photobioreactors using the Constructal Approach. *Chemical Engineering Science* 65:985–998. <https://doi.org/10.1016/j.ces.2009.09.052>
86. de Vree J, Bosma R, Janssen M, Barbosa MJ, Wijffels R (2015) Comparison of four outdoor pilot-scale photobioreactors. *biotechnology for biofuels* 8:. <https://doi.org/10.1186/s13068-015-0400-2>
87. Olaizola M, Duerr EO (1990) Effects of light intensity and quality on the growth rate and photosynthetic pigment content of *Spirulina platensis*. *J Appl Phycol* 2:97–104. <https://doi.org/10.1007/BF00023370>
88. Masojídek J, Torzillo G (2008) Mass Cultivation of Freshwater Microalgae. In: *Encyclopedia of Ecology*. pp 2226–2235

89. Whitton R, Ometto F, Pidou M, Jarvis P, Villa R, Jefferson B (2015) Microalgae for municipal wastewater nutrient remediation: mechanisms, reactors and outlook for tertiary treatment. *Environmental Technology Reviews* 4:133–148. <https://doi.org/10.1080/21622515.2015.1105308>
90. Chen H-B, Wu J-Y, Wang C-F, Fu C-C, Shieh C-J, Chen C-I, Wang C-Y, Liu Y-C (2010) Modeling on chlorophyll a and phycocyanin production by *Spirulina platensis* under various light-emitting diodes. *Biochemical Engineering Journal* 53:52–56. <https://doi.org/10.1016/j.bej.2010.09.004>
91. Photon management for augmented photosynthesis | Nature Communications. <https://www.nature.com/articles/ncomms12699>. Accessed 8 Jun 2023
92. Yim S-K, Ki D-W, Doo H-S, Kim H, Kwon T-H (2016) Internally illuminated photobioreactor using a novel type of light-emitting diode (LED) bar for cultivation of *Arthrospira platensis*. *Biotechnol Bioproc E* 21:767–776. <https://doi.org/10.1007/s12257-016-0428-6>
93. Kilimtzi E, Cuellar Bermudez S, Markou G, Goiris K, Vandamme D, Muylaert K (2019) Enhanced phycocyanin and protein content of *Arthrospira* by applying neutral density and red light shading filters: a small-scale pilot experiment. *Journal of Chemical Technology & Biotechnology* 94:2047–2054. <https://doi.org/10.1002/jctb.5991>
94. Markou G (2014) Effect of various colors of light-emitting diodes (LEDs) on the biomass composition of *Arthrospira platensis* cultivated in semi-continuous mode. *Appl Biochem Biotechnol* 172:2758–2768. <https://doi.org/10.1007/s12010-014-0727-3>
95. Ajayan KV, Selvaraju M, Thirugnanamoorthy K (2012) Enrichment of chlorophyll and phycobiliproteins in *Spirulina platensis* by the use of reflector light and nitrogen sources: An in-vitro study. *Biomass and Bioenergy* 47:436–441. <https://doi.org/10.1016/j.biombioe.2012.09.012>
96. Niangoran NUF, Buso D, Zissis G, Prudhomme T (2021) Influence of light intensity and photoperiod on energy efficiency of biomass and pigment production of *Spirulina* (*Arthrospira platensis*). *OCL* 28:37. <https://doi.org/10.1051/ocl/2021025>
97. White PJ (2012) Chapter 2 - Ion Uptake Mechanisms of Individual Cells and Roots: Short-distance Transport. In: Marschner P (ed) *Marschner's Mineral Nutrition of Higher Plants* (Third Edition). Academic Press, San Diego, pp 7–47
98. Yang Z, Xu B, Liu J, Zhan J (2022) Dynamic changes of growth and physiological parameters of *Spirulina* cultivated outdoors—a case study in *Spirulina* Industrial Park in Inner Mongolia, China. *Journal of Applied Phycology* 34:1–13. <https://doi.org/10.1007/s10811-021-02680-0>
99. Zeng X, Danquah MK, Zhang S, Zhang X, Wu M, Chen XD, Ng I-S, Jing K, Lu Y (2012) Autotrophic cultivation of *Spirulina platensis* for CO₂ fixation and phycocyanin production. *Chemical Engineering Journal* 183:192–197. <https://doi.org/10.1016/j.cej.2011.12.062>
100. Oliveira MACL de, Monteiro MPC, Robbs PG, Leite SGF (1999) Growth and Chemical Composition of *Spirulina Maxima* and *Spirulina Platensis* Biomass at Different Temperatures. *Aquaculture International* 7:261–275. <https://doi.org/10.1023/A:1009233230706>
101. Richmond A, Lichtenberg E, Stahl B, Vonshak A (1990) Quantitative assessment of the major limitations on productivity of *Spirulina platensis* in open raceways. *J Appl Phycol* 2:195–206. <https://doi.org/10.1007/BF02179776>
102. Brewer PG, Goldman JC (1976) Alkalinity changes generated by phytoplankton growth 1. *Limnology and Oceanography* 21:108–117. <https://doi.org/10.4319/lo.1976.21.1.0108>

103. Otero A, Vincenzini M (2003) Extracellular polysaccharide synthesis by *Nostoc* strains as affected by N source and light intensity. *Journal of Biotechnology* 102:143–152. [https://doi.org/10.1016/S0168-1656\(03\)00022-1](https://doi.org/10.1016/S0168-1656(03)00022-1)
104. Trabelsi L, Ben Ouada H, Bacha H, Ghoul M (2009) Combined effect of temperature and light intensity on growth and extracellular polymeric substance production by the cyanobacterium *Arthrospira platensis*. *J Appl Phycol* 21:405–412. <https://doi.org/10.1007/s10811-008-9383-8>
105. Kumar M, Kulshreshtha J, Singh GP (2011) Growth and biopigment accumulation of cyanobacterium *Spirulina platensis* at different light intensities and temperature. *Braz J Microbiol* 42:1128–1135. <https://doi.org/10.1590/S1517-838220110003000034>
106. Seyhaneyildiz Can S, Koru E, Cirik S (2017) Effect of temperature and nitrogen concentration on the growth and lipid content of *Spirulina platensis* and biodiesel production. *Aquacult Int* 25:1485–1493. <https://doi.org/10.1007/s10499-017-0121-6>
107. J K, J K, R MJ& JJ Taxonomic classification of cyanoprokaryotes (cyanobacterial genera) 2014, using a polyphasic approach. 86:
108. Nowicka-Krawczyk P, Mühlsteinová R, Hauer T (2019) Detailed characterization of the *Arthrospira* type species separating commercially grown taxa into the new genus *Limnospira* (Cyanobacteria). *Sci Rep* 9:694. <https://doi.org/10.1038/s41598-018-36831-0>
109. Rodrigues MS, Ferreira LS, Converti A, Sato S, Carvalho JCM (2010) Fed-batch cultivation of *Arthrospira* (*Spirulina*) *platensis*: Potassium nitrate and ammonium chloride as simultaneous nitrogen sources. *Bioresource Technology* 101:4491–4498. <https://doi.org/10.1016/j.biortech.2010.01.054>
110. Khanra S, Mondal M, Halder G, Tiwari ON, Gayen K, Bhowmick TK (2018) Downstream processing of microalgae for pigments, protein and carbohydrate in industrial application: A review. *Food and Bioproducts Processing* 110:60–84. <https://doi.org/10.1016/j.fbp.2018.02.002>
111. Brányiková I, Prochazkova G, Potočár T, Jezkova Z, Brányik T (2018) Harvesting of Microalgae by Flocculation. *Fermentation* 4:93. <https://doi.org/10.3390/fermentation4040093>
112. Zeng X, Guo X, Su G, Danquah MK, Chen XD, Lin L, Lu Y (2016) Harvesting of Microalgal Biomass. In: Bux F, Chisti Y (eds) *Algae Biotechnology: Products and Processes*. Springer International Publishing, Cham, pp 77–89
113. Singh G, Patidar SK (2018) Microalgae harvesting techniques: A review. *Journal of Environmental Management* 217:499–508. <https://doi.org/10.1016/j.jenvman.2018.04.010>
114. Javed F, Aslam M, Rashid N, Shamair Z, Khan AL, Yasin M, Fazal T, Hafeez A, Rehman F, Rehman MSU, Khan Z, Iqbal J, Bazmi AA (2019) Microalgae-based biofuels, resource recovery and wastewater treatment: A pathway towards sustainable biorefinery. *Fuel* 255:115826. <https://doi.org/10.1016/j.fuel.2019.115826>
115. Harvesting of Cyanobacterium *Arthrospira platensis* Using Inorganic Filtration Membranes: *Separation Science and Technology: Vol 40, No 15*. <https://www.tandfonline.com/doi/abs/10.1080/01496390500385046>. Accessed 28 Dec 2022
116. Laamanen CA, Ross GM, Scott JA (2016) Flotation harvesting of microalgae. *Renewable and Sustainable Energy Reviews* 58:75–86. <https://doi.org/10.1016/j.rser.2015.12.293>
117. Edzwald JK (1993) Algae, Bubbles, Coagulants, and Dissolved Air Flotation. *Water Science and Technology* 27:67–81. <https://doi.org/10.2166/wst.1993.0207>
118. Branyikova I, Prochazkova G, Potocar T, Jezkova Z, Branyik T (2018) Harvesting of Microalgae by Flocculation. *Fermentation* 4:93. <https://doi.org/10.3390/fermentation4040093>

119. Das P, Thaher MI, Abdul Hakim MAQM, Al-Jabri HMSJ, Alghasal GSHS (2016) Microalgae harvesting by pH adjusted coagulation-flocculation, recycling of the coagulant and the growth media. *Bioresource Technology* 216:824–829. <https://doi.org/10.1016/j.biortech.2016.06.014>
120. Huang K-X, Vadiveloo A, Zhou J-L, Yang L, Chen D-Z, Gao F (2023) Integrated culture and harvest systems for improved microalgal biomass production and wastewater treatment. *Bioresource Technology* 376:128941. <https://doi.org/10.1016/j.biortech.2023.128941>
121. Najjar YSH, Abu-Shamleh A (2020) Harvesting of microalgae by centrifugation for biodiesel production: A review. *Algal Research* 51:102046. <https://doi.org/10.1016/j.algal.2020.102046>
122. Kim GM, Kim Y-K (2022) Drying Techniques of Microalgal Biomass: A Review. *Applied Chemistry for Engineering* 33:145–150. <https://doi.org/10.14478/ace.2022.1007>
123. Khoo CG, Dasan YK, Lam MK, Lee KT (2019) Algae biorefinery: Review on a broad spectrum of downstream processes and products. *Bioresource Technology* 292:121964. <https://doi.org/10.1016/j.biortech.2019.121964>
124. Nelson JA (2015) Postharvest Degradation of Microalgae: Effect of Temperature and Water Activity
125. Brink J, Marx S (2013) Harvesting of Hartbeespoort Dam micro-algal biomass through sand filtration and solar drying. *Fuel* 106:67–71. <https://doi.org/10.1016/j.fuel.2012.10.034>
126. Sadeghi G, Taheri O, Mobadersani F (2012) NEW TECHNOLOGIES OF SOLAR DRYING SYSTEMS FOR AGRICULTURAL AND MARINE PRODUCTS
127. van Deventer H, Houben R, Koldeweij R (2013) New Atomization Nozzle for Spray Drying. *Drying Technology* 31:891–897. <https://doi.org/10.1080/07373937.2012.735734>
128. Mouahid A, Seengeon K, Martino M, Crampon C, Kramer A, Badens E (2020) Selective extraction of neutral lipids and pigments from *Nannochloropsis salina* and *Nannochloropsis maritima* using supercritical CO₂ extraction: Effects of process parameters and pre-treatment. *The Journal of Supercritical Fluids* 165:104934. <https://doi.org/10.1016/j.supflu.2020.104934>
129. Fasaei F, Bitter JH, Slegers PM, van Boxtel T (2018) Techno-economic evaluation of microalgae harvesting and dewatering systems. *Algal Research* 31:.. <https://doi.org/10.1016/j.algal.2017.11.038>
130. Sultana R, Hossen MdF (2023) A Literature Review for Improving the Solubility of Poorly Water-Soluble Drug
131. Khanlari A, Doğuş Tuncer A, Sözen A, Şirin C, Gungor A (2020) Energetic, environmental and economic analysis of drying municipal sewage sludge with a modified sustainable solar drying system. *Solar Energy* 208:787–799. <https://doi.org/10.1016/j.solener.2020.08.039>
132. Neves F de F, Demarco M, Tribuzi G, Neves F de F, Demarco M, Tribuzi G (2019) Drying and Quality of Microalgal Powders for Human Alimentation. In: *Microalgae - From Physiology to Application*. IntechOpen
133. Rekik C, Besombes C, Hajji W, Gliguem H, Bellagha S, Mujumdar AS, Allaf K (2021) Study of interval infrared Airflow Drying: A case study of butternut (*Cucurbita moschata*). *LWT* 147:111486. <https://doi.org/10.1016/j.lwt.2021.111486>
134. Baker CGJ, McKenzie KA (2005) Energy Consumption of Industrial Spray Dryers. *Drying Technology* 23:365–386. <https://doi.org/10.1081/DRT-200047665>
135. Lin LP Microstructure of Spray-Dried and Freeze-Dried Microalgal Powders

136. Rybak K, Parniakov O, Samborska K, Wiktor A, Witrowa-Rajchert D, Nowacka M (2021) Energy and Quality Aspects of Freeze-Drying Preceded by Traditional and Novel Pre-Treatment Methods as Exemplified by Red Bell Pepper. *Sustainability* 13:2035. <https://doi.org/10.3390/su13042035>
137. Chen W, Xu J, Yu Q, Yuan Z, Kong X, Sun Y, Wang Z, Zhuang X, Zhang Y, Guo Y (2020) Structural insights reveal the effective *Spirulina platensis* cell wall dissociation methods for multi-output recovery. *Bioresource Technology* 300:122628. <https://doi.org/10.1016/j.biortech.2019.122628>
138. Rame R, Nilawati, Silvy D, Novarina IH, Agus P, Ganang RDH (2018) Cell-wall disruption and characterization of phycocyanin from microalgae: *Spirulina platensis* using Catalytic ozonation. *E3S Web Conf* 73:08010. <https://doi.org/10.1051/e3sconf/20187308010>
139. Rahman MM, Hosano N, Hosano H (2022) Recovering Microalgal Bioresources: A Review of Cell Disruption Methods and Extraction Technologies. *Molecules* 27:2786. <https://doi.org/10.3390/molecules27092786>
140. Pez Jaeschke D, Rocha Teixeira I, Damasceno Ferreira Marczak L, Domeneghini Mercali G (2021) Phycocyanin from *Spirulina*: A review of extraction methods and stability. *Food Research International* 143:110314. <https://doi.org/10.1016/j.foodres.2021.110314>
141. Geciova J, Bury D, Jelen P (2002) Methods for disruption of microbial cells for potential use in the dairy industry—a review. *International Dairy Journal* 12:541–553. [https://doi.org/10.1016/S0958-6946\(02\)00038-9](https://doi.org/10.1016/S0958-6946(02)00038-9)
142. Goettel M, Eing C, Gusbeth C, Straessner R, Frey W (2013) Pulsed electric field assisted extraction of intracellular valuables from microalgae. *Algal Research* 2:401–408. <https://doi.org/10.1016/j.algal.2013.07.004>
143. Käferböck A, Smetana S, de Vos R, Schwarz C, Toepfl S, Parniakov O (2020) Sustainable extraction of valuable components from *Spirulina* assisted by pulsed electric fields technology. *Algal Research* 48:101914. <https://doi.org/10.1016/j.algal.2020.101914>
144. Chew KW, Yap JY, Show PL, Suan NH, Juan JC, Ling TC, Lee D-J, Chang J-S (2017) Microalgae biorefinery: High value products perspectives. *Bioresource Technology* 229:53–62. <https://doi.org/10.1016/j.biortech.2017.01.006>
145. González LE, Díaz GC, Aranda DAG, Cruz YR, Fortes MM (2015) Biodiesel Production Based in Microalgae: A Biorefinery Approach. *Natural Science* 07:358. <https://doi.org/10.4236/ns.2015.77039>
146. Eppink MHM, Ventura SPM, Coutinho JAP, Wijffels RH (2021) Multiproduct Microalgae Biorefineries Mediated by Ionic Liquids. *Trends in Biotechnology* 39:1131–1143. <https://doi.org/10.1016/j.tibtech.2021.02.009>
147. Mitra M, Mishra S (2019) Multiproduct biorefinery from *Arthrospira* spp. towards zero waste: Current status and future trends. *Bioresource Technology* 291:121928. <https://doi.org/10.1016/j.biortech.2019.121928>
148. Ranjith Kumar R, Hanumantha Rao P, Arumugam M (2015) Lipid Extraction Methods from Microalgae: A Comprehensive Review. *Frontiers in Energy Research* 2:
149. Zygler A, Słomińska M, Namieśnik J (2012) 2.04 - Soxhlet Extraction and New Developments Such as Soxtec. In: Pawliszyn J (ed) *Comprehensive Sampling and Sample Preparation*. Academic Press, Oxford, pp 65–82

150. Pinto LFR, Ferreira GF, Beatriz FP, Cabral FA, Filho RM (2022) Lipid and phycocyanin extractions from *Spirulina* and economic assessment. *The Journal of Supercritical Fluids* 184:105567. <https://doi.org/10.1016/j.supflu.2022.105567>
151. Hadiyanto H, Adetya NP (2018) Response surface optimization of lipid and protein extractions from *Spirulina platensis* using ultrasound assisted osmotic shock method. *Food Sci Biotechnol* 27:1361–1368. <https://doi.org/10.1007/s10068-018-0389-y>
152. de Sousa e Silva A, Moreira LM, de Magalhães WT, Farias WRL, Rocha MVP, Bastos AKP (2017) Extraction of biomolecules from *Spirulina platensis* using non-conventional processes and harmless solvents. *Journal of Environmental Chemical Engineering* 5:2101–2106. <https://doi.org/10.1016/j.jece.2017.04.008>
153. Pohndorf RS, Camara AS, Larrosa APQ, Pinheiro CP, Strieder MM, Pinto LAA (2016) Production of lipids from microalgae *Spirulina* sp.: Influence of drying, cell disruption and extraction methods. *Biomass and Bioenergy* 93:25–32. <https://doi.org/10.1016/j.biombioe.2016.06.020>
154. Zhang B, Feng H, He Z, Wang S, Chen H (2018) Bio-oil production from hydrothermal liquefaction of ultrasonic pre-treated *Spirulina platensis*. *Energy Conversion and Management* 159:204–212. <https://doi.org/10.1016/j.enconman.2017.12.100>
155. Bitwell C, Indra SS, Luke C, Kakoma MK (2023) A review of modern and conventional extraction techniques and their applications for extracting phytochemicals from plants. *Scientific African* 19:e01585. <https://doi.org/10.1016/j.sciaf.2023.e01585>
156. Zhang Q-W, Lin L-G, Ye W-C (2018) Techniques for extraction and isolation of natural products: a comprehensive review. *Chin Med* 13:20. <https://doi.org/10.1186/s13020-018-0177-x>
157. Albuquerque BR, Prieto MA, Barreiro MF, Rodrigues A, Curran TP, Barros L, Ferreira ICFR (2017) Catechin-based extract optimization obtained from *Arbutus unedo* L. fruits using maceration/microwave/ultrasound extraction techniques. *Industrial Crops and Products* 95:404–415. <https://doi.org/10.1016/j.indcrop.2016.10.050>
158. Jovanović AA, Đorđević VB, Zdunić GM, Pljevljakušić DS, Šavikin KP, Gođevac DM, Bugarski BM (2017) Optimization of the extraction process of polyphenols from *Thymus serpyllum* L. herb using maceration, heat- and ultrasound-assisted techniques. *Separation and Purification Technology* 179:369–380. <https://doi.org/10.1016/j.seppur.2017.01.055>
159. Tavanandi HA, Mittal R, Chandrasekhar J, Raghavarao KSMS (2018) Simple and efficient method for extraction of C-Phycocyanin from dry biomass of *Arthrospira platensis*. *Algal Research* 31:239–251. <https://doi.org/10.1016/j.algal.2018.02.008>
160. Taufikurahman T, Ilhamsyah DPA, Rosanti S, Ardiansyah MA (2020) Preliminary Design of Phycocyanin Production from *Spirulina platensis* Using Anaerobically Digested Dairy Manure Wastewater. *IOP Conf Ser: Earth Environ Sci* 520:012007. <https://doi.org/10.1088/1755-1315/520/1/012007>
161. Ruiz-Domínguez MC, Jáuregui M, Medina E, Jaime C, Cerezal P (2019) Rapid Green Extractions of C-Phycocyanin from *Arthrospira maxima* for Functional Applications. *Applied Sciences* 9:1987. <https://doi.org/10.3390/app9101987>
162. El-Zahlanieh S, Sivabalan S, Tribouilloy B, Benoit T, Brunello D, Vignes A, Dufaud O (2021) Lifting the Fog Off Hydrocarbon Mist Explosions

163. Soria AC, Brokł M, Sanz ML, Martínez-Castro I (2012) 4.11 - Sample Preparation for the Determination of Carbohydrates in Food and Beverages. In: Pawliszyn J (ed) *Comprehensive Sampling and Sample Preparation*. Academic Press, Oxford, pp 213–243
164. Zhang K, Wong JW (2011) 4.12 - Solvent-Based Extraction Techniques for the Determination of Pesticides in Food. In: Pawliszyn J (ed) *Comprehensive Sampling and Sample Preparation*. Academic Press, Oxford, pp 245–261
165. Barp L, Višnjevec AM, Moret S (2023) Pressurized Liquid Extraction: A Powerful Tool to Implement Extraction and Purification of Food Contaminants. *Foods* 12:2017. <https://doi.org/10.3390/foods12102017>
166. Wianowska D, Gil M (2019) Critical approach to PLE technique application in the analysis of secondary metabolites in plants. *TrAC Trends in Analytical Chemistry* 114:314–325. <https://doi.org/10.1016/j.trac.2019.03.018>
167. Papoutsis K, Grasso S, Menon A, Brunton NP, Lyng JG, Jacquier J-C, Bhuyan DJ (2020) Recovery of ergosterol and vitamin D2 from mushroom waste - Potential valorization by food and pharmaceutical industries. *Trends in Food Science & Technology* 99:351–366. <https://doi.org/10.1016/j.tifs.2020.03.005>
168. Perez-Vazquez A, Carpena M, Barciela P, Cassani L, Simal-Gandara J, Prieto MA (2023) Pressurized Liquid Extraction for the Recovery of Bioactive Compounds from Seaweeds for Food Industry Application: A Review. *Antioxidants* 12:612. <https://doi.org/10.3390/antiox12030612>
169. Hempel M de SS, Colepicolo P, Zambotti-Villela L (2023) Macroalgae Biorefinery for the Cosmetic Industry: Basic Concept, Green Technology, and Safety Guidelines. *Phycology* 3:211–241. <https://doi.org/10.3390/phycology3010014>
170. Dini I, Laneri S (2021) The New Challenge of Green Cosmetics: Natural Food Ingredients for Cosmetic Formulations. *Molecules* 26:3921. <https://doi.org/10.3390/molecules26133921>
171. Radjenović J, Jelić A, Petrović M, Barceló D (2009) Determination of pharmaceuticals in sewage sludge by pressurized liquid extraction (PLE) coupled to liquid chromatography-tandem mass spectrometry (LC-MS/MS). *Anal Bioanal Chem* 393:1685–1695. <https://doi.org/10.1007/s00216-009-2604-4>
172. Eletskaia PM, Mironenko OO, Kukushkin RG, Sosnin GA, Yakovlev VA (2018) Catalytic Steam Cracking of Heavy Oil Feedstocks: A Review. *Catal Ind* 10:185–201. <https://doi.org/10.1134/S2070050418030042>
173. da Silva MF, Casazza AA, Ferrari PF, Aliakbarian B, Converti A, Bezerra RP, Porto ALF, Perego P (2017) Recovery of phenolic compounds of food concern from *Arthrospira platensis* by green extraction techniques. *Algal Research* 25:391–401. <https://doi.org/10.1016/j.algal.2017.05.027>
174. Zhou J, Wang M, Carrillo C, Zhu Z, Brncic M, Berrada H, Barba FJ (2021) Impact of Pressurized Liquid Extraction and pH on Protein Yield, Changes in Molecular Size Distribution and Antioxidant Compounds Recovery from *Spirulina*. *Foods* 10:2153. <https://doi.org/10.3390/foods10092153>
175. Herrero M, Martín-Álvarez PJ, Señoráns FJ, Cifuentes A, Ibáñez E (2005) Optimization of accelerated solvent extraction of antioxidants from *Spirulina platensis* microalga. *Food Chemistry* 93:417–423. <https://doi.org/10.1016/j.foodchem.2004.09.037>
176. Ch S, Cs L, Pc Y, Ks S, Cc C (2014) Solid-liquid extraction of phycocyanin from *Spirulina platensis*: Kinetic modeling of influential factors. *Sep Purif Technol* 123:64–68

177. The Optimized Concentration and Purity of *Spirulina platensis* C-Phycocyanin: A Comparative Study on Microwave-Assisted and Ultrasound-Assisted Extraction Methods - Vali Aftari - 2015 - Journal of Food Processing and Preservation - Wiley Online Library. <https://ifst-onlinelibrary-wiley-com.lama.univ-amu.fr/doi/10.1111/jfpp.12573>. Accessed 15 Jan 2024
178. Sundaram KM (2022) Chapter 9 - Permeability of unimodal pore system. In: Sundaram KM, Mukherjee S (eds) *Developments in Petroleum Science*. Elsevier, pp 613–733
179. Bogialli S, Di Corcia A, Nazzari M (2007) Chapter 9 - Extraction procedures. In: Picó Y (ed) *Food Toxicants Analysis*. Elsevier, Amsterdam, pp 269–297
180. Sundaram KM (2022) Chapter 4 - Pore space attributes of nonconventional reservoirs. In: Sundaram KM, Mukherjee S (eds) *Developments in Petroleum Science*. Elsevier, pp 161–226
181. Michalak I, Dmytryk A, Wieczorek P, Rój E, Awska B, Gorka B, Messyasz B, Lipok J, Mikulewicz M, Wilk R, Schroeder G, Chojna K (2015) Supercritical Algal Extracts: A Source of Biologically Active Compounds from Nature. *Journal of Chemistry* 597140:. <https://doi.org/10.1155/2015/597140>
182. Tzima S, Georgiopoulou I, Louli V, Magoulas K (2023) Recent Advances in Supercritical CO₂ Extraction of Pigments, Lipids and Bioactive Compounds from Microalgae. *Molecules* 28:1410. <https://doi.org/10.3390/molecules28031410>
183. Supercritical Carbon Dioxide Extraction of Molecules of Interest from Microalgae and Seaweeds | Industrial & Engineering Chemistry Research. <https://pubs-acsc-org.lama.univ-amu.fr/doi/10.1021/ie102297d>. Accessed 15 Jan 2024
184. Wang W, Rao L, Wu X, Wang Y, Zhao L, Liao X (2021) Supercritical Carbon Dioxide Applications in Food Processing. *Food Eng Rev* 13:570–591. <https://doi.org/10.1007/s12393-020-09270-9>
185. Del Valle JM, Rivera O, Mattea M, Ruetsch L, Daghero J, Flores A (2004) Supercritical CO₂ processing of pretreated rosehip seeds: effect of process scale on oil extraction kinetics. *The Journal of Supercritical Fluids* 31:159–174. <https://doi.org/10.1016/j.supflu.2003.11.005>
186. Kubovics M, Rojas S, López AM, Fraile J, Horcajada P, Domingo C (2021) Fully supercritical CO₂ preparation of a nanostructured MOF composite with application in cutaneous drug delivery. *The Journal of Supercritical Fluids* 178:105379. <https://doi.org/10.1016/j.supflu.2021.105379>
187. Soh SH, Lee LY (2019) Microencapsulation and Nanoencapsulation Using Supercritical Fluid (SCF) Techniques. *Pharmaceutics* 11:21. <https://doi.org/10.3390/pharmaceutics11010021>
188. Capuzzo A, Maffei ME, Occhipinti A (2013) Supercritical Fluid Extraction of Plant Flavors and Fragrances. *Molecules* 18:7194–7238. <https://doi.org/10.3390/molecules18067194>
189. Gadkari PV, Balaraman M (2015) Solubility of caffeine from green tea in supercritical CO₂: a theoretical and empirical approach. *J Food Sci Technol* 52:8004–8013. <https://doi.org/10.1007/s13197-015-1946-5>
190. Soares GC, Learmonth DA, Vallejo MC, Davila SP, González P, Sousa RA, Oliveira AL (2019) Supercritical CO₂ technology: The next standard sterilization technique? *Materials Science and Engineering: C* 99:520–540. <https://doi.org/10.1016/j.msec.2019.01.121>
191. Warambourg V, Mouahid A, Crampon C, Galinier A, Claeys-Bruno M, Badens E (2023) Supercritical CO₂ sterilization under low temperature and pressure conditions. *The Journal of Supercritical Fluids* 203:106084. <https://doi.org/10.1016/j.supflu.2023.106084>

192. Chen L, Dean B, Liang X (2021) A technical overview of supercritical fluid chromatography-mass spectrometry (SFC-MS) and its recent applications in pharmaceutical research and development. *Drug Discovery Today: Technologies* 40:69–75. <https://doi.org/10.1016/j.ddtec.2021.10.002>
193. Bagheri H, Notej B, Shahsavari S, Hashemipour H (2022) Supercritical carbon dioxide utilization in drug delivery: Experimental study and modeling of paracetamol solubility. *European Journal of Pharmaceutical Sciences* 177:106273. <https://doi.org/10.1016/j.ejps.2022.106273>
194. Díaz-Reinoso B, Moure A, Domínguez H, Parajó JC (2006) Supercritical CO₂ Extraction and Purification of Compounds with Antioxidant Activity. *J Agric Food Chem* 54:2441–2469. <https://doi.org/10.1021/jf052858j>
195. Ha MY, Yoon TJ, Tlustý T, Jho Y, Lee WB (2018) Widom Delta of Supercritical Gas–Liquid Coexistence. *J Phys Chem Lett* 9:1734–1738. <https://doi.org/10.1021/acs.jpcllett.8b00430>
196. Mouahid A, Boivin P, Diaw S, Badens E (2022) Widom and extrema lines as criteria for optimizing operating conditions in supercritical processes. *The Journal of Supercritical Fluids* 186:105587. <https://doi.org/10.1016/j.supflu.2022.105587>
197. Sanzo GD, Mehariya S, Martino M, Larocca V, Casella P, Chianese S, Musmarra D, Balducchi R, Molino A (2018) Supercritical Carbon Dioxide Extraction of Astaxanthin, Lutein, and Fatty Acids from *Haematococcus pluvialis* Microalgae. *Mar Drugs* 16:334. <https://doi.org/10.3390/md16090334>
198. Tippelt M (2019) From lab scale to pilot and production scale using scCO₂ at 1000 bar with special focus on *Haematococcus pluvialis*. 17th European meeting on supercritical fluids 2019
199. Cassanelli M, Prosapio V, Norton I, Mills T (2018) Design of a Cost-Reduced Flexible Plant for Supercritical Fluid-Assisted Applications. *Chemical Engineering & Technology* 41:1368–1377. <https://doi.org/10.1002/ceat.201700487>
200. Benaissi K Le CO₂ supercritique appliqué à l'extraction végétale. In: *Techniques de l'Ingénieur*. <https://www.techniques-ingenieur.fr/base-documentaire/procedes-chimie-bio-agro-th2/intensification-des-procedes-et-methodes-d-analyse-durable-42493210/le-co2-supercritique-applique-a-l-extraction-vegetale-chv4015/>. Accessed 15 Jan 2024
201. Badgujar KC, Badgujar VC, Bhanage BM (2022) Chapter 18 - Recent advances of lipase-catalyzed greener production of biodiesel in organic reaction media: economic and sustainable viewpoint. In: Gurunathan B, Sahadevan R (eds) *Biofuels and Bioenergy*. Elsevier, pp 453–482
202. Taberero A, Valle EMM del, Galan MA (2013) Microalgae Technology: A Patent Survey. *International Journal of Chemical Reactor Engineering* 11:733–763. <https://doi.org/10.1515/ijcre-2012-0043>
203. Valderrama JO, Perrut M, Majewski W (2003) Extraction of Astaxanthin and Phycocyanine from Microalgae with Supercritical Carbon Dioxide. *J Chem Eng Data* 48:827–830. <https://doi.org/10.1021/je020128r>
204. Golmakani M-T, Mendiola JA, Rezaei K, Ibáñez E (2012) Expanded ethanol with CO₂ and pressurized ethyl lactate to obtain fractions enriched in γ -Linolenic Acid from *Arthrospira platensis* (*Spirulina*). *The Journal of Supercritical Fluids* 62:109–115. <https://doi.org/10.1016/j.supflu.2011.11.026>
205. Careri M, Furlattini L, Mangia A, Musc M, Anklam E, Theobald A, von Holst C (2001) Supercritical fluid extraction for liquid chromatographic determination of carotenoids in *Spirulina Pacifica* algae: a chemometric approach. *J Chromatogr A* 912:61–71. [https://doi.org/10.1016/S0021-9673\(01\)00545-3](https://doi.org/10.1016/S0021-9673(01)00545-3)

206. Herrero M, Ibáñez E, Señoráns J, Cifuentes A (2004) Pressurized liquid extracts from *Spirulina platensis* microalga: Determination of their antioxidant activity and preliminary analysis by micellar electrokinetic chromatography. *Journal of Chromatography A* 1047:195–203. <https://doi.org/10.1016/j.chroma.2004.07.001>
207. Sajilata MG, Singhal RS, Kamat MY (2008) Supercritical CO₂ extraction of γ -linolenic acid (GLA) from *Spirulina platensis* ARM 740 using response surface methodology. *Journal of Food Engineering* 84:321–326. <https://doi.org/10.1016/j.jfoodeng.2007.05.028>
208. Mendiola J, Jaime L, Santoyo S, Reglero G, Cifuentes A, Ibáñez E, Señoráns F (2007) Screening of functional compounds in supercritical fluid extracts from *Spirulina Platensis*. *Food Chemistry* 102:1357–1367. <https://doi.org/10.1016/j.foodchem.2006.06.068>
209. Mendiola JA, García-Martínez D, Rupérez FJ, Martín-Álvarez PJ, Reglero G, Cifuentes A, Barbas C, Ibañez E, Señoráns FJ (2008) Enrichment of vitamin E from *Spirulina platensis* microalga by SFE. *The Journal of Supercritical Fluids* 43:484–489. <https://doi.org/10.1016/j.supflu.2007.07.021>
210. Shi J (2006) *Functional Food Ingredients and Nutraceuticals: Processing Technologies*. CRC Press
211. Pronyk C, Mazza G (2009) Design and scale-up of pressurized fluid extractors for food and bioproducts. *Journal of Food Engineering* 95:215–226. <https://doi.org/10.1016/j.jfoodeng.2009.06.002>
212. Laurent A, Lack E, Gamse T, Marr R, Gamse T, Marr R (2001) Chapter 6 - Separation Operations and Equipment. In: Bertuccio A, Vetter G (eds) *Industrial Chemistry Library*. Elsevier, pp 351–403
213. Cussler EL (2009) *Diffusion: Mass Transfer in Fluid Systems*. Cambridge University Press
214. Silveira ST, Quines LK de M, Burkert CAV, Kalil SJ (2008) Separation of phycocyanin from *Spirulina platensis* using ion exchange chromatography. *Bioprocess Biosyst Eng* 31:477–482. <https://doi.org/10.1007/s00449-007-0185-1>
215. Suzuki Y, Sugimura Y, Itoh T (1985) A catalytic oxidation method for the determination of total nitrogen dissolved in seawater. *Marine Chemistry* 16:83–97. [https://doi.org/10.1016/0304-4203\(85\)90029-5](https://doi.org/10.1016/0304-4203(85)90029-5)
216. Jiang B, Tsao R, Li Y, Miao M (2014) Food Safety: Food Analysis Technologies/Techniques. In: Van Alfen NK (ed) *Encyclopedia of Agriculture and Food Systems*. Academic Press, Oxford, pp 273–288
217. Zavřel T, Chmelík D, Sinetova MA, Červený J (2018) Spectrophotometric Determination of Phycobiliprotein Content in *Cyanobacterium Synechocystis*. *J Vis Exp* 58076. <https://doi.org/10.3791/58076>
218. Alkaline Persulfate Oxidation for Determining Total Nitrogen in Microbial Biomass Extracts - Cabrera - 1993 - Soil Science Society of America Journal - Wiley Online Library. <https://access.onlinelibrary.wiley.com/doi/abs/10.2136/sssaj1993.03615995005700040021x>. Accessed 7 Aug 2023
219. Bennett A, Bogorad L (1973) COMPLEMENTARY CHROMATIC ADAPTATION IN A FILAMENTOUS BLUE-GREEN ALGA. *J Cell Biol* 58:419–435
220. Dubois M, Gilles K, Hamilton JK, Rebers PA, Smith F (1951) A Colorimetric Method for the Determination of Sugars. *Nature* 168:167–167. <https://doi.org/10.1038/168167a0>

221. Kurzyna-Szklarek M, Cybulska J, Zdunek A (2022) Analysis of the chemical composition of natural carbohydrates – An overview of methods. *Food Chemistry* 394:133466. <https://doi.org/10.1016/j.foodchem.2022.133466>
222. Depraetere O, Pierre G, Deschoenmaecker F, Badri H, Foubert I, Leys N, Markou G, Wattiez R, Michaud P, Muylaert K (2015) Harvesting carbohydrate-rich *Arthrospira platensis* by spontaneous settling. *Bioresource Technology* 180:16–21. <https://doi.org/10.1016/j.biortech.2014.12.084>
223. Mishra SK, Suh WI, Farooq W, Moon M, Shrivastav A, Park MS, Yang J-W (2014) Rapid quantification of microalgal lipids in aqueous medium by a simple colorimetric method. *Bioresource Technology* 155:330–333. <https://doi.org/10.1016/j.biortech.2013.12.077>
224. Iverson SJ, Lang SLC, Cooper MH (2001) Comparison of the bligh and dyer and folch methods for total lipid determination in a broad range of marine tissue. *Lipids* 36:1283–1287. <https://doi.org/10.1007/s11745-001-0843-0>
225. Chen W, Zhang C, Song L, Sommerfeld M, Hu Q (2009) A high throughput Nile red method for quantitative measurement of neutral lipids in microalgae. *Journal of Microbiological Methods* 77:41–47. <https://doi.org/10.1016/j.mimet.2009.01.001>
226. Cavonius LR, Carlsson N-G, Undeland I (2014) Quantification of total fatty acids in microalgae: comparison of extraction and transesterification methods. *Anal Bioanal Chem* 406:7313–7322. <https://doi.org/10.1007/s00216-014-8155-3>
227. 8.2 The Reaction of Biodiesel: Transesterification | EGEE 439: Alternative Fuels from Biomass Sources. <https://www.e-education.psu.edu/egge439/node/684>. Accessed 20 Dec 2023
228. Cooper MS, Hardin WR, Petersen TW, Cattolico RA (2010) Visualizing “green oil” in live algal cells. *Journal of Bioscience and Bioengineering* 109:198–201. <https://doi.org/10.1016/j.jbiosc.2009.08.004>
229. Jaramillo AM, Londoño LF, Orozco JC, Patiño G, Belalcazar J, Davrieux F, Talsma EF (2018) A comparison study of five different methods to measure carotenoids in biofortified yellow cassava (*Manihot esculenta*). *PLoS One* 13:e0209702. <https://doi.org/10.1371/journal.pone.0209702>
230. Olszowy-Tomczyk M (2021) How to express the antioxidant properties of substances properly? *Chem Pap* 75:6157–6167. <https://doi.org/10.1007/s11696-021-01799-1>
231. Huang D, Ou B, Prior RL (2005) The Chemistry behind Antioxidant Capacity Assays. *J Agric Food Chem* 53:1841–1856. <https://doi.org/10.1021/jf030723c>
232. Rodrigues MJ, Soszynski A, Martins A, Rauter AP, Neng NR, Nogueira JMF, Varela J, Barreira L, Custódio L (2015) Unravelling the antioxidant potential and the phenolic composition of different anatomical organs of the marine halophyte *Limonium algarvense*. *Industrial Crops and Products* 77:315–322. <https://doi.org/10.1016/j.indcrop.2015.08.061>
233. Abramovi H, Grobin B, Ulrih N, Cigic B (2017) The Methodology Applied in DPPH, ABTS and Folin-Ciocalteu Assays Has a Large Influence on the Determined Antioxidant Potential. *Acta Chimica Slovenica* 64:491–499. <https://doi.org/10.17344/acsi.2017.3408>
234. Brand-Williams W, Cuvelier ME, Berset C (1995) Use of a free radical method to evaluate antioxidant activity. *LWT - Food Science and Technology* 28:25–30. [https://doi.org/10.1016/S0023-6438\(95\)80008-5](https://doi.org/10.1016/S0023-6438(95)80008-5)
235. Shalaby E, Shanab S (2013) Antiradical and Antioxidant Activities of Different *Spirulina platensis* Extracts against DPPH and ABTS Radical Assays. *Journal of Marine Biology & Oceanography* 02: <https://doi.org/10.4172/2324-8661.1000105>

236. Dong J-W, Cai L, Xing Y, Yu J, Ding Z-T (2015) Re-evaluation of ABTS•+ Assay for Total Antioxidant Capacity of Natural Products. *Natural Product Communications* 10:1934578X1501001. <https://doi.org/10.1177/1934578X1501001239>
237. Hernández-Rodríguez P, Baquero LP, Larrota HR (2019) Chapter 14 Flavonoids Potential Therapeutic Agents by Their Antioxidant Capacity. In: *Bioactive Compounds*. pp 265–288
238. Vuolo MM, Lima VS, Maróstica Junior MR (2019) Chapter 2 - Phenolic Compounds: Structure, Classification, and Antioxidant Power. In: Campos MRS (ed) *Bioactive Compounds*. Woodhead Publishing, pp 33–50
239. Bashir S, Sharif MK, Butt MS, Shahid M (2016) Functional Properties and Amino acid Profile of *Spirulina platensis* Protein Isolates. *Biological Sciences - PJSIR* 59:12–19. <https://doi.org/10.52763/PJSIR.BIOL.SCI.59.1.2016.12.19>
240. Silva SC, Almeida T, Colucci G, Santamaria-Echart A, Manrique YA, Dias MM, Barros L, Fernandes Â, Colla E, Barreiro MF (2022) *Spirulina* (*Arthrospira platensis*) protein-rich extract as a natural emulsifier for oil-in-water emulsions: Optimization through a sequential experimental design strategy. *Colloids and Surfaces A: Physicochemical and Engineering Aspects* 648:129264. <https://doi.org/10.1016/j.colsurfa.2022.129264>
241. Ramírez-Rodrigues MM, Estrada-Beristain C, Metri-Ojeda J, Pérez-Alva A, Baigts-Allende DK (2021) *Spirulina platensis* Protein as Sustainable Ingredient for Nutritional Food Products Development. *Sustainability* 13:6849. <https://doi.org/10.3390/su13126849>
242. Balti R, Zayoud N, Hubert F, Beaulieu L, Massé A (2021) Fractionation of *Arthrospira platensis* (*Spirulina*) water soluble proteins by membrane diafiltration. *Separation and Purification Technology* 256:117756. <https://doi.org/10.1016/j.seppur.2020.117756>
243. Abdel-Latif HMR, El-Ashram S, Yilmaz S, Naiel MAE, Abdul Kari Z, Hamid NKA, Dawood MAO, Nowosad J, Kucharczyk D (2022) The effectiveness of *Arthrospira platensis* and microalgae in relieving stressful conditions affecting finfish and shellfish species: An overview. *Aquaculture Reports* 24:101135. <https://doi.org/10.1016/j.aqrep.2022.101135>
244. Napolitano G, Venditti P, Agnisola C, Quartucci S, Fasciolo G, Muscari Tomajoli MT, Geremia E, Catone CM, Ulgiati S (2022) Towards sustainable aquaculture systems: Biological and environmental impact of replacing fishmeal with *Arthrospira platensis* (Nordstedt) (*spirulina*). *Journal of Cleaner Production* 374:133978. <https://doi.org/10.1016/j.jclepro.2022.133978>
245. Rosenau S, Ciulu M, Reimer C, Mott AC, Tetens J, Mörlein D (2022) Feeding green: *Spirulina* (*Arthrospira platensis*) induced changes in production performance and quality of salmonid species. *Aquaculture Research* 53:4276–4287. <https://doi.org/10.1111/are.15925>
246. Plaza I, Garcia JL, Villarroel M (2018) Effect of spirulina (*Arthrospira platensis*) supplementation on tilapia (*Oreochromis niloticus*) growth and stress responsiveness under hypoxia. *Spanish Journal of Agricultural Research* 16:e0606–e0606. <https://doi.org/10.5424/sjar/2018161-11698>
247. Occurrence of poly-beta-hydroxybutyrate in *Spirulina* species. - PMC. <https://www.ncbi.nlm.nih.gov/pmc/articles/PMC208930/>. Accessed 13 Jul 2023
248. Shayesteh H, Laird DW, Hughes LJ, Nematollahi MA, Kakhki AM, Moheimani NR (2023) Co-Producing Phycocyanin and Bioplastic in *Arthrospira platensis* Using Carbon-Rich Wastewater. *BioTech* 12:49. <https://doi.org/10.3390/biotech12030049>
249. Jau M-H, Yew S-P, Toh PSY, Chong ASC, Chu W-L, Phang S-M, Najimudin N, Sudesh K (2005) Biosynthesis and mobilization of poly(3-hydroxybutyrate) [P(3HB)] by *Spirulina*

- platensis. *International Journal of Biological Macromolecules* 36:144–151.
<https://doi.org/10.1016/j.ijbiomac.2005.05.002>
250. Martín-Juárez J, Markou G, Muylaert K, Lorenzo-Hernando A, Bolado S (2017) 8 - Breakthroughs in bioalcohol production from microalgae: Solving the hurdles. In: Gonzalez-Fernandez C, Muñoz R (eds) *Microalgae-Based Biofuels and Bioproducts*. Woodhead Publishing, pp 183–207
 251. de Farias Silva CE, Bertucco A (2016) Bioethanol from microalgae and cyanobacteria: A review and technological outlook. *Process Biochemistry* 51:1833–1842.
<https://doi.org/10.1016/j.procbio.2016.02.016>
 252. Phwan CK, Ong HC, Chen W-H, Ling TC, Ng EP, Show PL (2018) Overview: Comparison of pretreatment technologies and fermentation processes of bioethanol from microalgae. *Energy Conversion and Management* 173:81–94. <https://doi.org/10.1016/j.enconman.2018.07.054>
 253. Rempel A, de Souza Sossella F, Margarites AC, Astolfi AL, Steinmetz RLR, Kunz A, Treichel H, Colla LM (2019) Bioethanol from *Spirulina platensis* biomass and the use of residuals to produce biomethane: An energy efficient approach. *Bioresource Technology* 288:121588.
<https://doi.org/10.1016/j.biortech.2019.121588>
 254. Alfonsín V, Maceiras R, Gutiérrez C (2019) Bioethanol production from industrial algae waste. *Waste Management* 87:791–797. <https://doi.org/10.1016/j.wasman.2019.03.019>
 255. Hawrot-Paw M, Koniuszy A, Ratomski P, Sasiadek M, Gawlik A (2023) Biogas Production from *Arthrospira platensis* Biomass. *Energies* 16:3971. <https://doi.org/10.3390/en16103971>
 256. Sumprasit N, Wagle N, Glanpracha N, Annachhatre AP (2017) Biodiesel and biogas recovery from *Spirulina platensis*. *International Biodeterioration & Biodegradation* 119:196–204.
<https://doi.org/10.1016/j.ibiod.2016.11.006>
 257. Herrmann C, Kalita N, Wall D, Xia A, Murphy JD (2016) Optimised biogas production from microalgae through co-digestion with carbon-rich co-substrates. *Bioresour Technol* 214:328–337. <https://doi.org/10.1016/j.biortech.2016.04.119>
 258. Lichtenthaler HK, Buschmann C (2001) Chlorophylls and Carotenoids: Measurement and Characterization by UV-VIS Spectroscopy. *Current Protocols in Food Analytical Chemistry* 1:F4.3.1-F4.3.8. <https://doi.org/10.1002/0471142913.faf0403s01>
 259. Stumm W, Morgan JJ (2012) *Aquatic Chemistry: Chemical Equilibria and Rates in Natural Waters*. John Wiley & Sons
 260. Moraes L, Rosa GM da, Souza M da RAZ de, Costa JAV (2018) Carbon Dioxide Biofixation and Production of *Spirulina* sp. LEB 18 Biomass with Different Concentrations of NaNO₃ and NaCl. *Braz arch biol technol* 61:. <https://doi.org/10.1590/1678-4324-2018150711>
 261. Templeton DW, Laurens LML (2015) Nitrogen-to-protein conversion factors revisited for applications of microalgal biomass conversion to food, feed and fuel. *Algal Research* 11:359–367. <https://doi.org/10.1016/j.algal.2015.07.013>
 262. Siaut M, Cuiné S, Cagnon C, Fessler B, Nguyen M, Carrier P, Beyly A, Beisson F, Triantaphyllidès C, Li-Beisson Y, Peltier G (2011) Oil accumulation in the model green alga *Chlamydomonas reinhardtii*: characterization, variability between common laboratory strains and relationship with starch reserves. *BMC Biotechnology* 11:7. <https://doi.org/10.1186/1472-6750-11-7>
 263. Système d'extraction accélérée par solvant Dionex™ ASE™ 350.
<https://www.thermofisher.com/order/catalog/product/fr/fr/083114>. Accessed 1 Dec 2023

264. Blainski A, Lopes GC, de Mello JCP (2013) Application and Analysis of the Folin Ciocalteu Method for the Determination of the Total Phenolic Content from *Limonium Brasiliense* L. *Molecules* 18:6852–6865. <https://doi.org/10.3390/molecules18066852>
265. Mouahid A, Bombarda I, Claeys-Bruno M, Amat S, Myotte E, Nisteron J-P, Crampon C, Badens E (2021) Supercritical CO₂ extraction of Moroccan argan (*Argania spinosa* L.) oil: Extraction kinetics and solubility determination. *Journal of CO₂ Utilization* 46:101458. <https://doi.org/10.1016/j.jcou.2021.101458>
266. Sovova H (2005) Mathematical model for supercritical fluid extraction of natural products and extraction curve evaluation. *Journal of Supercritical Fluids - J SUPERCRIT FLUID* 33:35–52. <https://doi.org/10.1016/j.supflu.2004.03.005>
267. Mouahid A, Crampon C, Toudji S-AA, Badens E (2013) Supercritical CO₂ extraction of neutral lipids from microalgae: Experiments and modelling. *The Journal of Supercritical Fluids* 77:7–16. <https://doi.org/10.1016/j.supflu.2013.01.024>
268. Brune DE, Novak JT (1981) The use of carbonate equilibrium chemistry in quantifying algal carbon uptake kinetics. *European J Appl Microbiol Biotechnol* 13:71–76. <https://doi.org/10.1007/BF00499691>
269. Ravelonandro PH, Ratianarivo DH, Joannis-Cassan C, Isambert A, Raherimandimby M (2011) Improvement of the growth of *Arthrospira* (*Spirulina*) *platensis* from Toliara (Madagascar): Effect of agitation, salinity and CO₂ addition. *Food and Bioproducts Processing* 89:209–216. <https://doi.org/10.1016/j.fbp.2010.04.009>
270. Gordillo FJL, Jimenez C, Figueroa FL, Niell FX Effects of increased atmospheric CO₂ and N supply on photosynthesis, growth and cell composition of the cyanobacterium *Spirulina platensis* (*Arthrospira*). 10
271. Danesi EDG, Rangel-Yagui CO, Sato S, Carvalho JCM de (2011) Growth and content of *Spirulina platensis* biomass chlorophyll cultivated at different values of light intensity and temperature using different nitrogen sources. *Braz J Microbiol* 42:362–373. <https://doi.org/10.1590/S1517-83822011000100046>
272. Danesi EDG, Rangel-Yagui CO, Carvalho JCM, Sato S (2004) Effect of reducing the light intensity on the growth and production of chlorophyll by *Spirulina platensis*. *Biomass and Bioenergy* 26:329–335. [https://doi.org/10.1016/S0961-9534\(03\)00127-2](https://doi.org/10.1016/S0961-9534(03)00127-2)
273. Chen C-Y, Kao P-C, Tsai C-J, Lee D-J, Chang J-S (2013) Engineering strategies for simultaneous enhancement of C-phycoyanin production and CO₂ fixation with *Spirulina platensis*. *Bioresource Technology* 145:307–312. <https://doi.org/10.1016/j.biortech.2013.01.054>
274. Richmond A, Lichtenberg E, Stahl B, Vonshak A (1990) Quantitative assessment of the major limitations on productivity of *Spirulina platensis* in open raceways. *J Appl Phycol* 2:195–206. <https://doi.org/10.1007/BF02179776>
275. Kim YS, Lee S-H (2018) Quantitative analysis of *Spirulina platensis* growth with CO₂ mixed aeration. *Environmental Engineering Research* 23:216–222. <https://doi.org/10.4491/eer.2017.193>
276. Park Y-I (David), Labrecque M, Lavoie J-M (2013) Influence of Elevated CO₂ and Municipal Wastewater Feed on the Productivity, Morphology, and Chemical Composition of *Arthrospira* (*Spirulina*) *platensis*. *ACS Sustainable Chem Eng* 1:1348–1356. <https://doi.org/10.1021/sc400230q>

277. Huijun C, Yang Z, Lu Z, Wang Q, Liu J (2019) Combination of utilization of CO₂ from flue gas of biomass power plant and medium recycling to enhance cost-effective *Spirulina* production. *Journal of Applied Phycology* 31:.. <https://doi.org/10.1007/s10811-019-1736-y>
278. Kuo C-M, Jian J-F, Sun Y-L, Lin T-H, Yang Y-C, Zhang W-X, Chang H-F, Lai J-T, Chang J-S, Lin C-S (2018) An efficient Photobioreactors/Raceway circulating system combined with alkaline-CO₂ capturing medium for microalgal cultivation. *Bioresour Technol* 266:398–406. <https://doi.org/10.1016/j.biortech.2018.06.090>
279. Bao Y, Liu M, Wu X, Cong W, Ning Z (2012) In situ carbon supplementation in large-scale cultivations of *Spirulina platensis* in open raceway pond. *Biotechnol Bioproc E* 17:93–99. <https://doi.org/10.1007/s12257-011-0319-9>
280. Shareefdeen Z, Elkamel A, Babar ZB (2023) Recent Developments on the Performance of Algal Bioreactors for CO₂ Removal: Focusing on the Light Intensity and Photoperiods. *BioTech* 12:10. <https://doi.org/10.3390/biotech12010010>
281. Chunzhuk EA, Grigorenko AV, Chernova NI, Kiseleva SV, Ryndin KG, Popel OS, Malaniy SY, Slavkina OV, de Farias Neves F, Leng L, Kumar V, Vlaskin MS (2023) Direct Study of CO₂ Capture Efficiency during Microalgae *Arthrospira platensis* Cultivation at High CO₂ Concentrations. *Energies* 16:822. <https://doi.org/10.3390/en16020822>
282. Rubio FC, Fernández FGA, Pérez JAS, Camacho FG, Grima EM (1999) Prediction of dissolved oxygen and carbon dioxide concentration profiles in tubular photobioreactors for microalgal culture. *Biotechnology and Bioengineering* 62:71–86. [https://doi.org/10.1002/\(SICI\)1097-0290\(19990105\)62:1<71::AID-BIT9>3.0.CO;2-T](https://doi.org/10.1002/(SICI)1097-0290(19990105)62:1<71::AID-BIT9>3.0.CO;2-T)
283. Yuvraj, Padmanabhan P (2017) Technical insight on the requirements for CO₂-saturated growth of microalgae in photobioreactors. *3 Biotech* 7:119. <https://doi.org/10.1007/s13205-017-0778-6>
284. Pruvost J, Le Borgne F, Artu A, Cornet J-F, Legrand JM (2016) Industrial Photobioreactors and Scale-Up Concepts. In: Elsevier (ed) *Advances Chemical Engineering*. pp 257–310
285. Moroney JV, Somanchi A (1999) How Do Algae Concentrate CO₂ to Increase the Efficiency of Photosynthetic Carbon Fixation? *Plant Physiology* 119:9–16
286. Rosa GM da, Moraes L, Cardias BB, Souza M da RAZ de, Costa JAV (2015) Chemical absorption and CO₂ biofixation via the cultivation of *Spirulina* in semicontinuous mode with nutrient recycle. *Bioresource Technology* 192:321–327. <https://doi.org/10.1016/j.biortech.2015.05.020>
287. Serrano-Bermúdez LM, Montenegro-Ruíz LC, Godoy-Silva RD (2020) Effect of CO₂, aeration, irradiance, and photoperiod on biomass and lipid accumulation in a microalga autotrophically cultured and selected from four Colombian-native strains. *Bioresource Technology Reports* 12:100578. <https://doi.org/10.1016/j.biteb.2020.100578>
288. Cuellar-Bermudez SP, Aguilar-Hernandez I, Cardenas-Chavez DL, Ornelas-Soto N, Romero-Ogawa MA, Parra-Saldivar R (2015) Extraction and purification of high-value metabolites from microalgae: essential lipids, astaxanthin and phycobiliproteins. *Microbial Biotechnology* 8:190–209. <https://doi.org/10.1111/1751-7915.12167>
289. Maroneze MM, Siqueira SF, Vendruscolo RG, Wagner R, de Menezes CR, Zepka LQ, Jacob-Lopes E (2016) The role of photoperiods on photobioreactors – A potential strategy to reduce costs. *Bioresource Technology* 219:493–499. <https://doi.org/10.1016/j.biortech.2016.08.003>
290. Iwasaki H, Kondo T (2000) The Current State and Problems of Circadian Clock Studies in Cyanobacteria. *Plant and Cell Physiology* 41:1013–1020. <https://doi.org/10.1093/pcp/pcd024>

291. Prates D da F, Radmann EM, Duarte JH, Morais MG de, Costa JAV (2018) Spirulina cultivated under different light emitting diodes: Enhanced cell growth and phycocyanin production. *Bioresource Technology* 256:38–43. <https://doi.org/10.1016/j.biortech.2018.01.122>
292. Zhu B, Shen H, Li Y, Liu Q, Jin G, Han J, Zhao Y, Pan K (2020) Large-Scale Cultivation of Spirulina for Biological CO₂ Mitigation in Open Raceway Ponds Using Purified CO₂ From a Coal Chemical Flue Gas. *Front Bioeng Biotechnol* 7:441. <https://doi.org/10.3389/fbioe.2019.00441>
293. Cornwall CE, Hepburn CD, McGraw CM, Currie KI, Pilditch CA, Hunter KA, Boyd PW, Hurd CL (2013) Diurnal fluctuations in seawater pH influence the response of a calcifying macroalga to ocean acidification. *Proceedings of the Royal Society B: Biological Sciences* 280:20132201. <https://doi.org/10.1098/rspb.2013.2201>
294. Krzemińska I, Pawlik-Skowrońska B, Trzcińska M, Tys J (2014) Influence of photoperiods on the growth rate and biomass productivity of green microalgae. *Bioprocess Biosyst Eng* 37:735–741. <https://doi.org/10.1007/s00449-013-1044-x>
295. Meseck SL, Alix JH, Wikfors GH (2005) Photoperiod and light intensity effects on growth and utilization of nutrients by the aquaculture feed microalga, *Tetraselmis chui* (PLY429). *Aquaculture* 246:393
296. Hidasi N (2018) Diurnal variation of various culture and biochemical parameters of *Arthrospira platensis* in large-scale outdoor raceway ponds. *Algal Research* 9
297. Seyfabadi J, Ramezanpour Z, Khoeyi ZA (2010) Protein, fatty acid, and pigment content of *Chlorella vulgaris* under different light regimes. *Journal of Applied Phycology*. <https://doi.org/10.1007/s10811-010-9569-8>
298. Belkoura M, Dauta A, Bouterfas R (2006) The effects of irradiance and photoperiod on the growth rate of three freshwater green algae isolated from a eutrophic lake. *Limnetica*, ISSN 0213-8409, Vol 25, N° 3, 2006, pags 647-656 25:. <https://doi.org/10.23818/limn.25.43>
299. Hobson LA, Hartley FA, Ketcham DE (1979) Effects of Variations in Daylength and Temperature on Net Rates of Photosynthesis, Dark Respiration, and Excretion by *Isochrysis galbana* Parke. *Plant Physiol* 63:947–951. <https://doi.org/10.1104/pp.63.5.947>
300. Zakar T, Laczko-Dobos H, Toth TN, Gombos Z (2016) Carotenoids Assist in Cyanobacterial Photosystem II Assembly and Function. *Frontiers in Plant Science* 7:
301. Purnamayati L, Dewi EN, Kurniasih RA (2018) Phycocyanin stability in microcapsules processed by spray drying method using different inlet temperature. *IOP Conf Ser: Earth Environ Sci* 116:012076. <https://doi.org/10.1088/1755-1315/116/1/012076>
302. Adjali A, Clarot I, Chen Z, Marchioni E, Boudier A (2022) Physicochemical degradation of phycocyanin and means to improve its stability: A short review. *Journal of Pharmaceutical Analysis* 12:406–414. <https://doi.org/10.1016/j.jpha.2021.12.005>
303. Saini RK, Keum Y-S (2018) Carotenoid extraction methods: A review of recent developments. *Food Chemistry* 240:90–103. <https://doi.org/10.1016/j.foodchem.2017.07.099>
304. Jaime L, Mendiola JA, Herrero M, Soler-Rivas C, Santoyo S, Señorans FJ, Cifuentes A, Ibáñez E (2005) Separation and characterization of antioxidants from *Spirulina platensis* microalga combining pressurized liquid extraction, TLC, and HPLC-DAD. *J Sep Sci* 28:2111–2119. <https://doi.org/10.1002/jssc.200500185>
305. Zaghdoudi K, Pontvianne S, Framboisier X, Achard M, Kudaibergenova R, Ayadi-Trabelsi M, Kalthoum-Cherif J, Vanderesse R, Frochot C, Guiavarc'h Y (2015) Accelerated solvent

- extraction of carotenoids from: Tunisian Kaki (*Diospyros kaki* L.), peach (*Prunus persica* L.) and apricot (*Prunus armeniaca* L.). *Food Chem* 184:131–139. <https://doi.org/10.1016/j.foodchem.2015.03.072>
306. Shi G, Gu L, Jung H, Chung W-J, Koo S (2021) Apocarotenals of Phenolic Carotenoids for Superior Antioxidant Activities. *ACS Omega* 6:25096–25108. <https://doi.org/10.1021/acsomega.1c04432>
307. Cvetkovic D, Marković D (2008) UV-effects on antioxidant activity of selected carotenoids in the presence of lecithin estimated by DPPH test. *Journal of the Serbian Chemical Society* 73:. <https://doi.org/10.2298/JSC0811051C>
308. Ndayishimiye J, Chun BS (2017) Optimization of carotenoids and antioxidant activity of oils obtained from a co-extraction of citrus (Yuzu ichandrin) by-products using supercritical carbon dioxide. *Biomass and Bioenergy* 106:1–7. <https://doi.org/10.1016/j.biombioe.2017.08.014>
309. Rahim A, Çakir C, Ozturk M, Şahin B, Soulimani A, Sibaoueih M, Nasser B, Eddoha R, Essamadi A, El Amiri B (2021) Chemical characterization and nutritional value of *Spirulina platensis* cultivated in natural conditions of Chichaoua region (Morocco). *South African Journal of Botany* 141:235–242. <https://doi.org/10.1016/j.sajb.2021.05.006>
310. Agustini T, Suzery M, Sutrisnanto D, Ma'ruf W, Hadiyanto H (2015) Comparative Study of Bioactive Substances Extracted from Fresh and Dried *Spirulina* sp. *Procedia Environmental Sciences* 23:282–289. <https://doi.org/10.1016/j.proenv.2015.01.042>
311. Materials | Free Full-Text | Modeling of the Kinetics of Supercritical Fluid Extraction of Lipids from Microalgae with Emphasis on Extract Desorption. <https://www.mdpi.com/1996-1944/9/6/423>. Accessed 20 Jan 2024
312. Sovová H, Stateva RP (2019) New developments in the modelling of carotenoids extraction from microalgae with supercritical CO₂. *The Journal of Supercritical Fluids* 148:93–103. <https://doi.org/10.1016/j.supflu.2019.03.002>
313. Colla LM, Bertolin TE, Costa JAV (2004) Fatty acids profile of *Spirulina platensis* grown under different temperatures and nitrogen concentrations. *Z Naturforsch C J Biosci* 59:55–59. <https://doi.org/10.1515/znc-2004-1-212>
314. Gershwin ME, Belay A (2007) *Spirulina in Human Nutrition and Health*. CRC Press
315. Hutner SH, Provasoli L, Schatz A, Haskins CP (1950) Some Approaches to the Study of the Role of Metals in the Metabolism of Microorganisms. *Proceedings of the American Philosophical Society* 94:152–170

Annex

Table 57 Zarrouk medium composition

Compound	g/L	Sigma-Aldrich™ reference
NaCl	1.0	S9888
CaCl ₂ ·2H ₂ O	0.04	223506
NaNO ₃	2.5	221341
FeSO ₄ · 7H ₂ O	0.01	1270355
EDTA (Na)	0.08	324503
K ₂ SO ₄	1.0	223492
MgSO ₄ ·7H ₂ O	0.2	230391
NaHCO ₃	16.8	S6014
K ₂ HPO ₄	0.5	P3786
Hutner solution	1 mL	N/A

Table 58 Hutner solution composition [315]

Compound	g/L	Sigma-Aldrich™ reference
EDTA (Na)	50	324503
ZnSO ₄ ·7H ₂ O	22	221376
H ₃ BO ₃	11.4	B0394
MnCl ₂ ·4H ₂ O	5.1	221376
FeSO ₄ ·7H ₂ O	5	215422
CoCl ₂ ·6H ₂ O	1.6	255599
CuSO ₄ ·5H ₂ O	1.16	209198
(NH ₄) ₆ Mo ₇ O ₂₄ ·4H ₂ O	1.1	A7302

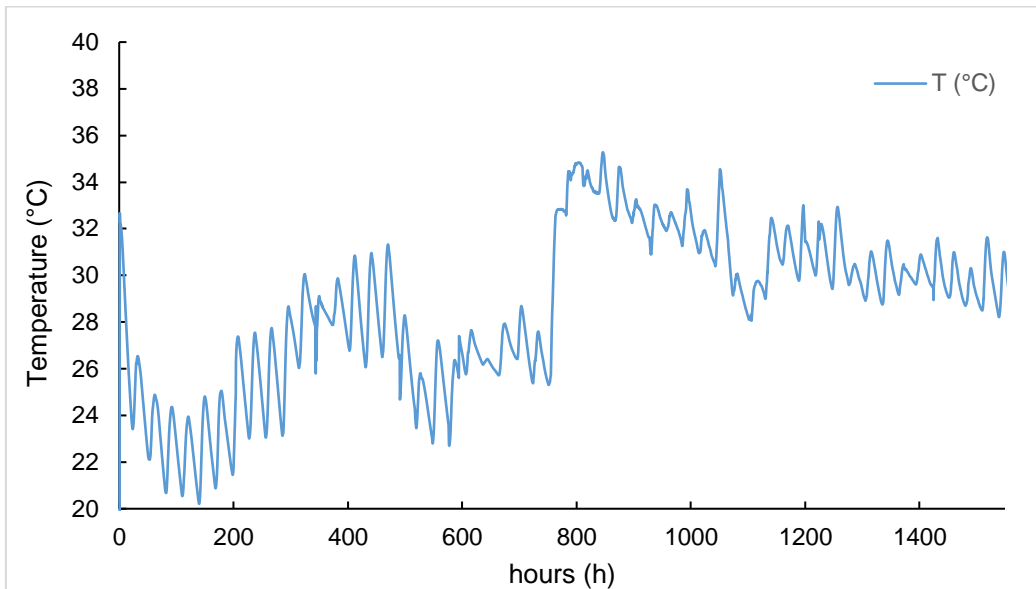


Figure 97 Temperature assessment in the 3 m³ raceway

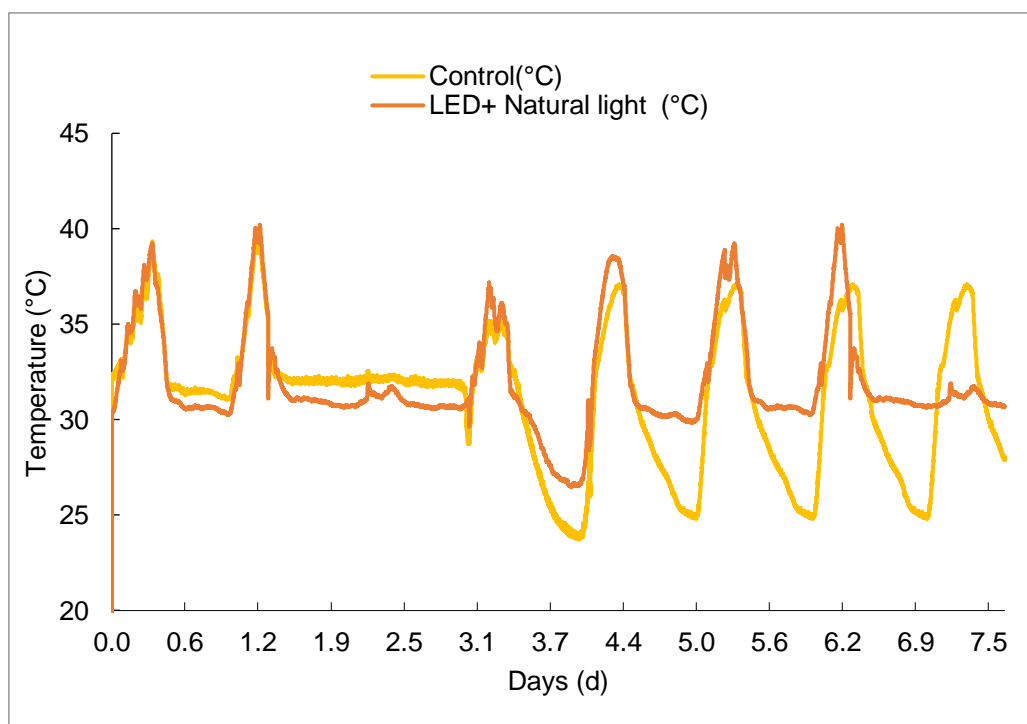


Figure 98 Temperature assessment in the natural light conditions experiment for pigment enhancement



Figure 99 scCO2 full extraction dry extract

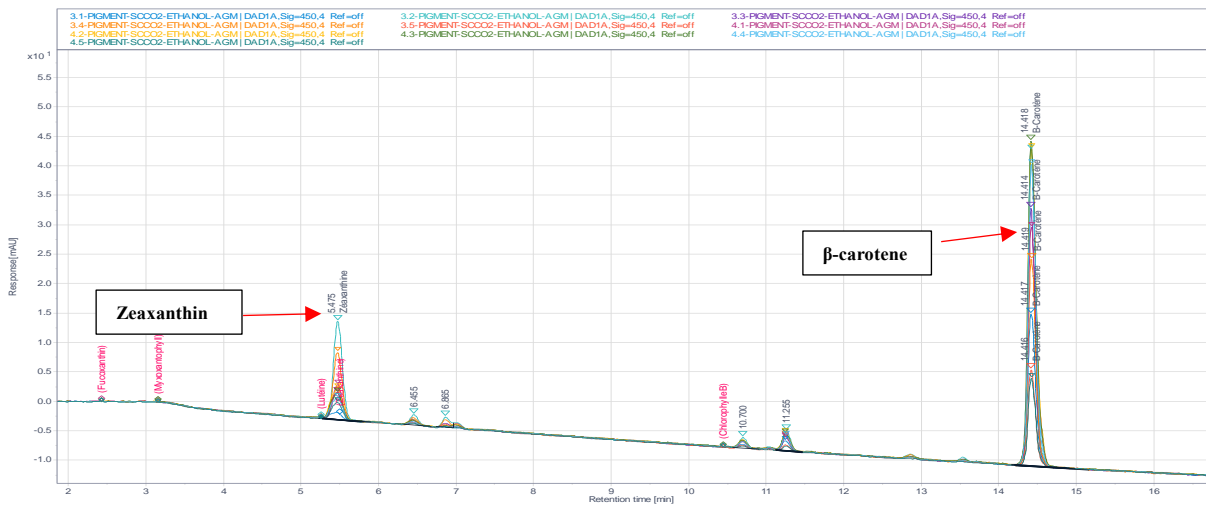


Figure 100 ScCO2extracted pigment chromatogram. Response (mA) as a function of the retention time

Table 59 FAMES fraction of the analyzed extracts by GC-FID

Point	C16:0	mean	C18:0	mean	C18:2 linoleate	mean	C20:3[cis- 8,11,14]	mean	Total FAMES
1.1	31.57%	31.55%	19.99%	20.24%	33.17%	32.94%	15.27%	15.27%	100.00%
1.2	31.54%		20.49%		32.71%		15.26%		100.00%
2.1	100.00%	100%	0.00%	0.00%	0.00%	0.00%	0.00%	0.00%	100.00%
2.2	100.00%		0.00%		0.00%		0.00%		100.00%
3.1	0.00%	0.00%	0.00%	0.00%	0.00%	0.00%	0.00%	0.00%	0.00%
3.2	0.00%		0.00%		0.00%		0.00%		0.00%
4.1	100.00%	100%	0.00%	0.00%	0.00%	0.00%	0.00%	0.00%	100.00%
4.2	100.00%		0.00%		0.00%		0.00%		100.00%
5.1	0.00%	0.00%	0.00%	0.00%	0.00%	0.00%	0.00%	0.00%	0.00%
5.2	0.00%		0.00%		0.00%		0.00%		0.00%

Figure 101 scCO₂ Lipid injection chromatogram

